

micropaleontology

volume 54, no. 1, 2008

Radiolarians in Paleoceanography

Selected Papers from InterRad XI

Edited by David Lazarus and Chris Hollis



RADIOLARIANS IN PALEOCEANOGRAPHY**Selected Papers from InterRad XI, Wellington, New Zealand, March 2006***Edited by David Lazarus and Chris Hollis*

- 2 David Lazarus and Chris Hollis**
Preface
- 3 Taniel Danelian**
Diversity and biotic changes of Archaeodictyomitrid Radiolaria from the Aptian/Albian transition (OAE1b) of southern Albania
- 15 Satoshi Funakawa and Hiroshi Nishi**
Radiolarian faunal changes during the Eocene-Oligocene transition in the Southern Ocean (Maud Rise, ODP Leg 113, Site 689) and its significance in paleoceanographic change
- 27 Yoshiyuki Ishitani, Kozo Takahashi, Yusuke Okazaki and Seiji Tanaka**
Vertical and geographic distribution of selected radiolarian species in the North Pacific
- 41 D.B. Lazarus, C.J. Hollis and M. Apel**
Patterns of opal and radiolarian change in the Antarctic mid-Paleogene: clues to the origin of the Southern Ocean
- 49 Vanessa Lüer, Christopher J. Hollis and Helmut Willems**
Late Quaternary radiolarian assemblages as indicators of paleoceanographic changes north of the subtropical front, offshore eastern New Zealand, southwest Pacific
- 71 Yusuke Okazaki, Kozo Takahashi and Hirofumi Asahi**
Temporal fluxes of radiolarians along the W-E transect in the central and western equatorial Pacific, 1999-2002

Radiolarians in Paleoceanography

Selected papers from InterRad XI, Wellington, New Zealand, March 2006

Edited by David Lazarus and Chris Hollis

The Micropaleontology Project, Inc.
New York, 2008

Preface

The six articles in this special issue of *Micropaleontology* were selected from papers presented at the 11th international meeting of radiolarian researchers (InterRad XI), which was held in Wellington, New Zealand, 19-24 March, 2006. Despite being held in a location far from the Northern Hemisphere centers of radiolarian research the conference attracted 120 participants from 19 countries, including 35 participants from Japan. Perhaps the key attractions of this first Southern Hemisphere radiolarian conference, were the well-attended field trips that combined spectacular radiolarian-rich rock successions with pristine natural scenery. The conference was hosted by InterRad, the International Association of Radiolarian Paleontologists, IGCP Project 467, the Subcommittee on Triassic Stratigraphy and GNS Science.

The articles in this special issue illustrate how our understanding of modern radiolarian ecology continues to improve, and demonstrates the application of ecological knowledge to important questions in paleoceanography at various time scales. Six articles in a companion special issue of *Stratigraphy* demonstrate the diverse applications for radiolarian micropaleontology in correlation and geologic dating. The next international radiolarian conference, InterRad XII, will be held in Nanjing, China, in September 2009.

David Lazarus
Museum für Naturkunde
Humboldt Universität zu Berlin, Germany

Chris Hollis
GNS Science New Zealand

Diversity and biotic changes of Archaeodictyomitrid Radiolaria from the Aptian/Albian transition (OAE1b) of southern Albania

Taniel Danelian

University Pierre and Marie Curie (Paris 6), UMR 5143

Palaeobiodiversity and Palaeoenvironments, C.104, 4 place Jussieu, 75252 Paris Cedex 05, France

email: danelian@ccr.jussieu.fr

ABSTRACT: Moderately well-preserved Archaeodictyomitrid radiolarian assemblages extracted from the Aptian/Albian transition interval (zones NC7 and NC8 of calcareous nannofossils) of the Sopot section in southern Albania provide new data for the Radiolarian record during the lower Albian Oceanic Anoxic Event (OAE1b), which was previously unexplored in Tethyan sediments. Two new species (*Archaeodictyomitra ioniana* n.sp. and *Mita amphora* n.sp.) are described and the age range of a number of Archaeodictyomitrid species is specified. The introduction of *Mita amphora* and *M. gracilis* at the base of the Albian reflects a biotic change that is highlighted by a longer/larger overall test size, wide intercostal pores and the development of robust costae throughout the test. These morphological changes are tentatively regarded as the biotic response of Archaeodictyomitrid radiolarian communities within the Ionian Zone to the palaeoceanographic changes that took place during the Aptian/Albian boundary interval.

INTRODUCTION

The family Archaeodictyomitridae is a Nassellarian clade characterized by long costae running throughout a multisegmented test. A row of pores (primary or relict) is situated between adjacent costae (Pessagno 1977). The family appears to have originated during the Early Jurassic (De Wever et al. 2001), with its last representatives found in Palaeocene strata (Hollis 1997).

Following the work by O'Dogherty (1994) the record of mid Cretaceous Archaeodictyomitrid Nassellaria is much improved. He suggested a number of evolutionary lineages based on the study of relatively rich assemblages yielded from pelagic carbonates of the Umbria-Marche Basin in Italy. However, important gaps still remain, especially for the Upper Aptian to Lower Albian interval, due to the poor preservation of radiolaria in the marly facies that developed in the Umbria-Marche Basin during this interval.

The Archaeodictyomitridae were important constituents of radiolarian communities in mid Cretaceous oceans and quite abundant in intervals punctuated by Oceanic Anoxic Events (OAEs; Salvini and Marcucci-Passerini 1998, Danelian et al. 2002, 2004). The OAE1b is manifested as an extended interval of generalized dysoxia and multiple discrete black shales across various parts of Tethys. It is recorded in the Aptian-Albian transitional interval and is characterized by major changes in the ocean-climate system, with possible consequences for the plankton response and evolution (Leckie et al. 2002).

The objective of this paper is to document the diversity of Archaeodictyomitrid Radiolaria from the OAE1b interval of the Ionian zone of Albania. Based on good age control provided by calcareous nannofossils (and dinoflagellates; Danelian et al. 2007) I reassess the age range of some of the species of this nassellarian family. I also discuss the importance of the observed biotic changes in relation to the background palaeoceanographic changes that took place during the Aptian/Albian transitional interval.

MATERIAL

The studied material comes from the Sopot section of southern Albania (text-fig. 1). The section displays two prominent

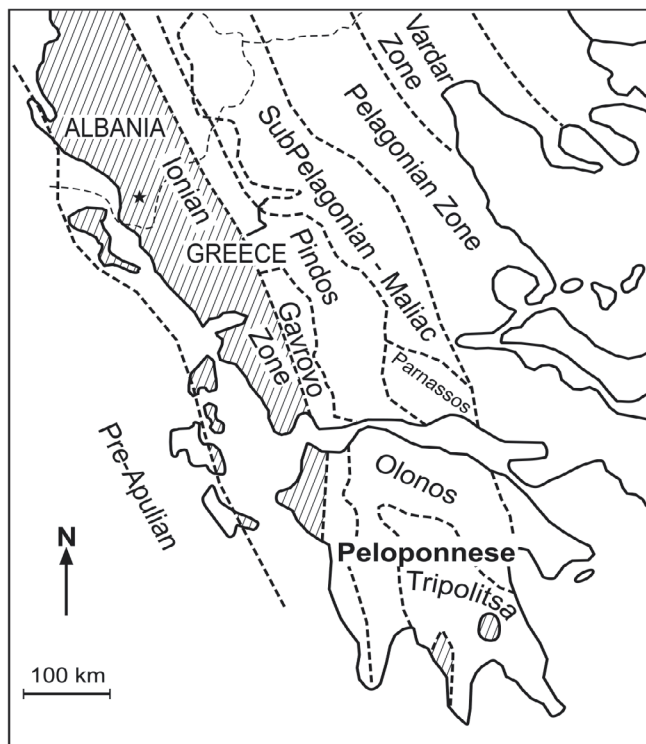
siliceous-marly intervals (text-fig. 2), punctuating a Lower Cretaceous Maiolica-type pelagic carbonate sequence: the Vigla Limestone formation. The litho- and biostratigraphy of the Sopot section is discussed in detail elsewhere (Danelian et al. 2007) and therefore will be only briefly presented below.

The lower shaly-siliceous interval is relatively rich in carbonates and radiolarians and contains many levels rich in organic matter of marine origin. Its age is constrained by Radiolaria (U.A. 1-4 of O'Dogherty 1994) and calcareous nannofossils (Zone NC6 of Bralower et al. 1995) as latest Barremian to early Aptian. It is therefore regarded as the equivalent of the Fourcade Level of Greece that corresponds to the OAE1a event.

All Radiolaria discussed in this study come from the upper shaly-siliceous interval, which is richer in both carbonates and radiolarians and displays a fair number of dark grey marly to black shale levels. Organic matter, measured by Rock-Eval pyrolysis, is preserved only in some black shale layers with Total Organic Carbon content always below 1% (Danelian et al. 2007). Radiolarians recovered from this interval can be assigned to the middle Albian *Mallanites romanus* Subzone (U.A. 10-11) of O'Dogherty (1994), bearing in mind that a substantial part of the upper Aptian to lower Albian interval is unzoned in O'Dogherty's Tethyan biozonation. Calcareous nannofossils identified throughout the upper siliceous horizon are indicative of zones NC7c and NC8a-b of Bralower et al. (1995) and neatly constrain the emplacement of the Aptian/Albian transition (text-fig. 2). Moreover, an early Albian age is also confirmed by dinoflagellates (presence of species *Kleithrisphaeridium atlasiense*) for the top of this interval. Based on its age, the scattered presence of organic matter and radiolarian abundance, the upper shaly-siliceous interval is considered as equivalent to the OAE1b (Danelian et al. 2007).

METHODS

All Archaeodictyomitrid Radiolaria discussed in this study come from three chert beds, selected for their preservation, and were extracted with the use of diluted hydrofluoric acid (4% HF) for 24h, repeated 5-6 times. Residues were collected with a sieve of a mesh of 63µm and washed through gently running water. Radiolarians were dry picked under a stereomicroscope. They are



TEXT-FIGURE 1
Outcrops of the Ionian zone in Greece and Albania. Star indicates the location of Sopoti section in Albania.

in general poorly preserved; the average assemblage in the collected residue displays a Preservation Index 5 to 8 on the scale of Kiessling (1996). Amongst Nassellaria, Archaeodictyomitridae are more abundant and in general better preserved (Preservation Index 3 to 4) and for this reason are the focus of this study. For details about the radiolarian assemblages identified in the studied samples, including the ones yielded from the Fourcade level, and their biostratigraphic significance, the reader is referred to Danelian et al. (2007).

SYSTEMATICS

All material illustrated in the present paper, including the type material of the new species described herein, is housed at the Muséum National d'Histoire Naturelle (Paris). Holotypes and paratypes are catalogued with Museum numbers (MNHN).

Order NASSELLARIA Ehrenberg 1875
Family ARCHAEODICTYOMITRIDAE Pessagno 1976

Genus *Archaeodictyomitra* Pessagno 1976
Type species: *Archaeodictyomitra squinaboli* Pessagno 1976

Remarks: The genus is characterized by a row of barely open (relict) pores situated between adjacent costae. As it stands the distinction between the genera *Archaeodictyomitra* and *Mita* is based solely on the presence of small, relict versus primary and wide open, intercostal pores on the postabdominal segments. However, it is possible to find both character stages within one single morphospecies and thus to consider them as being part of the morphological variation of the species. For example, some of the specimens assigned in this study to *Thanarla brouweri*

gr. display rather open intercostal pores (pl. 2, fig. 18), while the majority of specimens displays small ones. It is actually possible to consider that the extent to which pores are open within the same species is an ecophenotypic variation (dependent on environmental conditions). On the other hand, a clear-cut distinction between small and wide open pores is often difficult. This is why even species that consistently display distinctly open pores (i.e. *A. ioniana* n.sp.) are here assigned to genus *Archaeodictyomitra*.

***Archaeodictyomitra ioniana* Danelian n.sp.**
Plate 2, figures 1-6

Description: Test elongate inflated conical or gently ovoidal in its overall shape. Apical part is pointed and displays a conical outline. It is comprised of four short and imperforate segments (cephalis, thorax, abdomen and the first postabdominal segment), that are distinctive in the presence of a single transverse row of pores at their base.

The rest of the test displays a gently ovoidal outline, as segmental width decreases distally. The boundary between the various segments is unclear in this distal part of the test. 10-12 continuous costae run throughout the postabdominal segments. They are separated by a single row of wide circular pores surrounded by rectangular pore frames. Last segment (preserved only on the holotype) decreases gently distally.

Dimensions (in μm , based on 8 specimens):
Total height of the conical apical part: 55-80
Total height of the remaining gently ovoidal part (excluding last segment on holotype): 155-182
Maximum width: 120-130

Types: Holotype, pl. 2, fig. 1 (MNHN F62 172); Paratypes, pl.2, fig. 2 (MNHN F62 177), pl. 2, fig. 3 (MNHN F62 178).

Remarks: *Archaeodictyomitra ioniana* n.sp. shares a number of similar characters with *Archaeodictyomitra longovata* Dumitrica (in Dumitrica et al. 1997). However, it differs in its much less ovoidal overall shape, the presence of large open pores situated between the continuous costae and by a last segment which decreases only gradually distally. *A. ioniana* appears to be a rather short-lived species. It is common in sample SO PAL 107 but was not observed with certainty in the underlying and overlying samples. Related morphotypes assigned questionably to *A. ioniana* are rare throughout the studied interval. *A. ioniana* is here tentatively considered as an opportunistic species that originated from *A. longovata* and proliferated during the uppermost Aptian of Tethys.

Etymology: indicating its original description from material of the Ionian Zone.

Material: 11 specimens.

***Archaeodictyomitra* sp. cf. *A. ioniana* Danelian n. sp.**
Plate 1, figure 1; plate 2, figures 7-8

Remarks: This morphotype differs from *A. ioniana* n.sp. in its smaller size and more oval shape, narrower maximal width and lesser number of costae (9-10 per half circumference). Also only the three first imperforate segments are externally distinctive on the apical part, instead of four as for typical specimens of *A. ioniana*. This morphotype also resembles *A. longovata* Dumitrica

(in Dumitrica *et al.* 1997) but no funnel-shaped last segment was observed.

Material: 4 specimens.

Archaeodictyomitra montisserei (Squinabol)

Plate 1, figure 2; plate 2, figures 9-10; plate 3, figures 1-2

Stichophormis montisserei SQUINABOL 1903, p. 137, pl. 8, fig. 38.

Archaeodictyomitra sp. – SCHAAF 1981, pl. 3, fig. 14a-b.

Dictyomitra montisserei (Squinabol). – O'DOGHERTY 1994, p. 77, pl. 3, figs. 1-29 (and entire synonymy). – GALLICCHIO *et al.* 1996, pl. 1, fig. 3. – SALVINI and MARCUCCI PASSERINI 1998, fig-text. 7r. – BRAGINA 2004, p. S374, pl. 8, figs. 4, 7, non fig. 2, 3 (= *A. simplex*). – MUSAVU-MOUSSAVOU and DANELIAN 2006, p. 11, pl. 1, fig. 5.

Archaeodictyomitra montisserei (Squinabol). – GORICAN and SMUC 2004, pl. 3, fig. 2, 3.

Archaeodictyomitra sliteri Pessagno. – ERBACHER 1994, p. 93, pl. 20, fig. 3. – PIGNOTTI 1994, pl. 1, fig. 7. – non BRAGINA 2004, p. S372, pl. 7, figs. 6, 10, 11; pl. 8, figs. 8-10, 12; pl. 34, fig. 6.

Archaeodictyomitra sp. MUNASRI and BAMBANG 1994, fig-text. 7. 1.

Remarks: The previously known age range of this species was Middle Albian to lowermost Turonian (O'Dogherty, 1994). The material of this study establishes its presence in Upper Aptian and Lower Albian levels.

Material: Thirteen specimens.

Archaeodictyomitra vulgaris Pessagno

Plate 1, figure 3; plate 2, figures 11-12

Archaeodictyomitra vulgaris PESSAGNO 1977, p. 44, pl. 6, fig. 15. – SCHAAF 1981, p. 14, pl. 4, fig. 2. – THUROW 1988, p. 398, pl. 6, fig. 19. – non VISHNEVSKAYA 2001, p. 150, pl. 86, figs. 1, 4, pl. 116, fig. 7. – non BRAGINA 2004, p. S374, pl. 33, fig. 18 (= *A. montisserei*).

Remarks: The specimens illustrated by Vishnevskaya (2001) on plate 86 display a double transverse row of pores situated above and below segmental divisions that are prominent on the shell surface. They are separated by wide intersegmental parts devoid of any pores. The specimen illustrated on plate 116 is barrel-shaped than rounded conical. The specimen illustrated by Bragina (2004) is assigned to *A. montisserei* because of the several constrictions it displays in its distal part, which are underlined by a single transverse row of pores.

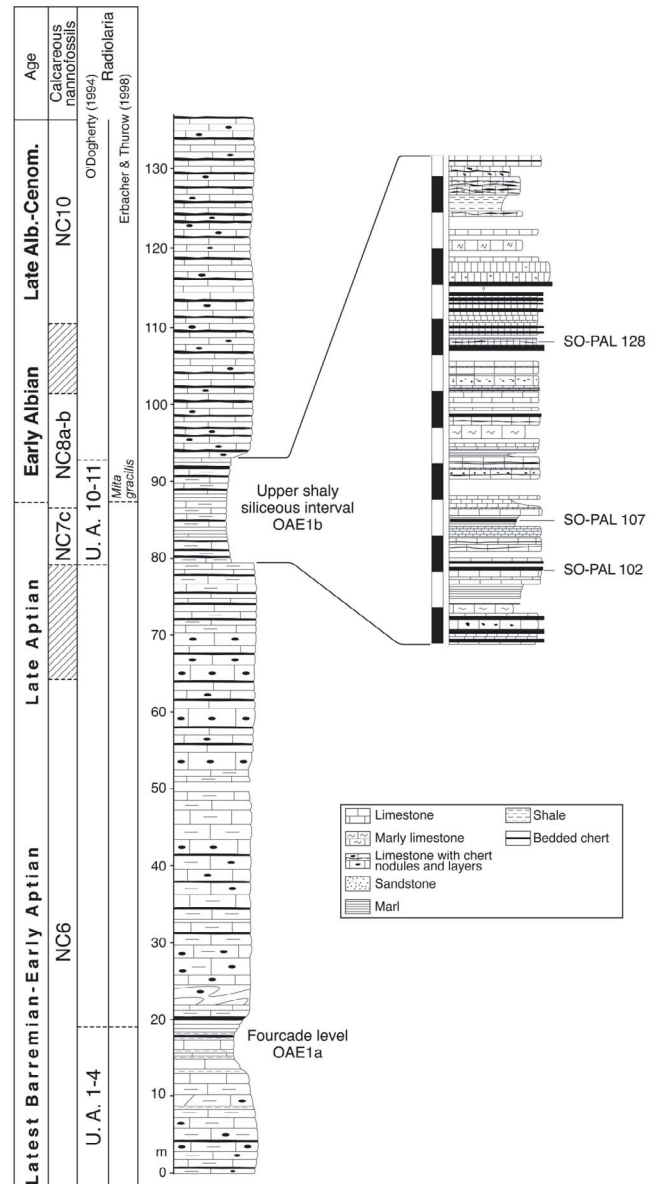
Occurrence: Upper Valanginian to uppermost Aptian of California (Pessagno 1977); Upper Barremian of the Mid-Pacific Mountains (DSDP site 463, Schaaf 1981) and of the Galicia Margin of the northern Atlantic (DSDP site 638; Thurow 1988); Upper Aptian of southern Albania (this study).

***Archaeodictyomitra* sp. A**

Plate 1, figure 4

Description: Large elongated form. The proximal half displays a conical outline and no constrictions. The distal part is gently constricted at two levels. Ten continuous costae run throughout the test and narrow at the thoracic (or abdominal ?) area. By its elongated form and constricted outline this morphotype is comparable to *A. montisserei*. However, it has a wider conical outline and wider intercostal zones.

Material: One specimen



TEXT-FIGURE 2
Lithostratigraphy, detail of the upper shaly-siliceous interval and biostratigraphic framework of the studied Sopot section, including position of samples discussed in the present study.

***Archaeodictyomitra* sp. B**

Plate 1, figure 5; plate 2, figure 13

Description: The proximal part of the test is conical formed by five (?) segments. It is followed by two gently lobated postabdominal segments. Width of the last segment gradually decreases distally. Twelve costae run throughout the test and narrow apically. A single row of small circular pores is situated between costae.

Material : Three specimens.

***Archaeodictyomitra* sp. C**

Plate 2, figure 14

Description: Proximal part of the test displays a conical outline. It is separated by a gentle shoulder from a distal cylindrical part covering two thirds of the test.

Material: One specimen.

Genus *Mita* Pessagno 1977

Type species: *Mita magnifica* Pessagno 1977

Remarks: As discussed under the genus *Archaeodictyomitra*, there are clearly many problems related to the use of primary vs relict intercostal pores as the only distinguishing characteristic between *Archaeodictyomitra* and *Mita*. It is suggested here that the development of costae throughout the test also be taken into account. On the type-species (*M. magnifica*), but also on the new species *M. amphora*, not all costae are raised on the distal half of the test. Moreover, some of the costae are only developed distally, starting well below the proximal part of the test. On the contrary, in most cases of *Archaeodictyomitra* species, all costae become proximally thinner and closer to each other, but all reach the area close to or around the cephalis.

***Mita amphora* Danelian n.sp.**

Plate 3, figure 3-7

? *Mita* (?) sp. D THUROW 1988, pl.6, fig. 22.

Description: Test bulb-shaped. A slight indent separates a conical and sharply-pointed apical part from a barrel-shaped distal part. The test is costate throughout, but only every second costae is well developed and raised on the surface of the barrel-shaped distal part. Costae continuous, decrease in number and converge apically on the conical proximal part. Primary, wide open pores occur between costae on postabdominal chambers.

No segmental distinctions can be seen on the test outline. The total number of segments is unknown.

Dimensions (in μm , based on 9 specimens):

Total height of the conical apical part: 100-133

Total height of the barrel-shaped distal part : 150-237

Maximum width: 150-210

Types: Holotype, pl. 3, fig. 3 (MNHN F62 171); Paratypes, pl. 3, fig. 4 (MNHN F62 179), pl. 3, fig. 5 (MNHN F62 180).

Remarks: *M. amphora* shares a number of common characteristics with the types-species *M. magnifica* Pessagno, namely the fact that not all costae are prominent, but in many cases only every second costae. It also shares many common characteristics with *M. spoletensis* (O'Dogherty) from which it differs by its longer proximal conical part, its less inflated barrel-shaped distal part and unequal development of costae throughout its test. The specimen illustrated by Thurow (1988) as *Mita* (?) sp. D from Upper Barremian levels of the DSDP Site 638 (Galicia margin) displays smaller pores and less well developed costae.

Etymology: from "amphora", referring to its overall shape.

Material: Nine specimens.

Mita gracilis (Squinabol)

Plate 3, figure 8-9

Sethoconus gracilis n. sp. – SQUINABOL 1903, p. 131, pl. 10, fig. 13.

Mita gracilis (Squinabol) – GORICAN 1987, p. 187, pl. 3, fig. 22-23; ERBACHER 1994, p. 102, pl. 9, figs. 10, 11; GORICAN 1994, p. 75, pl. 21, fig. 14-16 (only); ERBACHER 1998, p. 370, pl. 1, fig. 13; ERBACHER and THUROW 1998, Fig. 6-4.

Dictyomitra gracilis (Squinabol) - O'DOGHERTY 1994, p. 73, pl. 1, figs. 12-25 (and entire synonymy); GALLICCHIO et al. 1996, pl. 1, fig. 4. *Archaeodictyomitra chalilovi* (Aliev) – JUD 1994, p. pl. 3, fig. 13-14 (only); Baumgartner et al. 1995, p. 100, pl. 5582, fig. 1-2 (only). non *Thanarla gracilis* (Squinabol) - BRAGINA 2004, p. S369, pl. 7, fig. 9.

Remarks: The broad taxonomic concept by O'Dogherty (1994) is followed in this study, including forms displaying a large variability in the inflated nature of their distal part. They are all characterised by a long test and a sharply pointed apical part. Although the two specimens illustrated by Jud (1994) are poorly preserved and the pore pattern is not clearly visible, they are tentatively included here under this species because of their general outline and pointed apical part, and also because not all costae developed on the median part of the test reach its apical part.

Occurrence: Hauterivian/Barremian of Italy (Jud 1994); middle Albian – middle Cenomanian of Italy and Spain (Erbacher 1994 ; O'Dogherty, 1994), lower Albian to upper Cenomanian of the Atlantic (Erbacher 1994, 1998), upper Albian to Santonian of the Pacific (Schaaf 1981, Taketani 1982), Lowermost Albian of Albania (this study).

Material: Fifteen specimens.

Genus *Thanarla* Pessagno 1977

Type species: *Phormocyrtis veneta* Squinabol 1903

Thanarla brouweri (Tan) group

Plate 1, figure 7-9; plate 2 figure 15-18; plate 3, figure 10

Eucyrtidium Brouweri spec. nov. typ. TAN 1927, p. 58, pl. 11, fig. 89a-b. *Thanarla brouweri* (Tan) - O'DOGHERTY 1994, p.86, pl.5, fig. 1-12 (and entire synonymy), ZIABREV et al. 2003, fig. 3-43. *Thanarla conica* (Aliev) –MEKIK 2000, pl. 5, fig. 28.

Material: Nineteen specimens.

Thanarla conica (Squinabol)

Plate 1, figure 6; plate 3, figure 11

Carpocanistrum conicum SQUINABOL 1903, p. 128, pl.8, fig. *Thanarla conica* (Squinabol). – O'DOGHERTY 1994, p. 90, pl. 5, fig. 23-27 (and entire synonymy).

Remarks : Morphotype characterized by its shell-shaped outline devoid of any constriction. The specimens found in our material are slightly larger (about 100 μm), with more numerous costae (11 per circumference) than the ones found by O'Dogherty (1994).

Material: Six specimens.

Thanarla praeveneta Pessagno

Plate 1, fig.10; plate 2, figures 19-22; plate 3, figure 12

Thanarla praeveneta n.sp. PESSAGNO 1977, p. 46, pl. 7, fig. 11, 16, 18, 23, 27. – GORICAN 1994, p. 91, pl. 21, fig. 3?, 4 (and entire synonymy).

Remarks: *T. praeveneta* was considered by Pessagno (1977) as first occurring during the Albian. Following Goricani (1994), I here confirm the occurrence of this species in upper Aptian and lower Albian levels. Pessagno (1977) suggested also that *T. praeveneta* gave rise to *T. veneta* in early Cenomanian times. However, Thurow (1988) found *T. veneta* occurring first in upper

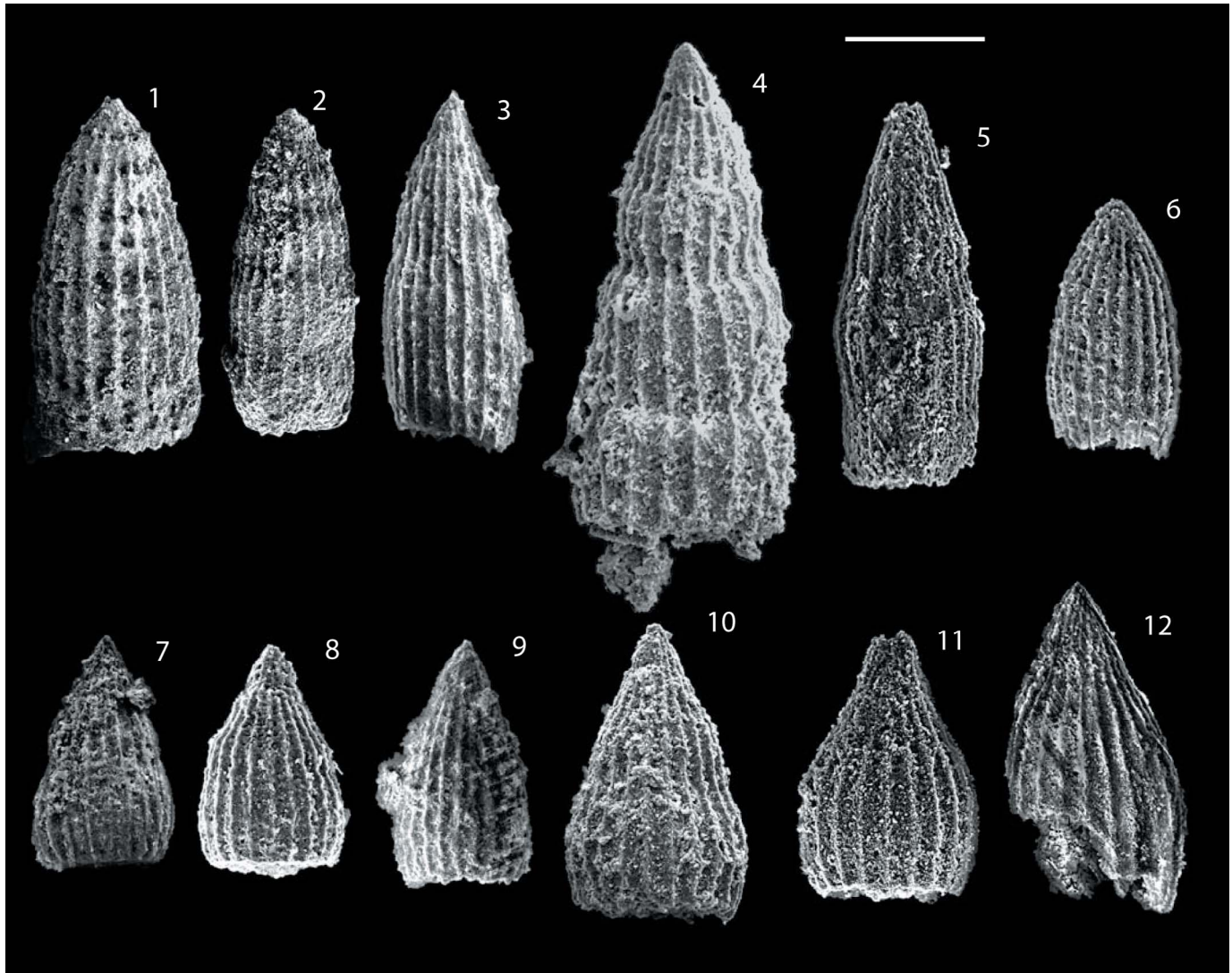


PLATE 1

Archaeodictyomitrud Radiolaria from the Upper Aptian sample SO PAL-102 of the Sopot section. Scale corresponds to 100µm for all specimens.

- | | |
|---|--|
| 1. <i>Archaeodictyomitra</i> sp.cf. <i>A. ioniana</i> n.sp. | 6. <i>Thanarla conica</i> (Squinabol) |
| 2. <i>Archaeodictyomitra montisserei</i> (Squinabol) | 7-9. <i>Thanarla brouweri</i> (Tan) gr. |
| 3. <i>Archaeodictyomitra vulgaris</i> Pessagno | 10. <i>Thanarla praeveneta</i> Pessagno |
| 4. <i>Archaeodictyomitra</i> sp. A. | 11-12. <i>Thanarla pulchra</i> (Squinabol) gr. |
| 5. <i>Archaeodictyomitra</i> sp. B. | |

Albian sediments of the Atlantic (Site 398). O'Dogherty (1994) considered species *T. praeveneta* as a junior synonym of *T. veneta* and regarded the latter species as originating from *T. pulchra*. I here regard *T. praeveneta* as a valid species and suggest that the *T. praeveneta*/*T. veneta* lineage originated from a *T. brouweri* stock. Some morphotypes of our material that display a more pronounced and wider triangular bilobate distal part (pl. 1, fig. 10, pl.2, fig. 19-20) may be regarded as transitional forms.

Material: Ten specimens.

Thanarla pulchra (Squinabol) group
Plate 1, figures 11-12

Sethamphora pulchra n. sp. SQUINABOL 1904, p. 213, pl. 5, fig. 8.
Thanarla pulchra (Squinabol). – O'DOGHERTY 1994, p. 91, pl. 5, figs 28-33 (and entire synonymy). – SALVINI and MARCUCCI-PASSERINI 1998, fig. 6u. – BAK 1999, pl. 1, fig. 9
Thanarla elegantissima (Cita). – BAK 1995, p. 21, fig-text. 10k, l. – SALVINI and MARCUCCI-PASSERINI 1998, fig. 6t.

Material: Four specimens.

TABLE 1

Occurrence of Archaeodictyomitrid Radiolaria identified in the three studied samples from the “upper shaly-siliceous interval” of the Sopot section.

	SO-PAL-102	SO-PAL-107	SO-PAL-128
<i>Archaeodictyomitra ioniana</i> n.sp.		♦	
<i>Archaeodictyomitra</i> sp. cf. <i>A. ioniana</i> n.sp.	♦	♦	♦
<i>Archaeodictyomitra montisserei</i> (Squinabol)	♦	♦	♦
<i>Archaeodictyomitra vulgaris</i> Pessagno	♦	♦	
<i>Archaeodictyomitra</i> sp. A	♦	♦	
<i>Archaeodictyomitra</i> sp. B	♦		
<i>Archaeodictyomitra</i> sp. C		♦	
<i>Mita amphora</i> n.sp.			♦
<i>Mita gracilis</i> (Squinabol)			♦
<i>Thanarla brouweri</i> (Tan) gr.	♦	♦	♦
<i>Thanarla conica</i> (Squinabol)	♦		♦
<i>Thanarla praeveneta</i> Pessagno	♦	♦	♦
<i>Thanarla pulchra</i> (Squinabol) gr.	♦	♦	

RESULTS

Table 1 displays the occurrence of morphospecies and morphotypes discussed in the present study. All three assemblages were yielded from chert lithologies, and the Archaeodictyomitridae studied display more or less the same average degree of preservation (Preservation Index 3 to 4 on the scale of Kiessling 1996). One of the most noticeable changes in the diversity of the three succeeding assemblages is the introduction of *Mita amphora* n.sp. and *M. gracilis* in the Lower Albian sample SO PAL-128. The common occurrence of *A. ioniana* n.sp. in the uppermost Aptian sample SO PAL-107 is also striking.

The age range of some Archaeodictyomitrid species can be better constrained or confirmed. Thus, (i) the earliest known first occurrence (F.O.) of *A. montisserei* in the upper Aptian and Lower Albian is here established for the first time; (ii) the upper age limit of *Archaeodictyomitra vulgaris* in the upper Aptian is here confirmed for Tethys, following its establishment in the palaeo-Pacific (Pessagno 1977). Moreover, the local F.O. of *Mita gracilis* in the Ionian Zone towards the base of the Albian (sample SO PAL-128) is coeval with the Atlantic record (Erbacher

and Thurow 1998). It is noteworthy that this species appears to first occur much earlier (Hauterivian/Barremian) in the Umbria-Marche Basin (Jud 1994) and later (Late Albian) in the Pacific (Schaaf 1981, Taketani 1982).

Finally, the Archaeodictyomitrids preserved throughout the three examined assemblages display a general morphological trend towards larger and longer tests. More particularly, although small Archaeodictyomitrids (i.e. *Thanarla brouweri*) are abundant in the oldest of our samples (SO PAL-102), they become increasingly rare in the younger sample (SO PAL-128), in which large morphospecies (i.e. *M. gracilis*) are common. Morphometric data for Archaeodictyomitrids picked up randomly from the dried residues for SEM observations provide quantitative evidence for this general trend. Indeed, as shown on Table 2, the 95% confidence intervals for both maximum width and maximum length of Archaeodictyomitrids yielded from the three successive assemblages do not overlap.

DISCUSSION

The late Aptian-early Albian OAE 1b is of considerable importance for heterotrophic biomineralising plankton. For example, Leckie et al. (2002) showed that planktic foraminifera experienced a severe faunal turnover and drastic reduction in their average size. With respect to Radiolaria, the little data currently available for the Aptian/Albian transition come from Deep Sea Drilling sites of the Atlantic ocean, where Erbacher (1994) and Erbacher and Thurow (1997) found a stepwise extinction pattern in the Upper Aptian and lowermost Albian, which was followed by a diversification. More recently, O’Dogherty and Guex (2002) argued for a longer extinction interval covering the late early Aptian to early Albian, followed by an important diversification in the middle Albian.

Although the number of samples studied here is somewhat limited, the results merit discussion as a guide for future research, especially in the context of global palaeoenvironmental changes across the Aptian/Albian transition.

The F.O. of large *Mita* species (i.e. *M. gracilis* and *M. amphora*) in the lowermost Albian of the Sopot section is clearly an introduction (migration ?) of new Archaeodictyomitrid species into the Ionian Zone.

Another interesting case of ecological significance might be the common presence of *A. ioniana* in the uppermost Aptian sample SO PAL 107. Its morphological resemblance to *A. longovata* and

PLATE 2

Archaeodictyomitrid Radiolaria extracted from the Uppermost Aptian sample SO PAL-107 of the Sopot section. Scale corresponds to 100µm for all specimens.

- | | |
|---|--|
| 1-6. <i>Archaeodictyomitra ioniana</i> n.sp.; fig. 1: Holotype, arrows indicate the beginning of the last segment, fig. 2-3: paratypes. | 13. <i>Archaeodictyomitra</i> sp. B. |
| 7-8. <i>Archaeodictyomitra</i> sp.cf. <i>A. ioniana</i> n.sp. | 14. <i>Archaeodictyomitra</i> sp. C. |
| 9-10. <i>Archaeodictyomitra montisserei</i> (Squinabol) | 15-18. <i>Thanarla brouweri</i> (Tan) gr. |
| 11-12. <i>Archaeodictyomitra vulgaris</i> Pessagno | 19-22. <i>Thanarla praeveneta</i> Pessagno |

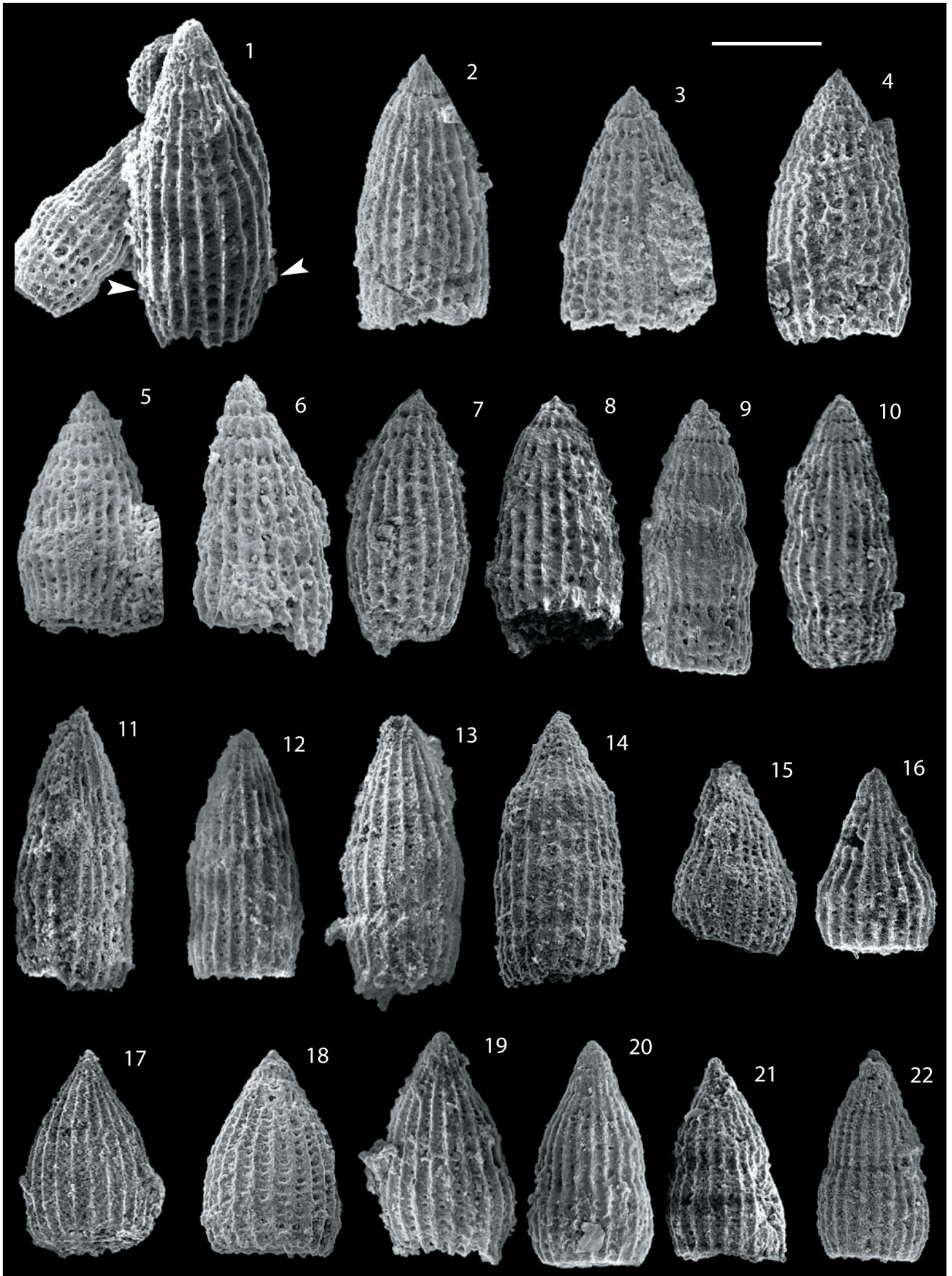


TABLE 2

Morphometric data for Archaeodictyomitrid specimens picked up randomly from dried residues of the three studied samples. Lmax = Maximum Length; Wmax = Maximum Width; (μ) = mean; (σ) = Standard deviation; (C.I.) = Confidence Interval.

	Lmax (μ)	Lmax (σ)	Lmax (95% C.I.)	Wmax (μ)	Wmax (σ)	Wmax (95% C.I.)	n° of specimens
SO PAL-102	202.9	41.3	193-212.8	105.3	14.5	101.8-108.7	68
SO PAL-107	218	46.4	208-227.4	114.3	18.8	110.6-118	93
SO PAL-128	282.2	62.3	266.4-297.9	132.9	30.2	125.2-140.5	60

the rare presence of related morphotypes throughout this material (cf. *A. ioniana*) suggests that this species might have been an opportunistic ecophenotype of *A. longovata* that developed a wider more conical outline, stronger costae and large intercostal pores. Sample SO PAL 107 represents the most radiolarian-rich level (over 40% of radiolaria, according to the chart by Baccele and Bosellini 1965) within the OAE1b interval of the Sopot section (Danelian et al. 2007). The entire upper siliceous interval is itself rich in radiolaria (30% on average). It contrasts with the radiolarian paucity in the underlying and overlying Maiolica facies limestones, considered as accumulations under stratified oligotrophic waters. Radiolarian richness in the upper siliceous interval of the Sopot section is thus regarded as the result of higher plankton productivity. This correlates well with the abundance of siliceous plankton in coeval sections of other well documented areas, such as radiolarian abundance in the tropical DSDP site 545, west of Africa (Leckie et al. 2002), radiolarian accumulation on Shatsky Rise of the Pacific ocean (Robinson et al. 2004) and the accumulation of high latitude diatomites near Antarctica (Gersonde and Harwood 1990, Harwood and Gersonde 1990).

The occurrence of *A. ioniana* n.sp. in the uppermost Aptian of the Sopot section and the introduction of *M. gracilis* and *M. amphora* n.sp. at the lowermost Albian levels underline the preference of a considerable number of Archaeodictyomitrid Radiolaria of the Ionian Zone for wider intercostal pores and larger test size, with more robust/strengthened costae. This tendency towards larger and stronger test construction might have been developed as a response of Archaeodictyomitrids to the establishment of more eutrophic conditions in the Ionian Zone.

CONCLUSIONS

Study of the diversity and average test size of Archaeodictyomitrids throughout the Aptian/Albian transitional interval of the Sopot section of Albania provides some insights into the radiolarian response to the OAE1b event in the Ionian Zone and Tethys.

The introduction of relatively large species, such as *Mita amphora* sp. nov. and *M. gracilis*, in the earliest Albian of the Ionian Zone highlights an overall trend within the Archaeodictyomitrid communities to develop a larger average test size, with well defined, robust costae and wide open intercostal pores. These biotic changes took place in the background of profound palaeoceanographic changes which favoured biosiliceous accumulation and contrast with the planktic foraminiferal response which was expressed by a reduction in their average test size.

Given the good age control of the studied interval provided by calcareous nannofossils (and dinoflagellates), the age range of some species is further specified (i.e. *A. montisserei*) or confirmed for Tethys (i.e. *A. vulgaris*).

ACKNOWLEDGMENTS

C. Chancogne helped with SEM work and C. Abrial with the plate preparation. Paulian Dumitria, Spela Gorican, Luis O'Dogherty, Elspeth Urquhart and Valentina Vishnevskaya provided valuable remarks which greatly improved the manuscript.

REFERENCES

- BACCELLE, L. and BOSELLINI, A., 1965. Diagrammi per la stima visiva della composizione percentuale nelle rocce sedimentary. *Annali dell'Università di Ferrara (Nuovo Serie)*, Sezione IX, Scienze Geologiche e Paleontologiche 1 : 117-153.
- BAK, M., 1995. Mid Cretaceous Radiolaria from the Pienny Klippen Belt, Carpathians, Poland. *Cretaceous Research* 16: 1-23.
- , 1999. Cretaceous radiolarian zonation in the Polish part of the Pienny klippen belt (Western Carpathians). *Geologica Carpathica* 50(1): 21-31.
- BAUMGARTNER, P. O., O'DOGHERTY, L., GORICAN, S., DUMITRICA-JUD, R., DUMITRICA, P., PILLEUIT, A., URQUHART, E., MATSUOKA, A., DANELIAN, T., BARTOLINI, A., CARTER, E. S., DE WEVER, P., KITO, N., MARCUCCI, M. and STEIGER, T., 1995. Radiolarian catalogue and systematics of Middle Jurassic to Early Cretaceous Tethyan genera and species. In: Baumgartner, P.O., O'Dogherty, L., Gorican, S., Urquhart, E., Pilleuit, A. and De Wever, P., Eds; Middle Jurassic to Lower Cretaceous Radiolaria of Tethys: Occurrences, Systematics, Biochronology, *Mémoires de Géologie (Lausanne)* 23, 37-685.
- BRAGINA, L. G., 2004. Cenomanian-Turonian Radiolarians of Northern Turkey and Crimean Mountains. *Paleontological Journal*, supplement 38: S325-S456.
- BRALOWER, T.J., LECKIE, R.M., SLITER, W.V., THIERSTEIN, H.R. 1995. An integrated Cretaceous microfossil biostratigraphy. SEPM Special Publication, 54, 65-79. DANELIAN, T., BAUDIN, F., GARDIN, S., BELTRAN, C. and MASURE, E., 2002. Early Aptian productivity increase as recorded in the Forcale level of the Ionian zone of Greece. *Comptes Rendus Géoscience*, 334, 1087-1093.
- DANELIAN, T., TSIKOS, H., GARDIN, S., BAUDIN, F., BELLIER, J.-P. and EMMANUEL, L., 2004. Global and regional palaeoceanographic changes as recorded in the mid-Cretaceous (Aptian-Albian) sequence of the Ionian zone (northwestern Greece). *Journal of the Geological Society, London*, 161, 703-709.

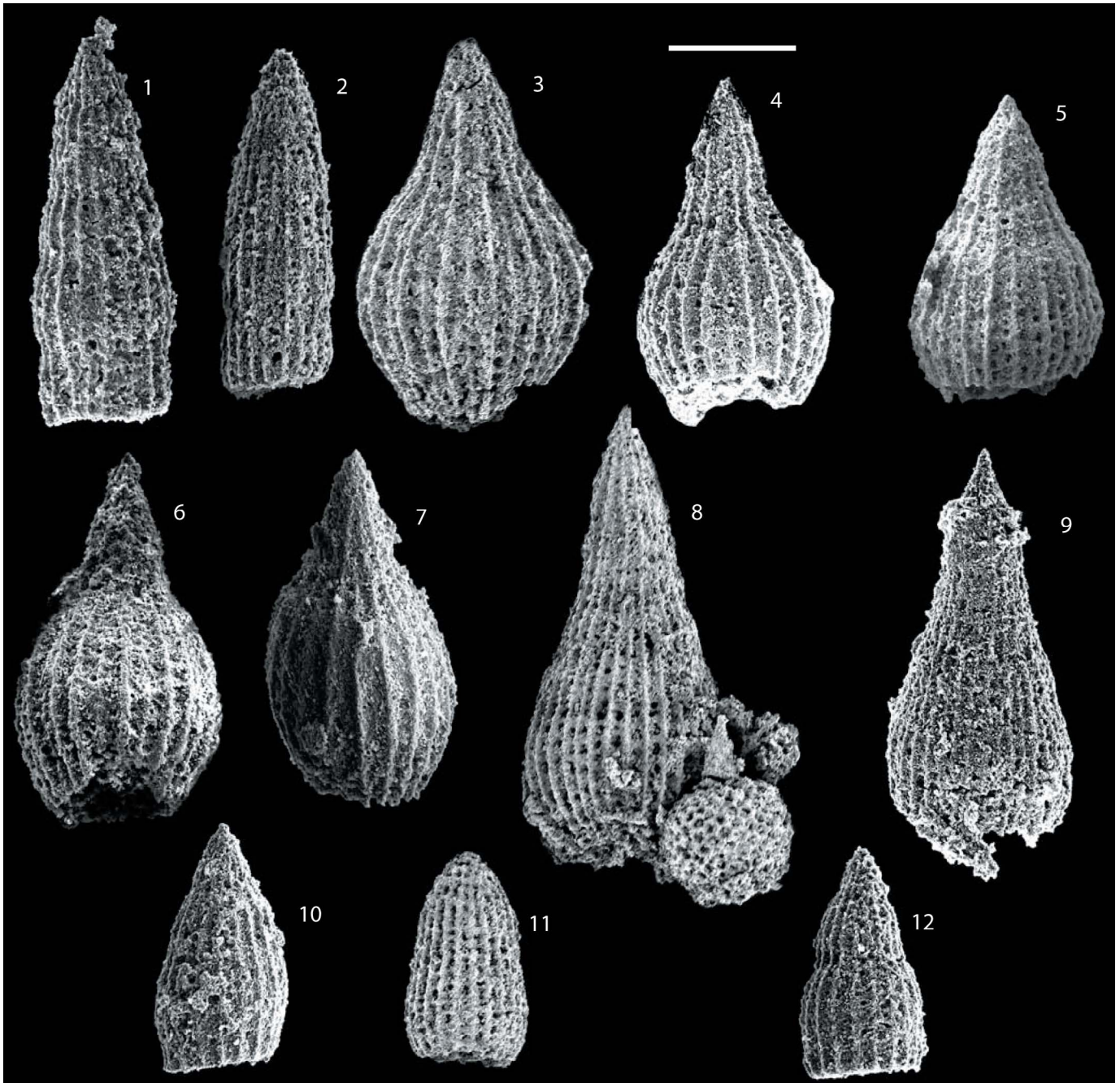


PLATE 3

Archaeodictyomitrid Radiolaria extracted from the Lower Albian sample SO PAL-128 of the Sopot section. Scale corresponds to 100µm for all specimens.

1-2. *Archaeodictyomitra montisserei* (Squinabol)

3-7: *Mita amphora* n.sp. Fig. 3: Holotype, Figs. 4-5: Paratypes.

8-9: *Mita gracilis* (Squinabol)

10. *Thanarla brouweri* (Tan) gr.

11: *Thanarla conica* (Squinabol)

12. *Thanarla praeveneta* Pessagno

- DANELIAN, T., BAUDIN, F., GARDIN, S., MASURE, E., RICORDEL C., FILI I., MECIT. and MUSKA K. (2007). The record of mid Cretaceous Oceanic Anoxic Events from the Ionian zone of southern Albania. *Revue de Micropaléontologie*, 50: 225-237.
- DE WEVER, P., DUMITRICA, P., CAULET, J.P., NIGRINI, C., CARIDROIT, M., 2001. Radiolarians in the Sedimentary Record, Gordon and Breach Science Publishers, 533p.
- DUMITRICA, P., IMMENHAUSER, A. and DUMITRICA-JUD, R. 1997. Mesozoic Radiolarian biostratigraphy from Masirah Ophiolite, Sultanate of Oman. Part I: Middle Triassic, Uppermost Jurassic and Lower Cretaceous Spumellarians and multisegmented Nassellarians. *Bulletin of the National Museum of Natural Science*, 9: 1-105.
- EHRENBERG, C. G., 1875. Fortsetzung der mikrogeologischen Studien als Gesamt-Uebersicht der mikroskopischen Palaontologie gleichartig analysirter Gebirgsarten der Erde, mit specieller Rücksicht auf den Polycystinen-Mergel von Barbados. *Königliche Akademie der Wissenschaften zu Berlin, Abhandlungen*, Jahre: 1-225.
- ERBACHER, J., 1994. Entwicklung und Paläoozeanographie mittelkretazischer Radiolarien der westlichen Tethys (Italien) und des Nordatlantiks. *Tübinger Mikropaläontologische Mitteilungen*, Institut und Museum für Geologie und Paläontologie der Universität Tübingen. 12: 120p.
- ERBACHER, J., 1998. Mid-Cretaceous radiolarians from the Eastern equatorial Atlantic and their paleoceanography. In Mascle, J., Lohmann, G.P., and Moullade, M., Eds; *Proceedings of the Ocean Program, Scientific Results* 159: 363-373.
- ERBACHER, J. and THUROW, J., 1997. Influence of oceanic anoxic events on the evolution of mid-Cretaceous radiolaria in the North Atlantic and west Tethys. *Marine Micropaleontology* 30: 139-158.
- ERBACHER, J. and THUROW, J., 1998. Mid-Cretaceous radiolarian zonation for the North Atlantic: an example of oceanographically controlled evolutionary processes in the marine biosphere? In: Cramp, A., Macleod, C.J., Lee, S.V. and Jones, E.J.W., Eds. *Geological Evolution of Ocean Basins: Results from Ocean Drilling Program*. Geological Society, London Special Publications 131: 71-82.
- GALLICCHIO, S., MARCUCCI, M., PIERI, P., PREMOLI SILVA, I., SABATO and L., SALVINI, G., 1996. Stratigraphical data from a Cretaceous claystones sequence of the "Argile Varicolori" in the Southern Apennines (Basilicata, Italy). *Palaeopelagos* 6: 261-272.
- GERSONDE, R. and HARWOOD, D.M. 1990. Lower Cretaceous diatoms from ODP Leg 113 Site 693 (Weddell Sea), part 1, Vegetative cells. *Proceedings Ocean Drilling Program Scientific Results*, 113, 365-402.
- GORICAN, S. 1987. Jurassic and Cretaceous radiolarians from the Budva zone (Montenegro, Yugoslavia). *Revue de Micropaléontologie* 30: 177-197.
- 1994. Jurassic and Cretaceous radiolarian biostratigraphy and sedimentary evolution of the Budva Zone (Dinarides, Montenegro). *Mémoires de Géologie (Lausanne)* 18: 177 p.
- GORICAN, S. and SMUC, A., 2004. Albian Radiolaria and Cretaceous stratigraphy of Mt Mangart (Western Slovenia). *Razprave IV. Razreda sazu XLV-3*: 29-49.
- HARWOOD, D.M. and GERSONDE, R. 1990 – Lower Cretaceous diatoms from ODP Leg 113 Site 693 (Weddell Sea), part 2, Resting spores, Chrysophycean cysts, and endoskeletal dinoflagellates, and notes on the origin of diatoms. *Proceedings Ocean Drilling Program Scientific Results*, 113, 403-426.
- HOLLIS C.J. 1997. Cretaceous – Paleocene Radiolaria from Eastern Marlborough, New Zealand. Institute of Geological and Nuclear Sciences Monograph 17, 152 p.
- JUD, R., 1994. Biochronology and Systematics of Early Cretaceous Radiolaria of the Western Tethys. *Mémoires de Géologie (Lausanne)* 19: 147 p., 24 pls.
- KIESSLING, W., 1996. Facies characterization of Mid-Mesozoic deep-water sediments by quantitative analysis of siliceous microfossils. *Facies* 35: 237-274.
- LECKIE, R.M., BRALOWER, T.J. and CASHMAN, R. 2002. Oceanic anoxic events and plankton evolution: Biotic response to tectonic forcing during the mid-Cretaceous. *Paleoceanography*, 17, 13-1 – 13-29.
- MEKIK, F., 2000. Early Cretaceous Pantanelliidae (Radiolaria) from northwest Turkey. *Micropaleontology*, 46/1: 1-30.
- MUNASRI, K. W. and BAMBANG, W., 1994. Cretaceous radiolarians from the Luk-Ulo Melange Complex in the Karangsambung area, central Java, Indonesia. *Journal of Southeast Asian Earth Sciences* 9(1/2): 29-43.
- MUSAVU-MOUSSAVOU, B. and DANELIAN, T. 2006. The Radiolarian biotic response to Oceanic Anoxic Event 2 in the southern part of the Northern proto-Atlantic (Demerara Rise, ODP Leg 207). In: Erbacher J. *et al.* Eds Demerara Rise (Leg 207): Equatorial Cretaceous and Paleogene Stratigraphy and Palaeoceanography – *Revue de Micropaléontologie* 49: 141-163.
- O'DOGHERTY, L., 1994. Biochronology and paleontology of Mid-Cretaceous radiolarians from Northern Apennines (Italy) and Betic Cordillera (Spain). *Mémoires de Géologie (Lausanne)* 21: 411p.
- O'DOGHERTY, L. and GUEX, J., 2002. Rates and pattern of evolution among Cretaceous radiolarians: relations with global paleoceanographic events. *Micropaleontology* 48 (suppl. n°1): 1-22.
- PESSAGNO, E. A. Jr., 1976. Radiolarian zonation and stratigraphy of the Upper Cretaceous of the Great Valley Sequence, California Coast Ranges. *Micropaleontology special publication* 2: 1-95.
- , 1977. Lower Cretaceous radiolarian biostratigraphy of Great Valley Sequence and Franciscan complex, California Coast Ranges. *Cushman Foundation for foraminiferal research, special publication* 15: 1-87.
- PIGNOTTI, L., 1994. The Cenomanian - Turonian siliceous-anoxic event in the Scisti Policromi (Tuscan succession, Northern Apennines): data on radiolarian and foraminiferal biostratigraphy. *Palaeopelagos* 4: 141-153.
- ROBINSON, S.A., WILLIAMS, T. and BOWN, P.R., 2004. Fluctuations in biosiliceous production and the generation of Early Cretaceous oceanic anoxic events in the Pacific Ocean (Shatsky Rise, Ocean Drilling Program Leg 198). *Paleoceanography*, 19: 1.
- SALVINI, G. and MARCUCCI PASSERINI, M., 1998. The radiolarian assemblages of the Bonarelli Horizon in the Umbria-Marches Apennines and Southern Alps, Italy. *Cretaceous Research* 19: 777-804.
- SCHAAF, A., 1981. Late Early Cretaceous Radiolaria from Leg 62. *Init. Repts DSDP*, Washington (D.C.), vol. 62: 419-470.
- SQUINABOL, S., 1903. Le Radiolarie dei noduli selciosi nella Scaglia degli Euganei. *Contribuzione. Rivista Italiana di Paleontologia* 19: 127-130.
- , 1904. Radiolarie cretacee degli Euganei. *Atti e memorie dell'Accademia di scienze, lettere ed arti. Padova, new series* 20: 171-244.

TAKETANI, Y., 1982. Cretaceous radiolarian biostratigraphy of the Urakawa and Obira areas, Hokkaido. *Science Reports of the Tohoku University*, 2 1/1-2: 1-75.

TAN, S.H., 1927. Over de samenstelling en het ontstaan van krijt-en mergel-gesteenten van de Molukken. In: Brouwer, H.A., Ed.: *Jaarboek van het mijnwezen in Nederlandsch Oost-Indie*, Jaargang 55, 1926, verhandelingen, 3rd gedeelte, 5-165.

THUROW, J., 1988. Cretaceous Radiolarians of the North Atlantic Ocean: ODP Leg 103 (Sites 638, 640 and 641) and DSDP Legs 93 (Site 603) and 47B (Site 398). In: Boillot, G., Winterer, E.L., et al.

Eds: *Proceedings of the Ocean Drilling Program, Scientific Results* 103: 379-418.

VISHNEVSKAYA, V., 2001. Jurassic to Cretaceous Radiolarian biostratigraphy of Russia. *Geos*, 374 pp.

ZIABREV, S.V., AITCHISON, J.C., ABRAJEVITCH, A.V., BADENG-ZHU, DAVIS, A.M. and LUO, H., 2003. Precise radiolarian age constraints on the timing of ophiolite generation and sedimentation in the Dazhuqu terrane, Yarlung-Tsangpo suture zone, Tibet. *w*, 160, 591-599.

Radiolarian faunal changes during the Eocene-Oligocene transition in the Southern Ocean (Maud Rise, ODP Leg 113, Site 689) and its significance in paleoceanographic change

Satoshi Funakawa¹ and Hiroshi Nishi²

¹*Nishi-akada 273-2, Nasu-Shiobara, Tochigi 329-2744, Japan*

²*Department of Earth and Planetary Sciences, Graduate School of Science, Hokkaido University, Sapporo, 060-0810, Japan*
e-mail: funakawa@msg.biglobe.ne.jp; hnishi@ep.sci.hokudai.ac.jp

ABSTRACT: Quantitative analysis of radiolarian assemblages from the late middle Eocene to late Oligocene at Hole 689B (ODP Leg 113, Maud Rise, Southern Ocean) reveal that radiolarian faunal turnovers occurred at ~38.5 Ma (Subchron C18n1n), ~36.3 Ma (Subchron C16n2n), 34.5-33.9 Ma (Subchron C13r), ~28.3 Ma (Subchron C9r), ~26.9 Ma (Subchron C8r), and 26.4-26.2 Ma (Subchron C8n2n). These faunal turnovers are characterized by an increase or decrease of the Antarctic-diagnostic assemblage. Furthermore, species diversity indexes such as species richness, diversity and equitability and total accumulation rate of radiolarians decreases significantly near the turnover events. The patterns of increase and decrease in the Antarctic group suggest that the faunal turnover events are interpreted as replacement events between the Antarctic and Subantarctic assemblages. The intervals with higher levels of the Antarctic group at 38.5-36.3 Ma, 34.5-33.9 Ma, and 28.3-26.9 Ma were under the influence of the Antarctic bioprovince. Two faunal turnover events at 34.5-33.9 Ma and ~28.3 Ma are correlated with the positive shift of $\delta^{18}\text{O}$ isotopes in the early stage of Oi-1 glaciation and Oi-2a event, respectively. Events at ~36.3 Ma and 26.9-26.2 Ma when the Antarctic-dominant assemblages decreased correspond to warming events in late Eocene and the late Oligocene warming, respectively. Thus, faunal changes in radiolarians can be used to monitor paleoceanographic change in the Southern Ocean and migration of the high-latitude water mass boundary during the Eocene-Oligocene interval.

INTRODUCTION

The transition from the early Paleogene hothouse to the Neogene icehouse is well-documented by $\delta^{18}\text{O}$ and Mg/Ca curves in benthic foraminifers (e.g., Lear et al. 2000; Zachos et al. 2001; Billups and Schrag 2003). Particularly, climatic change at the Eocene-Oligocene transition started by mid-Eocene, with glaciation at high-latitudes in both hemispheres (Tripathi et al. 2005), followed by late Eocene cooling (Vonhof et al. 2000), and finally resulted in large glaciations near the Eocene/Oligocene boundary and at the early/late Oligocene boundary that are named the Oi-1 and Oi-2a isotope events, respectively (Miller et al. 1991; Zachos et al. 1993, 2001). Short intervals of late Eocene (Bohaty and Zachos 2003) and late Oligocene warming (Zachos et al. 2001; Villa and Persico 2006) interrupted the long-term cooling during the Eocene through Miocene.

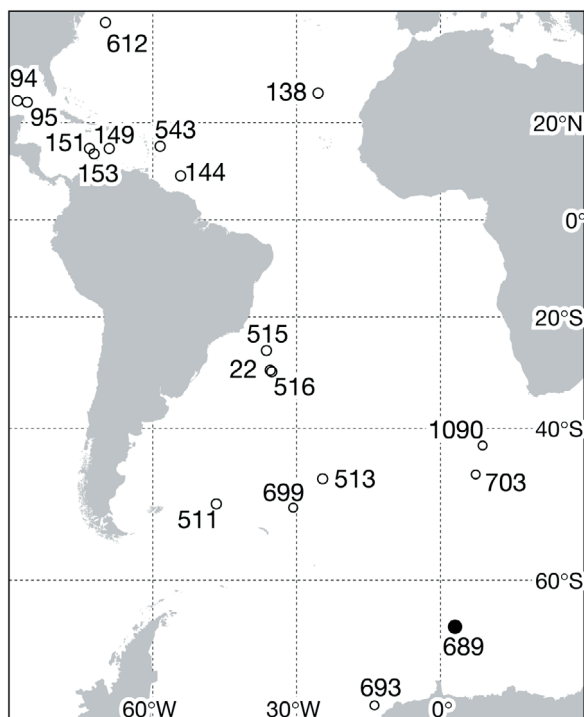
Biotic evolution during the Eocene-Oligocene transition has been discussed by many authors based on the results from several DSDP (Deep Sea Drilling Project) and ODP (Ocean Drilling Program) sites (e.g., Kennett and Warnke 1991, 1993; Prothero and Berggren 1992; Wei et al. 1992; Prothero et al. 2003; Persico and Villa 2004; Sluijs et al. 2005; Funakawa et al. 2006). The faunal analysis of benthic foraminifers indicates that the deep ocean environment changed in the middle to late Eocene (e.g., Thomas 1990; Schröder-Adams 1991; Mackensen and Berggren 1992). Floral analysis of calcareous nannofossils indicates a cooling of surface ocean starting in the late Eocene, and a large turnover from temperate to cool water assemblages occurring near the Eocene/Oligocene boundary (Wei et al. 1992; Persico and Villa 2004). Moreover, the faunal change from Subantarctic to Antarctic assemblages in radiolarians occurred during the late Paleogene in the Southern Ocean (Lazarus and Caulet 1993).

The Southern Ocean is one of the key areas to reconstruct ancient climatic conditions during the greenhouse-icehouse transi-

tion, because Antarctic ice-sheet formation would have affected global climate by increasing global albedo and strengthening the atmospheric Polar High, and because the formation of cold intermediate and bottom water around Antarctica would have drawn heat from lower latitude oceans. In the modern southern high-latitude oceans, the important water mass boundaries are the Subtropical Convergence and the Antarctic Polar Front (AAPF). The AAPF is characterized as the boundary between cold Antarctic surface water and warm Subantarctic surface water, and represents a sharp horizontal thermal gradient. The AAPF is also known as the boundary between the Antarctic and Subantarctic bioprovinces (e.g., Smith and Schnack-Schiel 1990). Endemic radiolarian faunas suggest that Antarctic assemblages are found in the ocean south of the AAPF (Lombardi and Boden 1985; Abelmann et al. 1999).

There are two interpretations on the late Paleogene AAPF condition. One is the relatively stable positioned AAPF (Lazarus and Caulet 1993). The other is the mobile AAPF migrated northwardly in association with the climate change (Weaver 1983; Cooke et al. 2002). Because the migration and position of the AAPF strongly affect the surface circulation pattern and oceanographic characteristics of the Southern Ocean, the change of planktic assemblages in some time intervals may be a very useful proxy in recognizing this hydrographic change. The radiolarian fauna is an important group in the Southern Ocean plankton, and is one of the most appropriate proxies to use in defining oceanographic conditions in the Southern Ocean not only in the modern ocean but also in the Eocene-Oligocene sediments (e.g., Abelmann 1990; Caulet 1991; Takemura 1992; Lazarus and Caulet 1993; Takemura and Ling 1997; Funakawa and Nishi 2005).

In the present paper, we first present the results of a quantitative analysis of the radiolarian assemblages obtained from Site 689 located in the Southern Ocean and then reconstruct the biopro-



TEXT-FIGURE 1
Map of the modern Atlantic Ocean showing ODP Site 689 and other DSDP and ODP sites penetrating late Paleogene radiolarian bearing sediments.

vincial change of the assemblages at this site during the Eocene-Oligocene interval. Finally, we discuss the relationship between bioprovincial changes of radiolarian faunas and the possible migration of the AAPF from the viewpoint of global climate change during the Eocene-Oligocene transition.

MATERIALS AND METHODS

ODP (Ocean Drilling Program) Hole 689B was drilled in the Weddell Sea, South Atlantic (text-figure 1), near the crest of Maud Rise (64°31'S, 03°06'E). Upper Paleogene sediments were recovered from the upper middle Eocene (Chron C18) to upper Oligocene (Subchron C7A) with a continuous paleomagnetic record (Florindo and Roberts 2005). The sediments contain abundant calcareous and siliceous microfossils (Barker et al. 1988). We analyzed 103 samples from Sample 113-689B-8H-5, 50-55cm (69.0 mbsf, Lithologic Unit II) to 16H-7, 30-35cm (148.7 mbsf, Unit II). Unit II is subdivided into the Subunit IIA and IIB. The former consists of the upper Oligocene to upper Miocene diatom nannofossil ooze above 72.1 mbsf, while the latter is composed of middle Eocene to upper Oligocene nannofossil ooze with radiolarians from 72.1 to 149.1mbsf (Barker et al. 1988). Examination of smear slides shows that radiolarian shells are abundant in the top of Subunit IIB above Section 113-689B-10H-5 (87.7 mbsf), Section 113-689B-12H-6 to 13H-2 (108.5-113.6 mbsf), Section 113-689B-13H-6 to 14H-2 (118.1-123.2 mbsf), and Section 113-689B-15H-1 to 15H-5 (129.9-137.4 mbsf) (Barker et al. 1988). Paleogene ice rafted debris was observed in Subunit IIB within Core 113-689B-10H (82.40, 88.88 and 91.30 mbsf; Barker et al. 1988). Sampling intervals range from 25 to 320 cm.

Dried and weighed samples were treated with a solution of 3% hydrochloric acid (HCl). After the reaction ceased, the samples were sieved at 63µm. The residue was cleaned using an approx.

3% hydrogen peroxide (H₂O₂) solution with a small amount of sodium diphosphate decahydrate (Na₄P₂O₇•10H₂O) and then sieved again at 63µm. Dried residue was repeatedly split equally into smaller portions until divided residues contained several hundred to several thousand radiolarian tests, appropriate for mounting on a slide. A split was randomly scattered on a slide, on which thin gum tragacanth was spread. Canada balsam and 22 x 40 mm glass covers were used to mount the tests.

More than 500 radiolarian shells were counted for most samples except for several samples (see next section), in which fragmented radiolarian shells were dominant. We counted all specimens up to the end of the traverse line in which 500 specimens were exceeded. We applied a magnetobiochronologic framework developed by Florindo and Roberts (2005). The Global Polarity Time Scale of Berggren et al. (1995) is used for age calibration of paleomagnetic events. A total of ca.100 species were counted (listed in Funakawa and Nishi 2005). Among them, taxonomic characters of three species groups are revised from Funakawa and Nishi (2005) and are described in Appendix A. Numeric data for twelve selected species (see next section) in this study are given in Appendix B.

RESULTS

Radiolarian preservation

Radiolarian preservation is moderate to very good except for the interval from 96.1 to 108.23 mbsf (text-figure 2). This interval is characterized by the abundant occurrence of fragmented radiolarian shells. In several samples of this interval, orospherid fragments range up to five times as abundant as other radiolarian shells in the fraction larger than 63µm.

To examine radiolarian assemblages in which counts provide comparable accuracy, we exclude samples from this interval in the following discussion.

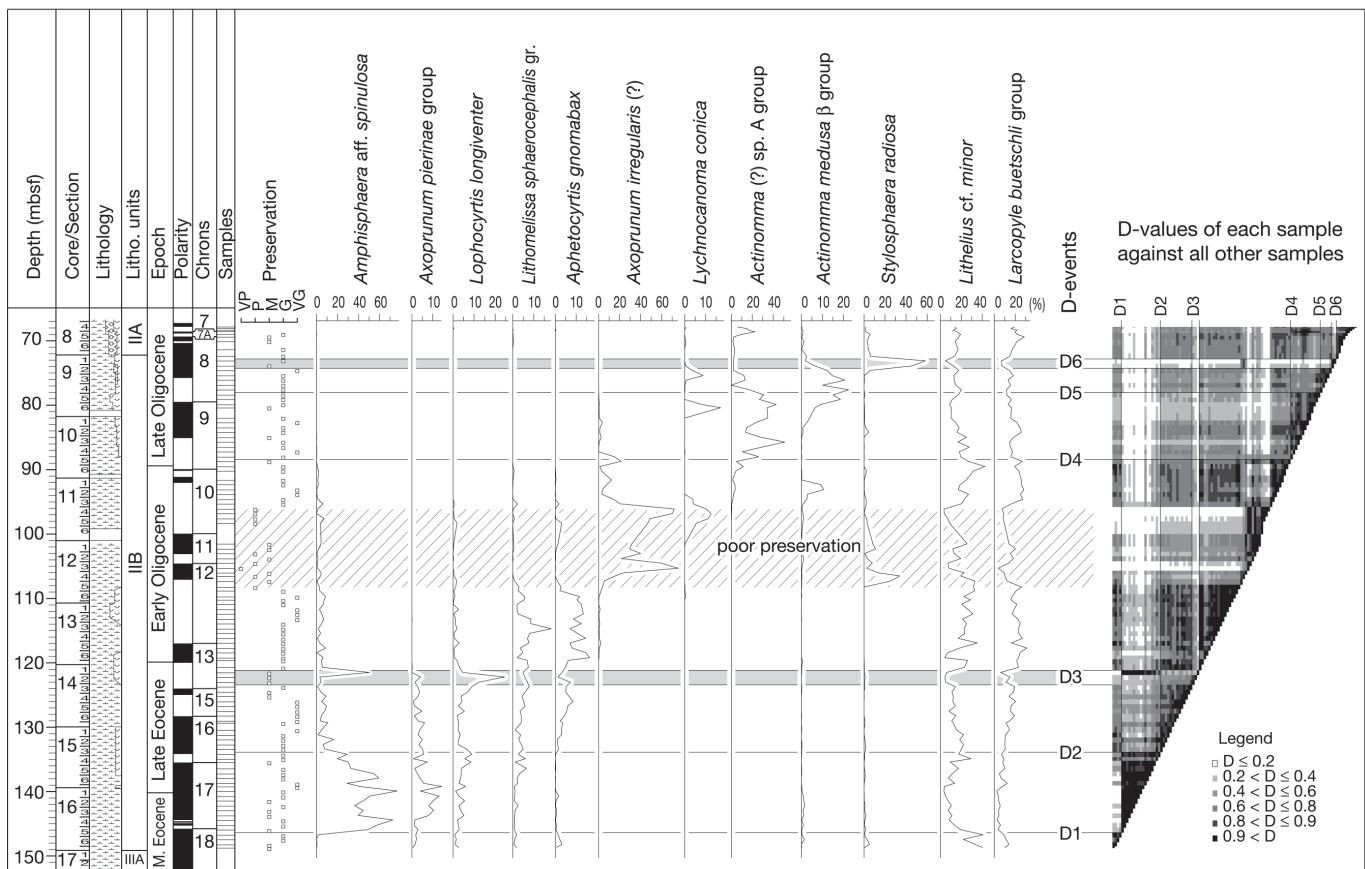
Radiolarian assemblages and faunal abundance change

For the description of radiolarian assemblages, we selected twelve species that continually occur at more than 5% in relative abundance (text-figure 2). Within Chron 18 of the middle Eocene, *Lithelius* sp. cf. *minor* is a dominant species. Across the middle/upper Eocene boundary, the radiolarian assemblage is characterized by the abundant occurrence of *Amphisphaera* sp. aff. *A. spinulosa* between 145.9 and 133.4 mbsf. This species decreases during the upper Eocene where the *Axoprunum pierinae* group, *Lophocyrtis longiventer*, the *Lithomelissa sphaerocephalis* group, *Aphetocyrtis gnomabax*, *L. sp. cf. minor*, and the *Larcopyle buetschlii* group are common species. However, *L. longiventer* and *A. sp. aff. spinulosa* reach sharp abundance peaks at 122.2 and 121.5 mbsf, respectively.

The *L. sphaerocephalis* group, *A. gnomabax*, *L. sp. cf. minor*, and the *L. buetschlii* group are dominant species in the lower Oligocene (117.7 to 108.23 mbsf). In the upper Oligocene, the dominant species are *Actinomma* (?) sp. A group (88.0 to 78.4 mbsf), *Actinomma medusa* β group (79.1 to 75.4 mbsf), and *Stylosphaera radiosa* (74.6 to 72.5 mbsf). *L. cf. minor* and the *L. buetschlii* group also remain dominant in the upper Oligocene.

Degree of overlap

Degree of overlap (D) describes the faunal continuity between two samples ($D_{ij} = \sum P_{ij} P_{ij} / \{ \sum (P_{ij})^2 \}^{1/2} \{ \sum (P_{ij})^2 \}^{1/2}$; where P_{ij} and P_{ji} are products of the proportion species "j" in samples "i" and



TEXT-FIGURE 2

Stratigraphic variation of radiolarian shell preservation and relative abundance changes of selected 12 radiolarian species from the upper middle Eocene to upper Oligocene at Hole 689B. Degree of overlap (D) values for each sample relative to all other samples is also shown in the right-hand panel. D-value events from D1 through D6 are drawn as horizontal lines and grey bars. Shaded area indicates the interval where radiolarian preservation is poor.

“h”). The D-value equals one if all species are present in the same proportion in both samples and approaches zero as fewer species co-exist in sample pairs. Hence, a low-value interval of this index indicates a large faunal turnover. We calculated the D-values for each sample relative to all other samples and expressed the results as a stratigraphic density plot of D-value (text-figure 2).

The D-values between adjacent samples fluctuate between 0.28 and 1.00 (Appendix B). Six faunal turnovers (D1 to D6) are found in the record based on the density plot of D-values (Table 1; text-figure 2). The oldest D-value event (D1) is recorded in the middle Eocene (uppermost Subchron C18n1n) at 145.9-146.7 mbsf where *A. aff. spinulosa* rapidly increases. Turnover D2 is situated in the lower upper Eocene (Subchron C16n2n) at 133.4-134.2 mbsf and results from a decrease of *A. aff. spinulosa*. The D3 turnover event occurs in the uppermost Eocene (Subchron C13r) between 120.7 and 123.7 mbsf. This interval includes a rapid increase of the *L. longiventer* group and a rapid increase followed closely by a rapid decline of *A. sp. aff. spinulosa*. In the upper Oligocene, three D events are recognized, one at 88.0-88.7 mbsf (D4) near the lower/upper Oligocene boundary (lower Subchron C9r) and one at 77.6-78.4 mbsf (D5, Subchron C8r). These events correspond to the rapid increase and the subsequent decrease of the *Actinomma* (?) sp. A group, respectively (Table 1; text-figure 2). The uppermost turnover event occurs at 72.4-74.6 mbsf (D6: Subchron C8n2n), where *S. radiosa* reaches its peak

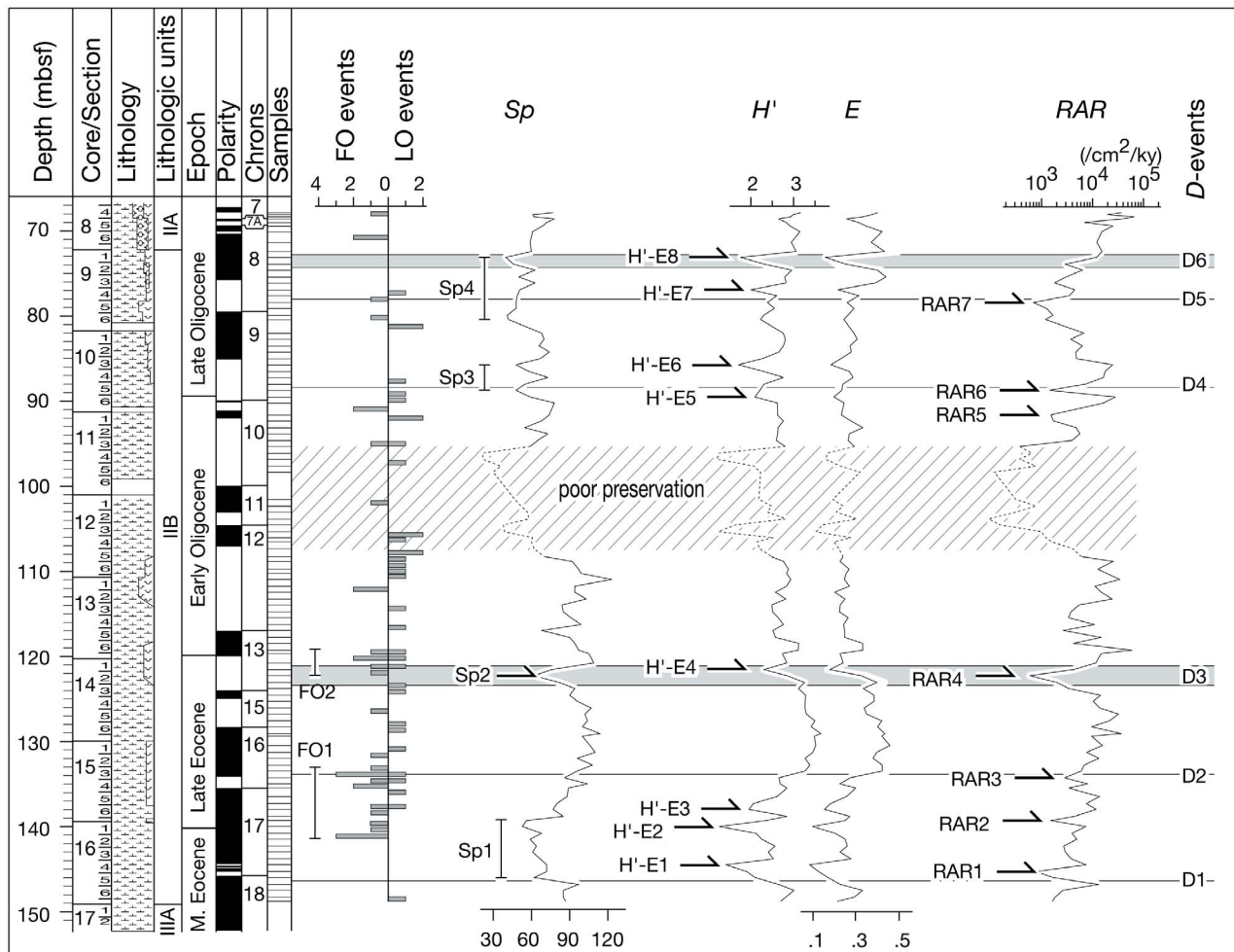
abundance, coincident with a rapid decrease in the *Actinomma medusa* β group.

Pattern of FO and LO events

Funakawa and Nishi (2005) reported a total of 65 individual species radiolarian events in the studied interval, including the 31 first occurrence (FO) and 34 last occurrence (LO) events (text-figure 3). The FO events are commonly found during the Eocene, particularly two distinct intervals of FO1 (14 events, 132.7-141.4 mbsf, Subchrons C16n to C17n1n) and FO2 (5 events, 119.2-122.2 mbsf, Subchrons C13n to C13r). FO events are fewer during the Oligocene. The LO events are dispersed more evenly throughout the studied interval (text-figure 3).

Species richness, diversity and equitability

For each sample, species richness, Shannon-Wiener diversity, and equitability were calculated (text-figure 3). Species richness (Sp) is the number of species in each sample. The Sp-value, ranging from 22 to 123, is generally high in the Eocene through the lower lower Oligocene and low in the upper lower to upper Oligocene (text-figure 3). There are four low-Sp-value intervals (Sp1 to Sp4) in the studied section. Intervals Sp1 and Sp2 occur across the middle/upper Eocene boundary from 139.2 to 145.9 mbsf (Chron C17) between the D1 and D2 events and in the uppermost Eocene at 122.2 mbsf (Subchron C13r) within the D3 event, respectively. In the upper Oligocene, Sp3 and Sp4 are recognized from 85.7 to 88.7 mbsf (Subchron C9r) across the D4



TEXT-FIGURE 3

Stratigraphic variations of the number of FO and LO events, species richness (Sp), diversity (H'), equitability (E), and radiolarian accumulation rate (RAR). All Sp, H', E, and RAR events and D-value events are indicated.

event and from 73.1 to 80.4 mbsf (Subchrons C8n to C9n) across the D5 and D6 events, respectively (text-figure 3).

The Shannon-Wiener index (H') describes species diversity, taking into account the relative proportion of each species within a sample ($H' = -\sum P_i \ln P_i$; where P_i is the proportion of each species). Equitability (E) is a measure of the evenness of the species distribution within a sample. This index is calculated using the Shannon-Wiener diversity and the species number ($E = e^{H'}/S$; where S is the number of species in counted area and H' is Shannon-Wiener diversity). Equitability equals one if all species are present in the same proportion and approaches zero when one species dominates the fauna.

Diversity and equitability are covariant throughout the studied section (text-figure 3). The H'- and E-values range from 1.21 to 3.63 and 0.08 to 0.46, respectively (Appendix B). Low H'-E-values are recognized at eight levels (H'-E1 to H'-E8 events). Events H'-E1 to H'-E3 are found in the middle to upper Eocene within Subchron C17n at 144.4 mbsf, 139.9 mbsf, and 137.9 mbsf, respectively. They are included in the interval between the D1 and D2 events. The H'-E4 event occurs in the uppermost Eocene (Subchron C13r) at 121.5 mbsf within the D3 event. In the upper Oligocene, the H'-E5 and H'-E6 events are located near the D4 event at 89.5 and 85.7 mbsf (Subchron C9r), respectively. The H'-

E7 and H'-E8 events are bound between the D5 and D6 events at 76.9 (Subchron C8r) and 73.1 mbsf (Subchron C8n), respectively (text-figure 3).

Radiolarian accumulation rate

The radiolarian accumulation rate is the number of shells deposited on one square cm in one thousand years ($RAR = LSR \times DBD \times n_R \times 1000$; where n_R is the number of radiolarian specimens per one mg of dry sediment; DBD is dry bulk density in grams per cubic cm calculated from wet bulk density (WBD) and porosity data by the formula (Barker et al. 1988): $DBD = WBD - 1.026 \times \text{porosity}/100$).

The RAR-value ranges from 0.04-7.0 ($\times 10^4/\text{cm}^2/\text{ky}$). The low-RAR-value intervals are labeled as RAR1 through RAR7 (text-figure 3). From the middle to upper Eocene, RAR1 to RAR3 are observed between the D1 and D2 events at 145.2 mbsf (Subchron C17r), 139.2 mbsf (Subchron C17n), and 134.2 mbsf (Subchron C16r), respectively. Around the Eocene/Oligocene boundary, a low-RAR-value horizon is recognized at 122.2 mbsf (RAR4; Subchron C13r) within the D3 event. Around the lower/upper Oligocene boundary, RAR5 and RAR6 are located at 91.6 (Subchron C10n1n) and 88.7 mbsf (Subchron C9r), respectively, near the D4 event. The RAR7 event (Subchron C8r) occurs at 78.4 mbsf (text-figure 3), close to the D5 event.

TABLE 1

D-value events and major radiolarian faunal changes in ODP Hole 689B.

D-event	core-section, interval	mbsf	Characteristics in faunal change
113-689B-			
6	9H-1, 30-35 cm/	72.4/	peak of <i>Stylosphaera radiosa</i> (63 %);
	9H-2, 100-105 cm	74.6	<i>Actinomma medusa</i> β gr. (15 \rightarrow 3 %)
5	9H-4, 100-105 cm/	77.6/	<i>Actinomma</i> sp. A gr. (32 \rightarrow 18 %)
	9H-5, 30-35 cm	78.4	
4	10H-5, 30-35 cm/	88.0/	<i>Actinomma</i> sp. A gr. (5 \rightarrow 27 %)
	10H-5, 100-105 cm	88.7	
3	13H-5, 130-135 cm/	117.7/	peak of <i>Amphisphaera</i> aff. <i>spinulosa</i> (50 %)
	14H-2, 50-55 cm	122.2	
2	15H-3, 50-55cm/	133.4/	<i>Amphisphaera</i> aff. <i>spinulosa</i> (29 \rightarrow 8 %)
	15H-3, 130-135 cm	134.2	
1	16H-5, 50-55 cm/	145.9/	<i>Amphisphaera</i> aff. <i>spinulosa</i> (2 \rightarrow 48 %)
	16H-5, 130-135 cm	146.7	

The fluctuation pattern of RAR-values is basically correlated with those of species richness, diversity, and equitability (text-figure 3). However, the pattern of RAR is not consistent with that of diversity-equitability in the upper Oligocene (text-figure 3).

Bioprovince indexes of radiolarian species

To reconstruct the bioprovinces of radiolarian faunas from low- to high-latitudes during the Eocene-Oligocene interval, we examined the distribution of the twelve selected dominant species (text-figure 2, Appendix B). The distribution patterns are based on the observation of sediment samples from Atlantic DSDP and ODP sites (text-figure 1, Appendix C), which are deposited in the DSDP/ODP Micropaleontology Reference Center, National Museum of Nature and Science, Tokyo, and Utsunomiya University, Japan.

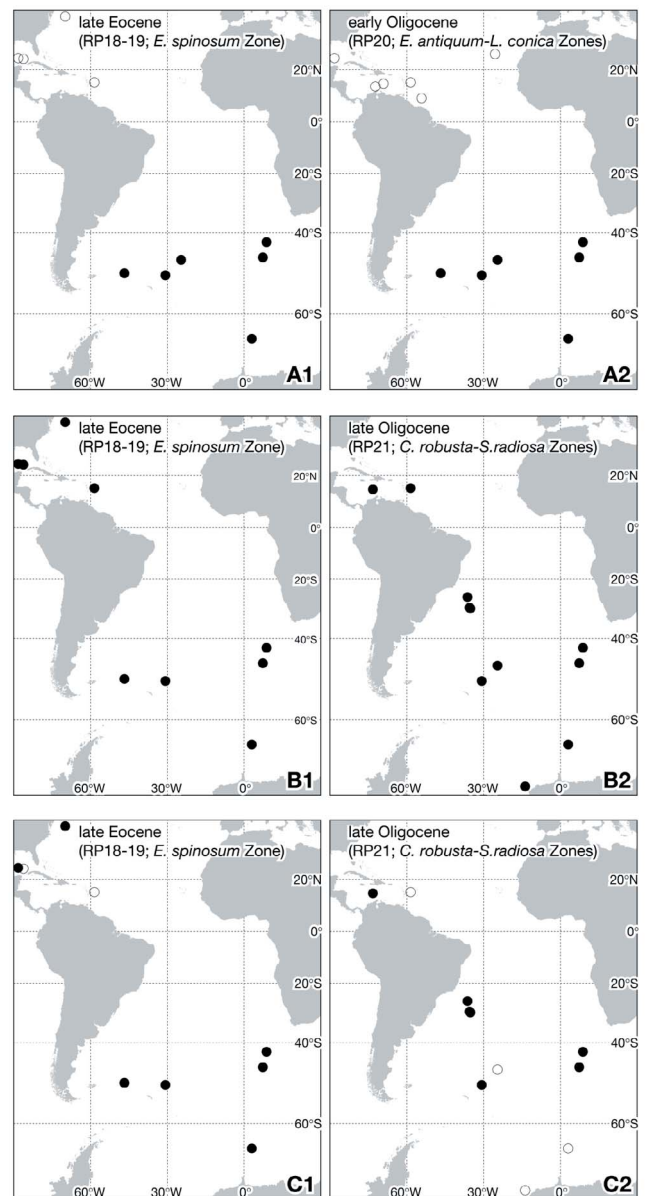
To summarize the distribution pattern of radiolarians in the Atlantic Ocean, eight species (*Lychnocanoma conica*, the *Actinomma medusa* β group, *Axoprunum irregularis* (?), *Amphisphaera* sp. aff. *spinulosa*, *Lophocyrtis longiventer*, the *Lithomelissa sphaerocephalis* group, the *Actinomma* (?) sp. A group, and *Aphetocyrtis gnomabax*) are recognized in southern high latitudes throughout their stratigraphic ranges (text-figure 4A), and designated Antarctic species (AN). Three species (*Stylosphaera*

radiosa, *Lithelius* cf. *minor*, and the *Larcopyle buetschlii* group) are widely distributed from low latitude to the Antarctic margin (text-figure 4B), and are grouped as cosmopolitan species (CP). Although the *Axoprunum pierinae* group occurs from low to high latitudes, the last occurrence in high latitude is significantly earlier than in low to mid latitudes (text-figure 4C; Appendix C). Therefore this group is classified as low to high-latitude species (LH).

DISCUSSION

Bioprovinciality based on quantitative analysis

Based on quantitative analysis of radiolarian assemblages using the degree of overlap index (D), six faunal turnovers are recognized during the late middle Eocene through late Oligocene interval at ODP Site 689 on Maud Rise. One of the most characteristic changes during these faunal turnovers is an increasing/decreasing trends in the AN group. The D1, D3, and D4 turnover events mark rapid increases in the AN group, while the other

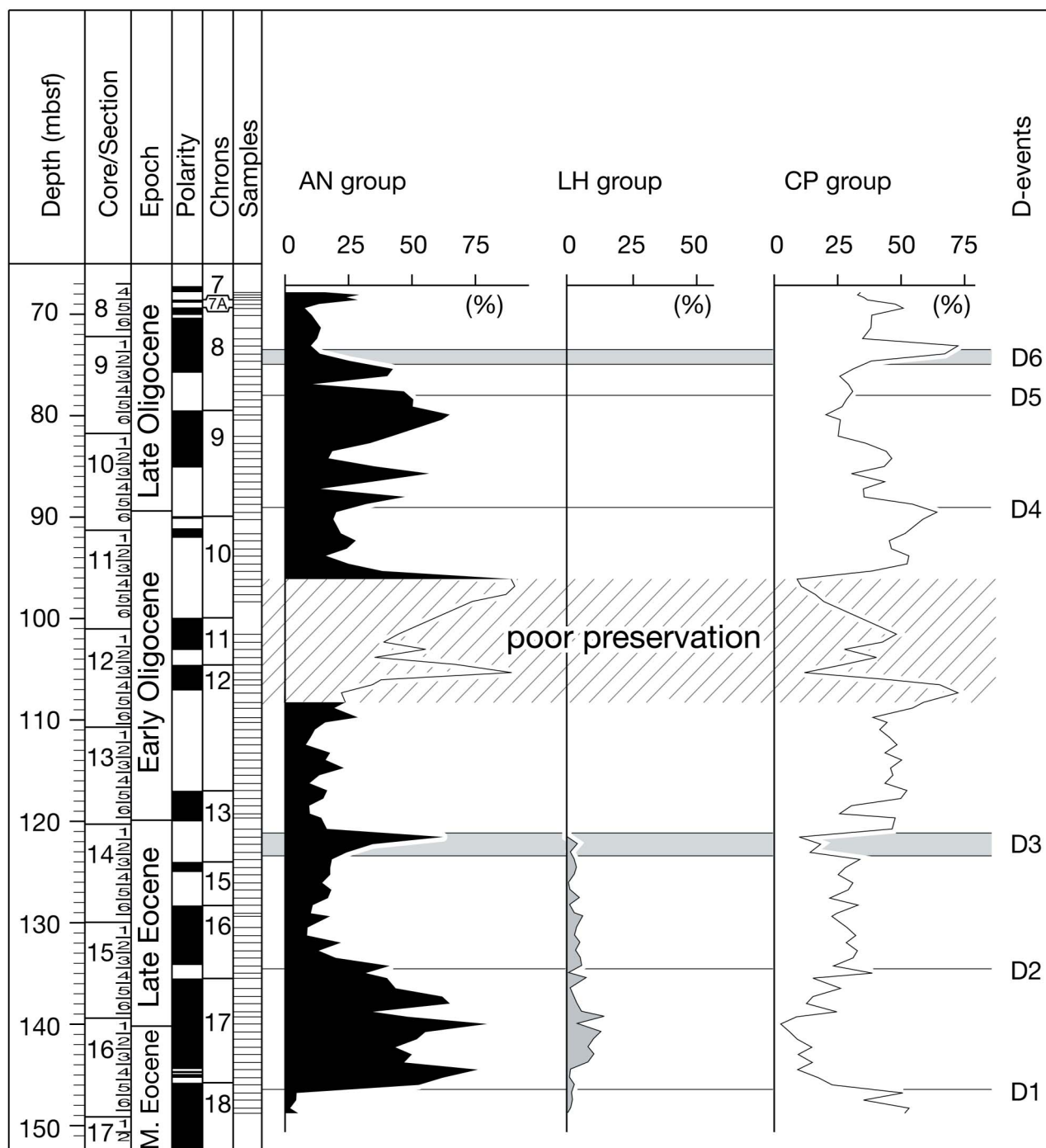


TEXT-FIGURE 4

Eocene and Oligocene paleobiogeographic distribution of three radiolarian species in DSDP and ODP drill sites in the Atlantic ocean. *Amphisphaera* aff. *spinulosa* (AN species), *Stylosphaera radiosa* (CP species), and *Axoprunum pierinae* group (LH species) are shown in text-figs. 4A, 4B, and 4C, respectively.

events (D2, D5, and D6) correspond to rapid decreases in the AN group (text-figure 5). In addition, species diversity indexes (Sp, H', and E) and RAR also drop at or near each D-value-event (text-figure 3).

In the modern Southern Ocean, the Antarctic and Subantarctic bioprovinces are bounded by the Antarctic Polar Front (e.g., Smith and Schnack-Schiel 1990). The water column in the Antarctic region is characterized by an extremely low vertical thermal gradient, where the radiolarian faunas are dominated

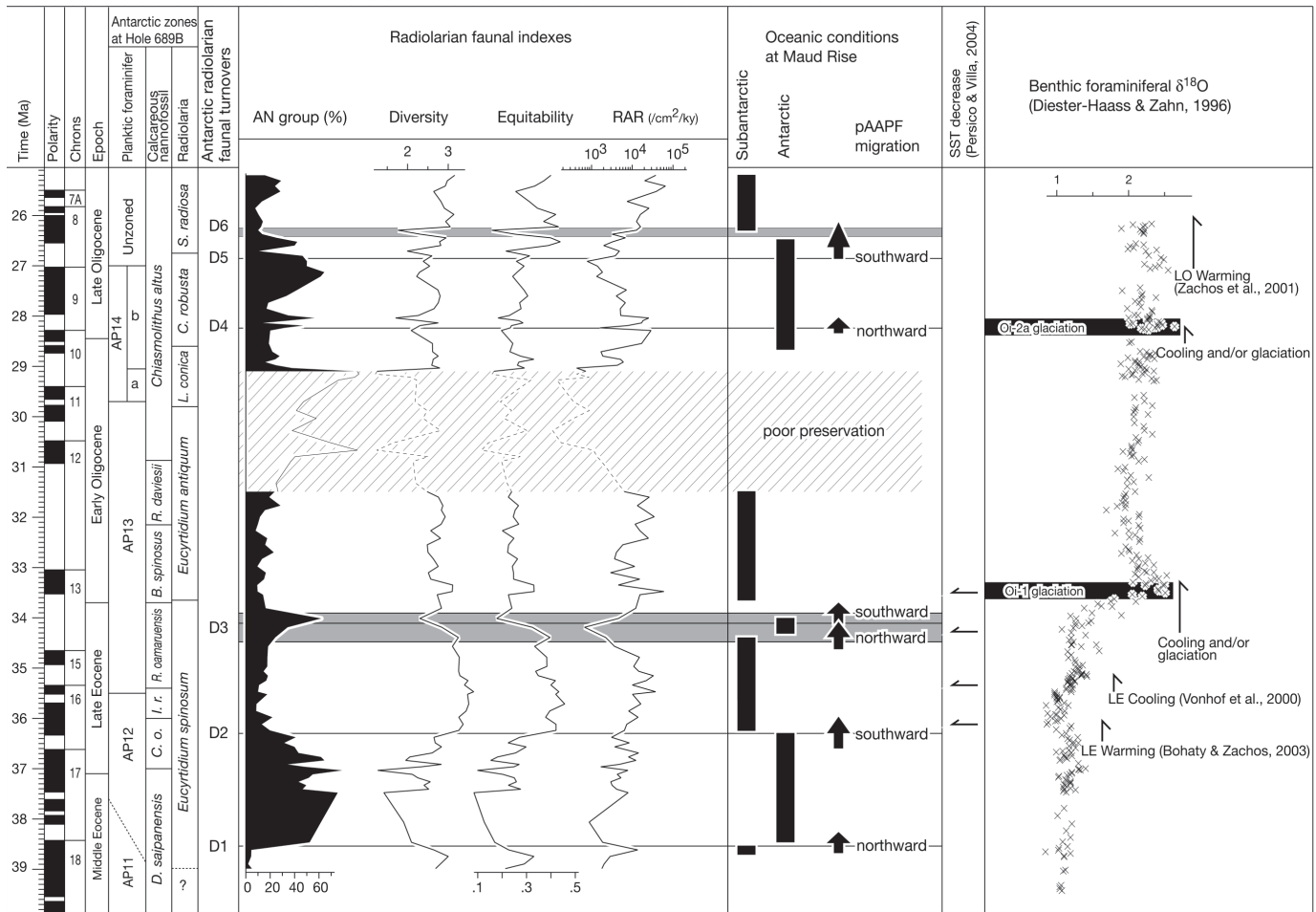


TEXT-FIGURE 5
 Stratigraphic variation of the abundance of AN, LH, CP groups at Hole 689B. D-value events and an interval with poorly preserved radiolarians are indicated by horizontal lines/bars and shaded area, respectively.

by over 50% Antarctic species (Abelmann et al. 1999) with low species diversity (Boltovskoy 1987). On the other hand, the water column in the Subantarctic region represents a larger vertical thermal gradient, and the faunas show higher species diversity than the Antarctic fauna (Boltovskoy 1987). Hence, the Antarctic-dominant radiolarian fauna with low-diversity indicates a water column environment corresponding to modern Antarctic condition, while relatively high diversity with less common Antarctic species implies a Subantarctic condition. Furthermore, the D events are characterized by rapid changes in the Antarctic assemblage and sudden drops of species diversity and radiolarian

accumulation rates. These characteristics of the fauna around the D events are thought to represent the frontal condition between Antarctic and Subantarctic regions (text-figure 6). Here, we name this frontal condition as the proto -Antarctic Polar Front (pAAPF).

One alternate interpretation for the Paleogene radiolarian faunal changes in the Southern Ocean has been pointed out by Lazarus and Cautlet (1993). In their model, radiolarian faunal changes occurred in one water mass and it was gradual rather than abrupt. It seems that the continuous occurrence of Antarctic species in



TEXT-FIGURE 6

Temporal change of the AN group, diversity, equitability, and radiolarian accumulation rate. Oceanic conditions and possible front migration pattern suggested by radiolarian assemblage are shown in the middle column. Surface water cooling from nanofossil assemblage analysis by Persico and Villa (2004) and benthic foraminiferal δ¹⁸O curve by Diester-Haass and Zahn (1996) are also drawn.

the studied section (text-figure 6) supports their model. However, Antarctic species occur in the Subantarctic region and a conspicuous abundance change of them corresponds with the front (Lombardi and Boden 1985; Abelmann et al. 1999). This fact and the abrupt faunal change shown by sudden drop of D-value suggest that repeated faunal turnovers between the Antarctic-dominant fauna and the fauna with less common AN group are caused by the migrations of front system. Further study at other sites in Southern Ocean are needed to confirm this hypothesised migration pattern.

Paleoceanographic change in Maud Rise

The abundance changes of the AN group in the studied section indicate bioprovincial changes of radiolarian assemblages linked with the migration of the pAAPF back and forth across the Maud Rise site during the late middle Eocene through late Oligocene (text-figure 6). The D1 and D4 events are associated with rapid increases in the AN assemblage. The shift from Subantarctic to Antarctic bioprovinces occurred at ~38.5 Ma and at ~28.3 Ma. These changes are probably caused by the northward migration of the pAAPF over the Maud Rise. In contrast, the subsequent decrease of the AN assemblage at the D2, D5, and D6 events suggests that the Antarctic bioprovince return to Subantarctic condition due to the southward migration of the pAAPF over Maud Rise at ~36.3 Ma, 26.9 Ma, and 26.2 Ma. The D3 event is a short interval, spanning from 34.5 to 33.9 Ma in the lat-

est Eocene. Here, the AN assemblage rapidly increases and then decreases. This faunal change could represent a northward, followed closely by a southward migration of pAAPF over Maud Rise (text-figure 6).

The environmental history of cooling/warming of the Antarctic bottom water has been documented by the δ¹⁸O record measured in benthic foraminiferal shells obtained from Hole 689B (Diester-Haass and Zahn 1996) (text-figure 6). Among the sharp increases events in the AN group (D1, D3, and D4), the D4 event (~28.3 Ma) corresponds to the Oi-2a positive isotope shift event near the early/late Oligocene boundary (Miller et al. 1991; Zachos et al. 1993). The early part of the D3 event (34.5-34.1 Ma) is correlated with the beginning of a positive shift of δ¹⁸O below the Oi-1 glaciation or a decrease of sea surface temperature based on the change of nanofossil assemblages (Miller et al. 1991; Zachos et al. 1993; Persico and Villa 2004). The latter part of this event (34.1-33.9 Ma) is located just below the peak of Oi-1 glaciation and corresponds to the rapid increase in δ¹⁸O. The positive shift of δ¹⁸O was caused by the decrease in bottom water temperature, and by the increase in volume of trapped water on the Antarctic continent. The development of Antarctic glaciers needs not only cold condition for freezing of water on the continent but also a humid air supply to the continent. The southward migration of the pAAPF at the late part of D3 event (34.1-33.9 Ma) suggests that the southward advance of warm surface water

might contribute to the humid condition on the continent. However, the oldest sharp increase in the AN group (D1, ~38.5 Ma) is not identical with the positive isotope shift previously reported in many isotope studies (text-figure 6). On the other hand, two sharp decreases in the AN group are recognized in the late Eocene (D2, ~36.3 Ma) and late Oligocene (D5 to D6, 26.9-26.2 Ma). These correspond to the late Eocene warming (Bohaty and Zachos 2003) and the late Oligocene warming (Zachos et al. 2001; Villa and Persico 2006), respectively. Thus, the increase of the AN group suggests the northward migration of pAAPF and the subsequent faunal change from the Subantarctic to Antarctic faunas associated with global cooling. In contrast, the decrease of the AN group results from the southward migration of the pAAPF and a return from Antarctic conditions to Subantarctic ones. This change could be caused by global warming or interglacial conditions.

CONCLUSION

In ODP Site 689 on Maud Rise, in the Weddell Sea sector of the South Atlantic, six radiolarian faunal turnover events are identified in the upper middle Eocene through upper Oligocene: D1 at ~38.5 Ma (Subchron C18n1n), D2 at ~36.3 Ma (Subchron C16n2n), D3 from 34.5 to 33.9 Ma (Subchron C13r), D4 at ~28.3 Ma (Subchron C9r), D5 at ~26.9 Ma (Subchron C8r), and D6 from 26.4 to 26.2 Ma (Subchron C8n2n). These turnover events mark rapid increases or decreases in the antarctic endemic (AN) group, and are concurrent with drastic drops of equitability-diversity and radiolarian accumulation rate. These faunal characteristics suggest that radiolarian faunal turnovers are related to the migration of a proto-Antarctic Polar Front (pAAPF) and the associated shift in bioprovinces between the Antarctic and Subantarctic regions. Three intervals (D1-D2, D3, and D4-D5) are characterized by the dominance of the AN group and low species diversity. These characteristics suggest that faunal assemblages changed from Subantarctic to Antarctic bioprovinciality at D1, the beginning of D3, and D4 events. This faunal change could be related with the northward movement of the pAAPF that passed over the drilling site on Maud Rise. In contrast, the abundance of the AN group become less common in the D2-D3 and upper

D5 intervals. Faunal changes from the Antarctic to Subantarctic assemblages occurred at the D2 and D5 events and this change would be explained by the southward migration of pAAPF. The events marking an increase in the AN group or the northward migrations of the pAAPF occurred at 34.5-34.1 Ma and ~28.3 Ma and coincide with the beginning of Oi-1 glaciation around the Eocene-Oligocene boundary and Oi-2a event near the early/late Oligocene boundary, respectively. The events marking a decrease in the AN group or the southward migration of the pAAPF are observed at ~36.3 Ma and 26.9-26.2 Ma and correspond to late Eocene and late Oligocene warming, respectively. Thus global climate change during the Eocene-Oligocene transition is an important factor controlling abundance change in the AN group and is associated with the latitudinal migration of the frontal zone between the Antarctic and Subantarctic regions of the Southern Ocean.

ACKNOWLEDGMENTS

Samples from ODP Hole 689B were supplied through the assistance of the U.S. National Science Foundation, and those from other DSDP and ODP sites were provided through the assistance of the DSDP/ODP Micropaleontology Reference Centers at The National Science Museum and Utsunomiya University, Japan. We express sincere thanks to Theodore C. Moore and Annika Sanfilippo for their critical reviews on our manuscript to improve it. We acknowledge Toyosaburo Sakai for valuable discussion. We also wish to thank David Lazarus and Atsushi Takemura for helpful and critical comments on the manuscript. Some of the work was carried out at the Micropaleontology Reference Center, Utsunomiya University, Japan.

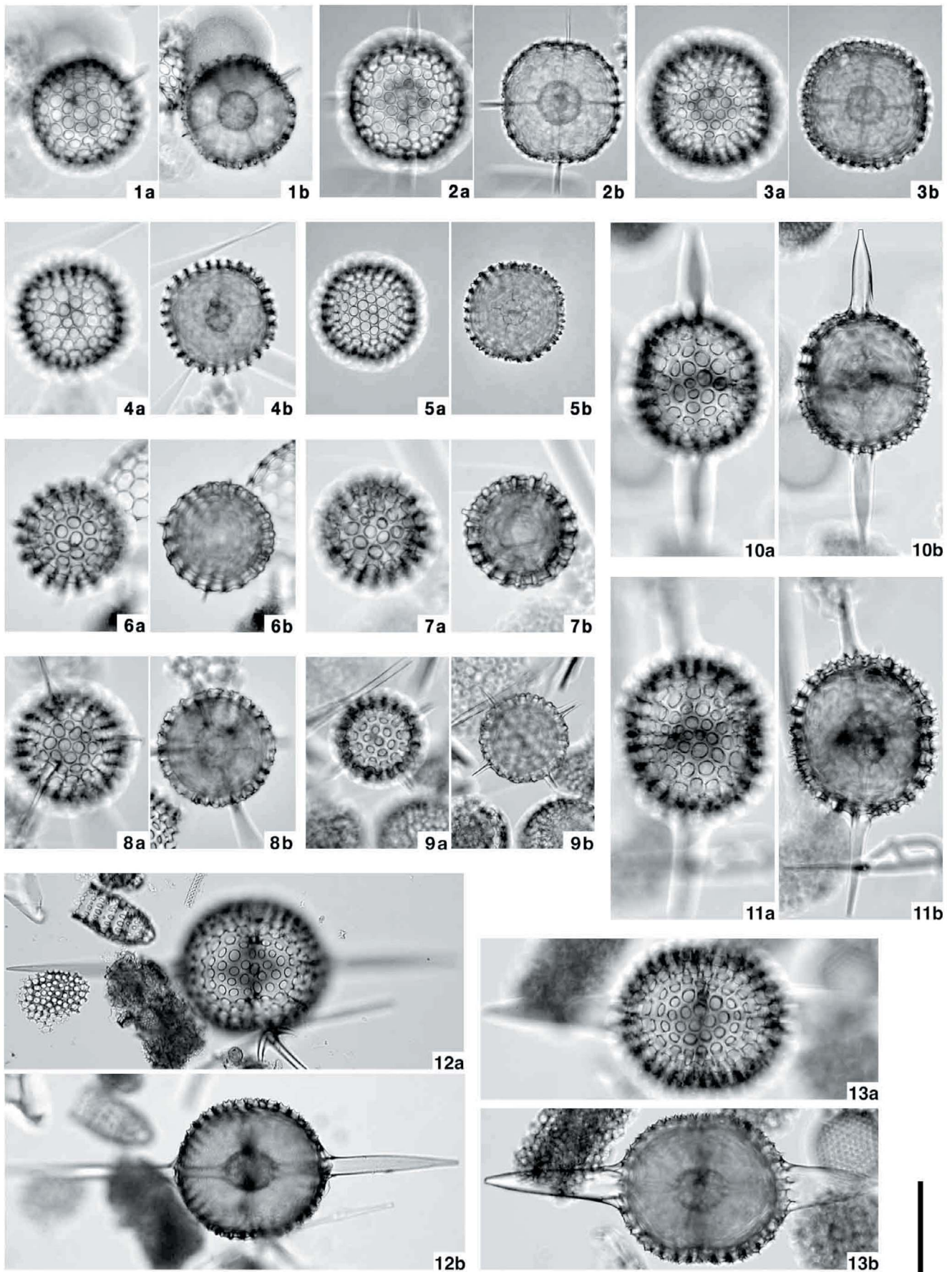
REFERENCES

- ABELMANN, A., 1990. Oligocene to middle Miocene radiolarian stratigraphy of southern high latitudes from Leg 113, Sites 689 and 690, Maud Rise. In: Barker, P. F., Kennett, J. P., et al., Eds., *Proceedings of Ocean Drilling Program, Scientific Results*, vol. 113: 675-708. College Station, Texas: Ocean Drilling Program.
- ABELMANN, A., BRATHAUER, U., GERSONDE, R., SIEGER, R.

PLATE 1

Transmitted microphotographs of selected radiolarians from upper Paleogene sediments from several Atlantic DSDP and ODP sites. Specimens are located using England Finder coordinates (No. 5077-E by Iwamoto Mineral, Japan; radiolarian slide label positioned to the left). Scale bar is 100µm.

- | | |
|---|--|
| <p>1-5 <i>Actinomma medusa</i> β group; 1, Sample 113-689B-13H-2, 130-135cm, K46/0, early Oligocene <i>Eucyrtidium antiquum</i> Zone; 2, Sample 113-689B-11H-2, 100-105cm, S46/4, early Oligocene <i>Lychnocanoma conica</i> Zone; 3, Sample 113-689B-9H-3, 100-105cm, G40/0, late Oligocene <i>Stylosphaera radiosa</i> Zone; 4, Sample 113-689B-9H-1, 30-35cm, N34/0, late Oligocene <i>Stylosphaera radiosa</i> Zone; 5, Sample 113-689B-9H-1, 30-35cm, W23/2, late Oligocene <i>Stylosphaera radiosa</i> Zone.</p> <p>6-8 <i>Actinomma</i> (?) sp. A group; 6, Sample 71-513A-17-5, 29-34cm, G10/1, late Oligocene <i>Stylosphaera radiosa</i> Zone; 7, Sample 113-689B-8H-5, 10-15cm, K32/1, late Oligocene <i>Stylosphaera radiosa</i> Zone; 8, Sample 113-</p> | <p>689B-9H-4, 20-25cm, R32/0, late Oligocene <i>Stylosphaera radiosa</i> Zone.</p> <p>9 <i>Hexacantium</i> sp., Sample 113-689B-10H-6, 30-35cm, L46/0, late Oligocene <i>Clinorhabdus robusta</i> Zone.</p> <p>10-13 <i>Axoprunum pierinae</i> group; 10, Sample 113-689B-14H-6, 130-135cm, Q32/2, late Eocene <i>Eucyrtidium spinosum</i> Zone; 11, Sample 113-689B-14H-6, 130-135cm, O27/1, late Eocene <i>Eucyrtidium spinosum</i> Zone; 12, Sample 177-1090B-36X-3, 20-26cm, W27/3 (MRC ID number: 003111), late Eocene <i>Eucyrtidium spinosum</i> Zone; 13, Sample 95-612-18-5, 75-84cm, J25/4 (MRC ID number: 002512), late Eocene Zone RP18.</p> |
|---|--|



Radiolarian zones	Leg-Core-Section, Interval (cm)	Depth (mbsf)	Preservation	Radiolarian species												Sp	H'	E	D	RAR
				<i>Actinomma meudae</i> f. gr.	<i>Actinomma</i> sp. A gr.	<i>Amphisphaera</i> aff. <i>spinulosa</i>	<i>Aphelocypris</i> <i>gnomabax</i>	<i>Apopurum irregularis</i> (?)	<i>Apopurum pleinae</i> gr.	<i>Larocypile buetschlii</i> gr.	<i>Lithelius</i> cf. <i>minor</i>	<i>Lithomelissa sphaerocephalis</i> gr.	<i>Lophocypris longiventris</i>	<i>Lychnocanoma conica</i>	<i>Stylosphaera radiosa</i>					
Stylosphaera radiosa	113-689B-8H-4, 85-90cm	67.85	VG	0.5	6.1						19.2	12.9	0.0	0.6	1.4	77	3.16	0.40	0.91	38110
	113-689B-8H-4, 110-115cm	68.1	G	0.7	15.6						15.8	14.7		0.4	1.8	61	2.98	0.37	0.94	20300
	113-689B-8H-4, 135-140cm	68.35	M	0.7	16.8						21.9	10.9	0.2	0.0	1.4	62	2.93	0.33	0.96	64970
	113-689B-8H-5, 10-15cm	68.6	M	0.7	23.3	0.0					19.7	15.5		0.0	0.0	78	2.64	0.26	0.90	39110
	113-689B-8H-5, 50-55cm	69	G	0.7	10.1	0.1					21.9	19.0	0.1	0.0	6.6	72	2.82	0.31	0.92	7490
	113-689B-8H-5, 90-95cm	69.4	M	0.2	2.3						29.3	17.0	0.2	0.2	4.6	69	2.91	0.34	0.96	25980
	113-689B-8H-6, 10-15cm	70.1	M	1.3	1.6						21.9	13.4	0.4	0.5	3.2	61	3.14	0.42	0.92	15940
	113-689B-8H-6, 135-140cm	71.35	G	0.2	3.3						17.0	16.4		4.5	59	2.94	0.37	0.86	12750	
	113-689B-9H-1, 30-35cm	72.4	G	2.6	2.8						14.5	12.9		6.8	60	3.05	0.43	0.42	16050	
	113-689B-9H-1, 100-105cm	73.1	G	1.9	2.2						6.2	3.3		62.6	40	1.76	0.16	0.97	12640	
	113-689B-9H-2, 30-35cm	73.9	M	6.7	1.9						6.8	11.7		0.5	48.9	46	2.32	0.25	0.52	3190
	113-689B-9H-2, 100-105cm	74.6	VG	12.7	2.2						14.1	17.1		3.9	6.4	63	2.95	0.40	0.86	6810
113-689B-9H-3, 30-35cm	75.4	G	15.2	12.5			0.0			18.1	12.0		9.1	0.2	50	2.79	0.44	0.93	3300	
113-689B-9H-3, 100-105cm	76.1	G	21.4	13.7			0.0			12.8	12.4		0.7	0.4	63	2.82	0.39	0.81	1990	
113-689B-9H-4, 30-35cm	76.9	G	10.4							15.4	14.0		0.2		51	1.99	0.22	0.78	4850	
113-689B-9H-4, 100-105cm	77.6	G	23.3	17.8			0.0			11.2	19.9		0.2		49	2.60	0.31	0.90	3810	
113-689B-9H-5, 30-35cm	78.4	G	15.7	32.1			0.2			11.5	16.5		0.8	0.8	48	2.38	0.26	0.97	780	
113-689B-9H-5, 100-105cm	79.1	G	19.3	27.7			0.3			16.1	10.5				48	2.55	0.29	0.90	1400	
113-689B-9H-6, 30-35cm	79.9	G	9.4	44.3			0.6			12.9	7.6		8.6	0.3	41	2.30	0.26	0.96	1860	
Cinorhabdus robusta	113-689B-9H-6, 80-85cm	80.4	M	6.8	35.4			0.4		16.4	9.4		17.7	0.4	42	2.22	0.24	0.91	1330	
	113-689B-10H-1, 30-35cm	82	G	3.9	35.9			0.6		15.4	9.2		0.0	0.6	68	2.75	0.29	0.92	7220	
	113-689B-10H-1, 100-105cm	82.7	VG	2.7	24.3			3.6		21.9	13.8		0.4	0.4	70	2.80	0.31	0.95	4040	
	113-689B-10H-2, 30-35cm	83.5	G	0.7	15.1			1.3		24.8	17.4		1.8	0.6	2.76	2.62	0.27	0.93	6790	
	113-689B-10H-2, 100-105cm	84.2	G	0.8	14.0		0.0	1.0		27.6	15.3		4.7	74	2.65	0.28	0.88	5080		
	113-689B-10H-3, 30-35cm	85	M	0.2	29.3	0.2		2.4		18.4	25.1	0.0			67	2.27	0.23	0.91	5200	
	113-689B-10H-3, 100-105cm	85.7	G	52.8		0.0	0.5			14.4	16.2				48	1.70	0.18	0.89	25530	
	113-689B-10H-4, 30-35cm	86.5	G	0.2	30.0	0.2	0.2			15.2	27.9		0.2	0.2	58	2.30	0.27	0.85	18350	
	113-689B-10H-4, 100-105cm	87.2	VG	11.0	0.2	0.0	0.0			17.3	17.7		0.2	0.2	73	2.75	0.29	0.77	17070	
	113-689B-10H-5, 30-35cm	88	G	0.2	27.0	0.2	14.9			15.6	19.2		0.2	0.2	55	2.30	0.24	0.79	7660	
	113-689B-10H-5, 100-105cm	88.7	M	5.0		0.7	0.0	2.1		27.2	27.0				48	2.21	0.23	0.82	1600	
	113-689B-10H-6, 30-35cm	89.5	G	11.8	0.7	0.0	1.2			19.5	44.2	0.1			59	2.09	0.20	0.96	28960	
113-689B-10H-6, 100-105cm	90.2	G	0.2	4.5	1.9	0.2	2.8		23.8	32.1	0.7	0.0	2.6	78	2.61	0.24	0.94	17020		
Lychnocanoma conica	113-689B-11H-1, 30-35cm	91.6	G	0.2	1.3	1.1	0.4	12.2		26.3	25.0	0.2	0.2	0.2	74	2.61	0.23	0.93	1700	
	113-689B-11H-1, 100-105cm	92.3	G	9.5	3.6	1.7	0.1	7.7		26.2	18.6	0.1	0.2	0.2	68	2.75	0.28	0.98	1890	
	113-689B-11H-2, 30-35cm	93.1	VG	11.1	3.9	0.2	0.0	3.6		28.8	16.4		0.2	0.2	55	2.63	0.33	0.92	5130	
	113-689B-11H-2, 100-105cm	93.8	VG	3.1	2.1	0.3	0.2	2.9		25.3	27.2		0.5	0.5	73	2.62	0.27	0.93	6070	
	113-689B-11H-3, 30-35cm	94.6	G	0.8	14.0			13.8		27.6	22.8	0.2	4.1	2.1	65	2.59	0.26	0.92	4320	
	113-689B-11H-3, 100-105cm	95.3	G	0.8	0.4	6.1	1.9	20.2		16.2	20.0	2.3	0.6	4.2	2.3	59	2.79	0.29	0.67	430
	113-689B-11H-4, 30-35cm	96.1	P	0.2	0.5	1.2		70.8		6.5	1.9	0.2	10.6	1.0	22	1.25	0.17	1.00	720	
	113-689B-11H-4, 100-105cm	96.8	P	0.8	0.3			69.2		8.4	2.2		0.3	13.0	22	1.21	0.16	0.98	430	
	113-689B-11H-5, 30-35cm	97.6	P	1.1		7.2	0.3	48.2		7.8	5.8	0.8	0.6	11.6	2.8	36	2.07	0.23	0.98	870
	113-689B-11H-5, 100-105cm	98.3	P	0.6		3.8	3.2	46.2		9.0	7.7		1.9	5.8	3.2	30	2.22	0.32	0.85	140
	113-689B-12H-1, 50-55cm	101.5	M			4.2	1.4	31.0		13.6	25.7	0.4	0.3	0.1	9.1	47	2.18	0.19	0.92	360
	113-689B-12H-1, 130-135cm	102.3	M			1.8	0.5	28.9		20.3	10.8	0.5	0.2	11.8	52	2.48	0.24	0.93	880	
113-689B-12H-2, 50-55cm	103	P	0.3		0.3	0.2	39.3		15.1	12.1			0.9	57	2.38	0.21	0.89	360		
113-689B-12H-2, 130-135cm	103.8	M	1.2		1.4	0.2	21.2		18.2	19.1	0.2	0.2	3.3	58	2.81	0.30	0.77	110		
113-689B-12H-3, 50-55cm	104.5	P	0.7		0.7		58.3		13.3	5.9			8.5	38	1.64	0.14	0.98	180		
113-689B-12H-3, 130-135cm	105.3	VP	0.3		1.0	0.1	74.5		2.8	6.8			2.8	39	1.24	0.12	0.71	1120		
113-689B-12H-4, 50-55cm	106	M			4.4		23.7		8.8	23.7		0.4		61	2.51	0.27	0.84	1360		
113-689B-12H-4, 100-105cm	106.5	P	0.3		3.8		15.5		9.7	19.0	0.2	0.5	36.8	60	2.14	0.20	0.89	1750		
113-689B-12H-5, 30-35cm	107.3	M	0.2		0.4	1.1	5.4		11.7	33.6	0.9	1.8	27.3	62	2.20	0.22	0.74	4410		
113-689B-12H-5, 123-125cm	108.23	P	0.2		2.6	3.0	3.5		26.6	32.3	3.1	1.2	70	2.48	0.24	0.99	6420			
113-689B-12H-6, 30-35cm	108.8	G			3.0	2.3	2.3		21.0	33.7	2.6	0.4		92	2.76	0.23	0.91	26360		
113-689B-12H-6, 121-123cm	109.71	VG	0.2		8.4	12.2	0.4		16.8	22.4	5.9	0.9		97	2.87	0.27	0.98	13350		
113-689B-12H-7, 20-25cm	110.2	G			7.2	10.7	0.3		15.6	29.1	5.7	0.3		99	2.83	0.25	0.94	19900		
Eucyrtidium antiquum	113-689B-13H-1, 50-55cm	110.9	G			6.3	12.8	0.1		21.7	20.2	2.1	0.1		123	2.93	0.25	0.97	34850	
	113-689B-13H-1, 130-135cm	111.7	VG			2.7	13.4	1.4		18.9	26.8	2.1	2.7		94	2.83	0.27	0.98	11780	
	113-689B-13H-2, 50-55cm	112.4	VG			4.9	13.9	0.3		16.9	31.7	2.6	0.3		94	2.57	0.20	0.92	15430	
	113-689B-13H-2, 130-135cm	113.2	VG	0.1		6.7	9.0	0.5	0.1	22.8	21.0	9.0	1.3		103	2.81	0.25	0.99	25060	
	113-689B-13H-3, 50-55cm	113.9	G			4.7	12.9	1.1		25.1	25.2	8.9	1.1		84	2.48	0.23	0.95	5870	
	113-689B-13H-3, 130-135cm	114.7	G			1.6	7.3	0.5		23.4	22.6	19.0	1.9		85	2.50	0.22	0.95	4090	
	113-689B-13H-4, 50-55cm	115.4	M	0.2		3.7	11.0	0.6		23.7	23.7	8.4	0.4		91	2.63	0.26	0.96	3670	
	113-689B-13H-4, 130-135cm	116.2	G			0.7	15.0	0.7		27.4	16.6	7.3	0.7							

- tributions. Cushman Foundation for Foraminiferal Research, Special Publication, 16A: 125 pp.
- MACKENSEN, A. and BERGGREN, W. A., 1992. Paleogene benthic foraminifers from the southern Indian Ocean (Kerguelen Plateau). In: Wise, S. W., Jr., Schlich, R., et al., Eds., *Proceedings of Ocean Drilling Program, Scientific Results*, vol. 120: 603-630. College Station, Texas: Ocean Drilling Program.
- MILLER, K. G., WRIGHT, J. D. and FAIRBANKS, R. G., 1991. Unlocking the icehouse: Oligocene-Miocene oxygen isotopes, eustasy, and margin erosion. *Journal of Geophysical Research*, 96: 6829-6848.
- PERSICO, D. and VILLA, G., 2004. Eocene-Oligocene calcareous nannofossils from Maud Rise and Kerguelen Plateau (Antarctica): paleoecological and paleoceanographic implications. *Marine Micropaleontology*, 52: 153-179.
- PROTHERO, D. R. and BERGGREN, W. A., 1992. *Eocene-Oligocene Climatic and Biotic Evolution*. Princeton, NJ, Princeton University Press: 568 pp.
- PROTHERO, D. R., IVANY, L. C. and NESBITT, E. A., 2003. *From Greenhouse to Icehouse. The marine Eocene-Oligocene transition*. New York: Columbia University Press, 541 pp.
- SCHRÖDER-ADAMS, C. J., 1991. Middle Eocene to Holocene benthic foraminifer assemblages from the Kerguelen Plateau (southern Indian Ocean). In: Barron, J., Larsen, B., et al., Eds., *Proceedings of Ocean Drilling Program, Scientific Results*, vol. 119: 611-630. College Station, Texas: Ocean Drilling Program.
- SLUIJS, A., PROSS, J. and BRINKHUIS, H., 2005. From greenhouse to icehouse; organic-walled dinoflagellate cysts as paleoenvironmental indicators in the Paleogene. *Earth-Science Reviews*, 68: 281-315.
- SMITH, S. L. and SCHNACK-SCHIEL, S. B., 1990. Polar zooplankton. In: Smith, W. O. Jr., Ed., *Polar Oceanography, Part B: Chemistry, Biology, and Geology*, 527-598. San Diego: Academic Press, Inc.
- TAKEMURA, A., 1992. Radiolarian Paleogene biostratigraphy in the southern Indian Ocean, Leg 120. In: Wise, S. W., Jr., Schlich, R., et al., Eds., *Proceedings of Ocean Drilling Program, Scientific Results*, vol. 120: 735-756. College Station, Texas: Ocean Drilling Program.
- TAKEMURA, A. and LING, H. Y., 1997. Eocene and Oligocene radiolarian biostratigraphy from the Southern Ocean: correlation of ODP Legs 114 (Atlantic Ocean) and 120 (Indian Ocean). *Marine Micropaleontology*, 30: 97-116.
- THOMAS, E., 1990. Late Cretaceous through Neogene deep-sea benthic foraminifers (Maud Rise, Weddell Sea, Antarctica). In: Barker, P. F., Kennett, J. P., et al., Eds., *Proceedings of Ocean Drilling Program, Scientific Results*, vol. 113: 571-594. College Station, Texas: Ocean Drilling Program.
- TRIPATI, A., BACKMAN, J., ELDERFIELD, H. and FERRETTI, P., 2005. Eocene bipolar glaciation associated with global carbon cycle changes. *Nature*, 436: 341-346.
- VILLA, G. and PERSICO, D., 2006. Late Oligocene climatic changes: Evidence from calcareous nannofossils at Kerguelen Plateau Site 748 (Southern Ocean). *Palaeogeography, Palaeoclimatology, Palaeoecology*, 231: 110-119.
- VONHOF, H. B., SMIT, J., BRINKHUIS, H., MONTANARI, A. and NEDERBRAGT, A. J., 2000. Global cooling accelerated by early late Eocene impacts? *Geology*, 28: 689-690.
- WEAVER, F. M., 1983. Cenozoic radiolarians from the southeast Atlantic, Falkland Plateau region, Deep Sea Drilling Project Leg 71. In: Ludwig, W. J., et al., Eds., *Initial Reports of the Deep Sea Drilling Project*, vol. 71: 667-686. Washington, DC: US Government Printing Office.
- WEI, W., VILLA, G. and WISE, S. W. JR., 1992. Paleoceanographic implications of Eocene-Oligocene calcareous nannofossils from Sites 711 and 748 in the Indian Ocean. In: Wise, S. W., Jr., Schlich, R., et al., Eds., *Proceedings of Ocean Drilling Program, Scientific Results*, vol. 120: 979-999. College Station, Texas: Ocean Drilling Program.
- ZACHOS, J. C., LOHMANN, K. C., WALKER, J. C. G. and WISE, S. W., 1993. Abrupt climate change and transient climates during the Paleogene: a marine perspective. *Journal of Geology*, 101: 191-213.
- ZACHOS, J., PAGANI, M., SLOAN, L., THOMAS, E. and BILLUPS, K., 2001. Trends, rhythms, and aberrations in global climate 65 Ma to present. *Science*, 292: 686-693.

Vertical and geographic distribution of selected radiolarian species in the North Pacific

Yoshiyuki Ishitani¹, Kozo Takahashi¹, Yusuke Okazaki², and Seiji Tanaka¹

¹Department of Earth and Planetary Sciences, Graduate School of Science, Kyushu University, Fukuoka 812-8581, Japan

²Institute of Observational Research for Global Change, Japan Agency for Marine-Earth Science and Technology, Natsushima-cho, Yokosuka 237-0061, Japan
email: shitani@geo.kyushu-u.ac.jp

ABSTRACT: In this paper, we compile the plankton tow and sediment trap data previously obtained in the North Pacific and discuss the relevant results for ten representative radiolarian taxa. *Didymocyrtis tetrathalamus* and *Tetrapyle octacantha* group are controlled by warm water currents. *Tetrapyle octacantha* group is a Tropical-Subtropical indicator whose living zone is broader than that of *D. tetrathalamus*. *Pseudocubus obeliscus* is a productivity indicator. *Spongostichus glacialis* appears to be advected from the Subarctic Current through the California Current into the central Equatorial Pacific. *Pseudodictyophimus gracilipes*, *Stylochlamydidium venustum*, *Larcopyle butschlii*, and *Litharachnium tentorium* show distributions conformable with the “tropical submergence” hypothesis. *Botryostrobus aquilonaris* and *Stylodictya aculeata* seem to be associated with upwelling and we define them as “upwelling” taxa.

INTRODUCTION

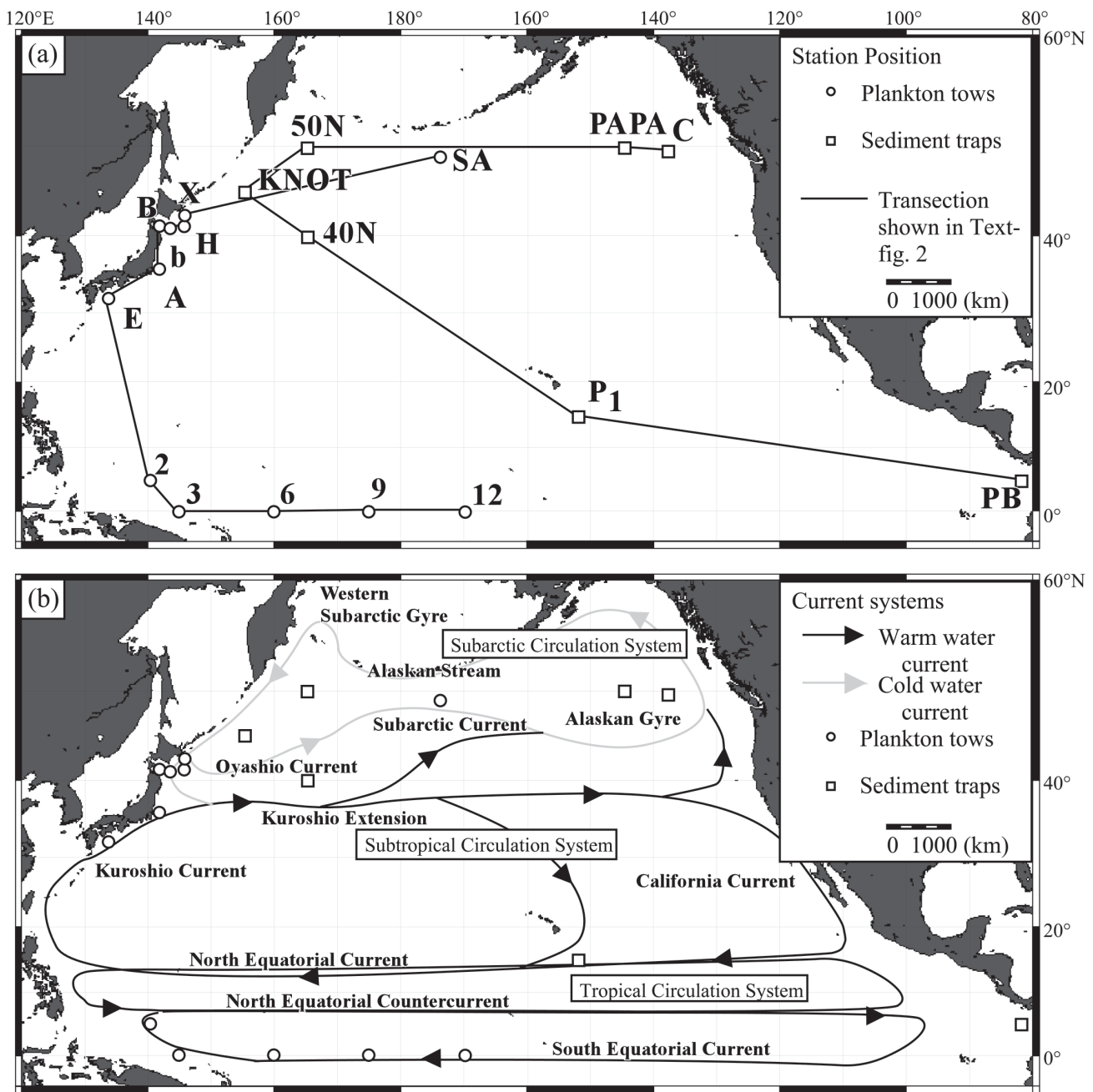
Radiolaria are marine zooplankton with siliceous shells. Their sinking shells are not readily dissolved en-route from the epipelagic to the bathypelagic and they are often preserved as fossils in marine sediments (e.g., Takahashi 1995). They appeared during the Cambrian in the fossil record, and at present they geographically extend from the Arctic to Antarctic regions (e.g., De Wever et al. 2001). New species with distinct morphologies have evolved throughout successive geologic ages in parallel with ever changing environments. As a result, their utility in earth science is not only as time markers but also as paleoenvironmental indicators, with the latter application not fully exploited because of poor information about their vertical and geographic distributions.

Living radiolarians were first extensively studied in the nineteenth century and their abundances and vertical distributions were investigated in more recent years. From these works, we can understand the relationship between some radiolarian taxa and specific water masses (e.g., Renz 1976; Boltovskoy and Riedel 1987; Welling et al. 1996). The purpose of this paper is to compile and discuss data for living radiolarians in the North Pacific in order to advance our knowledge of the relationship between radiolarians and specific environmental conditions. In order to avoid problems of differences in radiolarian taxonomy used by different workers, we mainly use the data generated by the members of one specific research group (Paleoenvironmental Laboratory of the Kyushu University), and the selected taxa are very carefully chosen by comparison of their morphology in each of the publications and personal communications.

OCEANOGRAPHIC SETTING

In the North Pacific, there are three main surface circulation systems in the upper 500m: the Tropical Circulation System, the Subtropical Circulation system, and the Subarctic Circulation System. Between 500 and 1000m, there are two intermediate water masses: the Antarctic Intermediate Water (AAIW) and the North Pacific Intermediate Water (NPIW). The Circumpolar Deep Water (CDW) occupies the water mass below 1000m (text-figs. 1 and 2; Sverdrup et al. 1941; Emery and Meincke 1986; Steel et al. 2001).

The Tropical Circulation System is characterized by relatively high salinity (>34.5psu) and temperature (7-23°C), and is comprised of three major currents: the westward North Equatorial Current, the eastward North Equatorial Countercurrent, and the westward South Equatorial Current. In the Equatorial region, there are two major water masses in the surface layer: the Western Pacific Warm Pool (WPWP) and the upwelled water in the Upwelling Region (UW) which is generated by the Trade Winds (Lukas and Lindstrom 1991). The WPWP, characterized by low salinity (34-35psu) and high temperature (>29.4°C), is oligotrophic in the surface layer because of the presence of a strong pycnocline. By contrast, the surface layer of the UW is characterized by nutrient rich conditions and a weak pycnocline because of the Equatorial Upwelling brought by the Trade Winds. Equatorial upwelling is distinct from Coastal Upwelling, which is generated by the strong wind force along the coast. Differences in the driving mechanism cause the features of each upwelling system to be different: the Equatorial Upwelling shows weak but long term (seasonal variation) upwelling from about 200m to the surface, while the Coastal Upwelling shows strong but short term (diurnal variation) rising from between 200 and 400m to the surface. In the Pacific region of our study, coastal upwelled waters are present only beyond the area of our sampling, in the Coastal Upwelling Region (CUW) off the Coast of Peru. The Subtropical Circulation System is characterized by high salinity (33.8-35.2psu) and temperatures (10-22°C), and is composed of four major currents: the North Equatorial Current, the Kuroshio Current, the Kuroshio Extension, and the California Current. The Subarctic Circulation System is characterized by relatively low salinity (<33.6psu) and temperatures (3-15°C), and is composed of the Subarctic Current, the Alaskan Gyre, the Alaskan Stream, the Western Subarctic Gyre, and the Oyashio Current. The zone between the Kuroshio and Oyashio Currents is characterized by high productivity because of mixing of warm and cool waters and due to upwelling (Yasuda 2003). The Subarctic Circulation System supports a high productivity biota which can be attributed to seasonal vertical mixing, inputs from enriched marginal seas such as the Bering and Okhotsk Seas, and the terminal location of the general abyssal circulation. The upper waters (0-500m) are subdivided into surface and subsurface (upper and lower surface layers) by the existence of permanent pycnocline (Steel et al. 2001). The position of the permanent pycnocline is mainly observed in the 100-200m intervals.



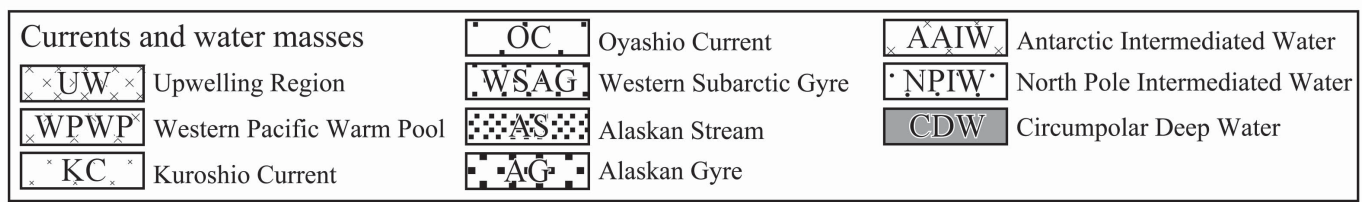
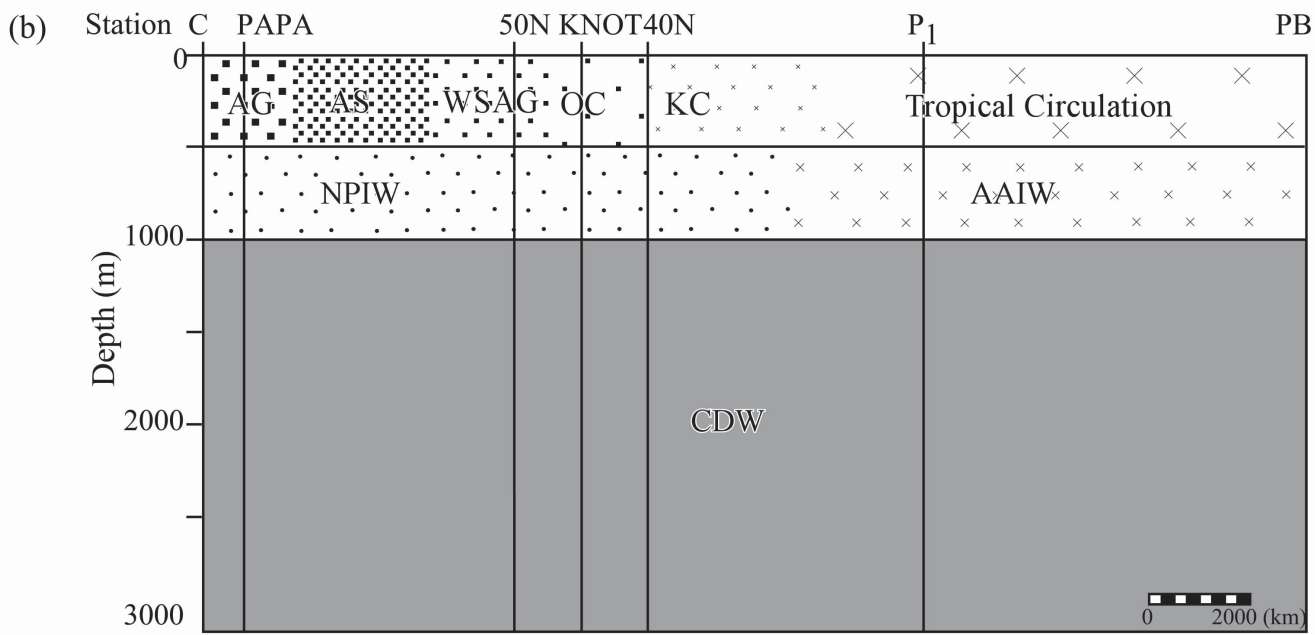
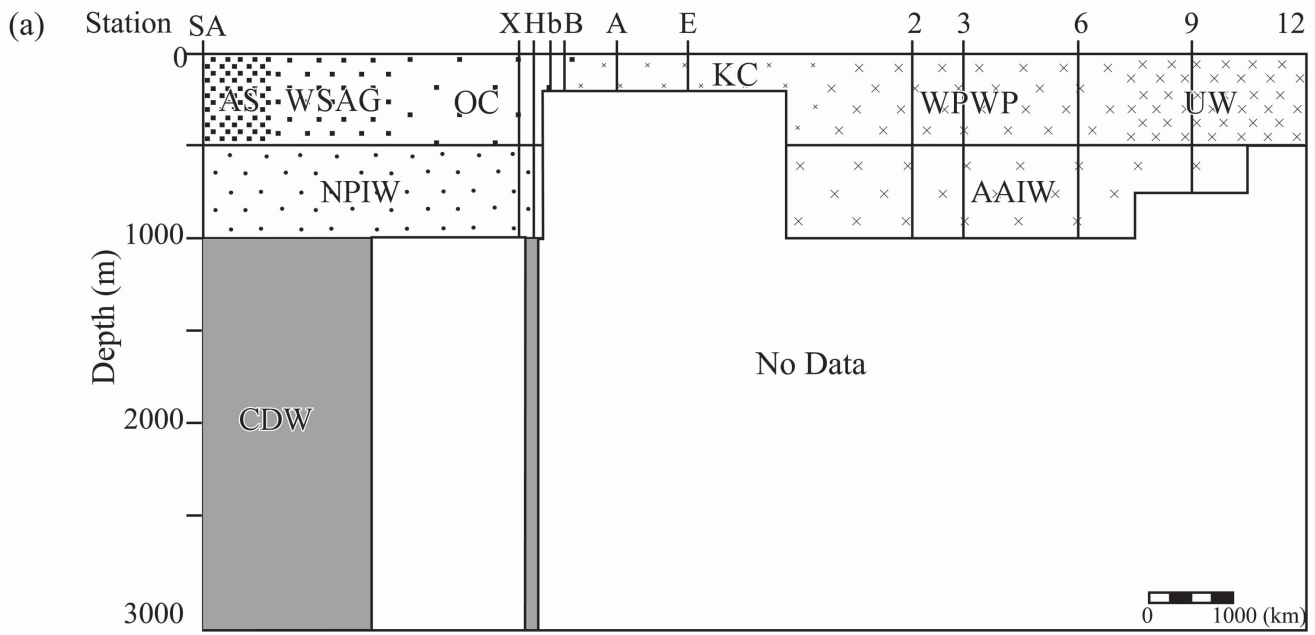
TEXT-FIGURE 1

Maps showing (a) twelve plankton tow stations and seven sediment trap stations. The track connecting the stations is the transect shown in Text-fig. 2, and (b) the major oceanographic circulation systems and currents in the North Pacific: the Tropical Circulation System is comprised of the North Equatorial Current, North Equatorial Countercurrent, and South Equatorial Current. The Subtropical Circulation System is made of the North Equatorial Current, Kuroshio Current, Kuroshio Extension, and California Current. The Subarctic Circulation System is composed of the Subarctic Current, Alaskan Gyre, Alaska Stream, Western Subarctic Gyre, and Oyashio Current.

The AAIW is characterized as a low salinity layer whose distribution is restricted to waters of high potential density (27.2kg m⁻³), low temperatures (2-10°C), and high dissolved oxygen (4-6ml l⁻¹). The NPIW, with higher temperatures (5-12°C) and lower dissolved oxygen (<4ml l⁻¹) than the AAIW, has a distinctive low salinity layer marked by low potential density (26.8kg m⁻³) (Johnson and McPhaden 1999). The CDW is characterized by low temperatures (<2°C), low salinity (34.6-34.7psu), and low dissolved oxygen (2-4ml l⁻¹).

MATERIALS AND METHODS

All data, acquired by plankton tows and sediment traps, are located in the North Pacific (text-fig. 1a). The plankton tow data from twelve stations are compiled in this paper (data sources in Table 1 and sampled locations in text-fig. 1a). The samples cover different water intervals because of the differences among the studies plankton tow depths. Sediment trap data used in this paper are composed of seven stations which have previously been published (data sources in Table 2 and sampled locations in Text-figure 1a). The data for Station P1 at the southern margin of the

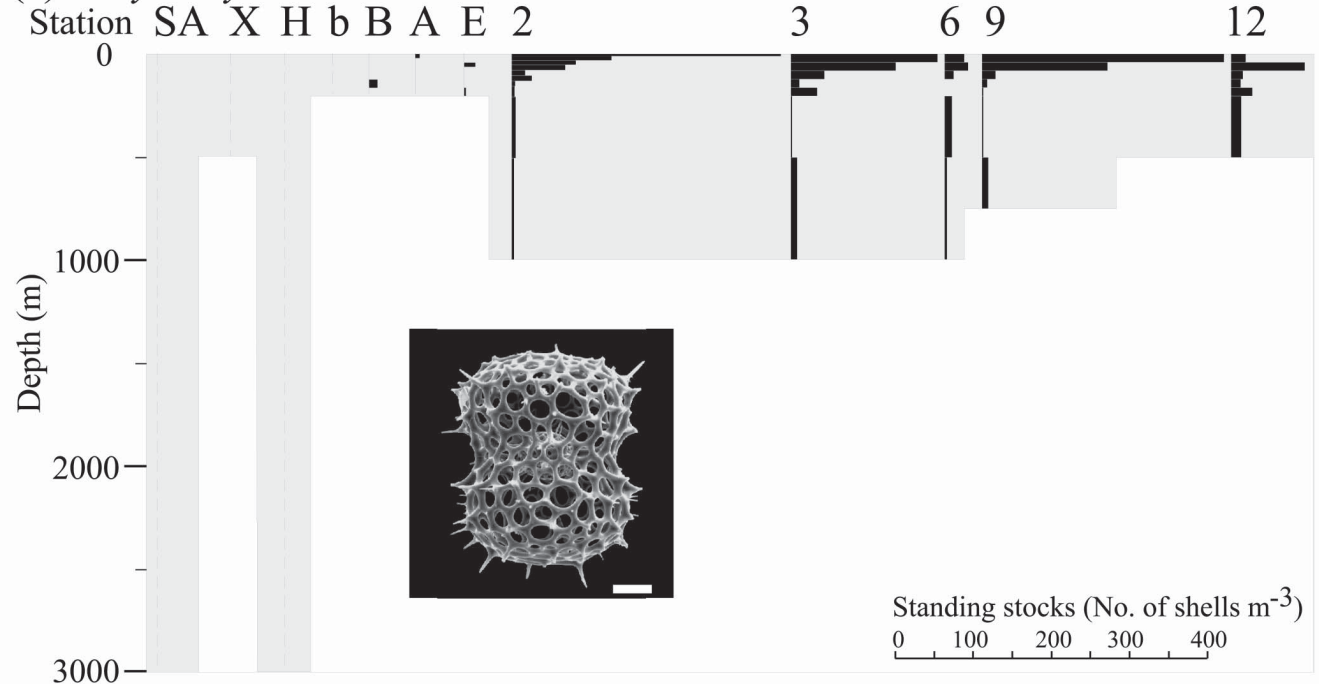


TEXT-FIGURE 2
 Transects showing the water masses below the stations in Text-figure 1a. Transects for (a) plankton tow stations and (b) sediment trap stations are shown, respectively.

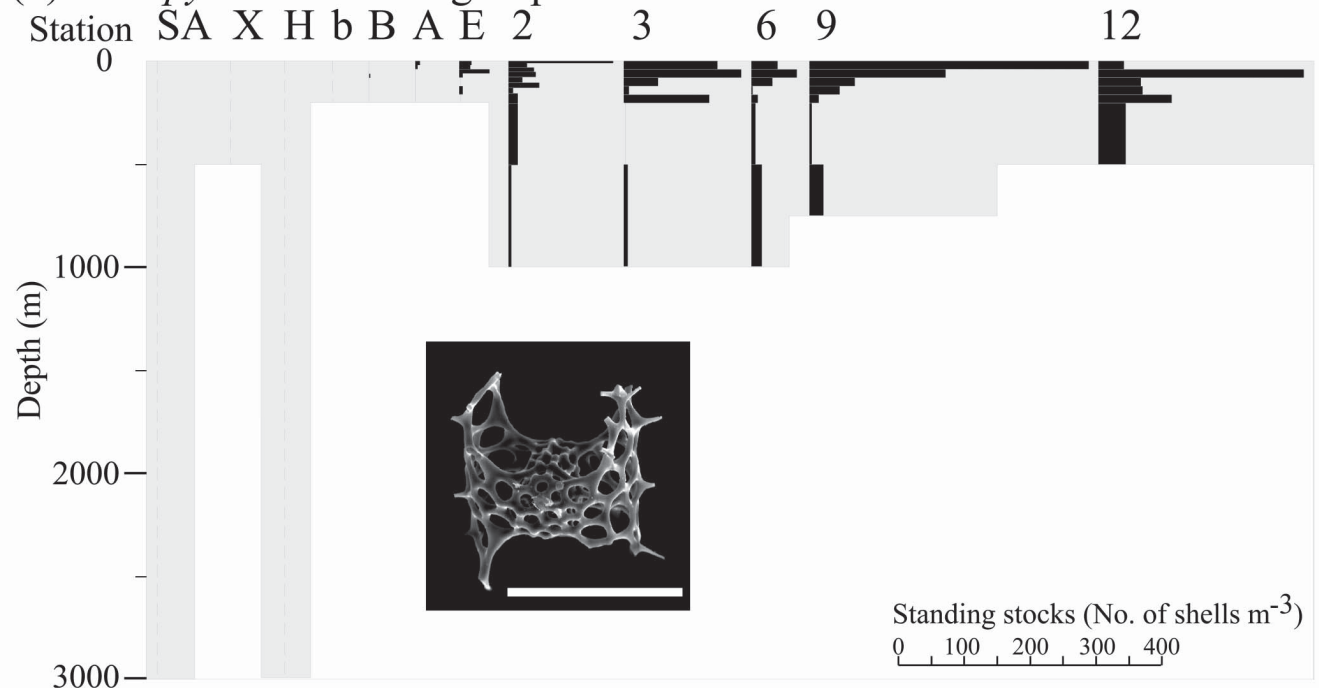
Central Pacific Gyre and Station PB in the Panama Basin were published in Takahashi (1991). Okazaki et al. (2005) showed the data at Station 40N adjacent to the western Subarctic Pacific and Stations KNOT and 50N in the western Subarctic Pacific, respectively. The data for Stations PAPA and C in the Gulf of Alaska are from Takahashi (unpublished data).

Various water masses for each depth interval (surface, intermediate, and deep) at plankton tow and sediment trap stations are shown in text-figure 2. The surface layer of plankton tows at Stations 6, 9, and 12 are located in the UW region of the South Equatorial Current, and Stations 2 and 3 are in the WPWP region of the South Equatorial Current. Station E is in the Kuroshio Current, Station A is in the mixing zone between the Ku-

(a) *Didymocyrtis tetralthalamus*



(b) *Tetrapyle octacantha* group



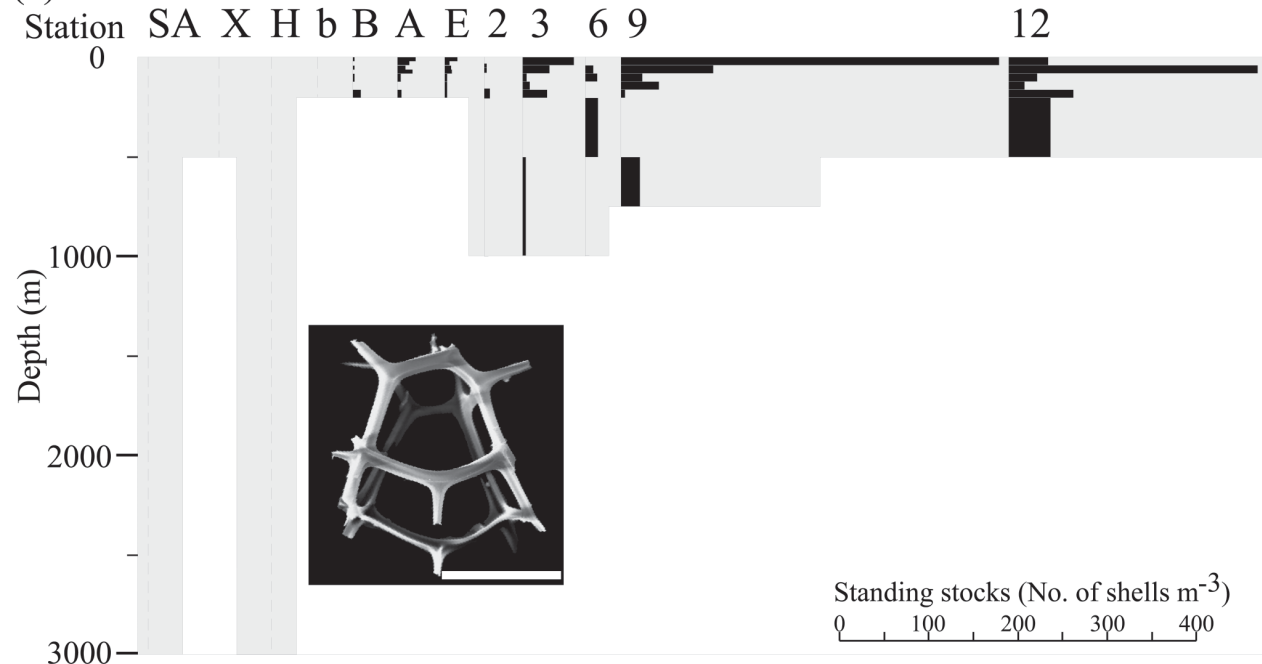
TEXT-FIGURE 3

Vertical and geographic distributions of *Didymocyrtis tetralthalamus* and *Tetrapyle octacantha* group, indicators of the Subtropical and Tropical Circulation Systems. The black bars within the gray zone of sampling represent standing stocks (No. of shells m^{-3}) at each of the depth. All scale bars in the photographs of text-figures 3 through 6 equal $30\mu m$. The photomicrographs with the white scale bars are taken with SEM and those with the black scale bars are taken with LM.

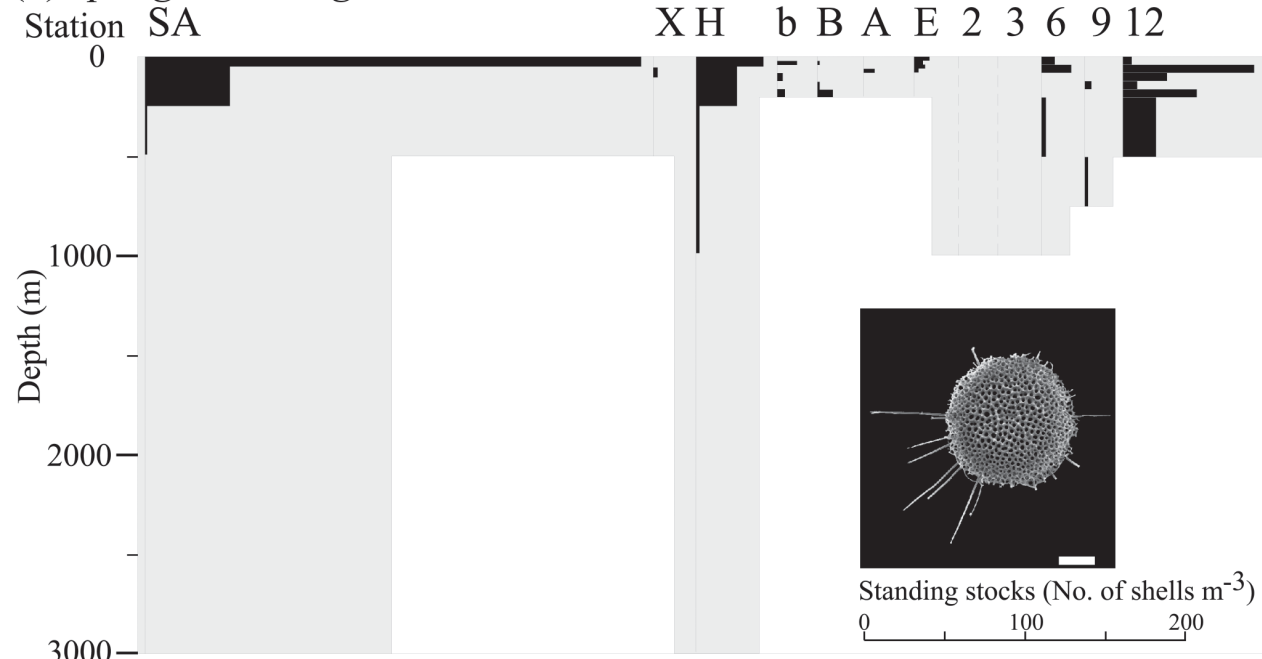
roshio and Oyashio Currents, and Stations B, b, H, and X are in the Oyashio Current. Station SA is located between the Alaskan Stream and Subarctic Current. In the intermediate layer, Stations 2, 3, 6, 9, and 12 are located in the AAIW, and other stations are in the NPIW. Below 1000m, there is the CDW at all stations

in the North Pacific. In the surface layer of sediment trap stations, Stations P1 and PB are in the Tropical Circulation System. Station 50N is in the Western Subarctic Gyre, Station KNOT is located in the Oyashio Current, and Station 40N is situated in the mixing zone between the Kuroshio and Oyashio Currents.

(a) *Pseudocubus obeliscus*



(b) *Spongotrochus glacialis*



TEXT-FIGURE 4

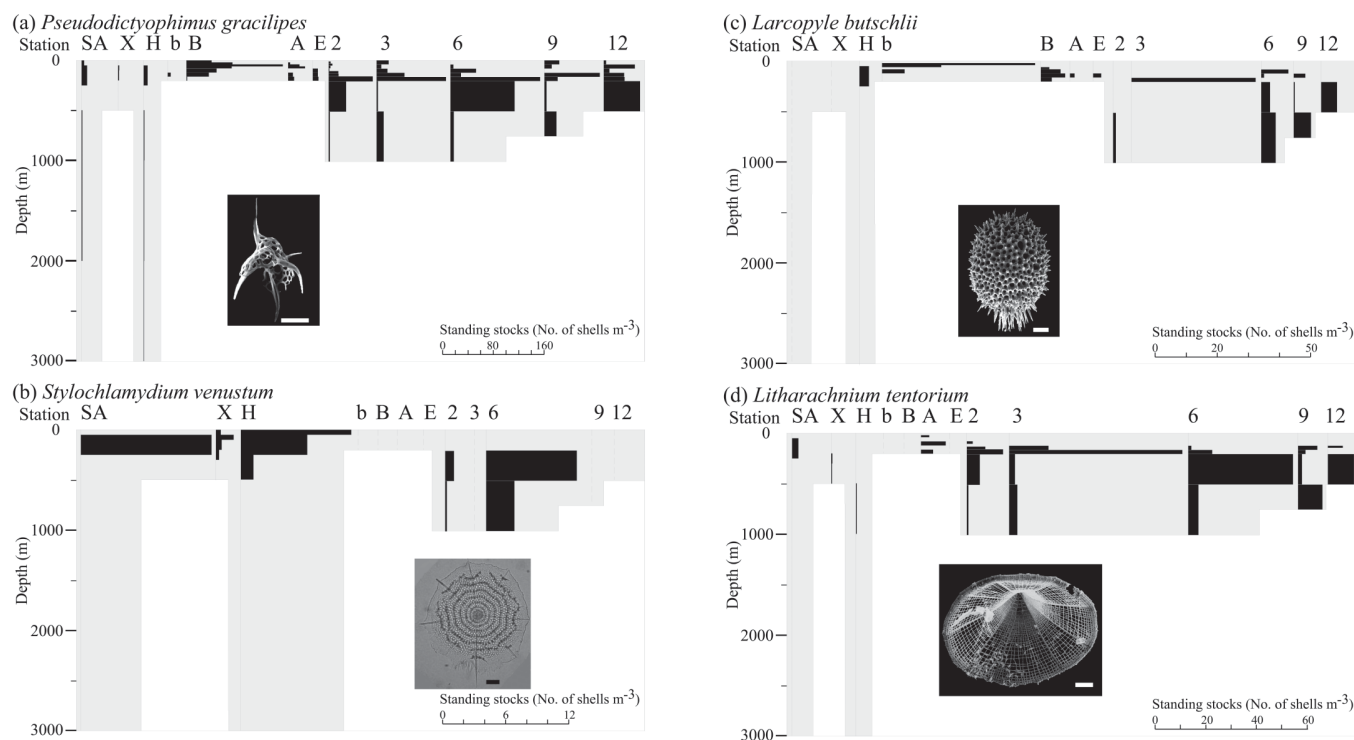
The vertical and geographic distributions of *Pseudocubus obeliscus* and *Spongotrochus glacialis*.

Stations PAPA and C are located in the Alaskan Gyre. In the Intermediate layer, Stations P1 and PB are situated in the AAIW and all other stations except for Stations P1 and PB are located in the NPIW. The water masses below 1000 m at all stations are accounted by the CDW.

In this study, we compiled data from four different studies (Yamashita et al. 2002; Okazaki et al. 2003; Ishitani and Takahashi 2007; Tanaka et al., submitted). These samples were obtained by the same plankton net with 63 μ m mesh, and were treated with the same methods. In synthesizing our data, one

problem is caused by radiolarian seasonal changes because of different sampling dates. However, in this study, our objective is to understand species' longer-term (annual) distributions. In order to resolve this problem, we compile temporal plankton tow data and longer-term sediment trap data, and contrast these data.

We chose ten representative taxa by first surveying vertical and geographic distribution of all data involving 332 taxa because of their regular and meaningful distributions. The taxonomic



TEXT-FIGURE 5

The vertical and geographic distributions of *Pseudodictyophimus gracilipes*, *Stylochlamydidium venustum*, *Larcopyle butschlii*, and *Litharachnium tentorium*, showing “tropical submergence”.

consistencies of all data for these ten taxa were checked by comparing their photomicrographs in each of the publications and/or through personal communications. Two taxa were specifically defined as follows. In *Tetrapyle octacantha* group, we included some ontogenetic stages of *Tetrapyle octacantha* except for *Octopyle stenozona* and *Phorticium pylonium*. In *Larcopyle butschlii*, we chose only adult forms to avoid confusion between *L. butschlii* (juvenile) and *Tholospira* spp.

RESULTS AND DISCUSSION

Ten taxa in the North Pacific showed characteristic vertical and geographic distributions (text-figures 3-6). For each taxon, we summarize the distribution (Table 3), and compare them with other published data for plankton tows from the North Pacific (Kling 1979; Boltovskoy and Riedel 1987; Kling and Boltovskoy 1995; Welling et al. 1996) (Text-figure 7). Comparisons with sediment trap data, plankton tow data from other seas, and surface sediment data are described below.

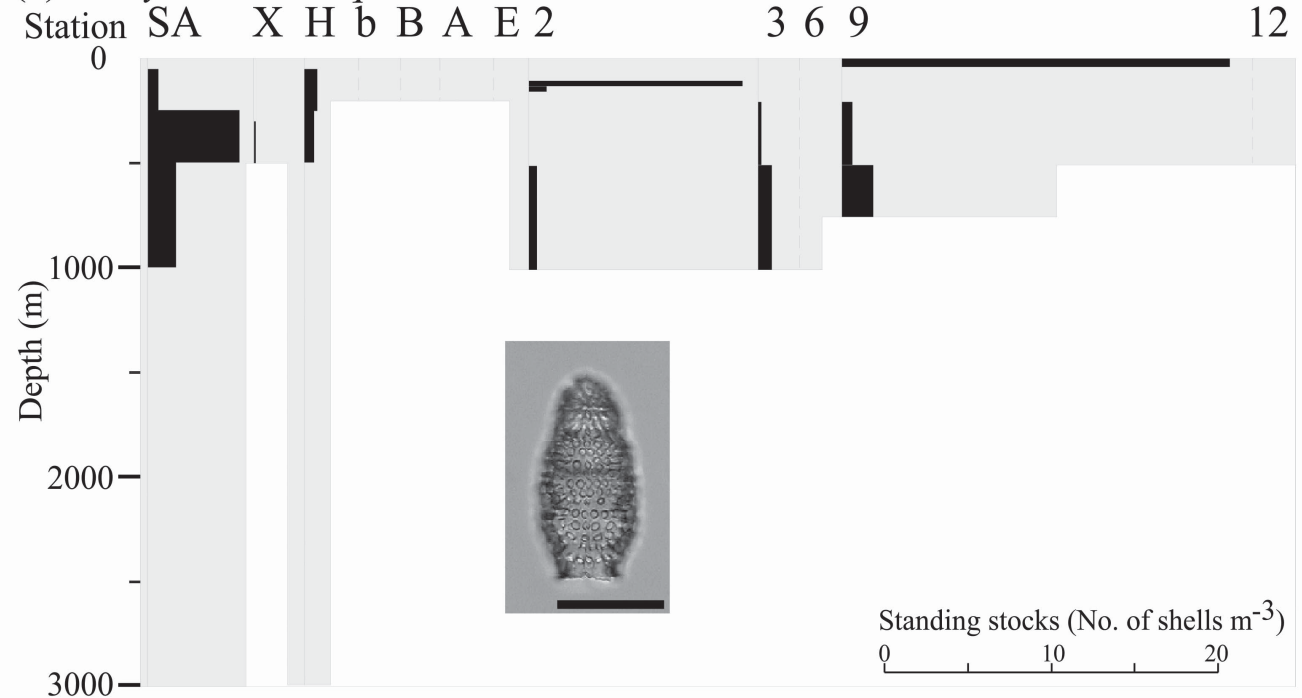
Didymocyrtis tetrathalamus and *Tetrapyle octacantha* group showed similar vertical and geographic patterns. *Didymocyrtis tetrathalamus* was mainly observed in the South Equatorial Current and the Kuroshio Current (Text-figure 3a). This taxon seems to favor the surface layer in the Tropical and Subtropical Circulation Systems. From other publications, *Didymocyrtis tetrathalamus* is known to be an indicator of tropical-subtropical waters (upper 100m: Kling and Boltovskoy 1995; Boltovskoy and Riedel 1987). According to Welling et al. (1996), this taxon belonged to the West Pacific Factor which was dominant in the WPWP region. This taxon is only observed in the surface layer of the Subtropical and Tropical Circulation Systems, and it is dominant in the west Pacific. Therefore, *D. tetrathalamus* is controlled by warm water currents.

Tetrapyle octacantha group was mainly observed in the South Equatorial Current and the Kuroshio Current (Text-figure 3b). It favors the surface layer of the Tropical and Subtropical Circulation Systems. In other publications, *Tetrapyle octacantha* group follows the tropical-subtropical waters (upper 100m: Kling and Boltovskoy 1995; Boltovskoy and Riedel 1987; Kling 1979; Welling et al 1996). In our study, this taxon is most abundant in the UW. Thus, it is possible to conclude that the distribution of *T. octacantha* group is controlled by warm water currents and is more dominant in high productivity regions.

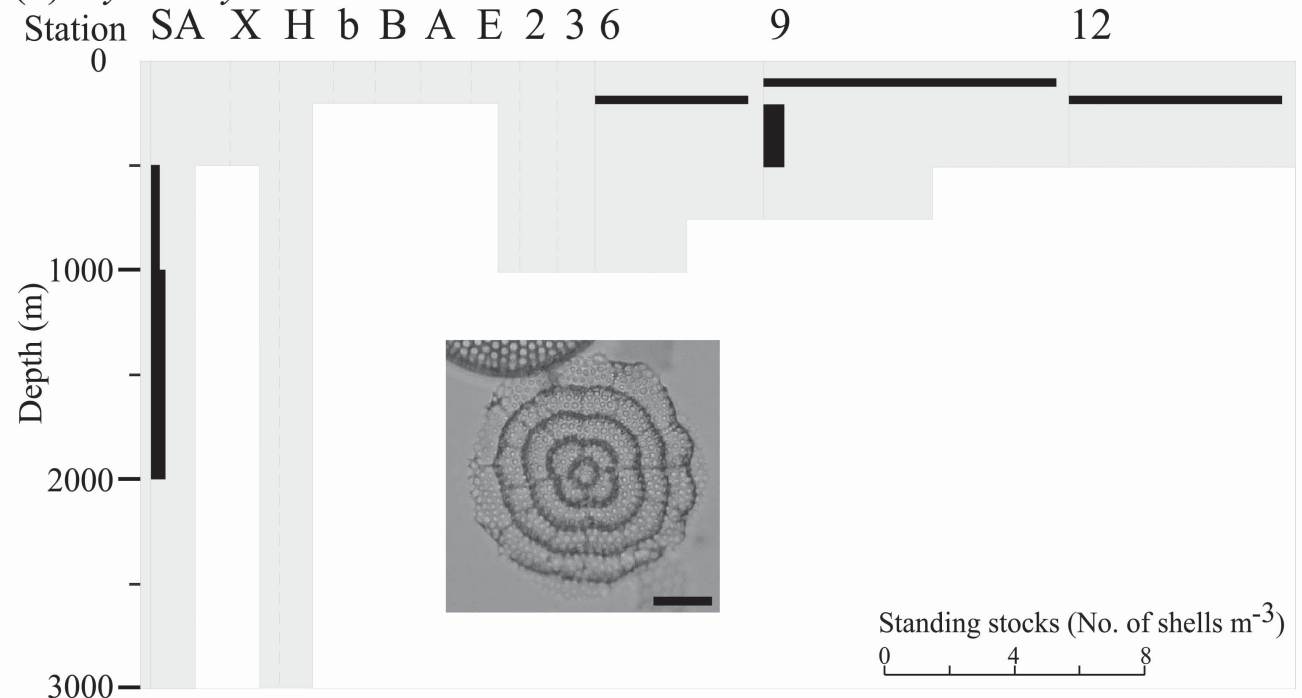
Pseudocubus obeliscus was abundant in the UW and the region of mixing between the Kuroshio and the Oyashio Currents, which is characterized by high productivity (text-figure 4a). This taxon is observed in high productivity regions in the Tropical and Subtropical Circulation Systems in the other publications. *Pseudocubus obeliscus* was numerous in the California Current, and even more abundant in the cold-transitional area than in the tropical area (Boltovskoy and Riedel 1987). This taxon was observed only in the Subtropical and Tropical Circulation Systems, and showed high standing stocks in the high productivity areas. From these observations, *P. obeliscus* is a productivity indicator restricted in the Subtropical and Tropical Circulation Systems.

Spongostrochus glacialis was abundant in the Subarctic Current and was rare in the west of the South Equatorial Current (text-figure 4b). In the central Equatorial Pacific region and the Kuroshio Current, the abundance of *S. glacialis* was very low. As *Spongostrochus glacialis* was also observed in the California Current (Boltovskoy and Riedel 1987), this taxon seems to be advected from the Subarctic Current through the Kuroshio Extension and California Current into the central Equatorial Pacific region. During summer and early fall, the California Current

(a) *Botryostrobus aquilonaris*



(b) *Stylodictya aculeata*

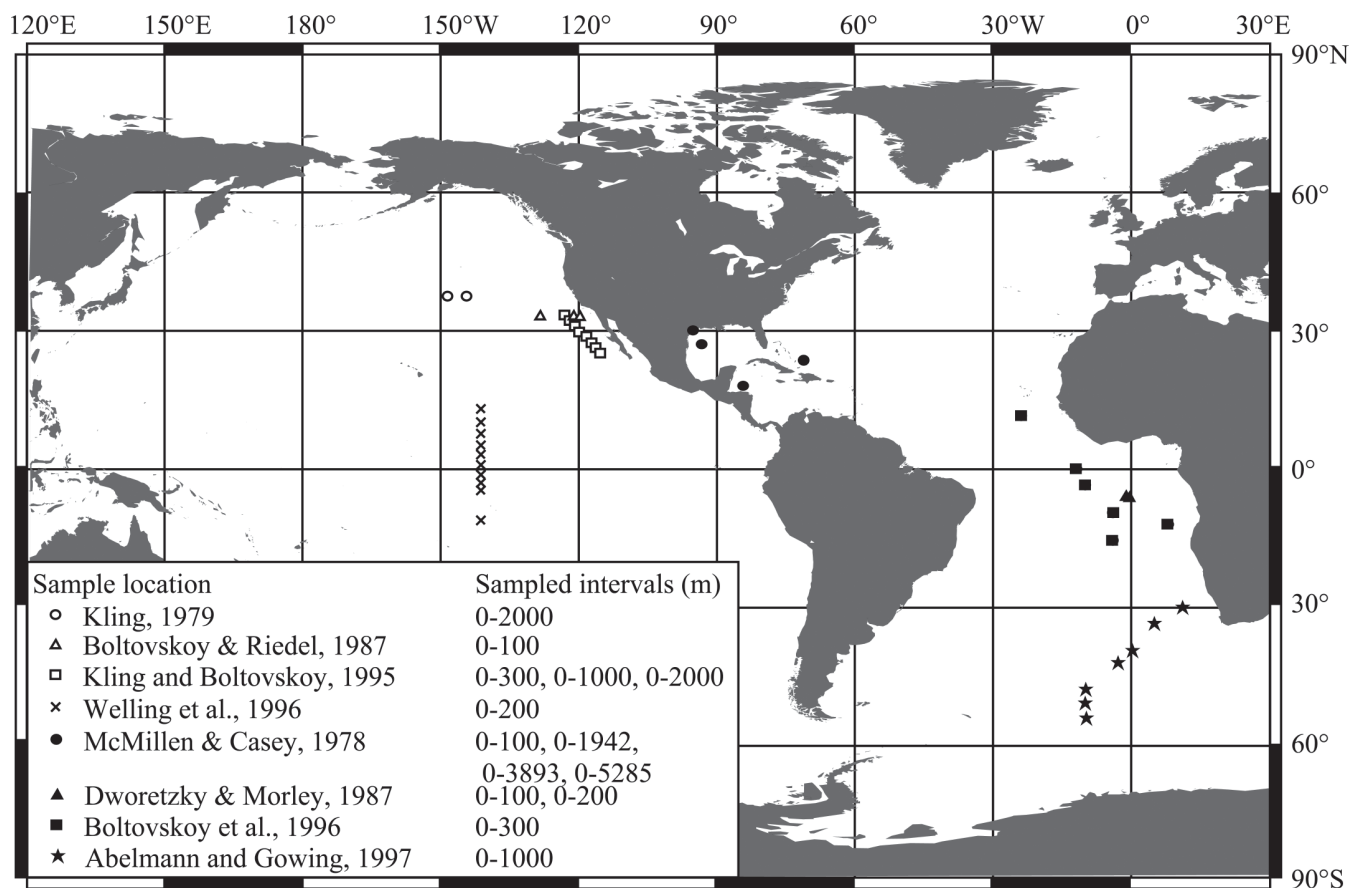


TEXT-FIGURE 6

The vertical and geographic distributions of *Botryostrobus aquilonaris* and *Stylodictya aculeata* identified as “upwelling” taxa.

reaches the central Equatorial Pacific region because of strong southern flow (Wyrтки 1965), thus this current provides a viable recruiting mechanism for this species to be present in the central Equatorial Pacific. Moreover, *Spongostrobus glacialis* belonged to the Subtropical Factor assemblage which was mainly related to the advection of the North Equatorial Current (Welling et al 1996).

Text-figure 5 shows the vertical and geographic distributions of taxa conforming to Casey’s (1971) “tropical submergence” hypothesis, i.e. living in shallower waters at high latitudes and deeper waters at low latitudes. The pattern is suggested as a result of adaptation to temperature (Boltovskoy 1988). He proposed that distribution patterns of two radiolarian taxa (*Castanidium ap-*



TEXT-FIGURE 7

Location of plankton tow stations and sampled intervals reviewed in the Results and Discussions section.

stini and *C. variabile*) are an evidence of bipolar distributions because they migrated to the deeper layer around the equator and their abundances were lower than those in the high latitude due to high water temperature. Such “tropical submergence” patterns are observed in several plankton groups (Radiolaria, Foraminifera, and Pteropoda) and are regarded as the proof of the bipolar distributions (Boltovskoy 1988; Boltovskoy 1994).

Pseudodictyophimus gracilipes was abundant in the lower South Equatorial Current (below 200m) and the upper Kuroshio and Oyashio Currents (upper 200m) (text-fig. 5a). Welling et al. (1996) and Ishitani and Takahashi (2007) considered *P. gracilipes* as a typical “tropical submergence” group. Practically, they are abundant in the upper surface layer (upper 200m) of the high latitudes (25-50m in the Chukuchi and Beaufort Seas: Itaki et al. 2003), and numerous in the lower surface layer (below 200m) of the low latitudes (200m: Kling 1979; 100m: Kling and Boltovskoy 1995). These results confirm that *P. gracilipes* is a typical species “tropical submergence” form.

Stylochlamydidium venustum was abundant in the lower South Equatorial Current and the upper Subarctic Current (text-fig. 5b). In other publications, *Stylochlamydidium venustum* was observed in the upper surface layer (upper 100 m) of the California Current (Kling and Boltovskoy 1995; Boltovskoy and Riedel 1987) and the central North Pacific (Kling 1979). However, in our study, this taxon was observed in the AAIW. Considering these results, we suggest *S. venustum* as a “tropical submergence” species.

Larcopyle buetschlii and *Litharachnium tentorium* were sub-

merged at lower latitudes analogous to *P. gracilipes*. *Larcopyle buetschlii* was observed in the upper surface layer of the Oyashio Current and in the lower surface layer of the Subtropical and Tropical Circulation Systems (text-fig. 5c). In Kling and Boltovskoy (1995), *Larcopyle buetschlii* was dominant in the upper surface layer (<200m) of the California Current, which is in the Subtropical Circulation System. Consequently, this taxon is observed in the upper surface layer of the high latitudes and in the lower surface layer of the low latitudes. *Litharachnium tentorium* was abundant in the upper surface layer of the Oyashio Current and in the lower surface layer of the Subtropical and Tropical Circulation Systems (text-fig. 5d). Comparing with other publications, *Litharachnium tentorium* was observed in the upper surface layer (<200m) of the California Current (Kling and Boltovskoy 1995) and the central North Pacific (Kling 1979). This species mainly dwells in the upper surface layer of the high latitudes and in the lower surface layer of the low latitudes analogous to *L. buetschlii*. These results suggest that *L. buetschlii* and *L. tentorium* are “tropical submergence” species.

Botryostrobus aquilonaris was observed in the AAIW, NPIW, and South Equatorial Current (text-fig. 6a). Values in the South Equatorial Current and UW were higher than those in the WPWP. If these occurrences were transported from the surface currents (i.e., the California and North Equatorial Currents), this taxon should have been observed in the surface layer of the California Current. However, in the California Current, *Botryostrobus aquilonaris* was represented as an intermediate water dweller (Kling and Boltovskoy 1995). Hence, this taxon rises up into the surface layer between the California Current and the UW. The

upwelling water among this route is caused by the CUW off the Coast of Peru or the UW. The upwelling force of the CUW is higher than that of the UW, and thus this taxon may move up into the surface layer by using the upwelling force of the CUW. Therefore, the origin of *Botryostrobus aquilonaris* is perhaps in the Intermediate Water of the California Current, and rising up off the Coast of Peru before advected into the WPWP region. Its high standing stocks were observed in the surface layer of the region following the CUW.

Stylodictya aculeata was abundant in the UW of the South Equatorial Current and rare in the CDW (Text-figure 6b). This species dwells shallower in the UW than the other regions examined in this study. This vertical and geographic distribution is similar to that of *B. aquilonaris*. Therefore, we have categorized *B. aquilonaris* and *S. aculeata* as “upwelling” taxa.

As a supplemental data set for vertical and geographic distributions of Radiolaria in the North Pacific, the data from sediment traps (Table 2) in the North Pacific were also compared with our plankton tow results.

Didymocyrtis tetrathalamus was only observed in abundance at Stations P1 and PB both of which belonged to the Tropical Circulation System, and was rare at Stations 50N, KNOT, and 40N in or adjacent to the western Subarctic Pacific. From these results, we emphasize that *Didymocyrtis tetrathalamus* is a Tropical-Subtropical indicator.

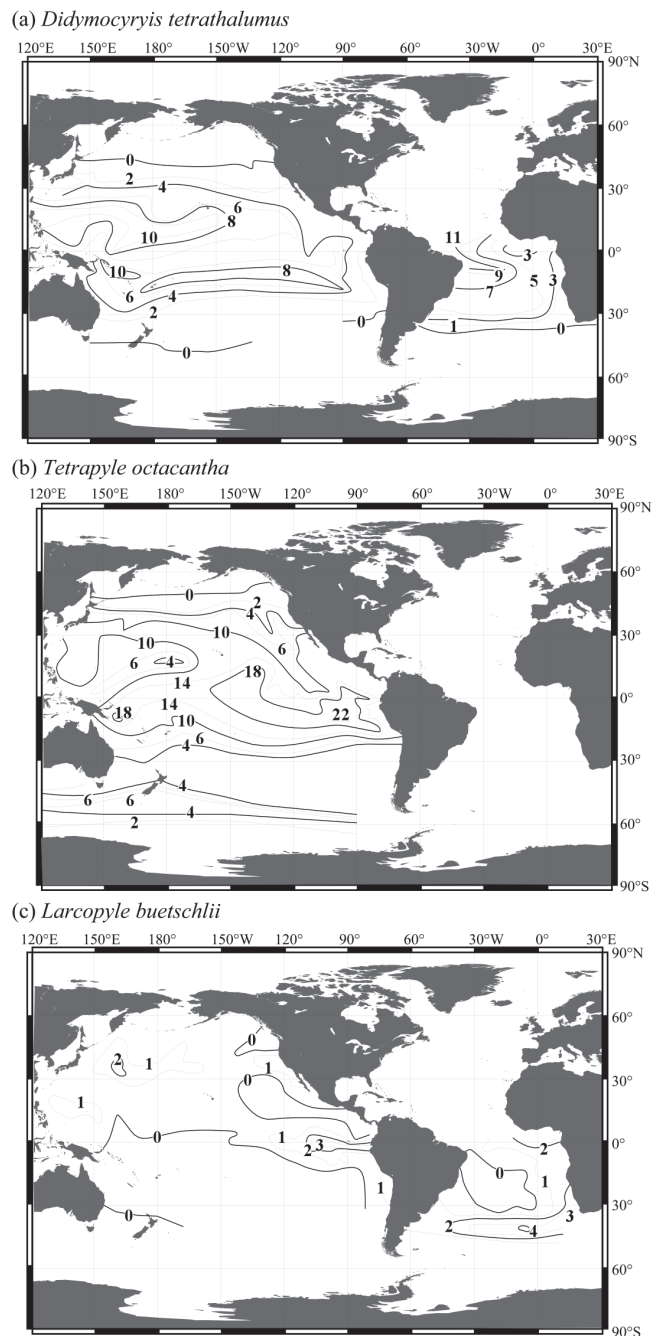
Tetrapyle octacantha group was abundant at Stations P1 and PB, and rare at Station 40N, which was located in the Transitional Zone between the Subtropical and Subarctic Zone. Therefore, *Tetrapyle octacantha* group is a Tropical-Subtropical indicator whose living zone is broader than that of *D. tetrathalamus*.

Larcopyle butschlii was consistently absent in the upper 1000m at Station P1. This result strengthens our interpretation that this taxon favors the surface water in the high latitudes and the intermediate water in the low latitudes.

Stylochlamydidium venustum is rare or absent at Stations E, A, B, and b, however, it is abundant (6.1%) at Station 40N whose latitude is a little lower than Stations B and b. The maximum sampling depth at Stations E, A, B and b was 200m, and the mooring depth at Station 40N was 2986m. Consequently, this taxon is rare or absent at Stations E, A, B, and b because that this taxa has already submerged below 200m at the latitude of 40°N. This result implies that *S. venustum* is a “tropical submergence” taxon.

It is also useful to view these vertical distributions with those outside of the North Pacific. We compare them with other published Atlantic plankton tow data (McMillen and Casey 1978; Dworetzky and Morley 1987; Boltovskoy et al. 1996; and Abelmann and Gowing 1997). Their locations are shown in text-figure 7.

In the Atlantic, *Didymocyrtis tetrathalamus* is observed in the upper surface layer of the Tropical and Subtropical regions (0-100m in the Gulf of Mexico and Caribbean Sea: McMillen and Casey 1978; 0-200m in the eastern Equatorial Atlantic: Dworetzky and Morley 1987; 0-300m in the eastern Equatorial Atlantic: Boltovskoy et al. 1996). *Didymocyrtis tetrathalamus* is also observed only in the Tropical and Subtropical regions analogous to that in the North Pacific.



TEXT-FIGURE 8
Map showing the geographic distribution of (a) *Didymocyrtis tetrathalamus*, (b) *Tetrapyle octacantha* group, and (c) *Larcopyle butschlii* in surface sediments (simplified from Lombardi and Boden 1985). The isopleths show their relative abundances in total radiolarian contents in the surface sediments.

Tetrapyle octacantha group is observed in the upper surface layer of the Tropical and Subtropical regions (0-50m in the Gulf of Mexico and Caribbean Sea: McMillen and Casey 1978; 0-200m in the eastern Equatorial Atlantic: Dworetzky and Morley 1987; 0-300m in the eastern Equatorial Atlantic: Boltovskoy et al. 1996; 0-150m in southeastern South Atlantic: Abelmann and Gowing 1997). In Abelmann and Gowing (1997), *Tetrapyle octacantha* group belonged to the Southeast Atlantic Factor whose occurrence area was in the Subtropical Zone. *Tetrapyle octacantha* group is observed in a region broader than that of *Didymocyrtis tetrathalamus*, as we suggested based on our Pacific data.

TABLE 1

Plankton tow samples at twelve stations: Yamashita et al. (2002); Okazaki et al. (2003); Ishitani and Takahashi 2007; and Tanaka et al., submitted.

Reference	Station ID	Depth interval (m)	Publication	Station ID	Depth interval (m)
Yamashita et al., 2002	Station 12	0-40	Ishitani and Takahashi, 2007	Station E	0-20
	Position 0°00'N	40-80		Position 32°10'N	20-40
	170°07'W	80-120		133°53'E	40-60
	Date 15/Jan/1999	120-160		Date 27/May/2002	60-80
	Sampling time 0:07-2:09	160-200		Sampling time 09:00-10:16	80-120
	Bottom depth 5397 m	200-500		Bottom depth 2660 m	120-160
	Station 9	0-40			160-200
	Position 0°01'N	40-80		Station A	0-20
	174°58'E	80-120		Position 36°01'N	20-40
	Date 12/Jan/1999	120-160		141°47'E	40-60
Sampling time 0:32-2:52	160-200	Date 25/May/2002	60-80		
Bottom depth 4831 m	200-500	Sampling time 09:52-11:18	80-120		
	500-750	Bottom depth 2220 m	120-160		
Station 6	0-40		160-200		
Position 0°01'N	40-80	Station B	0-20		
159°59'E	80-120	Position 41°34'N	20-40		
Date 7-8/Jan/1999	120-160	141°54'E	40-60		
Sampling time 23:58-2:45	160-200	Date 3/Jan/2002	60-80		
Bottom depth 2800 m	200-500	Sampling time 09:02-10:18	80-120		
	500-1000	Bottom depth 1000 m	120-160		
Station 3	0-40		160-200		
Position 0°00'N	40-80	Station b	0-20		
144°59'E	80-120	Position 41°09'N	20-40		
Date 4/Jan/1999	120-160	143°23'E	40-60		
Sampling time 0:23-3:21	160-200	Date 4/Jan/2002	60-80		
Bottom depth 3638 m	200-500	Sampling time 09:01-10:08	80-120		
	500-1000	Bottom depth 2077 m	120-160		
Station 2	0-10		160-200		
Position 5°02'N	10-30	Tanaka et al., submitted	Station H	0-50	
140°07'E	30-50	Position 41°30'N	50-250		
Date 2/Jan/1999	50-75	145°47'E	250-500		
Sampling time 0:36-3:17	75-100	Date 21/Aug/2004	500-1000		
Bottom depth 4175 m	100-125	Bottom depth 6900 m	1000-2000		
	125-150		2000-3000		
	150-200	Station SA	0-50		
	200-500	Position 49°00'N	50-250		
	500-1000	174°00'W	250-500		
Okazaki et al., 2003	Station X	0-50	Date 10/Aug/2004	500-1000	
Position 42°52'N	50-100	Bottom depth 5480 m	1000-2000		
145° 55'E	100-200		2000-3000		
Date 26/Sept/1995	200-300				
	300-500				
	500-1000				

Stylochlamydidium venustum is observed in the upper surface layer of the southeastern South Atlantic (Abelmann and Gowing 1997) and the lower surface layer of the Gulf of Mexico and Caribbean Sea (McMillen and Casey 1978). In the southeastern South Atlantic, *S. venustum* is related with the Polar Front Surface Water Factor whose depth distribution is 0-100m (Abelmann and Gowing 1997). In the Gulf of Mexico and Caribbean Sea, *S. venustum* is observed in the 203-700m zone (McMillen and Casey 1978). Analogous to the North Pacific, the living depth of *S. venustum* increases with decreasing latitude.

Lastly, we compare our vertical distribution data to the geographic distribution patterns obtained from surface sediments which were shown in Lombardi and Boden (1986). The geographic distributions of three taxa (*D. tetrathalamus*, *Tetrapyle octacantha* group, and *L. buetschlii*) in surface sediments are illustrated in text-figure 8 (simplified from Lombardi and Boden 1986).

Didymocyrtis tetrathalamus is distributed between 45°N and 45°S, and its relative abundance is high in the oligotrophic re-

gion (the Tropical Circulation System except for the UW) (text-fig. 8a). Hence, its distribution is restricted in the Tropical and Subtropical Circulation Systems, and it favors the oligotrophic conditions. This result is similar to the result of Motoyama and Nishimura (2005). *Didymocyrtis tetrathalamus* is known to be a high temperature indicator (e.g., Anderson et al. 1990) and symbiotroph taxon (e.g., Sugiyama and Anderson 1998). Therefore, it can be an indicator of the Tropical and Subtropical Circulation Systems. In addition, *Didymocyrtis tetrathalamus* can live in the oligotrophic conditions attributing to the food supply by the symbiotic algae.

The geographic distribution of *T. octacantha* group is broader than that of *D. tetrathalamus* (text-fig. 8b). This result is supported by the above discussion in this study. Hence, *T. octacantha* group can live in a broader temperature range than that of *D. tetrathalamus*. The relative abundance of *T. octacantha* group is high in the UW characterized as the eutrophic region whereas *D. tetrathalamus* is dominant in the oligotrophic conditions. *Tetrapyle octacantha* group favors the eutrophic and warm region. Thus, while *Didymocyrtis tetrathalamus* and *T. octacantha*

group both favor warm water conditions, Probably, *Didymocyrtis tetrathalamus* shows low tolerance to nutrients, while *T. octacantha* group has a high tolerance to temperature.

Larcopyle buetschlii is abundant in the mixing zone between the Kuroshio and Oyashio Currents, the California Current, and the UW. These areas are eutrophic regions. Its geographic distribution may be associated with high productivity. In this study, *Larcopyle buetschlii* lives at approximately 50m water depths of the mid latitudes, and 200m water depths of the low latitudes, and thus this taxon is suggested as a “tropical submergence” taxon. In Boltovskoy (1988), the phenomenon called the “tropical submergence” has as a result that cold water taxa can survive in other regions in favorable temperature conditions. As we ascertain the association between temperature and this taxon, we use the annual temperature data observed in 2001 (Conkright et al., 2002). The temperature showing high relative abundance (50m water depths of mid latitudes, and 200m water depths of low latitudes) is approximately 13°C. This taxon is distributed in the high productivity region, and associated with low temperature (approximately 13°C).

CONCLUSIONS

1. *Didymocyrtis tetrathalamus* and *Tetrapyle octacantha* group are controlled by the warm water currents (text-figure 3a-b). *Tetrapyle octacantha* group is a Tropical-Subtropical indicator whose living zone is broader than that of *D. tetrathalamus*.

2. *Pseudocubus obeliscus* is restricted in the Subtropical and Tropical Circulation Systems and it is a productivity indicator (text-fig. 4a).

3. *Spongotrochus glacialis* appears to be advected from the Subarctic Current through the California Current into the central Equatorial Pacific (Text-figure 4b).

4. *Pseudodictyophimus gracilipes*, *Stylochlamydidium venustum*, *Larcopyle butschlii*, and *Litharachnium tentorium* are typical “tropical submergence” species (text-fig. 5). The depth of their maximum population deepened from the high latitudes to the low latitudes. This phenomenon is suggested to be associated with temperature gradients. *Larcopyle butschlii* shows the association with low temperature (Approximately 13°C).

5. *Botryostrobos aquilonaris* and *Stylodictya aculeata*, are defined as “upwelling” taxa (text-figs. 6a-c). These taxa live mainly in intermediate or deep water masses. However, in the upwelling region, they dwell in the surface layer with increased standing stocks. They may rise up into the surface layer by using the strong upwelling force near the coast.

These taxa can be used as indicators of various water masses. Further examinations of plankton tow, sediment trap, and surface sediment data, especially from other ocean basins than the North Pacific, are warranted in order to improve our knowledge of water mass-radiolarian relationships.

ACKNOWLEDGMENTS

We thank Dr. David Lazarus and Dr. Demetrio Boltovskoy for their constructive reviews as prereviewers of the first draft of this paper. We are grateful to Dr. Stan Kling and Dr. Guiseppa Cortese for their critical reading the manuscript as reviewers. We thank the members of the Paleoenvironmental Science Laboratory at the Kyushu University for helpful discussions and sugges-

TABLE 2

The information for sediment trap samples at seven stations: Takahashi (1991); Okazaki et al. (2005); and Takahashi, unpublished.

Reference	Station	Position	Date	Mooring depth (m)
Takahashi (1991)	P1	15°N, 151°W	Jul. 1978-Nov. 1978	378, 978, 2778, 4280, 5582
	PB	5°N, 81°W	Aug. 1979-Dec. 1979	667, 1268, 2869, 3769, 3791
Okazaki et al. (2005)	50N	50°N, 165°E	Dec. 1997-May. 2000	3260
	KNOT	44°N, 155°E	Dec. 1997-May. 2000	2957
	40N	40°N, 165°E	Dec. 1997-May. 2000	2986
Takahashi (unpublished)	PAPA	50°N, 145°W	Sep. 1982-Apr. 1986	1000 * 3800
	C	49.5°N, 138°W	May. 1985-Nov. 1985	3500

*Samplings were performed only from March to September 1983, and from May 1985 to April 1986.

tions. This study was supported by the following research programs: MEXT Grants-in-Aid-for Scientific Research B2 Project No. 15310001 and JSPS B Project No. 17310009.

REFERENCES

ABELMANN, A., and GOWING, M.M., 1997. Spatial distribution of living polycystine radiolarian taxa – baseline study for paleoenvironmental reconstructions in the Southern Ocean (Atlantic sector). *Marine Micropaleontology*, 30(1): 3-28.

ANDERSON, O. R., BRYAN, M., and BENNETT, P., 1990. Experimental and observational studies of radiolarian physiological ecology: 4. Factors determining the distribution and survival of *Didymocyrtis tetrathalamus tetrathalamus* with implications for paleoecological interpretations. *Marine Micropaleontology*, 16(2): 155-167.

BOLTOVSKOY, D., 1988. Equatorward sedimentary shadows of near-surface oceanographic patterns. *Speculations in Science and Technology*, 11(3): 219-232

———, 1994. The sedimentary record of pelagic biogeography. *Progress in Oceanography*, 34(2): 135-160.

BOLTOVSKOY, D., and RIEDEL, W.R., 1987. Polycystine Radiolaria of the California Current region: seasonal and geographic patterns. *Marine Micropaleontology*, 12: 65-104.

BOLTOVSKOY, D., OBERHANSLI, H., and WEFER, G., 1996. Radiolarian assemblages in the eastern tropical Atlantic: patterns in the plankton and in sediment trap samples. *Journal of Marine Systems*, 8(1): 31-51.

CASEY, R.E., 1971. Distribution of polycystine radiolaria in the oceans in relation to physical and chemical conditions. In: Funnel, B.M., Riedel, W.R., Eds., *The Micropaleontology of Oceans*, 151-159.

CONKRIGHT, M.E., et al. 2002: World Ocean Atlas 2001: Objective Analyses, Data Statistics, and Figures, CD-ROM Documentation. National Oceanographic Data Center, Silver Spring, MD, 17 pp.

DE WEVER, P., DUMITRICA, P., CAULET, J.P., NIGRINI, C., CARIDROIT, M., 2001. Radiolarian in the Sedimentary Record. *Gordon and Breach Science Publishers*, 533 pp.

DWORETZKY, B.A., and MORLEY, J.J., 1987. Vertical distribution of radiolaria in the eastern equatorial Atlantic: analysis of a multiple series of closely-spaced plankton tows. *Marine Micropaleontology*, 12: 1-19.

EMERY, W.J., and MEINCKE, J., 1986. Global water masses: summary and review. *Oceanologica acta*, 9(4): 383-391.

ISHITANI, Y., and TAKAHASHI, K., accepted. The vertical distribution of Radiolaria in the waters surrounding Japan. *Marine Micropaleontology*.

ITAKI, T., 2003. Depth-related radiolarian assemblage in the water-column and surface sediments of the Japan Sea. *Marine Micropaleontology*, 47(3): 253-270.

TABLE 3
Compiled standing stock data (No. of shells m⁻³) for the selected taxa.

Station ID	Station 2										Station 3						
Depth interval (m)	0-10	10-30	30-50	50-75	75-100	100-125	125-150	150-200	200-500	500-1000	0-40	40-80	80-120	120-160	160-200	200-500	500-1000
<i>Didymocystis tetrathalamus</i>	418.6	155.3	99.5	83.6	20.8	31.0	5.2	4.1	6.0	3.1	227.8	163.0	52.0	12.9	41.1	1.7	9.7
<i>Tetrapyle octacantha</i> group	158.4	27.9	39.2	41.8	20.8	46.5	7.3	14.3	13.7	4.6	142.4	177.8	52.0	7.8	130.0	1.1	6.5
<i>Pseudocubus obeliscus</i>	0	0	3.0	2.8	0	0	0	6.1	0	0	56.9	29.6	4.3	7.8	27.4	0.2	3.2
<i>Spongostochus glaciaris</i>	0	0	0	0	0	0	0	0	0	0	0	0	0	0	0	0	0
<i>Larcopyle butschlii</i>	0	0	0	0	0	0	0	0	0	1.0	0	0	0	0	41.1	0	0
<i>Litharacanthium tentorium</i>	0	0	0	0	2.3	0	7.3	14.3	5.1	0.7	0	0	0	15.5	68.4	2.3	3.2
<i>Pseudodicyophimus gracilipes</i>	0	3.1	6.0	2.8	1.2	15.5	15.7	69.7	27.5	2.0	19.0	7.4	17.3	44.0	109.5	2.3	11.3
<i>Stylochlamyidum venustum</i>	0	0	0	0	0	0	0	0	0.9	0.2	0	0	0	0	0	0	0
<i>Boiryostrobis aquilonaris</i>	0	0	0	0	0	12.9	1.0	0	0	0.5	0	0	0	0	0	0.2	0.8
<i>Dorydruppa bensoni</i>	0	0	0	0	0	0	0	0	0	0	0	0	0	0	0	0	0
<i>Stylodictya aculeata</i>	0	0	0	0	0	0	0	0	0	0	0	0	0	0	0	0	0
<i>Spongurus pylomaticus</i>	0	0	0	0	0	0	0	0	0	0	0	0	0	0	0	0	0

Station ID	Station 6							Station 9						
Depth interval (m)	0-40	40-80	80-120	120-160	160-200	200-500	500-1000	0-40	40-80	80-120	120-160	160-200	200-500	500-750
<i>D. tetrathalamus</i>	30.6	36.8	13.5	1.0	0	11.5	3.4	376.1	195.2	21.0	7.6	2.0	1.6	9.6
<i>T. octacantha</i> group	39.9	69.1	31.5	1.5	9.4	5.8	16.2	423.1	206.6	69.1	45.7	14.1	3.5	21.1
<i>P. obeliscus</i>	0	9.2	13.5	0	0	13.8	0	423.1	103.3	24.0	41.9	4.0	1.0	21.1
<i>S. glaciaris</i>	8.0	18.4	0	0.5	0	2.9	0	0	0	0	3.8	0	1.0	1.9
<i>L. butschlii</i>	0	0	9.0	1.0	0	2.9	4.7	0	0	0	3.8	0	0.3	5.7
<i>L. tentorium</i>	0	0	0	1.3	9.4	41.5	4.1	0	0	0	7.6	3.0	1.6	9.6
<i>P. gracilipes</i>	0	4.6	40.5	16.5	141.4	101.4	5.4	23.5	11.5	0	87.7	21.1	3.5	19.1
<i>S. venustum</i>	0	0	0	0	0	8.6	2.7	0	0	0	0	0	0	0
<i>B. aquilonaris</i>	0	0	0	0	0	0	0	23.5	0	0	0	0	0.6	1.9
<i>D. bensoni</i>	0	0	0	0.5	0	11.5	0	0	0	0	0	1.0	0	1.9
<i>S. aculeata</i>	0	0	0	0	4.7	0	0	0	0	9.0	0	0	0.6	0
<i>S. pylomaticus</i>	0	0	0	0	0	0	0	0	0	0	0	0	0	0

Station ID	Station 12					
Depth interval (m)	0-40	40-80	80-120	120-160	160-200	200-500
<i>D. tetrathalamus</i>	22.1	114.7	18.4	14.7	32.8	15.6
<i>T. octacantha</i> group	38.7	311.3	64.3	67.4	111.6	41.7
<i>P. obeliscus</i>	44.2	278.5	32.1	17.6	72.2	46.9
<i>S. glaciaris</i>	5.5	81.9	27.5	8.8	45.9	20.8
<i>L. butschlii</i>	0	0	0	0	0	5.2
<i>L. tentorium</i>	0	0	0	5.9	0	10.4
<i>P. gracilipes</i>	3.7	49.2	9.2	32.3	32.8	57.3
<i>S. venustum</i>	0	0	0	0	0	0
<i>B. aquilonaris</i>	0	0	0	0	0	0
<i>D. bensoni</i>	0	0	0	2.9	0	0
<i>S. aculeata</i>	0	0	0	0	6.6	0
<i>S. pylomaticus</i>	0	0	0	0	0	0

Station ID	Station E							Station A						
Depth interval (m)	0-20	20-40	40-60	60-80	80-120	120-160	160-200	0-20	20-40	40-60	60-80	80-120	120-160	160-200
<i>D. tetrathalamus</i>	32.6	0	17.6	0	0	0	3	6.8	0	0	0	0	0	0
<i>T. octacantha</i> group	18.6	17.2	45.7	5.3	0	5.4	0	6.8	3.3	0	0	0	0	0
<i>P. obeliscus</i>	14.0	5.7	7	8	2.7	2.7	3	20.3	13	8.9	16.8	3.3	0	4.7
<i>S. glaciaris</i>	9.3	5.7	7	2.7	0	0	0	0	0	0	6.7	0	0	0
<i>L. butschlii</i>	0	0	0	0	0	2.7	0	0	0	0	0	0	1.5	0
<i>L. tentorium</i>	0	0	0	0	0	0	0	0	3.3	0	0	9.8	0	4.7
<i>P. gracilipes</i>	0	0	0	0	8.2	8	9.1	0	3.3	17.7	26.8	0	7.5	9.5
<i>S. venustum</i>	0	0	0	0	0	0	0	0	0	0	0	0	0	0
<i>B. aquilonaris</i>	0	0	0	0	0	0	0	0	0	0	0	0	0	0
<i>D. bensoni</i>	0	0	0	0	0	0	0	0	0	0	0	0	0	0
<i>S. aculeata</i>	0	0	0	0	0	0	0	0	0	0	0	0	0	0
<i>S. pylomaticus</i>	0	0	0	0	0	0	0	0	0	0	0	0	0	0

Station ID	Station B							Station b						
Depth interval (m)	0-20	20-40	40-60	60-80	80-120	120-160	160-200	0-20	20-40	40-60	60-80	80-120	120-160	160-200
<i>D. tetrathalamus</i>	0	0	0	0	0.9	12.6	0	0	0	0	0	0	0	0
<i>T. octacantha</i> group	1	0	0	1.4	0.9	0	0	0	0	0	0	0	0	0
<i>P. obeliscus</i>	1.9	0	1.6	0	1.9	0	8.4	0	0	0	0	0	0	0
<i>S. glaciaris</i>	0	1.6	0	0	0	1.1	9.6	0	12.7	0	0	3.7	0	4.8
<i>L. butschlii</i>	0	0	0	2.8	6.5	8	3.6	0	50.7	19.6	0	7.5	0	0
<i>L. tentorium</i>	0	0	0	0	0	0	0	0	0	0	0	0	0	0
<i>P. gracilipes</i>	39.8	72.8	152.2	71.7	47.7	35.5	1.2	0	0	0	0	0	4.6	0
<i>S. venustum</i>	0	0	0	0	0	0	0	0	0	0	0	0	0	0
<i>B. aquilonaris</i>	0	0	0	0	0	0	0	0	0	0	0	0	0	0
<i>D. bensoni</i>	0	0	0	0	0	0	0	0	0	0	0	0	0	0
<i>S. aculeata</i>	0	0	0	0	0	0	0	0	0	0	0	0	0	0
<i>S. pylomaticus</i>	0	0	0	0	0	2.3	0	0	0	0	0	0	0	0

Station ID	Station X					Station H					Station SA						
Depth interval (m)	0-50	50-100	100-200	200-300	300-500	0-50	50-250	250-500	500-1000	1000-2000	2000-3000	0-50	50-250	250-500	500-1000	1000-2000	2000-3000
<i>D. tetrathalamus</i>	0	0	0	0	0	0	0	0	0.3	0	0	0	0	0	0	0	0
<i>T. octacantha</i> group	0	0	0	0	0	0	0.8	0	0	0.1	0	0	0	0	0	0	0
<i>P. obeliscus</i>	0	0	0	0	0	0	0	0	0.3	0	0	0	0.6	0	0	0	0
<i>S. glaciaris</i>	0.9	2.8	0.3	0.2	0.1	42	25.2	1.8	2.1	0.1	0	309.1	52.9	1.5	0.6	0.3	0
<i>L. butschlii</i>	0	0	0	0	0	0	3.2	0	0	0	0	0	0	0	0	0	0
<i>L. tentorium</i>	0	0	0	0.4	0.2	0	0	0	0	0.3	0	0	2.5	0	0	0	0
<i>P. gracilipes</i>	0.2	1.9	1.7	0.4	0	0	6.3	0	1.3	1	0.6	4.2	8.7	0	1.4	1.3	0.2
<i>S. venustum</i>	0.5	1.7	0.5	0.3	0	10.5	6.3	1.2	0	0	0	0	12.4	0	0	0	0
<i>B. aquilonaris</i>	0	0	0	0	0.1	0	0.8	0.6	0	0	0	0	0.6	5.5	1.7	0	0
<i>D. bensoni</i>	1.4	1.9	0.2	0	0	0	0.8	0	0	1.2	0	0	0	0	0	0.4	0.2
<i>S. aculeata</i>	0	0	0	0	0	0	0	0	0	0	0	0	0	0	0.3	0.4	0
<i>S. pylomaticus</i>	0	0.2	0	0	0.1	0	0	1.2	0	0	0	0	0.6	0	0	0.1	0

- ITAKI, T., ITO, M., NARITA, H., AHAGON, N., SAKAI, H., 2003. Depth distribution of radiolarians from the Chukchi and Beaufort Seas, western Arctic. *Deep-Sea Research I*, 50(12): 1507-1522.
- JOHNSON, G. C., and MCPHADEN, M. J., 1999. Interior pycnocline flow from the Subtropical to the Equatorial Pacific Ocean. *Journal of Physical Oceanography*, 29(12): 3073-3089.
- KLING, S.A., 1979. Vertical distribution of polycystine radiolarians in the central North Pacific. *Marine Micropaleontology*, 4: 295-318.
- KLING, S.A., and BOLTOVSKOY, D., 1995. Radiolarian vertical distribution patterns across the southern California Current. *Deep-Sea Research I*, 42(2): 191-231.
- LUKAS, R., and LINDSTROM, E., 1991. The mixed layer of the western Equatorial Pacific Ocean. *Journal of Geophysical Research*, 96(Supplement), 3343-3357.
- LOMBARI, G., and BODEN, G., 1985. Modern Radiolarian Global Distributions. *Cushman Foundation for Foraminiferal research, Special Publication 1* 6A, 125pp.
- MCMILLEN, K.J., and CASEY, R.E., 1978. Distribution of living polycystine radiolarians in the Gulf of Mexico and Caribbean Sea, and comparison with the sedimentary record. *Marine Micropaleontology*, 3(2): 121-145.
- MOTOYAMA, I., and NISHIMURA, A., 2005. Distribution of radiolarians in North Pacific surface sediments along the 175E meridian. *Paleontological Research*, 9(2): 95-117.
- OKAZAKI, Y., TAKAHASHI, K., ITAKI, T., and KAWASAKI, Y., 2004. Comparison of radiolarian vertical distributions in the Okhotsk Sea near Kuril Islands and the northwestern North Pacific off Hokkaido Island. *Marine Micropaleontology*, 51(3-4): 257-284.
- OKAZAKI, Y., TAKAHASHI, K., ONODERA, J., and HONDA, C. M., 2005. Temporal and spatial flux changes of radiolarians in the northwestern Pacific Ocean during 1997-2000. *Deep-Sea Research I*, 52(16-18), 2240-2274.
- RENZ, G.W., 1976. The distribution and ecology of radiolaria in the central Pacific: plankton and surface sediments. *Bulletin of the Scripps Institution of Oceanography*, 22. 267pp.
- SCHLITZER, R., Ocean Data View, <http://www.awi-bremerhaven.de/GEO/ODV>, 2003.
- STEEL, J. H., THORPE, S. A., TUREKIAN, K. K., 2001. *Encyclopedia of Ocean Science*. Academic Press. 3399 pp.
- SUGIYAMA, K., and ANDERSON, O. R., 1998. Cytoplasmic organization and symbiotic associations of *Didymocyrtis tetrathalamus* (Haeckel) (Spumellaria, Radiolaria). *Micropaleontology*, 44(3): 277-289.
- SVERDRUP, H. U., JOHNSON, M. W., FLEMING, R. H., 1941. *The Oceans*. Prentice Hall Inc., 1087 pp.
- TAKAHASHI, K., 1991. Radiolaria: flux, ecology, and taxonomy in the Pacific and Atlantic. In: Honjo, S., Ed., *Ocean Biocoenosis, Series 3*. Woods Hole, MA: Woods Hole Oceanography Inst. Press, 303 pp.
- , 1995. Opal particle flux in the Subarctic Pacific and Bering sea and sidocoenosis preservation hypothesis. In: Tsunogai, S., et al., Eds., *Global fluxes of Carbon and Its Related Substances in the Coastal Sea-Ocean-Atmosphere System, Proceedings of the 1994 Sapporo IGBP Symposium*, 458-466. Yokohama: M&J International.
- WELLING, L.A., PISIAS, N.G., JOHNSON, E.S., and WHITE, J.R., 1996. Distribution of polycystine radiolaria and their relation to the physical environment during the 1992 El Nino and flowing cold event. *Deep-Sea Research I*, 43(4-6): 1413-1434.
- YAMASHITA, H., TAKAHASHI, K., and FUJITANI, N., 2002. Zonal and vertical distribution of radiolarians in the western and central Equatorial Pacific in January 1999. *Deep-Sea Research I*, 49(13-14): 2823-2862.
- YASUDA, I., 2003. Hydrographic structure and variability in the Kuroshio-Oyashio transition area. *Journal of Oceanography*, 59(4): 389-402.

Patterns of opal and radiolarian change in the Antarctic mid-Paleogene: clues to the origin of the Southern Ocean

D.B. Lazarus,^{1,3} C.J. Hollis² and M. Apel¹

¹*Museum f. Naturkunde, Invalidenstrasse 43, 10115 Berlin*

²*GNS Science, 1 Fairway Drive, Avalon 5010, PO Box 30-368, Lower Hutt 5040, New Zealand*

³*Corresponding author: david.lazarus@rz.hu-berlin.de*

ABSTRACT: The timing of the origin of the Southern Ocean is important for studies of Antarctic biologic evolution and for understanding past climate change. The long standing theory that separation of Australia from Antarctica at the end of the Eocene allowed the development of a circumpolar ocean circulation, isolating the Antarctic continent and causing ice-sheet growth at the Eocene-Oligocene boundary, has recently been challenged by ODP Leg 189 drilling south of Australia. Based on these new cores it has been proposed that separation and Southern Ocean formation had already occurred within the late Eocene, approximately 2 my before the Antarctic became glaciated. This proposal however extrapolates data from a limited area to the history of a large circumpolar ocean region. To better determine Southern Ocean history we have compiled data from a large number of locations around Antarctica on opal accumulation and have analyzed circum-polar radiolarian faunas for development of endemism and evolutionary turnover. Our results show that opal deposition was widespread in the late Eocene Antarctic oceans with concentrations similar to that of the early Oligocene; substantial endemism was already present in late Eocene radiolarian faunas, and that most evolutionary turnover, in particular the origin of taxa characteristic of the early Oligocene, had already taken place within the late Eocene (ca 35 Ma). We conclude that there is a significant (ca 2 my) gap between a late Eocene Southern Ocean origin and later, Eocene-Oligocene boundary Antarctic glaciation.

INTRODUCTION

The origin and subsequent evolution of the Southern Ocean is one of the most significant events in the Cenozoic. The Southern Ocean today is the single largest source of the world ocean's bottom waters, plays a major role in regulating the global climate, and hosts a diverse biota, whose unique adaptations and evolutionary history are of great biologic interest. The dominant theory of Southern Ocean origins for three decades has been that of Kennett (1977). This theory postulates that the plate-tectonic driven separation of Australia from Antarctica at the end of the Eocene allowed a wind-driven circumpolar ocean current to develop that prevented warmer temperate waters from reaching and warming the Antarctic continent. The subsequent cooling of the continent led to glaciation, with further cooling and intensification of circumpolar Southern Ocean circulation due to the effects of glaciation on climate (Kennett 1977).

Although a true circumpolar circulation system requires an open passage between Australia and Antarctica, there are many still unresolved questions about Kennett's theory. These include the development of passages at other points around the Antarctic continent, in particular when the Drake Passage between Antarctica and South America opened (Barker and Burrell 1977; Barker and Thomas 2004); and more generally, to what extent a circumpolar circulation truly regulates climate on the Antarctic continent. Ocean circulation simulations had by the early 1990s already suggested that even in the absence of true circumpolar circulation significant regional frontal systems would be present that would have largely prevented lower latitude currents from warming the Antarctic continent (Barron and Peterson 1991). More recent computer models of climate and ocean circulation (Huber et al. 2004) have reached similar conclusions. Decreasing late Paleogene atmospheric CO₂ concentrations have been suggested instead as an alternative mechanism for initiating Antarctic glacia-

tion (De Conto and Pollard 2003). This proposed mechanism is not necessarily mutually exclusive to that of ocean circulation, in that ocean circulation driven changes in export production of organically fixed carbon may play a major role in controlling the atmospheric concentration of CO₂.

In order to test these different hypotheses, accurate data is needed on the timing and degree of development of the Southern Ocean, the effect this had on oceanic export productivity, and the relationship in time between Southern Ocean development, tectonic development of oceanic passageways, Antarctic glaciation, ocean temperature change, and atmospheric CO₂ concentration, among other parameters. Many of these parameters are still poorly constrained, although much progress has also been made in many areas. Recent deep sea drilling south of Australia for example (Scientific Party 2002) has provided new data that better constrains the separation of Australia from Antarctica and the development of this oceanic gateway. From this work it has been suggested that the gateway between Australia and Antarctica had already largely opened by the mid-late Eocene (Stickley et al. 2004a, b), and thus that ocean circulation change substantially preceded (by ca 2 my) the end-Eocene glaciation of Antarctica, with the implication that tectonics and circulation change did not have a simple, direct effect on continental climate change (Huber et al. 2004).

This conclusion however is somewhat tentative, in part due to the limited geographic extent of the cores used in the studies. These are largely located near the southeastern end of the Australian continent, and partially in shallow, nearshore settings, so that the possibility exists that more local oceanographic changes might be dominating the signal, rather than the oceanographic history of the much larger circumpolar region. In this paper we therefore provide a summary of several paleoceanographically sensitive parameters from mid-Paleogene sediments from a wider variety of locations around the

Radiolarian faunal turnover in the Antarctic Neogene is known to be closely linked to changes in Southern Ocean environments (Lazarus 2002). It is therefore reasonable to expect that as the distinctive characteristics of the Southern Ocean first evolved in the Paleogene due to changing patterns of ocean circulation, that radiolarian faunas would evolve in response. Periods of relatively rapid faunal turnover should therefore mark intervals of relatively rapid or extensive change in Southern Ocean conditions. Further, in that a species' evolution is a response to the environmental pressures felt over the entire biogeographic range of the species, evolutionary patterns of change, particularly when compiled from entire faunas, are likely to be more reliable indicators of regional patterns of change in environment than change in taxa abundances noted in a small number of geographically restricted sections.

In this study we have attempted to provide, for the first time, a comprehensive survey of the stratigraphic distribution and development of Antarctic Paleogene radiolarian taxa. All forms encountered in a survey of standard (45 µm) random-strewn slides made from 85 samples from two geographically widely spaced composite sections constructed from four DSDP and ODP sites (table 1) were digitally imaged, assigned to provisional taxonomic categories, and the distribution of each form in each location was tabulated in standard occurrence tables (supplemental data, available at www.pangea.de). For purposes of providing an overview of radiolarian evolutionary change throughout the Antarctic, all of our data were compiled into a single circum-Antarctic composite occurrence table. The ranges of species were determined by visual inspection of ranges; error bars for ranges were based on average gap size - similar methods have been employed previously (Lazarus 2002) and are well established in paleobiological research. Few taxa had first or last occurrence uncertainties that extended beyond ca 1 my, and we do not feel range uncertainties significantly affect our conclusions. Because many of the more than 200 taxa encountered are new and still in open nomenclature, we are not yet able to combine these data with coeval data from other geographic regions to provide an improved biogeographic analysis of Antarctic Paleogene radiolarian faunas. Changes of the radiolarian faunas within the Antarctic over time, and in particular intervals of relatively rapid faunal turnover, are however quite robust and are unlikely to be significantly affected by additional taxonomic research. In this paper we therefore present a summary of the stratigraphic range data and the evolutionary metrics derived from it. Additional details and a full taxonomic documentation of the forms used are given in Apel (2005).

MATERIAL

Text-figure 1 and table 1 provide an overview of the materials and sources synthesized in this paper. In addition to a variety of DSDP and ODP Holes (including many ODP Holes from Legs drilled after the earlier synthesis of Lazarus and Caulet (1993)), we include older data from piston cores first given in Lazarus and Caulet (1993) as well as previously unsynthesized data from relevant onshore New Zealand sections (North Island and Oamaru diatomites, summarized in O'Connor 2000).

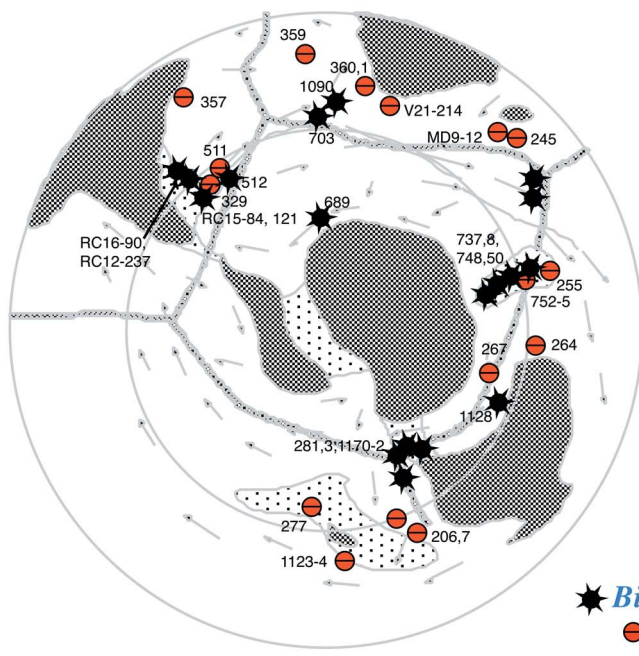
RESULTS

Opal Geographic Distribution

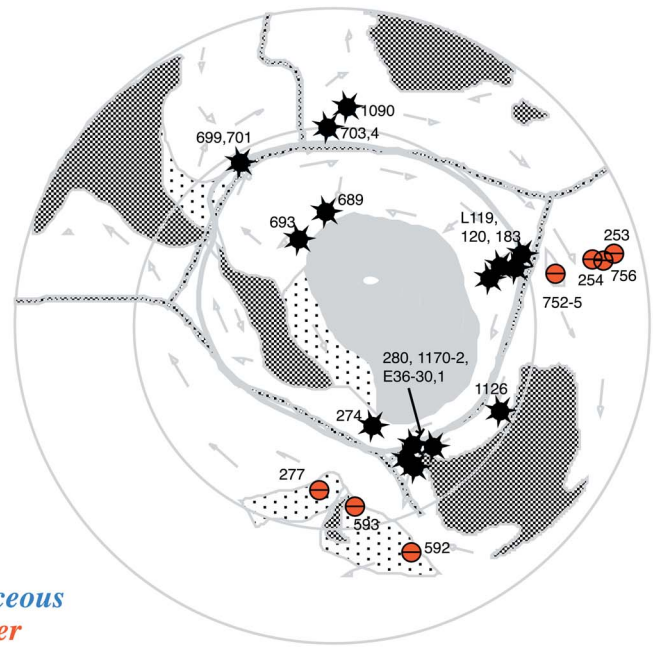
Geographic syntheses of data from Antarctic Paleogene sediments are a compromise between number of data points avail-

TABLE 1
Sediment cores and published sources of information used in this paper.
Time Series - E: evolution; O: opal.

Site	Latitude	Longitude	Time Series
206	-32.01	165.45	
207	-36.96	165.43	
245	-31.53	52.30	
253	-24.88	87.37	
254	-30.97	87.90	
255	-31.13	93.73	
264	-34.97	112.04	
267	-59.26	104.49	
274	-69.00	173.43	
277	-52.22	166.19	
280	-48.96	147.23	
281	-48.00	147.76	
283	-43.91	154.28	
329	-50.66	-46.10	
357	-30.00	-35.56	
359	-34.98	-4.50	
360	-35.85	18.10	
361	-35.07	15.45	
511	-51.00	-46.97	E
512	-49.87	-40.85	
592	-36.47	165.44	
593	-40.51	167.67	
689	-64.52	3.10	E,O
693	-70.83	-14.57	
699	-51.54	-30.68	
701	-51.98	-23.21	
703	-47.05	7.89	
704	-46.88	7.42	
737	-50.23	73.03	
738	-62.71	82.79	
748	-58.44	79.00	E,O
750	-57.59	81.24	
752	-30.89	93.58	
753	-30.84	93.59	
754	-30.94	93.57	
755	-31.03	93.55	
756	-27.36	87.60	
1090	-42.91	8.90	O
1123	-41.79	-171.50	
1124	-39.50	-176.53	
1126	-33.51	128.07	
1128	-34.39	127.59	
1138	-53.55	75.97	E
1170	-47.15	146.05	
1171	-48.50	149.11	
1172	-43.96	149.93	
RC16-90	-41.17	-52.54	
RC12-237	-47.47	-57.39	
RC15-84	-50.29	-44.43	
RC15-121	-49.37	-55.54	
V24-214	-37.03	24.57	
MD9-12	-32.38	50.47	
E36-30	-54.04	155.00	
E36-31	-55.00	155.00	



TEXT-FIGURE 2
Eocene opal distribution. Black stars indicate Eocene sediment with at least several percent biogenic opal and/or at least moderately preserved opaline microfossils. All other sediment types, including pure carbonate oozes to barren red clays are marked with red barred circles.



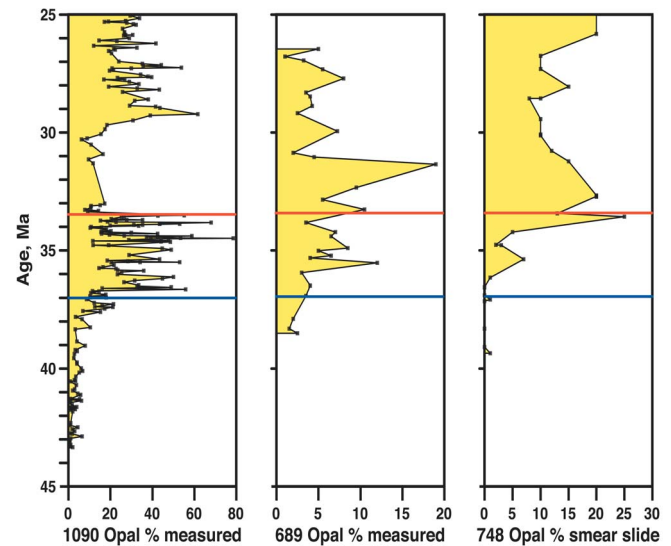
TEXT-FIGURE 3
Early Oligocene opal distribution. Symbol plotting conventions as in text-figure 2.

able and the temporal resolution of the reconstructed time interval. Our opal distribution maps (text-figures 2 and 3) are, as was true for those of Lazarus and Caulet (1993) limited to just 'Eocene' and 'Early Oligocene', although, as shown in the following section, most of the Eocene data on opal are likely to be of Late Eocene age. Other than a couple of minor corrections to the analysis of Lazarus and Caulet (1993) (Sites 703 and 704 are here classified as containing opal), the major differences are due to the addition of new data from more recently drilled ODP sites, e.g. Leg 177 Site 1090 in the South Atlantic (Scientific Party 1999), and several sites from Legs 182, 183 and 189 in the south Australian and southwest Pacific sectors of the Antarctic (Scientific Party 2000a, b; 2002). The addition of these data simply reinforce the more tentative conclusions reached by Lazarus and Caulet (1993), that biosiliceous sedimentation was widespread in the (late) Eocene Antarctic oceans. There is no indication from the available data that there was any significant change in the areal extent of opal deposition between the (late) Eocene and early Oligocene. However, to determine this more accurately more precisely dated opal abundance data are needed, and in a more quantitative form than the relatively crude presence-absence type of information used for our geographic reconstructions.

Opal Time Series

Quantitative time series of opal abundance in late Eocene-early Oligocene Antarctic sediments have been published recently by Diekmann et al. (2004) for Site 1090 and Schumacher and Lazarus (2004) for Sites 689 and 748, the latter two based on Initial Reports smear slide and geochemical data, the first Site on new geochemical measurements of sample material. These sites form a transect from north of the current position of the Polar Front to locations well south of the Polar Front, and are from both the Atlantic and Indian Ocean sectors of the Antarctic ocean. The data

from these Sites (text-fig. 4) show a remarkably coherent pattern, with significant opal deposition beginning somewhat below, or near the base of the late Eocene and increasing through the late Eocene to values typical of the subsequent opal-rich sediments of the Oligocene. There is a weak suggestion that early Oligocene opal accumulation was somewhat more geographically partitioned, with opal content being reduced in the most northerly Site 1090 in comparison to the more southerly Sites 689 and 748. This inference is however based on just three locations and, for



TEXT-FIGURE 4
Time series of opal abundance in Eocene-Oligocene sections from the Antarctic ocean. Replotted from data presented in Diekmann et al. (2004) (Site 1090) and Schumacher and Lazarus (2004) (Sites 689 and 748; the latter publication also gives details of age models used and primary sources for both of the latter data sets). Lines at 37 Ma and 33.7 Ma mark boundaries of Late Eocene.

the sole northerly Site 1090, is complicated by the inferred presence of a hiatus in the early Oligocene (Schumacher and Lazarus 2004).

Radiolarian Biogeographic Patterns

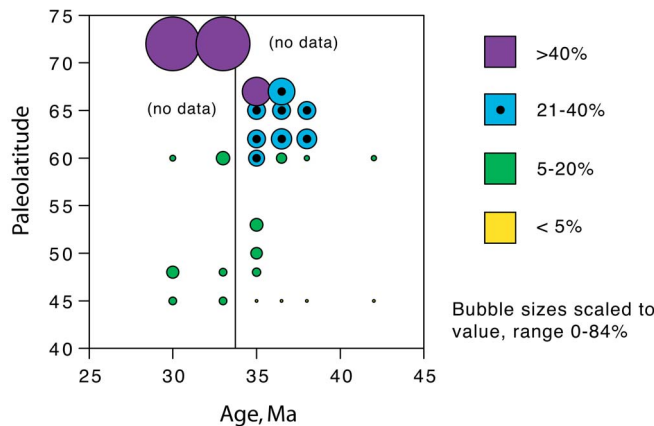
Other than Site 1090, for which no detailed radiolarian census data has been published, most new data suitable for biogeographic analysis comes from the Australian-southwest Pacific sector of Antarctic ocean, and we therefore restrict our analysis to this region. A benefit from this is the ability to better correlate data in this more restricted data set over more precise time intervals, so that in our analysis data can be binned into ca 3 my long intervals, based on various austral biozonations (table 2). The numerical values for each binned interval are plotted vs paleolatitude and age in text-fig. 5. Despite many gaps in coverage, significant percentages of polar forms, and a clear gradient in the relative abundance of polar radiolarian faunas can be seen which extends at least as far back as the early late Eocene. Although the highest values for polar faunal content are found in the early Oligocene, these are also in the highest paleolatitude locations and comparable high paleolatitude data for the late Eocene are not available, so it is not clear if the Eocene-Oligocene boundary marked a significant increase in polar faunal development or not.

The late Eocene is the time interval with the most complete paleolatitudinal coverage for radiolarian biogeographic data. To place these data in context, they are plotted on the recently published numerically modeled paleoceanographic reconstruction for the late Eocene Australo-southwest Pacific of Huber et al. (2004) (text-fig. 6). Despite limited geographic coverage the available radiolarian paleobiogeographic data for the late Eocene agrees very well with Huber et al.'s (2004) inferred oceanographic conditions for this region.

Radiolarian Evolutionary Turnover

Summary radiolarian taxa ranges for all taxa in our survey are presented graphically in text-fig. 7. Two views of the data are given - with ranges sorted by first appearance (origins) and by last occurrence (extinctions).

Approximately half of the taxa in our data appear either prior to the time interval studied or shortly thereafter (text-fig. 7a). However, as preservation of radiolarians is very poor near the base of our study interval (e.g. prior to ca 37 Ma) many of the apparent



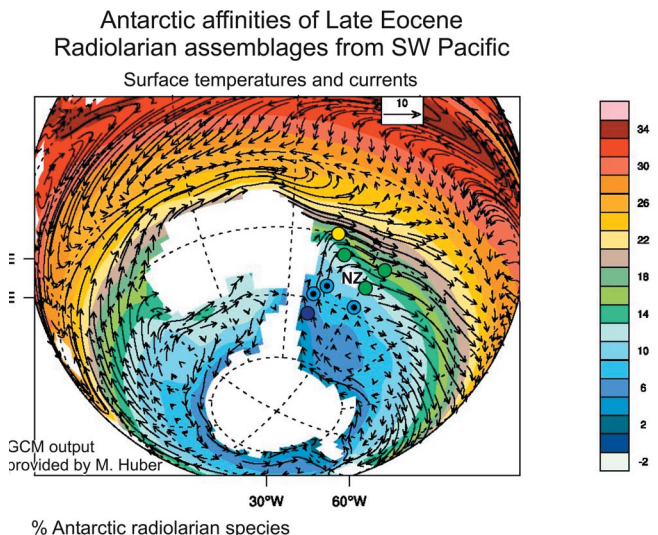
TEXT-FIGURE 5
Endemic+bipolar radiolarian taxa, by age and paleolatitude, southwest Pacific Paleogene. Based on data given in table 2. Bubble diameters are proportional to numeric value, and are additionally color coded according to percent endemic+bipolar to allow direct comparison to text-figure 6.

TABLE 2
Percent endemic+bipolar taxa in radiolarian faunas by time interval in SW Pacific Paleogene sediments.

Site/Age Interval	Mean Age (Ma)	Paleo-latitude (°)	Endemic+ Polar(%)
206 LEO	30	45	0
206 EEO	33	45	0
206 LLE	35	45	0
206 ELE	36.5	45	0
206 LME	38	45	0
206 MME	42	45	0
North Island	30	45	8.9
North Island	33	45	8.9
1123 LEO	30	48	15.4
1123 EEO	33	48	8.3
1123 LLE	35	48	10
592 LLE	35	50	15
Oamaru Fm LLE	35	53	17.3
277 LEO	30	60	6
277 EEO	33	60	18
277 LLE	35	60	22
277 ELE	36.5	60	13
277 LME	38	60	5
277 MME	42	60	5
283 LLE	35	62	25
283 ELE	36.5	62	29
283 LME	38	62	28
1172 LLE	35	65	25
1172 ELE	36.5	65	25
1172 LME	38	65	25
281 LLE	35	67	43
281 ELE	36.5	67	38
280 LLE	35	67	40
280 ELE	36.5	67	40
274 LEO	30	72	84
274 EEO	33	72	84

originations between 36 and 37 Ma probably reflect incomplete sampling or taxa rarity in the small number of samples above the interval of poor preservation. A much larger pulse of originations occurs however at ca 35 +/- 0.5 Ma. Preservation is generally good in this time interval and sampling is thought to be adequate to resolve taxa ranges to within ca 1 my (see Methods), so this origination pulse is thought to be a real feature of the evolutionary history of radiolarians in the Antarctic region. Originations for the remainder of the study interval are more or less uniformly distributed over time from the latest Eocene through early Oligocene. There is no significant pulse of origination associated with the Eocene-Oligocene boundary. Funakawa and Nishi (2008 - this issue) in a higher temporal resolution analysis, albeit of assemblages at a single location (ODP Site 689) also note a series of important turnovers in the radiolarian fauna within the late Eocene, with two events at ca. 36.5 and 34 Ma.

Extinctions (text-fig. 7b), in contrast to the pattern of originations, do not show any significant intervals of enhanced turnover. The apparent truncation of taxa ranges near the top of the study interval at ca 28.2 Ma is, like its counterpart at the base of the study interval, almost certainly an example of the well known 'edge' effect, e.g. an artefact of incomplete sampling, gaps in in-



TEXT-FIGURE 6

Late Eocene endemic+bipolar radiolarian faunal percentages (colored dots near New Zealand) plotted on simulated late Eocene paleoceanography of Huber et al. (2004). Color codes of dots refer to relative percent endemic+bipolar forms, same scale as in text-figure 5. Ocean colors are simulated surface water temperature, scale given on figure right.

dividual occurrences, and the lack of additional samples beyond the range of the study interval that would extend taxa ranges to the study interval boundaries.

DISCUSSION AND CONCLUSIONS

The primary goal of this paper has been to review several paleoceanographically significant parameters from Antarctic Paleogene sediments to better constrain the timing and geographic extent of Southern Ocean development in the early Cenozoic. For this purpose we have used the presence of opal in sediments, as this is both a feature of the modern Southern Ocean and more generally an indicator of enhanced export productivity. Although there is some evidence that Paleogene opal deposition was more widespread, and thus less of a specific indicator for productivity, this pattern is primarily restricted to the early-mid Eocene, rather than the late Eocene interval of our study (McGowran 1989). Our results are also in general agreement with other studies of Antarctic productivity change in the mid Paleogene (e.g. Diester-Haass 1994; Diester-Haass and Zahn 1996; summary in Schumacher and Lazarus 2004) which include other types of proxy data including benthic foraminifera and other sedimentary parameters.

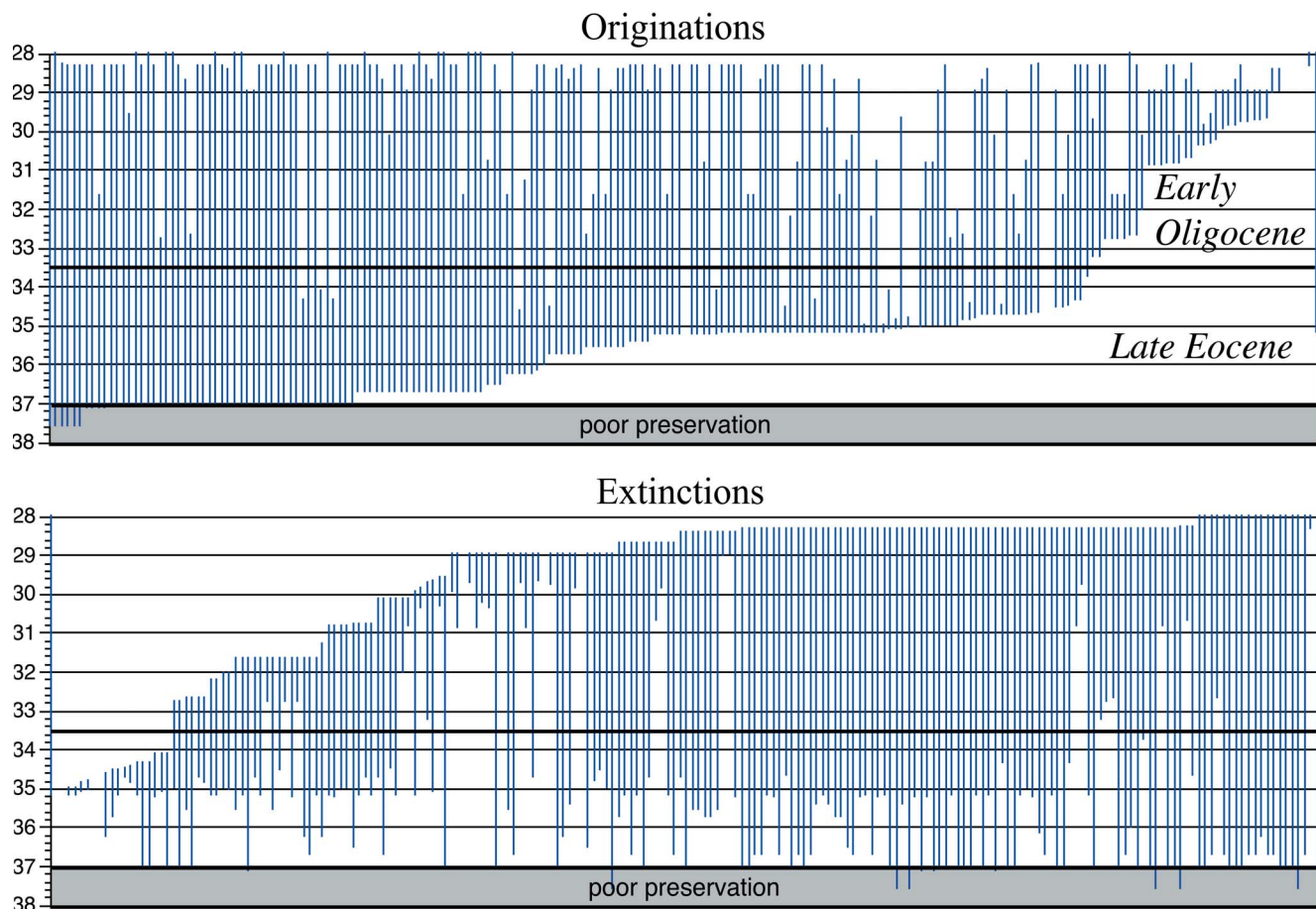
We have also summarized the development of radiolarian faunas in the Antarctic, using both biogeographic patterns and patterns of evolutionary turnover as descriptors of radiolarian faunal change. Although the modern radiolarian fauna largely originated in the mid Neogene (Lazarus 2002), radiolarian faunas today are sensitive markers for oceanic water mass boundaries and frontal systems throughout the world ocean, not only the Antarctic, and thus may be seen as reasonable probes of past oceanic conditions. Radiolarians have a particular advantage over other microfossil groups in being distributed over a broad depth range, including numerous deep water forms, so that changes in faunal composition are likely to reflect changes throughout the water column, not just changes in surface water environments. Limitations to our methods are equally important, particularly

in interpreting radiolarian faunal change. Although we can argue for change in ocean environment based on our radiolarian faunal analyses, without more detailed knowledge of these now mostly extinct species' ecology, including depth preferences, we can not specify in physical oceanographic terms what types of changes may have occurred. Nonetheless, substantial change in faunal composition almost certainly reflects substantial change in those characteristics of the modern Southern Ocean to which radiolarians are currently adapted - seasonally limited high productivity and weak and strongly variable water column stratification, among other factors. It is worth noting that among those of the modern Southern Ocean radiolarian taxa that are not actually endemic to the Antarctic, many are found only in other ocean regions where export productivity is high and seasonal and water column stratification is relatively weak and variable, e.g. low latitude upwelling zones, and the boreal North Pacific and Norwegian-Greenland Sea.

All of the data reviewed here suggests that most of the oceanographic changes that occurred in the Antarctic during the mid Paleogene were concentrated within the late Eocene time interval. Biogenic opal accumulation had already increased to approximately the same values seen in the subsequent Oligocene in sections where quantitative data are available, and, although limited by poor temporal resolution, the available data suggest that opal deposition and the implied elevated levels of export productivity was already very widespread in the Antarctic by the late Eocene. This is similar to the conclusion reached by Schumacher and Lazarus (2004) who reviewed opal and benthic foraminiferal data. Radiolarian faunas already show substantial levels of endemic and bipolar forms in the late Eocene, at least in the temporally best resolved data from the Australo-southwest Pacific sector, and most of the species that characterize the Oligocene Southern Ocean had already evolved within the late Eocene, with a particularly strong pulse of originations at ca 35 Ma. Thus, all evidence reviewed here suggests that the primary characteristics of the Southern Ocean, insofar as they were present in the Oligocene, had already developed within the late Eocene. The Eocene-Oligocene boundary by contrast does not appear to mark any significant changes in ocean characteristics in our study, despite this period being marked by the most dramatic change in the Cenozoic marine stable oxygen record, which is thought to record the growth of an Antarctic continental ice-sheet (Miller et al. 1987; Zachos et al. 2001).

The above conclusion is thus broadly in agreement with those of Huber et al., (2004). So far as we can determine from our data, Southern Ocean development temporally preceded, by about 2my, the origination of Antarctic continental glaciation. Further, the origination of the ice-sheet at the Eocene-Oligocene boundary did not by itself have any immediate, major impact on the environment of the Southern Ocean, at least as it affected surface or deep water plankton, or surface water productivity.

These conclusions are limited by the current nature of the data, including gaps in temporal and geographic recovery of mid-Paleogene sediments around Antarctica, and by poor taxonomic and ecologic knowledge of Antarctic Paleogene radiolarian faunas. Nor do these conclusions necessarily refute the broader aspects of Kennett's (1977) hypothesis that the separation of Antarctica and Australia played an important role in the development of Antarctic, and global Cenozoic climate. For example, we still do not, in our opinion, have a robust chronology for the opening of the relevant seaways around the Antarctic continent, due both to tectonic uncertainties, particularly for the Drake Passage, and due to our



TEXT-FIGURE 7

Radiolarian species ranges from a composite of Paleogene Antarctic sections, sorted by a) first occurrences and b) last occurrences. Ranges are based on occurrence data tables from four late Eocene and early Oligocene DSDP and ODP sections from both the Atlantic and Indo-Australian sectors of the Antarctic ocean. Range accuracy based on gap sizes in occurrence tables varies with species but generally is ca 1 my. Names of taxa (many of which are provisional or in open nomenclature) not given for clarity but are available with age ranges upon request to senior author. Age models, detailed taxonomic information for each species and all sections occurrence data given in Apel (2005).

limited knowledge of how extensive a seaway need be to have a substantial oceanographic influence. We also do not have a clear understanding of the relationships between oceanographic change, climate change, atmospheric CO₂ concentrations and ice-sheet development. De Conto and Pollard (2003) for example have suggested that the relationship between CO₂, climate change and ice-sheet growth may be complex and highly non-linear, with most ice-sheet growth occurring rapidly once a critical threshold in CO₂ regulated atmospheric temperature has been crossed. Similar links and possible non-linear feedback effects between oceanographic change, particularly ocean productivity, and climatic change still need to be explored.

ACKNOWLEDGMENTS

The authors wish to thank Cathy Stickley and Mat Huber for reviews of the manuscript and for sharing unpublished data and figures. Dr. Apel's work was supported by a DFG financed Graduate College stipend.

REFERENCES

- APEL, M., 2005. "Taxonomie, Evolution und Diversitätsparameter von obereozänen bis unteroligozänen Radiolarien im Südozean: Einfluss von Paläoozeanographie und Paläoökologie." Unpublished Ph.D. Thesis, Humboldt University, Berlin, ca 300 p. (Copies available on request from DBL)
- BARKER, P.F. and BURRELL, J., 1977. The opening of the Drake Passage. *Marine Geology*, 25: 15-34.
- BARKER, P.F. and THOMAS, E., 2004. Origin, signature and palaeoclimatic influence of the Antarctic Circumpolar Current. *Earth Science Reviews*, 66: 143-162.
- BARRON, E.J. and PETERSON, W.H., 1991. The Cenozoic ocean circulation based on ocean General Circulation Model results. *Paleogeography, Paleoclimatology, Paleoecology*, 83: 1-28.
- BERGER, W.H., LANGE, C.B. and WEFER, G., 2002. Upwelling history of the Benguela-Namibia system: A synthesis of leg 175 results. *Proceedings of the ODP, Scientific Results*, 175: 1-103.

- BERGGREN, W.A., KENT, D.V., SWISHER, I.C.C. and AUBRY, M.-P., 1995. A revised Cenozoic geochronology and chronostratigraphy. In: W.A. Berggren, D.V. Kent, M.P. Aubry and J. Hardenbol, Eds., *Geochronology, Time Scales and Stratigraphic Correlation: Framework for an Historical Geology*, pp. 129-212. Tulsa: Special Publication, Society of Economic Paleontologists and Mineralogists.
- CASEY, R.E., 1993. Radiolaria. In: J.E. Lipps, Ed., *Fossil Procar-yotes and Protists*. Boston: Blackwell, pp. 249-284.
- DE CONTO, R.M. and POLLARD, D., 2003. Rapid Cenozoic glaci-ation of Antarctica induced by declining atmospheric CO₂. *Nature*, 421: 245-249.
- DE WEVER, P., DUMITRICA, P., CAULET, J.P., NIGRINI, C. and CARIDROIT, M., 2001. *Radiolarians in the Sedimentary Record*. Amsterdam: Gordon and Breach, 533 pp.
- DIKMANN, B., KUHN, G., GERSONDE, R. and MACKENSEN, A., 2004. Middle Eocene to early Miocene environmental changes in the sub-Antarctic Southern Ocean: evidence from biogenic and terrigenous depositional patterns at ODP Site 1090. *Global and Planetary Change*, 40: 295-313.
- DIESTER-HAASS, L., 1994. Middle Eocene to early Oligocene paleoceanography of the Antarctic Ocean (Maud Rise, ODP Leg 113, Site 689): change from a low to a high productivity ocean. *Paleogeography, Paleoclimatology, Paleoecology*, 113(2-4): 311-334.
- DIESTER-HAASS, L. and ZAHN, R., 1996. Eocene-Oligocene transition in the Southern Ocean: History of water mass circulation and biological productivity. *Geology*, 24(2): 163-166.
- FUNAKAWA, S. and NISHI, H. 2008. Radiolarian faunal changes during the Eocene-Oligocene transition in the Southern Ocean (Maud Rise, ODP Leg 113, Site 689) and its significance in paleoceanographic change. *Micropaleontology*, 54(1) (this issue).
- HAYS, J.D., 1965. *Radiolaria and late Tertiary and Quaternary history of Antarctic Seas, Biology of Antarctic Seas*, pp. 125-184. Washington, DC: American Geophysical Union Antarctic Research Series 5.
- HUBER, M., BRINKHUIS, H., STICKLEY, C.E., DÖÖS, K., SLUIJS, A., WARNAAR, J., SCHELLENBERG, S.A. and WILLIAMS, G.L., 2004. Eocene circulation of the Southern Ocean: was Antarctica kept warm by subtropical waters? *Paleoceanog-raphy*, 19: 12 (web).
- KENNETT, J.P., 1977. Cenozoic evolution of Antarctic glaciation, the circum-Antarctic Ocean, and their impact on global paleoceanography. *Journal of Geophysical Research*, 82(27): 3843-3860.
- LAZARUS, D.B., 1994. The Neptune Project - A marine micropaleon-tology database. *Mathematical Geology*, 26(7): 817-832.
- LAZARUS, D. and CAULET, J.P., 1994. Cenozoic Southern Ocean re-constructions from sedimentologic, radiolarian, and other microfossil data. In: J.P. Kennett and D.A. Warnke, Eds., *The Antarctic Paleoenvironment: A Perspective on Global Change*. Part 2. Antarctic Research Series, pp. 145-174.
- LAZARUS, D.B., 2002. Environmental control of diversity, evolution-ary rates, and taxa longevities in Antarctic Neogene Radiolaria. *Pa-leontologica Electronica*, 5(1): ca 30 p. (web).
- , 2005. A brief review of radiolarian research. *Paläontologische Zeitschrift*, 79(1): 183-200.
- , 2007. Radiolarians and Silicoflagellates. p. 1682-1692 In: S.A. Elias, Ed., *Encyclopedia of Quaternary Science*. Amsterdam: Else-vier, 3365 pp.
- MILLER, K.G., FAIRBANKS, R.G. AND MOUNTAIN, G.S., 1987. Tertiary oxygen isotope synthesis, sea level history, and continental margin erosion. *Paleoceanography*, 2(1): 1-19.
- MCGOWRAN, B., 1989. Silica burp in the Eocene ocean. *Geology*, 17: 857-860.
- O'CONNOR, B., 2000. Stratigraphic and geographic distribution of Eo-cene-Miocene Radiolaria from the southwest Pacific. *Micropaleon-tology*, 46(3): 189-228.
- SCHUMACHER, S. and LAZARUS, D., 2004. Regional differences in pelagic productivity in the late Eocene to early Oligocene- a compar-ison of southern high latitudes and lower latitudes. *Paleogeography, Paleoclimatology, Paleoecology*, 214: 243-263.
- SCIENTIFIC PARTY, 1999. *Proceedings of the Ocean Drilling Pro-gram, Initial Reports, 177*. College Station, TX: Ocean Drilling Pro-gram, College Station, TX.
- , 2000a. *Proceedings of the Ocean Drilling Program, Initial Re-ports, 182*. College Station, TX: Ocean Drilling Program, College Station, TX.
- , 2000b. *Proceedings of the Ocean Drilling Program, Initial Re-ports, 183*. College Station, TX: Ocean Drilling Program, College Station, TX.
- , 2001. *Proceedings of the Ocean Drilling Program, Initial Re-ports, 189*. College Station, TX: Ocean Drilling Program, College Station, TX.
- STICKLEY, C.E., BRINKHUIS, H. and MCGONIGAL, K.L., 2004a. Late Cretaceous-Quaternary biomagnetostratigraphy of ODP Sites 1168, 1170, 1171, and 1172, Tasmanian Gateway. In: N.F. Exon, J.P. Kennett and M.J. Malone, Eds., *Proceedings of the Ocean Drilling Program, Scientific Results*, pp. 1-57 (web).
- STICKLEY, C.E., BRINKHUIS, H., SCHELLENBERG, S.A., SLUIJS, A., R...HL, U., FULLER, M., GRAUERT, M., HUBER, M., WAR-NAAR, J. and WILLIAMS, G.L., 2004b. Timing and nature of the deepening of the Tasmanian Gateway. *Paleoceanography*, 19: 1-18 (web).
- ZACHOS, J., PEGANI, M., SOLAN, L., THOMAS, E. and BILLUPS, K., 2001. Trends, rhythms and aberrations in global climate 65 Ma to present. *Science*, 292: 686-693.

Late Quaternary radiolarian assemblages as indicators of paleoceanographic changes north of the subtropical front, offshore eastern New Zealand, southwest Pacific

Vanessa Lüer^{1,2}, Christopher J. Hollis² and Helmut Willems¹

¹University of Bremen, Faculty of Geosciences, PO Box 330 440, 28334 Bremen, Germany

²GNS Science, PO Box 30 368, Lower Hutt, New Zealand

email: vlueer@uni-bremen.de

ABSTRACT: Abundant and diverse polycystine radiolarian faunas from ODP Leg 181, Site 1123 (0-1.2 Ma at ~21 kyr resolution) and Site 1124 (0-0.6 Ma, ~5 kyr resolution, with a disconformity between 0.42-0.22 Ma) have been used to infer Pleistocene-Holocene paleoceanographic changes north of the Subtropical Front (STF), offshore eastern New Zealand, southwest Pacific. The abundance of warm-water taxa relative to cool-water taxa was used to determine a radiolarian paleo-temperature index, the Subtropical (ST) Index. ST Index variations show strong covariance with benthic foraminifera oxygen isotope records from Site 1123 and exhibit similar patterns through Glacial-Interglacial (G-I) cycles of marine isotope stages (MIS)15-1. At Site 1123, warm-water taxa peak in abundance during Interglacials (reaching ~8% of the total fauna). Within Glacials cool-water taxa increase to ~15% (MIS2) of the fauna. Changes in radiolarian assemblages at Site 1124 indicate similar but much better resolved trends through MIS15-12 and 7-1. Pronounced increases in warm-water taxa occur at the onset of Interglacials (reaching ~15% of the fauna), whereas the abundance of cool-water taxa increases in Glacials peaking in MIS2 (~17% of the fauna). Overall warmer conditions at Site 1124 during the last 600 kyrs indicate sustained influence of the subtropical, warm East Cape Current (ECC). During Interglacials radiolarian assemblages suggest an increase in marine productivity at both sites which might be due to predominance of micronutrient-rich Subtropical Water. At Site 1123, an increased abundance of deep-dwelling taxa in MIS 13 and 9 suggests enhanced vertical mixing. During Glacials, reduced vigour of ECC flow combined with northward expansion of cool, micronutrient-poor Subantarctic Water occurs. Only at Site 1123 there is evidence of a longitudinal shift of the STF, reaching as far north as 41°S.

INTRODUCTION

Polycystine Radiolaria are a diverse group of marine microzooplankton, bearing fossilizable skeletons of opaline silica. This fossil group has been used extensively for Quaternary paleoceanographic studies in the Pacific (e.g. Molina-Cruz 1977; Moore 1978; Pisias and Mix 1997; Welling and Pisias 1998), Atlantic (e.g. Morley 1979; Abelmann and Gowing 1997; Dolven et al. 2002), Indian (e.g. Dow 1978; Johnson and Nigrini 1980, 1982) and Southern oceans (e.g. Cortese and Abelmann 2002). Radiolarian depth zonations and the relative abundance of depth restricted taxa can be used for paleoceanographic reconstructions and detection of the influence of certain water masses within a study area (e.g. Casey 1971; McMillen and Casey 1978; Kling and Boltovskoy 1995; Abelmann and Gowing 1997) and to investigate paleoceanographic events (Welling et al. 1996; Wang and Abelmann 2002; Yamashita et al. 2002)

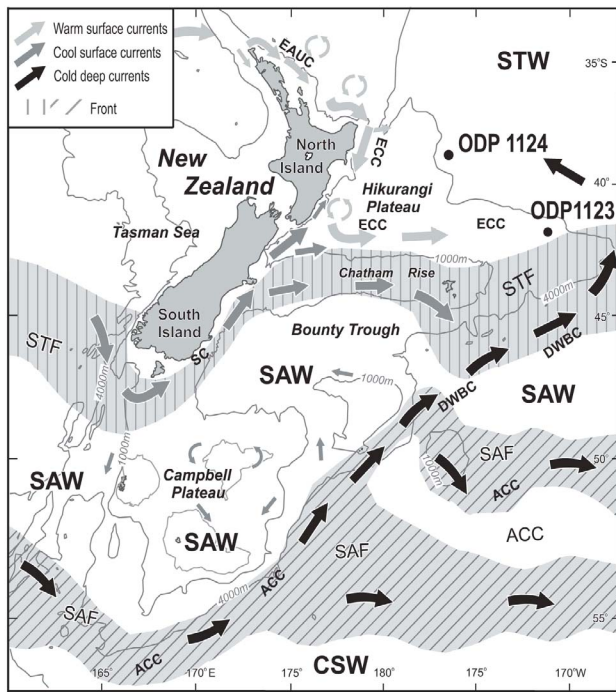
In contrast, there have been very few studies of Quaternary radiolarians (Hays 1965; Petrushevskaya 1967, 1975; Caulet 1986, see also Nelson et al. 1993; Carter et al. 1999b) and their application to paleoceanographic changes in the southern Pacific Ocean (Moore et al. 1978; Hollis et al. 2002; 2006). Our study of radiolarians from sediment cores from north of the STF (ODP Leg 181, Sites 1123, 1124), offshore eastern New Zealand, is the first detailed investigation of Late Quaternary assemblage variation in the region.

The two study locations, Sites 1123 and 1124, lie within a temperate climatic regime east of New Zealand and north of the Subtropical Front (STF). Our quantitative analysis of radiolarian assemblages aims to determine changes in the expression of the STF and associated currents during late Quaternary Glacial-Interglacial (G-I) climate cycles.

OCEANOGRAPHIC SETTING

The Subtropical Front (STF) is a prominent feature of the ocean regime offshore eastern New Zealand (text-fig. 1). It extends to a depth of ~350m (Heath 1976) and appears to have been locked to the Chatham Rise at ~45°S throughout the late Quaternary, including the Last Glacial Maximum (Heath 1985; Nelson et al. 1993; Chiswell 2002; Sikes et al. 2002). In the upper water-mass, however, the front is highly variable in strength. Satellite thermal imaging shows that meanders and eddies form at many different scales (Chiswell 1994). The STF is characterized by a 4-5° C drop in surface temperature and a ~1‰ drop in salinity over 200km (Chiswell 2001; Sikes et al. 2002). It separates high-salinity (~35.7‰), macronutrient-poor (nitrate, dissolved reactive phosphorus, silica), micronutrient-rich (iron and other trace metals), warm (>15°C summer) Subtropical Water (STW) from southern Subantarctic Water (SAW), which has lower salinity (~34.5‰), is macronutrient-rich, micronutrient-poor and cool (<15°C summer; Heath 1985; Nelson et al. 2000; Chiswell 2001, 2002). The high amount of micronutrients in STW triggers high primary production, especially in summer (Boyd et al. 2004). High nitrate, low chlorophyll (HNLC) SAW has low primary production with little seasonal variation (Boyd et al. 2004). The southern boundary of SAW is defined by the Subantarctic Front (SAF), which follows the submarine escarpment of Campbell Plateau (text-fig. 1). The SAF defines the northern extent of the Southern Ocean and Antarctic Circumpolar Current (ACC) and is associated with another drop in temperature of ~2°C and annual mean surface-water temperature of <10° C to the South. It restricts macronutrient-rich Circumpolar Subantarctic Water (CSW) to latitudes >55°S (Carter et al. 1999b).

The shallow subtropical East Cape Current (<350m; ECC) is a continuation of the East Australian Current (EAUC) that flows



TEXT-FIGURE 1
Location of ODP Sites 1123 and 1124 (black dots) and distribution of major water masses, currents and fronts offshore eastern New Zealand. CSW, Circum-Antarctic Surface Water; SAW, Subantarctic Surface Water; STW, Subtropical Surface Water; EAUC, East Australian Current; ECC, East Cape Current; SC, Southland Current; ACC, Antarctic Circumpolar Current; DWBC, Deep Western Boundary Current; STF, Subtropical Front; SAF, Subantarctic Front (modified from Carter 2001).

southward along North Island's east coast as a series of eddies before turning east at 2°S to follow the northern flank of Chatham Rise (Nelson et al. 2000; text-fig. 1). South of the STF, the cool shallow Southland Current (SC) flow travels around the bottom of South Island before turning northward (text-fig. 1). It is associated with the narrow Southland Front (SF), the landward expression of the STF that separates relatively warm, salty STW on the continental shelf from cool, relatively fresh SAW offshore (Sutton 2003). On its way north the SC mixes with offshore SAW on Campbell Plateau comprising ~90% SAW and ~10% STW before most of its flow is deflected to the east, south of Chatham Rise, while filaments of the SC pass through Mernoo Gap to combine with the ECC (Sutton 2003; text-fig. 1).

The remaining major current in this region is the Deep Western Boundary Current (DWBC), which separates from the Antarctic Circumpolar Current (ACC) at the SAF and flows northward, along the New Zealand continental margin (text-fig. 1). The DWBC has an upper boundary of 2000m (Carter et al. 1999a, b) and is a major component in the global ocean thermohaline circulation system, supplying 40% of the cold, saline Antarctic bottom water to the major ocean basins through the Pacific Ocean (Warren 1981). It is believed to have had a significant influence on the Earth's heat budget since its inception ~33 Ma (Clarke et al. 2001). The DWBC contains a mixture of Antarctic Bottom Water (AABW) and North Atlantic Deep Water (NADW; Carter et al. 1999b; Hall et al. 2001). These waters are entrained and mixed by the west wind-driven ACC to form Circumpolar Deep Water (CDW; Carter et al. 1999b).

The two study sites lie within STW north of the STF and have the potential to record variations in the influence of the ECC and STF in shallow waters and of the DWBC at depth.

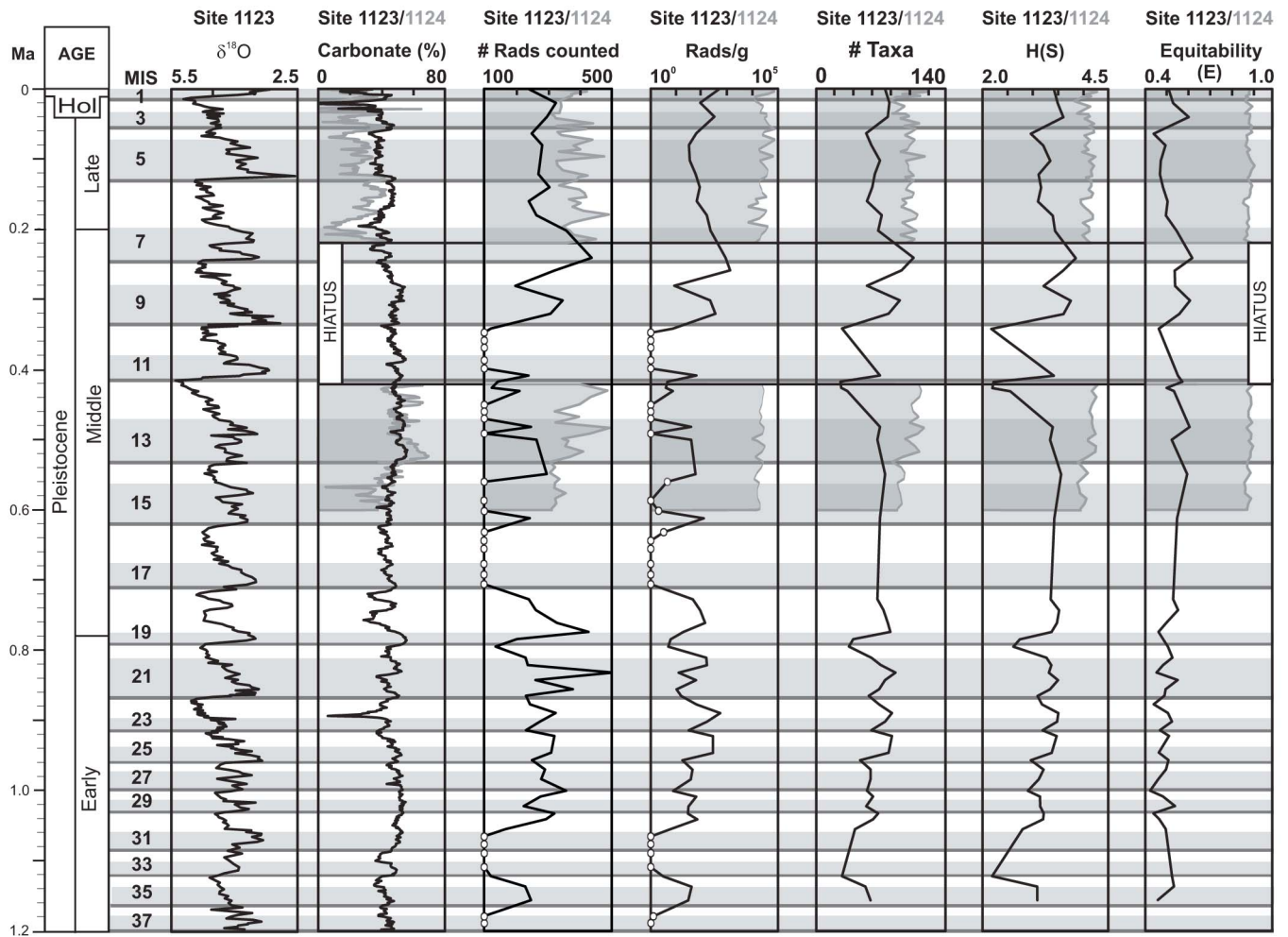
MATERIAL AND METHODS

Sediment samples and chronological framework

Sites 1123 (41°47'S; 71°30'W, 3290m water depth; text-fig. 1) and 1124 (39°30'S; 176°32'W, 3960m water depth) were APC/XCB cored during ODP Leg 181 (Carter et al. 1999b). Sediments of both cores consist of clayey nannofossil ooze, nannofossil ooze, nannofossil silty clay and intercalated tephra layers. Magnetic susceptibility and color reflectance records were used to identify overlapping intervals in Site 1123 Holes B and C, and Site 1124 Holes A-D in order to establish a continuous sedimentary record. Depths are based on these spliced records and are recorded as meters composite depth (mcd). Both sites have near complete Neogene records. In this study we provide an overview for the last 1.2 Myrs based on Site 1123 (based on Lüer 2003) and then compare records for the last 600 kyrs for both sites. 10 cc samples were taken every ~0.6 mcd (Site 1123) and ~0.36 mcd (Site 1124) to provide a temporal resolution of ~21 kyrs (Site 1123) and ~5 kyrs (Site 1124), respectively, during the last 600 kyrs. Unfortunately, Site 1124 has a hiatus at 0.42-0.22 Ma (Carter et al. 1999b; Hall et al. 2002; Aita and Suzuki 2003; Fenner and DiStefano 2004). For Site 1123 an orbitally tuned timescale was developed from benthic foraminiferal oxygen isotope records (Hall et al. 2001). The age model for Site 1124 is based on graphical correlation of color reflectance data with the record from Site 1123 (Hall et al. 2002). Two Late Quaternary radiolarian bioevents recorded in this study, the last occurrences of *Stylatractus universus* at 0.42 Ma and *Eucyrtidium calvertense* at 0.48 Ma, are in good agreement with previous studies (Hays and Shackleton 1976; Morley and Shackleton 1978; Lazarus 1992; Shackleton et al. 1995; Sanfilippo and Nigrini 1998; Aita and Suzuki 2003).

Sample processing

Because processing techniques were developed and refined in the course of this project, there are specific differences in the processing methodologies used for the two sites, especially in relation to the drying of sediments and residues, use of mesh size and the technique of strewn slide production. For Site 1123, we prepared strewn slides from a >63 µm fraction of oven-dried residue (see Appendix 3 for details). This method allowed comparison with the shipboard samples, which were prepared by this method (Carter et al. 1999b). However, because most paleoceanographic studies of Quaternary radiolarians are based on smaller size fractions (e.g. Wang and Abelmann 1997; Yamashita et al. 2002), the >45 µm fraction was analysed for Site 1124 to allow better comparison with other studies. In addition, samples were freeze-dried (Abelmann 1988) to reduce breakage of delicate radiolarian tests (Itaki and Hasegawa 2000) and a wet settling technique was adopted to ensure random distribution of radiolarian tests on the slides (Moore 1973; Abelmann 1988; Abelmann et al. 1999). A newly developed mounting technique was used to avoid the formation of air bubbles, especially within radiolarian tests. See Appendix 3 for details of processing methods. It is recognized that these differences in processing present problems in comparing assemblage data between the two sites. Diversity is expected to be greater at Site 1124, simply because of gentler drying methods and use of a smaller sieve size. A smaller sieve



TEXT-FIGURE 2

General features of radiolarian assemblages from ODP Site 1123 (0-1.2 Ma, black line) and Site 1124 (0-0.6 Ma, shaded grey) with benthic foraminiferal $\delta^{18}\text{O}$ record for Site 1123 and colour reflectance for Sites 1123 and 1124 for reference (from Hall et al. 2001, 2002): number of radiolarians counted in each sample (# Rads counted); radiolarians per gram of sediment (Rads/g), taxic richness (# Taxa), diversity (H(S)) and Equitability (E). Sparse samples (<100 specimens/sample) are shown as unfilled circles. Marine Isotope Stages (MIS) are calibrated according to the $\delta^{18}\text{O}$ and reflectance records at Site 1123. Glacial terminations are shown as dark grey horizontal lines and Interglacial Stages are shaded light grey. A hiatus at Site 1124 extends from uppermost MIS12 to mid-MIS7.

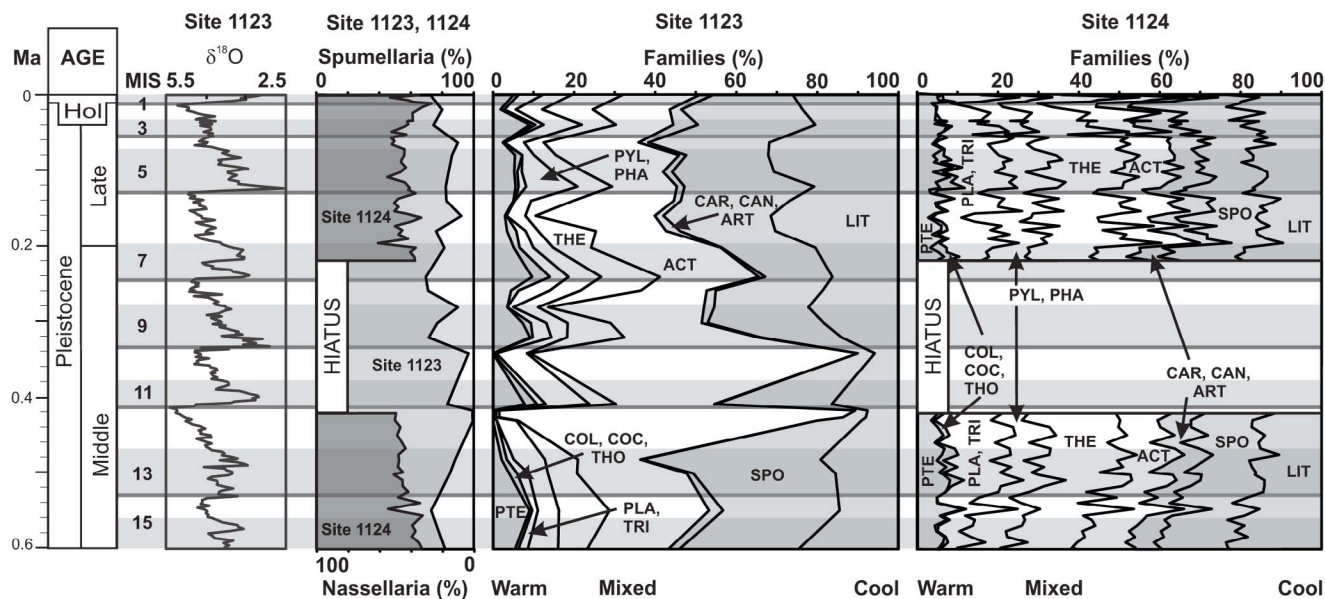
size is also expected to increase the diversity and abundance of nassellarians, which tend to be smaller than spumellarians

This study is based on the analysis of 151 samples, 79 from Site 1123 and 72 from Site 1124. The taxonomic level of counting groups ranges from subspecies to undifferentiated family and suborder categories. Generally, in case of incomplete or broken tests only radiolarians with >50% of the test preserved were counted. For nassellarians, only specimens with a cephalis present were counted. The ratio of radiolarian fragments over the total of counted specimens was used as a guide to radiolarian preservation within individual assemblages.

Bulk samples, radiolarian residues and strewn slides are stored and catalogued at GNS Science, Lower Hutt, New Zealand, (Site 1123) and at the University of Bremen, Germany (Site 1124). Raw data files are available at www.pangaea.de, an online archive for marine environmental scientific data.

Statistical analysis

For both sites we aimed for a minimum count of 300 specimens per sample in order to provide statistically significant abundance estimates (Cortese 2004). For Site 1123 we were not able to reach this number owing to the scarcity of radiolarians in some intervals. For our statistical analysis we included all samples with >100 specimens because, although errors are relatively large in counts of <300 specimens, general features of the assemblages are still meaningful (e.g. diversity, abundance of common species). Hayward et al. (1999) have established that counts of 100 specimens provide an adequate guide to general faunal character because the main statistical methods are primarily influenced by the abundance variations within the most common taxa. Diversity indices were calculated using a public domain data analysis software package, PAST (Paleontological Statistics; Hammer et al. 2001), including taxic richness (S = number of taxa in individual samples), Fisher α Index (α), Shannon-Wiener Information Function (H(S)) and Equitability (E). The linear coefficient



TEXT-FIGURE 3

Abundance of radiolarian orders (spumellarians, nassellarians) and families during the last 600 kyrs at ODP Sites 1123 and 1124 with benthic foraminiferal $\delta^{18}\text{O}$ record for reference (Hall et al. 2001). Warm-water affinities (shaded to left): Collosphaeridae (COL), Coccodiscidae (COC), Tholoniidae (THO), Pterocoryidae (PTE). Cool-water affinities (shaded to right): Spongodiscidae (SPO), Litheliidae (LIT), Carpaniidae (CAR), Can-nobotryidae (CAN), Artostrobiidae (ART). Mixed affinities: Actinommididae (ACT), Pyloniidae (PYL), Phacodiscidae (PHA), Theoperidae (THE), Plagoniidae (PLA), Trissocyclidae (TRI). Other shading and symbols as for text-figure 2.

of correlation (r ; Godfrey et al. 1988; Bevington and Robinson 1991) was used to examine patterns of covariance within radiolarian assemblage data and between radiolarian associations and paleoclimate proxies, such as oxygen isotopes (Hall et al. 2001, 2002).

Radiolarian paleotemperature and paleodepth indicators

Radiolarian assemblages at the two sites consist of a mixture of mainly transitional, subtropical and subantarctic species typical of temperate waters (Boltovskoy 1987) and transitional subzones TR1-3 of Hollis and Neil (2005). Based on local biogeographic data (Moore 1978; Boltovskoy 1987; Hollis and Neil 2005) 93 paleotemperature indicator species were identified (Appendix 1). These include 54 warm-water (tropical-subtropical) species and 33 cool-water (antarctic-subantarctic) species. Six taxa are considered to typify the transitional zone. The abundance of warm-water species relative to cool-water species was used to define the Subtropical Index (ST Index):

Subtropical (ST) Index: warm-water taxa [%]/cool-water taxa [%]

To examine water column structure radiolarians were also classified by depth zones utilising established depth zonations (Renz 1976; McMillen and Casey 1978; Kling 1979; Boltovskoy and Jankilevich 1985; Kling and Boltovskoy 1995; Abelmann and Gowing 1997). In this study radiolarian species that are restricted to the upper 100m of the water column or that have peak abundance at 100m are characteristic surface and subsurface dwellers and are classified as shallow dwellers. Deep-dwelling radiolarians are those that have their greatest abundance at >100m water depth and include species that are most abundant in intermediate watermasses (c. 200m) as well as those most abundant in deep waters (>300m). Altogether, 75 species were assigned to depth zones and 47 were classified as shallow dwellers whereas 28 were classified as deep-dwelling species (Appendix 1). It is

noted, however, that some radiolarians occur at different water depths in different latitudinal zones. Many radiolarian species that are classified as shallow-dwelling, cool-water species in high latitude surface waters are deep-dwelling species in lower latitudes (Casey 1971). For this reason, in the following section we are careful to rule out changes in water temperature as a cause for faunal changes prior to considering possible changes in water column structure or vertical mixing.

RESULTS

Variations in radiolarian abundance, diversity and preservation

Abundance and diversity are relatively high at Sites 1123 and 1124, which is consistent with the occurrence of rich radiolarian faunas in the transitional southwest Pacific, north of the STF (Hollis and Neil 2005). Overall, abundance is much higher at Site 1124 than at Site 1123, with maxima of ~70,000 and ~1,300 radiolarians per gram sediment (rads/g) and means of ~26,000 and ~100 rads/g, respectively (text fig 2). Diversity is also much higher at Site 1124, with a maximum of 122 vs 101 (Site 1123) taxa and averages of 98 and 53 taxa per sample (Site 1123), respectively. This marked difference is partly an artefact of differences in processing. In particular, the use of a 45 μm sieve, freeze-drying of samples and wet-mounting of residues are all likely to improve the recovery of radiolarians. However, other preservational differences and the very sparse assemblages in some intervals at Site 1123 indicate that these methodological differences serve to accentuate actual differences. Assemblages from Site 1124 are consistently richer, more diverse and better preserved than those from Site 1123. Radiolarians are mostly well- to very well-preserved at Site 1124, whereas preservation is much more variable at Site 1123 and ranges from poor, especially characterized by high fragmentation of radiolarian tests, to moderate and good to very good. Three samples from Site

1123 contain reworked Paleogene radiolarian specimens (1123B-3H-5, 126-128 cm; 1123B-6H-2, 19-23 cm; 1123C-5H-6, 17-21 cm).

Radiolarians from Site 1123 are generally rare to common, with most samples containing >500 radiolarians/g (text-fig. 2). Two intervals of low abundance are noted: near the base of the studied interval (MIS37-31) and in the middle Pleistocene (MIS17-10). Many of the sample residues from these two intervals contain <100 specimens (text-fig. 2) and, for this reason, these samples are not used for quantitative faunal analysis. A total of 163 taxa were recorded in samples from this site and assemblages are moderately diverse (maximum H(S) = 3.9; mean H(S) = 3.2; text-fig. 2). Equitability is also moderate to high (E = 0.4-0.6). Significant correlation between radiolarian abundance, diversity and oxygen isotopes was determined for samples from Site 1123 (Appendix 2). Generally, abundance and diversity tend to be highest at G-I transitions and decrease in Glacials, except in MIS31-30, 19-18 and 9-8, where the pattern is reversed (text-fig. 2).

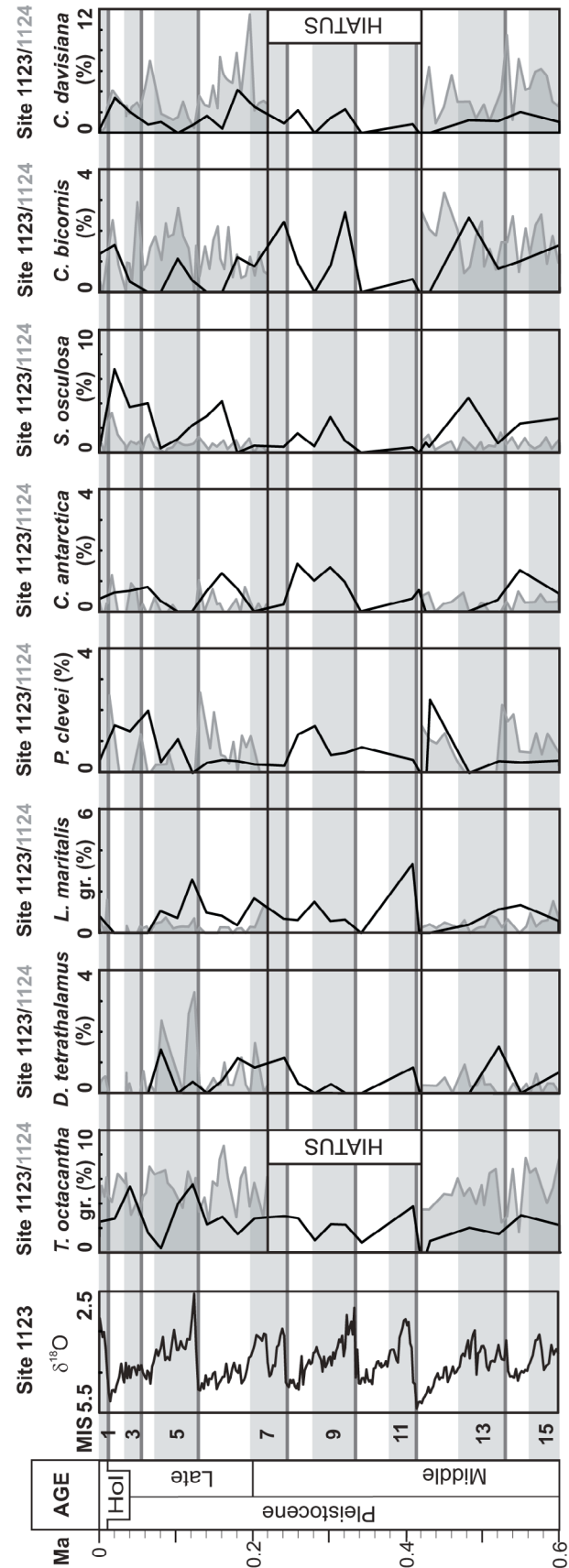
To examine the degree of covariance between radiolarian assemblage characteristics and global climatic changes we determined correlation coefficients for assemblage parameters and oxygen isotope values (Hall et al. 2001; 2002) for the same samples from Site 1123 (Appendix 2a, b). Although, significant positive correlations are evident between diversity parameters and abundance, only diversity exhibits a significant negative correlation with $\delta^{18}O$. From this pattern of covariance we infer that oceanographic changes, e. g. local changes in water temperature (e.g. Pahnke and Sachs 2006; Crundwell et al. in press) at this site during G-I cycles had greatest impact on radiolarian diversity, with a discernable but statistically insignificant effect on abundance. Specifically, radiolarian diversity increases in most Interglacials and is especially pronounced in the later Interglacials (MIS11 to MIS3).

Radiolarians are very abundant and very diverse at Site 1124 (text-fig. 2). A total of 271 taxa were recorded and diversity is significantly higher than at Site 1123 (maximum H(S) = 4.3; mean H(S) = 4.0). Taxa are also much more evenly distributed within assemblages than at Site 1123 (mean E = 0.89). The higher diversity, and possibly the higher Equitability, is probably due in part to processing differences (see above). In comparison with Site 1123, there is much less variation in abundance and diversity at Site 1124. Apart from distinct baseline increases in diversity at the bases of MIS13 and MIS1 (text-fig. 2), there is no obvious relationship between abundance and diversity parameters and G-I cycles.

As for Site 1123, abundance and diversity parameters are positively correlated although a significant correlation is not observed for abundance and Equitability (Appendix 2c). This is because Equitability is higher and less variable at Site 1124, compared to Site 1123. No $\delta^{18}O$ data are available for Site 1124.

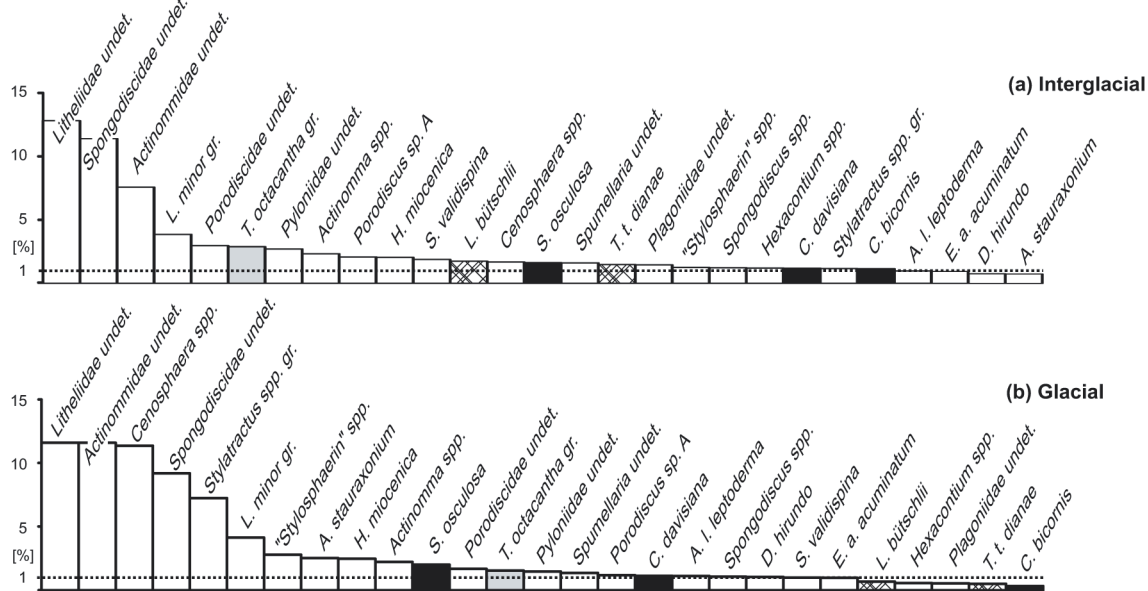
Radiolarian assemblage variation: orders and families

Spumellarians dominate radiolarian assemblages at Site 1123 (70-99.5%) and are slightly more common than nassellarians at Site 1124 (40-74%; text-fig. 3). This is typical of temperate South Pacific faunas (Boltovskoy 1987; Hollis and Neil 2005). The higher abundance of nassellarians at Site 1124 is due mainly to the greater abundance of small nassellarians (45-63 gm) and the better preservation of fragile nassellarian tests due to gentler preparation methods.

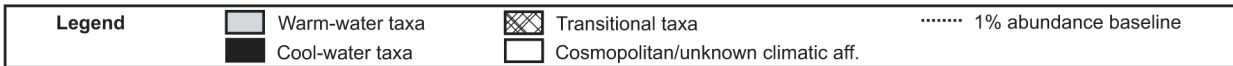
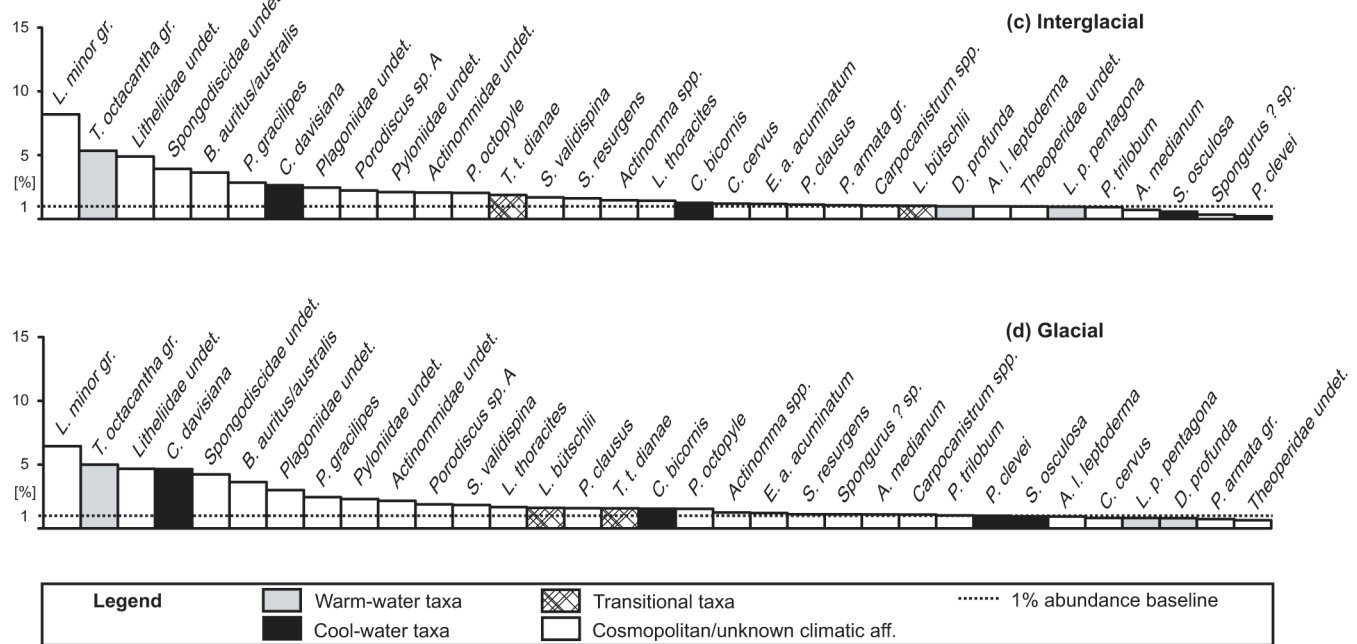


TEXT-FIGURE 4
Abundance of selected radiolarian taxa at ODP Sites 1123 (black line) and 1124 (shaded grey) during the last 600 kys with benthic foraminiferal $\delta^{18}O$ record for reference (Hall et al. 2001). Other shading and symbols as for text-figure 2.

Site 1123



Site 1124



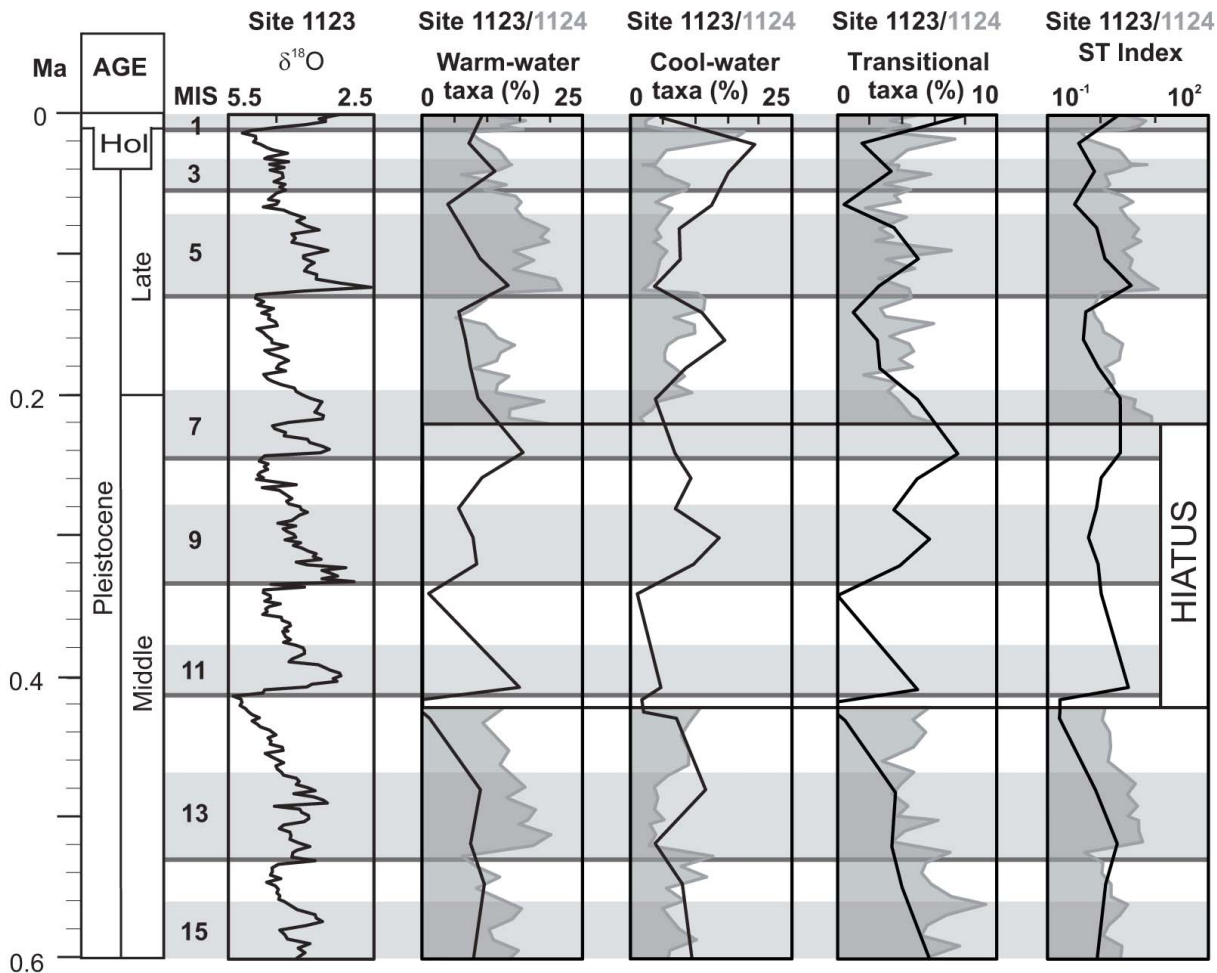
TEXT-FIGURE 5

Average frequency histograms for common taxa (>1%) and significant marker taxa (<1%) within Interglacial (a) and Glacial (b) samples at ODP Site 1123 and within Interglacial (c) and Glacial (d) samples at Site 1124.

Actinommiids, spongodiscids and litheliids are the most abundant spumellarian families at both sites (text-fig. 3). Average values for each family are at least 20% at Site 1123 and 12% at Site 1124, which is consistent with observations on Recent distribution patterns in surface sediments in the southwest Pacific (Boltovskoy 1987; Hollis and Neil 2005). Pyloniids, which are common in Recent radiolarian assemblages north of the STF (Boltovskoy 1987; Hollis and Neil 2005) average to 5% at Site 1123 and 10% at Site 1124. Collosphaeridae, Phacodiscidae, Coccodiscidae and Tholonidae are rare at both sites. Collosphaerids, phacodiscids, coccodiscids and, at Site 1124, tholoniids, are never more

abundant than 2.5% at Site 1123 and 3.5% at Site 1124. Generally, collosphaerids, coccodiscids and phacodiscids are rare in the transitional southwest Pacific (Boltovskoy 1987) and in the eastern New Zealand area (Hollis and Neil 2005).

Pterocoryids and theoperids dominate Recent nassellarian assemblages north of the STF (Boltovskoy 1987; Hollis and Neil 2005). With an average of 8% (Site 1123) and 19% (Site 1124), respectively, theoperids are the most common nassellarians in the study area (text-fig. 3). Pterocoryids, plagoniids, arstostrobids, and at Site 1124, trissocyclids, are also common (>5%). Car-



TEXT-FIGURE 6
Abundance of paleotemperature indicators at ODP Sites 1123 (black line) and 1124 (shaded grey) during the last 600 kyrs with benthic foraminiferal $\delta^{18}O$ record for reference (Hall et al. 2001). The Subtropical (ST) Index is the ratio of warm- to cool-water taxa. Other shading and symbols as for text-fig. 2.

ponaniids exceed 1% (Site 1123) and 3% (Site 1124) in individual samples. While cannobotryids are >1% in most assemblages at Site 1124, the family is very rare at Site 1123 (text fig. 3). The higher abundance of these small nassellarians at Site 1124 is due to the better preservation and incorporation of smaller radiolarian tests (>45 μ m).

Variation within G-I cycles at Sites 1123 and 1124 are very similar. Spumellarian collosphaerids, coccodiscids, tholoniids and nassellarian pterocoryids have increased abundance in Interglacials indicating that these families are dominated by warm-water taxa (text-fig. 3). Radiolarian assemblages within Glacials are dominated by spongodiscids and litheliids and have increased abundance of carpocaniids, cannobotryids and artostrobiids indicating the dominance of cool-water taxa within these families (text-fig. 3). Abundance trends of all other families show mixed affinities, including a mixture of warm- and cool-water species.

Radiolarian assemblage variation: key species and species groups

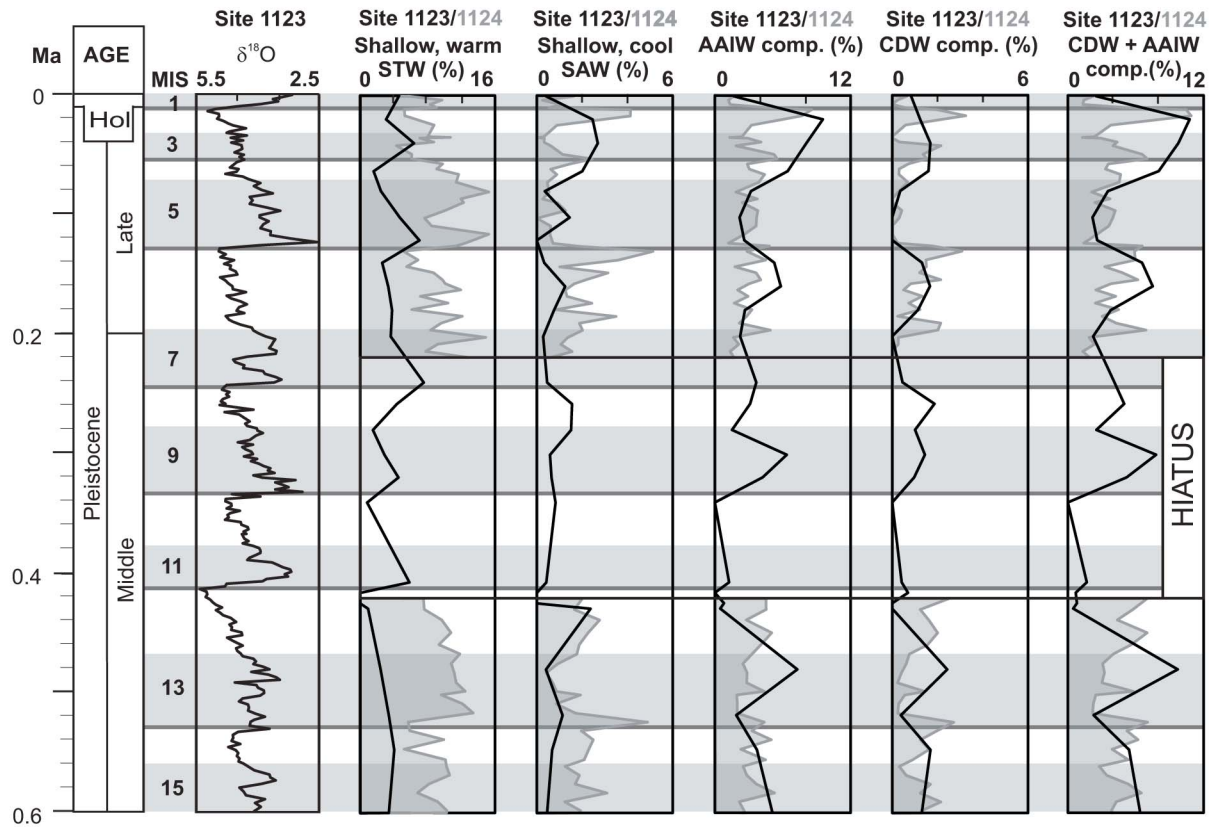
Abundance variations in key paleoenvironmental indicator species are used to further examine the changes in oceanographic conditions through the climate cycles identified at the two sites (text-fig. 4). Comparison of abundance variations between the

two sites also helps to clarify the effects of the different processing methodologies.

***Tetrapyle octacantha* group**

Tetrapyle octacantha gr. includes species of *T. octacantha* and *Octopyle stenozona*. Plankton and surface sediment studies identify peak abundances of *T. octacantha* gr. in the tropical (Renz 1976, Moore 1978; Boltovskoy and Jankilevitch 1985) and subtropical (Molina-Cruz 1977) Pacific. Moore's (1978) tropical factor is clearly dominated by this species group. Boltovskoy (1987) recorded highest abundance of *T. octacantha* gr. in the subtropical and tropical zones. Lombardi and Boden (1985) documented peaks of *T. octacantha* gr. in the tropical Pacific as well as in the vicinity of the Subtropical Front (STF). Hollis and Neil (2005) found higher abundance of *T. octacantha* gr. in Subtropical Water (STW), north of the STF. In the modern ocean *T. octacantha* gr. lives in shallow water masses and is most abundant in the upper 50m of the water column (e.g. Renz 1976; McMillen and Casey 1978; Kling 1979; Kling and Boltovskoy 1995).

At Site 1123, *T. octacantha* gr. abundance tends to increase in Interglacials (text-fig. 4), a feature that is corroborated by a significant negative correlation with the oxygen isotope record (r



TEXT-FIGURE 7

Abundance of radiolarian depth indicators at ODP Sites 1123 (black line) and 1124 (shaded grey) during the last 600 kyr with benthic foraminiferal $\delta^{18}\text{O}$ record for reference (Hall et al. 2001). Depth categories are shallow, warm Subtropical Surface Water (STW); shallow, cool Subantarctic Surface Water (SAW); Circumpolar Deep Water (CDW); Antarctic Intermediate Water (AAIW) components, and combined CDW and AAIW (deep, cool southern-sourced waters).

= -0.444; $r \geq 0.396$ is significant at $P = 0.05$, $N = 25$). A small peak in Glacial stage MIS8 is consistent with other indications, as discussed below, that this single sample has clear warm-water affinities. *T. octacantha* gr. also tends to be most common in Interglacials at Site 1124 although abundance peaks are recorded in Glacial stages MIS6, 4 and 2 (text-fig. 4). The reasons for these peaks are uncertain but they may reflect warming pulses within the Glacials or other oceanographic factors. In general, the abundance variation of *T. octacantha* gr. is in good agreement with the established species' ecology, i.e. a shallow-dwelling species that can be used to detect influences of STW and ECC flows. The higher abundance of *T. octacantha* gr. at Site 1124 reflects the stronger influence of these water masses at this site, particularly in Glacial stages in the late Pleistocene. Test sizes of individual specimens of the *T. octacantha* gr. included in this study are $>63\mu\text{m}$ and differences in the processing methods are expected to be minor.

Didymocyrtis tetrathalamus

D. tetrathalamus is very abundant in surface sediments in tropical to subtropical waters of the Pacific Ocean (Renz 1976; Molina-Cruz 1977; Moore 1978; Boltovskoy and Jankilevich 1985; Lombardi and Boden, 1985; Boltovskoy 1987) and is present north of the STF in the eastern offshore New Zealand area (Hollis and Neil 2005). The species is a shallow-water dweller, mainly living within the upper 50m of the water column (e.g. McMillen and

Casey 1978; Kling 1979; Kling and Boltovskoy 1995).

At Site 1123, *D. tetrathalamus* is common within Interglacials but is not recorded in Glacials, apart from rare occurrences in MIS8 and 6 (text-fig. 4). *D. tetrathalamus* occurs in both Interglacials and Glacials at Site 1124, except it is absent from MIS2. This species is most abundant in Interglacials and peaks in MIS5 (text-fig. 4). Due to its abundance within Interglacials at both sites, *D. tetrathalamus* is considered to be a reliable warm-water indicator, which agrees with the known species ecology. *D. tetrathalamus* has a weak negative correlation with oxygen isotopes at Site 1123 which is probably due the general scarcity ($<2\%$) of this species at this site ($r = -0.331$). *D. tetrathalamus* is used to indicate warm, shallow water masses of STW and ECC, herein. The impact of the different processing methods is believed to be minor because the species is generally larger than $63\mu\text{m}$ and has a relatively robust test.

Lamprocyclus maritilis group

The species included in the *Lamprocyclus maritilis* gr. are *L. maritilis maritilis* and *L. maritilis polypora*. *L. m. maritilis* is a common element of the tropical and subtropical zones whereas *L. m. polypora* is more abundant in the transitional zone of the southwest Pacific area according to Boltovskoy (1987). In the eastern New Zealand region both subspecies are common in surface sediments north of the STF, signaling their warm-wa-

TAXA	Ref 1	Comments	Site	Mor78	Bol87	sp. ID	H&N05 Temp	depth	Ref 2
COOL									
<i>Acanthosphaera pinchuda</i> Boltovskoy & Riedel	Bol 98		1		SA	19	cool		
<i>Acrosphaera arktios</i> (Nigrini)	N&M 79	As <i>Polysolenia</i>	1, 2				SA	cool	
<i>Actinomma antarcticum</i> (Haeckel)	N&M 79		1, 2		AA	20	SA	cool	surface 4,5
<i>Actinomma delicatulum</i> (Dogiel)	N&N 82		1				SA	cool	
<i>Androcyclas gamphonycha</i> (Jørgensen)	N&M 79	Includes <i>Lamprocyrtis</i> <i>? hammai</i> (Campbell & Clark) in N&M 79	1, 2		SA	172	SA	cool	deep 3
<i>Antarctissa cylindrica</i> (Petrushevskaya)	N&N 82		1, 2				SA	cool	
<i>Antarctissa denticulata</i> (Ehrenberg)	N&M 79		1, 2	AA-SA	AA	116	SA	cool	
<i>Antarctissa strelkovi</i> Petrushevskaya	Pet 67		1	AA-SA	AA	116		cool	surface 5
<i>Artostrobos annulatus</i> (Bailey)	Pet 67		1		SA	183		cool	
<i>Botryostrobos aquilonaris</i> (Bailey)	Bol 98		1, 2	SA	SA	184	SA	cool	deep 3
<i>Cenosphaera cristata?</i> Haeckel	N&M 79		1, 2	C-SA	AA	30	SA	cool	
<i>Cromyechinus antarctica</i> (Dreyer)	Bol 98		1, 2		AA	36	SA	cool	deep 5
<i>Cycladophora bicornis</i> (Popofsky)	N&M 79	As <i>Theocalyptra</i>	1, 2		C	165	SA	cool	intermediate 2,3,5
<i>Cycladophora davisiana</i> (Ehrenberg)	Bol 98		1, 2		C	165	SA	cool	intermediate 3,4
<i>Dictyophimus bicornis</i> (Ehrenberg)	Pet 67		1		AA	140		cool	
<i>Lithelius nautiloides</i> Popofsky	Bol 98		1, 2		AA	96	SA	cool	
<i>Peripyramis circumtexta</i> Haeckel	Bol 98		1, 2		SA	159	SA	cool	deep 3
<i>Phormacantha hystrix</i> (Jørgensen)	Bol 98		1		AA	130		cool	
<i>Phormospyris stabilis</i> (Goll) <i>scaphipes</i> (Haeckel)	N&M 79		1, 2				SA	cool	subsurface 3,4
<i>Phortidium clevei</i> (Jørgensen)	Bol 98		1, 2		A	92	SA	cool	surface 5
<i>Prunopyle titan</i> Campbell & Clark	Laz 90		1				SA	cool	
<i>Pseudocubus obeliscus</i> Haeckel	Bol 98		1		AA	131		cool	
<i>Saccospyris antarctica</i> Haecker	Bol 98		1, 2		AA	194	SA	cool	
<i>Sethophormis rotula</i> (Haeckel)	Bol 98		1		SA	108		cool	
<i>Siphocampe arachnea</i> (Ehrenberg) group	Nig 77		1, 2		SA	186		cool	
<i>Siphocampe lineata</i> (Ehrenberg) group	Nig 77		1, 2		SA	187		cool	
<i>Spongopyle osculosa</i> Dreyer	N&M 79		1, 2		SA	79	SA	cool	deep 2,4,5
<i>Spongostrochus glacialis</i> Popofsky	Bol 98		1, 2		C	80	SA	cool	surface 2,4,5
<i>Spongostrochus (?) venustum</i> (Bailey)	N&M 79		1, 2					cool	surface 5
<i>Spongurus pylomaticus</i> Riedel	Bol 98		1, 2		AA	82	SA	cool	deep 5
<i>Stylodictya aculeata</i> Jørgensen	Bol 98		1, 2				SA	cool	
<i>Styptosphaera (?) spumacea</i> Haeckel	N&M 79		1, 2		AA	64	SA	cool	
<i>Tricerapsyris antarctica</i> (Haecker)	Bol 98		1		AA	114		cool	

APPENDIX 1

Radiolarian biogeographic affinities and depth preferences for radiolarian taxa from (1) Site 1123 and (2) Site 1124. AA, Antarctic; SA, Subantarctic; TR, Transitional; ST, Subtropical; TT, Tropical zones; C, cosmopolitan. Ref 1, reference to taxon concept: Hk187, Haeckel 1887; Ben 66, Benson 1966; Pet 67, Petrushevskaya 1967; Pet 71, Petrushevskaya 1971b; Pet 72, Petrushevskaya 1972; P&K 72, Petrushevskaya and Kozlova 1972; Nig 77, Nigrini 1977; N&M 79, Nigrini and Moore 1979; N&N 82, Nakaseko and Nishimura 1982; Cau 86, Caulet 1986; C&N 88, Caulet and Nigrini 1988; Laz 90, Lazarus 1990; Tak 91, Takahashi 1991; Bol 98, Boltovskoy 1998. Biogeographic zonations: Mor78, Moore 1978; Bol87, Boltovskoy 1987 (followed by species identification number used in therein); H&N 05, Hollis and Neil 2005. Temp, water temperature affinity. Ref 2, reference to depth zonation: 1, Renz 1976; 2, McMillen and Casey 1978; 3, Kling 1979; 4, Kling and Boltovskoy 1995; 5, Abelmann and Gowing 1997.

ter affinities (Hollis and Neil 2005). In the Atlantic Ocean, the maximum occurrence of living *L. m. maritalis* is found in deep water and within AAIW north of the Polarfrontal Zone, where it is especially abundant in AAIW north of the STF (Abelmann and Gowing 1997).

L. maritalis gr. is most common in Interglacials at both sites, but is more abundant at Site 1123 (text-fig. 4). The warm-water preference of *L. maritalis* gr. is also shown by a negative correlation with $\delta^{18}O$ at Site 1123 ($r = -0.458$). The higher abundance of *L. maritalis* gr. at Site 1123 is probably an artifact of processing; the species group is relatively large and has a robust test.

Phortidium clevei

P. clevei is common in antarctic (Boltovskoy 1987) to subantarctic (Hollis and Neil 2005) waters of the southwest Pacific. It is rare in subtropical waters of the transitional zone (Boltovskoy 1987; Hollis and Neil 2005). *P. clevei* is a shallow dweller occurring with highest densities in the upper 100m of surface waters north and south of the Polarfrontal Zone (Atlantic Sector; Abelmann and Gowing 1997).

At Sites 1123 and 1124 (text-fig. 4), *P. clevei* is generally rare but exceeds 2% in Glacials. A preference for cooler waters is supported by a weak positive correlation with $\delta^{18}O$ at Site 1123 ($r = +0.331$). These features indicate that *P. clevei* is a useful cool-water indicator and it is used here to estimate the influence of shallow, cool SAW north of the STF. The scarcity of *P. clevei* in some Glacial intervals at site 1123 may be a processing artifact as the species is relatively delicate and some individuals are $<63\mu m$.

Cromyechinus antarctica

In the Pacific Ocean, *Cromyechinus antarctica* is a common faunal element in the antarctic and subantarctic zones south of the STF (Boltovskoy 1987; Hollis and Neil 2005). The species is a deep dweller, living in depths of 400-1000m in the Southern Ocean (Atlantic Sector) where *C. antarctica* represents a major component of Circumpolar Deep Water taxa (Abelmann and Gowing 1997).

At Sites 1123 and 1124, *C. antarctica* is relatively rare (never more than 2%) but increases in abundance in Glacial stages (text-fig. 4). *C. antarctica* is used to detect the influence of deep

Appendix 1 (continued)

TAXA	Ref 1	Comments	Site	Mor78	Bol87	sp. ID	H&N05 Temp	depth	Ref 2
WARM									
<i>Acanthodesmia vinculata</i> (Müller)	Tak 91		1		TT	100	warm	subsurface	1,2
<i>Acanthosphaera dodecastyla</i> Mast	Bol 98		1		ST	17	warm		
<i>Acrosphaera cyrtodon</i> (Haeckel)	Tak 91	Similar to <i>Odontosphaera cyrtodon</i> Haeckel, without curved spines in Hkl 87	1		TT	1	warm		
<i>Acrosphaera lappacea</i> (Haeckel)	N&M 79	As <i>Polysolenia</i>	1		C	2	warm	surface	2
<i>Acrosphaera spinosa</i> (Haeckel)	N&M 79	As <i>Polysolenia</i>	1, 2	TT	TT	4	ST	warm	
<i>Amphirhopalum ypsilon</i> Haeckel	Bol 98		1, 2		TT	68	ST	warm	intermediate 2
<i>Amphispyris reticulata</i> (Ehrenberg)	Bol 98		1		TT	101		warm	
<i>Anomalacantha dentata</i> (Mast)	N&M 79		1, 2		AA	26	ST	warm	
<i>Anthocyrtidium ophirensense</i> (Ehrenberg)	Bol 98		1		ST	173		warm	subsurface 3
<i>Anthocyrtidium zanguebaricum</i> (Ehrenberg)	Bol 98		1		ST	174		warm	
<i>Botryocyrtilis scutum</i> (Harting)	N&M 79		1		ST	191		warm	subsurface 1,2
<i>Carpocanarium papillosum</i> (Ehrenberg) group	N&M 79		1, 2		ST	169	ST	warm	
<i>Clathrocanium coarctatum</i> Ehrenberg	Tak 91		1		ST	119		warm	surface 4
<i>Collosphaera huxleyi</i> Müller	Tak 91		1, 2		C	6	ST	warm	
<i>Collosphaera macropora</i> Popofsky	Bol 98		1		TT	7		warm	
<i>Corocalyptra kruegeri</i> Popofsky	Bol 98		1		TT	137		warm	
<i>Cubotholus</i> spp.	Bol 98		1, 2		TT	99	ST	warm	
<i>Dictyocoryne profunda</i> Ehrenberg	Bol 98		1, 2	TT	TT	69	ST	warm	intermediate 3
<i>Dictyocoryne truncatum</i> (Ehrenberg)	Bol 98		2		TT	70		warm	
<i>Dictyophimus infabricatus</i> Nigrini	Bol 98		1, 2		ST	143		warm	intermediate 3,4
<i>Didymocyrtilis tetrathalamus</i> (Haeckel)	Bol 98		1, 2	C-TT	TT	87	ST	warm	surface 2,3,4
<i>Dipylissa bensoni</i> Dumitrica	Bol 98		1				ST	warm	
<i>Disolenia zanguebarica</i> (Ehrenberg)	N&M 79		1		TT	16		warm	surface 2
<i>Druppatractus irregularis</i> Popofsky	Ben 66		1		C	38	ST	warm	
<i>Euchitonia elegans/furcata</i> (Ehrenberg) group	Bol 98		1, 2	TT	TT	71	ST	warm	surface 1
<i>Eucyrtidium anomalum</i> (Haeckel)	Bol 98		1		TT	146	ST	warm	
<i>Eucyrtidium hexagonatum</i> Haeckel	N&M 79		1		TT	147		warm	surface 1,2
<i>Lamprocyclus maritilis maritilis</i> Haeckel	N&M 79		1, 2		TT	175	ST	warm	deep 5
<i>Lamprocyclus maritilis</i> Haeckel <i>polypora</i> Nigrini	N&M 79		1, 2		C	176	ST	warm	intermediate 3,5
<i>Lamprocyrtis nigriniae</i> (Caulet)	Bol 98		1, 2		ST	177	ST	warm	intermediate 3,4
<i>Lampromitra quadricuspis</i> Haeckel	Bol 98		1, 2		ST	153		warm	intermediate 4

southern-sourced water masses, particularly CDW at the studied sites.

Spongopyle osculosa

In Recent surface sediment samples *Spongopyle osculosa* occurs from the antarctic to subantarctic zone in the Atlantic Sector, with highest abundance in the Polarfrontal Zone (Petrushevskaya 1967; Abelmann and Gowing 1997). Boltovskoy (1987) recorded *S. osculosa* from the tropical to antarctic southwest Pacific but its highest occurrence is within the subantarctic zone and south of the STF offshore eastern New Zealand (Hollis and Neil 2005). Within plankton assemblages in the Atlantic Southern Ocean, Abelmann and Gowing (1997) recorded *S. osculosa* as one of two dominant deep dwellers within AAIW, in water depths of 400-1000 m (the other being *Cycladophora bicornis*; see below). *S. osculosa* is also common in AAIW in the northern subantarctic and subtropical zones (Abelmann and Gowing 1997). *S. osculosa* is recorded in deep water assemblages in the Gulf of Mexico and Caribbean Sea (McMillen and Casey 1978) and in the California Current (Boltovskoy and Riedel 1987). *S. osculosa* is commonly recorded in the vicinity of upwelling regimes, such as the Benguela Current System (Welling et al. 1992; Abelmann and Gowing 1997; Weinheimer 2001). Within the high productivity regime in the equatorial northwest Indian Ocean, Jacot Des Combes et al. (1999) describe *S. osculosa* as part of the thermocline layer assemblage.

S. osculosa exhibits an interesting pattern of occurrence at Site 1123 (text-fig. 4). In the lower part of the record (MIS 15-9), peak abundance is in Interglacials. However, in the late Pleistocene the peaks occur in Glacial stages MIS8, 6, 4 and 2. *S. osculosa* is

generally much less common at Site 1124 and exhibits very slight increases in abundance in Glacial stages MIS6, 4 and 2 (text-fig. 4). *S. osculosa* is thought to indicate the increased influence of AAIW in Glacial stages but in the lower part of Site 1123 it may be associated with enhanced mixing within Interglacials MIS15, 13 and 9. Given this species' robust and relatively large form it is possible that its greater abundance at Site 1123 is partly due to processing differences. However, the increases in Interglacials, which is not evident at Site 1124, signals a stronger influence of deep water mixing at Site 1123.

Cycladophora bicornis

Cycladophora bicornis is a common element of the subantarctic and antarctic Southern Ocean (Lombardi and Boden 1985). In the southwest Pacific, *C. bicornis* occurs in surface sediments north and south of the STF (Boltovskoy 1987), with higher abundance in subantarctic sediments (Hollis and Neil 2005). In the central north Pacific, Gulf of Mexico and Caribbean Sea, *C. bicornis* mainly lives in deep waters of 100-2000m and is most abundant at 200m (Kling 1979, McMillen and Casey 1978). In the Atlantic Sector of the Southern Ocean, *C. bicornis* is a prominent species in the AAIW plankton assemblage of the Polarfrontal Zone where it is most abundant at 100-300m (Abelmann and Gowing 1997). This same AAIW assemblage has also been found in depths between 100 and 500m close to the Namibia Upwelling Regime (Abelmann and Gowing 1997) where intermediate waters upwell along the southwestern African continental margin (Weinheimer 2001).

C. bicornis tends to be most common in Interglacials at Site 1123 (text-fig. 4), an observation supported by the negative correlation

Appendix 1 (continued)

TAXA	Ref 1	Comments	Site	Mor78	Bol87	sp. ID	H&N05	Temp	depth	Ref 2
<i>Larcospira quadrangula</i> Haeckel	Bol 98		1, 2		TT	95	ST	warm	surface	3,4
<i>Lipmanella bombus</i> (Haeckel)	Bol 98		1		TT	154		warm		
<i>Lipmanella dictyoceras</i> (Haeckel)	Bol 98		1, 2		ST	155	ST	warm	surface	4,5
<i>Litharachnium tentorium</i> Haeckel	Bol 98		1, 2		ST	156	ST	warm	subsurface	3,4
<i>Lithopera bacca</i> Ehrenberg	Bol 98		1		ST	157		warm	surface	3
<i>Lithostrobilus hexagonalis</i> Haeckel	Bol 98		1		TT	158		warm	surface	4
<i>Lophophaena hispida</i> (Ehrenberg)	Bol 98		1		ST	123		warm	subsurface	2
<i>Lophospyris pentagona pentagona</i> (Ehrenberg) emend. Goll	Bol 98		1, 2		TT	106		warm		
<i>Octopyle stenozona</i> Haeckel	N&M 79		1, 2		C	91	ST	warm	surface	3
<i>Peromelissa phalacra</i> (Haeckel)	Bol 98		1		ST	129		warm		
<i>Phormospyris stabilis stabilis</i> (Goll)	Bol 98		1		TT	107		warm	subsurface	3
<i>Pterocanium praetextum</i> (Ehrenberg) group	Bol 98		1, 2		TT	160	ST	warm	surface	1,2,4
<i>Pterocorys hertwigii</i> (Haeckel)	Bol 98		1, 2		TT	179		warm	surface	2,4
<i>Pterocorys minythorax</i> (Nigrini)	C&N 88		1		ST	180		warm	surface	4
<i>Pterocorys zancleus</i> (Müller)	Bol 98		1, 2		ST	181		warm	surface	2,4
<i>Saturnalis circularis</i> Haeckel	Bol 98		1		TT	55		warm		
<i>Siphonosphaera martensi</i> Brandt	Bol 98		1		C	10		warm		
<i>Siphonosphaera socialis</i> Haeckel	Tak 91		1		ST	11	ST	warm	surface	4,5
<i>Spirocorytis scalaris</i> Haeckel group	Bol 98		1, 2		ST	189		warm	surface	2,4
<i>Spongurus</i> sp. cf. <i>S. elliptica</i> (Ehrenberg)	N&M 79		1		ST	81		warm		
<i>Stylosphaera melpomene</i> Haeckel	Bol 98		1		ST	62		warm		
<i>Tetrapyle octacantha</i> Müller	N&M 79		1, 2	C-TT	C	91	ST	warm	surface	2,3,4,5
<i>Zygocircus productus</i> (Hertwig) group Hertwig	Bol 98		1, 2		ST	115		warm		
TRANSITIONAL										
<i>Actinomma sol</i> Cleve	Bol 98		1, 2		TR	24	TR	transit.	surface	4
<i>Eucyrtidium acuminatum octocolum</i> (Haeckel)	Bol 98		1, 2		TR	149	TR	transit.	intermediate	3
<i>Larcopyle bütschlii</i> Dreyer	Bol 98		1, 2		TR	94	TR	transit.	deep	4
<i>Thecosphaera inermis</i> (Haeckel)	Bol 98		1, 2		TR	65	TR	transit.		
<i>Theocorythium trachelium</i> (Ehrenberg) <i>dianae</i> (Haeckel)	N&M 79		1, 2		TR	182	TR	transit.	surface	3,4,5
<i>Theocorythium trachelium trachelium</i> (Ehrenberg)	N&M 79		1, 2		TR	182	TR	transit.	surface	3,4,5
COSMOPOLITAN										
<i>Acrospira murrayana</i> (Haeckel)	N&M 79	As <i>Polysolenia</i>	1		C	3		cosmop.	surface	2
<i>Actinomma leptoderma leptoderma</i> (Jørgensen)	N&M 79	<i>A. leptodermum</i> (Jørgensen) in N&M 79	1, 2		C	22	C	cosmop.	deep	5
<i>Actinomma medianum</i> Nigrini	N&M 79		1, 2	C	SA	23	C	cosmop.		
<i>Arachnocoallium calvata</i> Petrushevskaya	Pet 71		1		C	117		cosmop.		

with oxygen isotopes ($r = -0.477$). In contrast, *C. bicornis* shows a complex trend at Site 1124, where it has abundance peaks in specific Interglacials (MIS15, 5 and 3) and Glacials (MIS14, 12, 6 and 2) (text-fig. 4). The increased abundance of *C. bicornis* during Interglacials is intriguing given the cool water affinity noted above. Abundance peaks during Interglacials may signal increased deep-water influence or vertical mixing. Abundance peaks in Glacials at Site 1124, including a pronounced acme in MIS12, are consistent with cooling and an increased influence of AAIW at this site. Slightly higher abundance of *C. bicornis* at Site 1124 could be caused by differences in the processing methodology.

Cycladophora davisiana

In the Southern Ocean, *C. davisiana* is most abundant in antarctic waters (Lombardi and Boden 1985). East off New Zealand, the species occurs in surface sediments from north and south of the STF but is significantly more abundant in subantarctic samples (Boltovskoy 1987; Hollis and Neil 2005). In the central north Pacific and in the southern California Current, *C. davisiana* lives in the water column at 50-5000m and has peak abundance in intermediate waters in 100-200m depth (Kling 1979; Kling and Boltovskoy 1995). Nimmergut and Abelmann (2002) reported *C. davisiana* from sediment traps in 200-500m depths in the Okhotsk Sea. In the Antarctic and Polarfrontal Zone of the Atlantic Sector, living *C. davisiana* has been obtained from CDW samples between 400-1000m depth (Abelmann and Gowing 1997). In the western tropical Atlantic and in the Japan Sea, *C. davisiana* has been found in >500m depth (Takahashi and Honjo 1981; Itaki 2003). *C. davisiana* has been described from nearshore upwelling assemblages from the northern California Current (Welling et al. 1992), from the Benguela Current System

(Weinheimer 2001) and the northwest Indian Ocean (Jacot des Combes et al. 1999). The species is an important stratigraphic tool in carbonate-poor sediments in high latitudes as it is abundant in Glacial times but rare in Interglacials (Hays et al. 1976; Morley and Hays 1979; Abelmann and Gersonde 1988; Morley et al. 1995; Brathauer et al. 2001). Only in the Sea of Okhotsk (Ling 1974; Morley and Hays 1983) and Japan Sea (Itaki 2003), surface sediments contain >20-40% of *C. davisiana*. Hays and Morley (2003) discuss the Sea of Okhotsk as example for Ice Age Ocean conditions.

C. davisiana shows similar trends during the last 600 kyrs at Sites 1123 and 1124 (text-fig. 4). The species tends to be most common in Glacials (text-fig. 4). However, *C. davisiana* has abundance peaks in some Interglacials, especially those in which *C. bicornis* is also common (e.g. MIS15 at Site 1124, MIS9 at Site 1123). As with *C. bicornis*, this suggests that the deep-water influence is enhanced during some Interglacials at both sites. This complex abundance record indicates that, in contrast to high latitudes, *C. davisiana* is not a reliable guide for Glacial conditions in mid-latitudes. The higher abundance of this small species at Site 1124 could be due to processing differences between Sites 1123 and 1124.

Radiolarian assemblage variation: Glacial/Interglacial comparisons

Interglacial assemblages in 13 samples at Site 1123 are relatively diverse and are dominated by three undifferentiated spumellarian families (litheliids, spongodiscids, actinommids) (text-fig. 5a). *Larcopyle bütschlii* and *Theocorythium trachelium dianae* are the only transitional taxa to exceed 1% of the assemblage within Interglacials. *Tetrapyle octacantha* gr. is the only com-

Appendix 1 (continued)

TAXA	Ref 1	Comments	Site	Mor78	Bol87	sp. ID	H&N05	Temp	depth	Ref 2
<i>Axoprunum stauraxonium</i> Haeckel	N&M 79		1, 2		C	28	C	cosmop.		
<i>Botryopyle dictyocephalus</i> Haeckel	Bol 98		1		C	192		cosmop.		
<i>Botryostrobos auritus/australis</i> (Ehrenberg)	Bol 98		1, 2		C	185	C	cosmop. intermediate	3,4	
<i>Carpocanistrum</i> spp.	N&M 79		1, 2		ST	170,171	C	cosmop. intermediate	4	
<i>Ceratocyrtis histricosus</i> (Jørgensen)	Bol 98	<i>Helotholus histricosus</i> Jørgensen in Bol 98	1, 2		AA	121	C	cosmop. surface	4	
<i>Circodiscus microporus</i> (Stöhr)	P&K 72		1, 2				C	cosmop.		
<i>Cladoscenium ancoratum</i> Haeckel	Tak 91		1		C	118		cosmop.		
<i>Cornutella profunda</i> Ehrenberg	Bol 98		1, 2		SA	135	C	cosmop. intermediate	4	
<i>Corocalyptra cervus</i> (Ehrenberg)	Bol 98		1, 2				C	cosmop. intermediate	1,5	
<i>Corocalyptra columba</i> (Haeckel)	Bol 98		1		C	136		cosmop. deep	4	
<i>Cyrtopera laguncula</i> Haeckel	Bol 98		1, 2		C	139		cosmop. intermediate	3,4	
<i>Dictyophimus hirundo</i> (Haeckel)	Bol 98		1, 2		C	142	C	cosmop.		
<i>Eucyrtidium acuminatum acuminatum</i> (Ehrenberg)	N&M 79		1, 2		C	145	C	cosmop. surface	4	
<i>Eucyrtidium annulatum</i> (Popofsky)	Ben 66		1		C	151		cosmop.		
<i>Eucyrtidium hexastichum</i> (Haeckel)	Bol 98		1		C	148		cosmop. surface	4,5	
<i>Eucyrtidium teuscheri</i> (Haeckel)	Cau 86		1, 2				C	cosmop.		
<i>Gondwanaria dogieli</i> (Petrushevskaya)	N&N 82		1, 2				C	cosmop. deep	4	
<i>Haliometta miocenica</i> (Campbell & Clark)	N&N 82		1, 2				C	cosmop.		
<i>Heliodiscus asteriscus</i> Haeckel	Bol 98		1, 2		C	90	C	cosmop. surface	2,3	
<i>Hexacantium armatum/hostile</i> Cleve group	N&M 79	<i>H. enthacanthum</i> Jørgensen in N&M 79	1, 2		C	45,46	C	cosmop.		
<i>Hexacantium laevigatum</i> Haeckel	N&M 79		1		TT	49	C	cosmop.		
<i>Lithelius minor</i> Jørgensen group	Bol 98		1, 2	C			C	cosmop.		
<i>Phormostichoartus corbula</i> (Harting)	N&M 79		1		C	188		cosmop. subsurface	3	
<i>Pseudodictyophimus gracilipes</i> (Bailey)	Tak 91		1, 2		C	141	C	cosmop. intermediate	3,4,5	
<i>Pterocanium trilobum</i> (Haeckel)	Bol 98		1, 2		C	161	C	cosmop. surface	4	
<i>Pterocorys clausus</i> (Popofsky)	C&N 88		1, 2		SA	178	C	cosmop. subsurface	3,4	
<i>Pylolela armata</i> Haeckel group	Bol 98		1, 2		TT	93	C	cosmop. surface	2	
<i>Pylolella octopyle</i> Haeckel	Bol 98		1, 2		TT	98	C	cosmop.		
<i>Sethocomus (?) tabulatus</i> (Ehrenberg)	Pet 67		1, 2		C	162		cosmop.		
<i>Spongocore puella</i> Haeckel	N&M 79		1, 2		C	76	C	cosmop. intermediate	3	
<i>Spongodiscus resurgens</i> Ehrenberg	Bol 98		1, 2		C	77	C	cosmop. subsurface	3	
<i>Spongurus ? sp.</i>	N&M 79		1, 2		C	83	C	cosmop. deep	4, 5	
<i>Stichopilium bicornis</i> Haeckel	N&M 79		1		C	164		cosmop. subsurface	3	
<i>Stylatractus</i> spp. gr.	Bol 98		1, 2		C	60,61	C	cosmop.		

mon warm-water taxon (text-fig. 5a). Three cool-water taxa are abundant during Interglacials, including *Cycladophora bicornis* as noted above. Glacial assemblages in 12 samples are slightly less diverse (22 vs 24 taxa with an average abundance of >1% of the assemblage) but are similarly dominated by undifferentiated spumellarians (text-fig. 5b). A significant difference is the high abundance of the cool-water genus *Cenosphaera* (>10%). The warm-water *T. octacantha* gr. remains common but much less so than in Interglacials.

Because undifferentiated spumellarians are such a dominating feature of Glacial assemblages, only two definitively cool-water species occur at >1% in Glacial assemblages: *Spongopyle osculosa* and *Cycladophora davisiana*.

Assemblages from Site 1124 are generally more diverse than those from Site 1123, have high Equitability and have reduced dominance of undifferentiated spumellarians (text-fig. 5c, d). Interglacial assemblages in 39 samples are dominated by cosmopolitan taxa but the warm-water *T. octacantha* gr. is very common, exceeding 5% of the assemblage (text-fig. 5c). *Dictyocoryne profunda* and *Lophospyris pentagona pentagona* are two other common warm-water species. As discussed in the previous section, two subantarctic species, *C. davisiana* and *C. bicornis* are also relatively common in Interglacials. Glacial assemblages in 33 samples for Site 1124 are in general respects quite similar to Interglacial assemblages (text-fig. 5d). The main difference is the greater abundances of cool-water species, especially *C. davisiana*. In contrast to Site 1123 *L. bütschlii* and *T. t. dianae* are common transitional species within Interglacials and Glacials at Site 1124.

An exceptional species assemblage occurs in uppermost MIS8 at Site 1123 (1123B-2H-6, 80-82cm). The sample has an Interglacial character in terms of high abundance and diversity, as discussed above. Also, warm-water taxa (e.g. *Acrosphaera spinosa*, *Didymocyrtis tetrathalamus*) are much more common than cool-water taxa (e.g. *Cenosphaera cristata*, *Cycladophora bicornis*, *Botryostrobos aquilonaris*; Appendix 1). The sample may represent a warm anomaly within MIS8 or it might be out of place within the sedimentary succession. Unfortunately, no records for MIS8 are available for Site 1124 due to a hiatus.

Radiolarian paleotemperature indicators

Local information (Moore 1978; Boltovskoy 1987; Hollis and Neil 2005) on the modern biogeographic distribution of species and species groups encountered in this study has been used to assign 93 taxa to one of three categories: warm-water (tropical-subtropical), transitional, and cool-water (subantarctic-antarctic) (text-fig. 6; Appendix 1). As described earlier, the ratio of warm-water to cool-water species defines a new paleotemperature indicator: the Subtropical Index (ST index).

In the spumellarian-dominated record at Site 1123, paleotemperature indicator species rarely exceed 15% of the total fauna. Cool- and warm-water taxa have similar mean values (~6%) and, as expected, tend to vary antithetically in relation to oxygen isotope-defined climate cycles, especially in the upper part of the record (text-fig. 6). An exception to this pattern occurs in the lower part of the record where cool-water indicators show significant increases in Interglacials, notably MIS15, 13, 11 and 9. This is largely due to increases in deep-water indicators (*Cycladophora* spp., *S. osculosa*) and, as noted above, suggests increased deep-water influence during these middle Pleistocene Interglacials. The decline in cool-water taxa in uppermost parts

Appendix 1 (continued)

TAXA	Ref 1	Comments	Site	Mor78	Bol87	sp. ID	H&N05	Temp	depth	Ref 2
<i>Stylochlamidium</i> spp.	N&N 82		1, 2		C	84	C	cosmop.		
<i>Stylodictya validispina</i> Jørgensen	N&M 79		1, 2	C	C	85	C	cosmop. surface		2
<i>Theocorys veneris</i> Haeckel	Tak 91		1, 2		C	167		cosmop. subsurface		3, 4
<i>Theopilium tricostatum</i> (Haeckel)	Bol 98		1		C	168		cosmop. subsurface		2, 4

of Glacials MIS12 and 10 reflects the dominance of undifferentiated spumellarians, which cannot be assigned to biogeographic categories (see also text-fig. 5). Although the abundant genus *Cenosphaera* is dominated by cool-water species in this region, the presence of some warm-water elements precludes its use as a paleotemperature indicator (text-fig. 5). Transitional taxa make up ~3% of the total fauna on average and generally follow the pattern of warm-water taxa, increasing in Interglacials and decreasing in Glacials (text-fig. 6).

The high resolution record at Site 1124 shows well-defined antithetic variation in the abundance of paleotemperature indicator species in relation to climate cycles (text-fig. 6). On average, paleotemperature indicator species comprise >20% of the total fauna through the record. In contrast to the record at Site 1123, warm-water elements tend to be more common at Site 1124 and are rarely less than 10% (text-fig. 6). Transitional taxa average ~5% at Site 1124 and do not exhibit a clear trend in relation to climate cycles, with abundance peaks occurring in Glacials as well as Interglacials (text-fig. 6).

The Subtropical (ST) Index provides a useful summary of the trends discussed above and serves to accentuate the paleotemperature signal preserved in assemblages from both sites (text-fig. 6). Despite processing differences, the ST Index offsets between the two sites are consistent with the general biogeographic character of the assemblages, as discussed above, with the ST Index being generally higher at Site 1124, especially during Interglacials. The ST Index indicates that the warmest Interglacials are MIS11 (Site 1123 only), MIS7 and MIS5 and the coolest Glacials are MIS12 (at Site 1123), MIS6 and MIS2. Regarding Glacials at Site 1123 it has to be considered that MIS 12 is very depleted in paleotemperature indicator species and MIS2 is recorded by a single sample.

Local temperature changes throughout G-I climate cycles have been documented in local marine records using e. g. foraminifera and alkenones (Crundwell et al. in press; Pahnke and Sachs) which are in covariance with local (Hall et al. 2001, 2002) and global (Shackleton and Hall 1989) benthic foraminifera oxygen isotope records. Use of the radiolarian ST Index as a paleotemperature proxy is supported by a strong negative correlation of -0.728 with $\delta^{18}O$ at Site 1123 (Appendix 2b). However, it is interesting to note that while the percentage of warm-water indicators also shows a significant negative correlation with $\delta^{18}O$, there is no significant correlation with cool-water indicators. This reinforces the observation that temperature is not the sole influence on the abundance of cool-water taxa at Site 1123. This observation is reinforced by the absence of a correlation between warm- and cool-water indicators at Site 1123 (Appendices 2a, b), which contrasts with the strong negative correlation (-0.633) between these indicator groups at Site 1124 (Appendix 2c). Another important difference between the two sites in terms of covariance patterns is the significant positive correlation between diversity and both warm and cool paleotemperature indicators at Site 1123. This is not observed at Site 1124 and implies that the presence of identifiable paleotemperature indicators at Site 1123 may be a function of preservation. As preservation improves, the unexpected out-

come of the resulting diversity increase appears to be increases in the abundance of both warm- and cool-water indicator taxa. That no such correlation exists at Site 1124 is likely due to consistent good preservation through the late Pleistocene succession.

Radiolarian paleodepth indicators

It is difficult to differentiate paleodepth signals from paleotemperature signals in radiolarian assemblages because most of the species that inhabit surface or near-surface watermasses in high latitudes also inhabit deep watermasses at lower latitudes. In the preceding section, the paleotemperature records for both sites are based on variations in abundance of paleotemperature indicators from a range of depth zones. In this section, we subdivide the taxa according to depth preferences in order to determine if faunal changes help to identify changes in watermass structure at the two sites.

Variation in the abundance of shallow-dwelling taxa can be used to identify changes in the influence of surface watermasses north of the STF (text-fig. 7). Of the 29 shallow-dwelling taxa at Sites 1123 and 1124, warm-water elements are the most common and most diverse (23 warm-water and 6 cool-water taxa; Appendix 1). Especially at Site 1124, the ratio of warm-water taxa over cool-water taxa within shallow waters is almost twice as high as at Site 1123 which is partly due to differences in the processing methods. The abundance of warm-water, shallow dwelling taxa essentially mirrors that of the total warm-water cohort at both sites (text-fig. 6), peaking in Interglacials and decreasing through Glacials. In contrast, the cool-water shallow dwelling taxa differ from the total cool-water cohort in two important respects. Abundance peaks are intensified in a few Glacials, especially MIS12 at both sites and in uppermost MIS14 and MIS6 at Site 1124. This implies intensification of SAW flow at these times. Secondly, abundance peaks are muted in the Glacials in the late Middle to early Late Pleistocene at Site 1123, especially in MIS 10 and 6. This suggests relatively weak influence of SAW over Site 1123 at this time.

To determine the influence of intermediate water masses (AAIW) and deep southern-sourced currents (e.g. DWBC) at Sites 1123 and 1124 abundance of cool-water, deep-dwelling radiolarians has been investigated. Radiolarians living in depths >150m and have peak abundance at 200m water depths include *Cycladophora bicornis*, *Spongopyle osculosa*, *Peripyramis circumtexta*, *Androcyclas gamphonycha* and *Botryostrobus aquilonaris* (Appendix 1) and are inferred to be AAIW indicators (text-fig. 7). Deeper dwelling *Cromyechinus antarctica*, *Spongurus* ? sp. and *Spongurus pylomaticus* inhabit depths of >300m within CDW of the Southern Ocean (Abelmann and Gowing 1997). The influence of these southern-sourced, deep water masses is strongest in Glacials in the upper part of Site 1123 (MIS8 to MIS2) and throughout the interval examined at Site 1124 (text-fig. 7). In the lower part of Site 1123, this deep-water influence is strongest in the Interglacials (MIS15 to MIS9). The high abundance of deep-dwelling taxa in these Interglacials is a possible indication for enhanced vertical mixing. In MIS12 and 10, the weakness of a southern-sourced water mass signal is an artefact of the scarcity of paleoenvironmental indicators in spu-

Appendix 2 (a) Site 1123 (0-1.2 Ma)

	$\delta^{18}\text{O}$	rads/g	# taxa	α	H(S)	E	%SA	%ST	ST Index	%TR	shallow STW	shallow SAW	comb. CDW+AAIW	CDW comp.	AAIW comp.
$\delta^{18}\text{O}$	1.000	-0.032	-0.294	-0.255	-0.337	-0.002	0.242	-0.584	-0.557	-0.021	-0.501	0.306	0.110	0.207	0.069
rads/g		1.000	0.586	0.624	0.470	0.321	0.243	0.337	-0.067	0.014	0.390	0.223	0.239	0.317	0.189
# taxa			1.000	(0.968)	(0.944)	(0.250)	0.493	0.718	0.017	-0.294	0.696	0.234	0.518	0.339	0.514
α				1.000	(0.932)	(0.330)	0.522	0.664	-0.053	-0.272	0.653	0.273	0.538	0.399	0.520
H(S)					1.000	(0.331)	0.528	0.722	0.023	-0.301	0.671	0.249	0.554	0.319	0.562
E						1.000	0.298	0.200	-0.248	0.271	0.147	0.178	0.331	0.332	0.294
%SA							1.000	0.118	(-0.572)	-0.137	0.172	(0.593)	(0.917)	(0.598)	(0.910)
%ST								1.000	(0.497)	-0.220	(0.885)	-0.017	0.221	0.087	0.236
ST Index									1.000	-0.078	(0.354)	(-0.403)	(-0.431)	(-0.363)	(-0.404)
%TR										1.000	-0.241	-0.048	-0.173	0.069	-0.226
shallow STW											1.000	0.125	0.221	0.024	0.256
shallow SAW												1.000	0.422	0.291	0.415
CDW+AAIW													1.000	(0.704)	(0.977)
CDW comp.														1.000	0.538
AAIW comp.															1.000

Appendix 2 (b) Site 1123 (0-0.6 Ma)

	$\delta^{18}\text{O}$	rads/g	# taxa	α	H(S)	E	%SA	%ST	ST Index	%TR	shallow STW	shallow SAW	comb. CDW+AAIW	CDW comp.	AAIW comp.
$\delta^{18}\text{O}$	1.000	-0.127	-0.481	-0.490	-0.525	-0.083	0.167	-0.680	-0.728	0.206	-0.642	0.362	0.051	0.163	0.017
rads/g		1.000	0.639	0.651	0.475	0.293	0.089	0.422	0.173	0.019	0.470	0.073	0.109	0.235	0.068
# taxa			1.000	(0.981)	(0.960)	(0.465)	0.466	0.820	0.351	-0.159	0.766	0.084	0.507	0.396	0.506
α				1.000	(0.937)	(0.473)	0.443	0.809	0.349	-0.168	0.743	0.080	0.494	0.439	0.478
H(S)					1.000	(0.466)	0.508	0.818	0.339	-0.121	0.737	0.114	0.538	0.427	0.535
E						1.000	0.201	0.367	0.010	0.115	0.255	-0.044	0.296	0.369	0.257
%SA							1.000	0.187	(-0.422)	-0.165	0.154	(0.577)	(0.925)	(0.710)	(0.925)
%ST								1.000	(0.735)	-0.233	(0.946)	-0.079	0.269	0.149	0.285
ST Index									1.000	-0.269	(0.711)	(-0.367)	(-0.315)	(-0.276)	(-0.276)
%TR										1.000	-0.260	0.068	-0.318	-0.221	-0.325
shallow STW											1.000	-0.002	0.200	0.035	0.233
shallow SAW												1.000	0.378	0.247	0.390
CDW+AAIW													1.000	(0.817)	(0.987)
CDW comp.														1.000	0.715
AAIW comp.															1.000

Appendix 2 (c) Site 1124 (0-0.6 Ma)

	rads/g	# taxa	α	H(S)	E	%SA	%ST	ST Index	%TR	shallow STW	shallow SAW	comb. CDW+AAIW	CDW comp.	AAIW comp.
rads/g	1.000	0.452	0.383	0.428	0.216	-0.202	0.097	0.143	-0.127	0.071	-0.251	-0.195	-0.227	-0.136
# taxa		1.000	(0.851)	(0.876)	(0.248)	-0.146	0.211	0.153	-0.210	0.262	-0.112	-0.170	-0.183	-0.129
α			1.000	(0.851)	(0.416)	-0.157	0.227	0.129	-0.231	0.205	-0.132	-0.156	-0.184	-0.108
H(S)				1.000	(0.677)	-0.088	0.125	0.095	-0.203	0.129	-0.044	-0.089	-0.096	-0.067
E					1.000	-0.006	-0.039	-0.004	-0.060	-0.121	0.039	0.040	0.054	0.023
%SA						1.000	-0.633	(-0.767)	0.142	-0.457	(0.792)	(0.910)	(0.774)	(0.803)
%ST							1.000	(0.750)	-0.191	(0.795)	-0.571	-0.535	-0.668	-0.349
ST Index								1.000	-0.145	(0.514)	(-0.552)	(-0.716)	(-0.680)	(-0.590)
%TR									1.000	-0.244	0.241	0.152	0.312	0.028
shallow STW										1.000	-0.387	-0.469	-0.548	-0.328
shallow SAW											1.000	0.609	0.685	0.441
CDW+AAIW												1.000	(0.771)	(0.929)
CDW comp.													1.000	0.481
AAIW comp.														1.000

APPENDIX 2

Linear correlation coefficients for radiolarian assemblage characteristics (and $\delta^{18}\text{O}$ for Site 1123; from Hall et al. 2001) for (a) the entire 1.2 Myr record examined at ODP Site 1123 (N = 55; $r \geq 0.267$ is significant at $P = 0.05$), (b) the last 0.6 Myrs at Site 1123 (N = 25; $r \geq 0.396$ is significant at $P = 0.05$), and (c) the 0.6 Myr record at Site 1124 (N = 72; $r \geq 0.238$ is significant at $P = 0.05$). Significant correlations are in bold type. Correlations between non-independent radiolarian parameters are in brackets. %SA, abundance of cool-water taxa; %ST, abundance of warm-water taxa; %TR, abundance of transitional taxa. Other symbols as for text-figs. 2, 7.

mellarian-dominated assemblages at Site 1123 (text-fig. 7). From MIS7, a switch in the deep ocean regime seems to occur which strengthens the influence of deep, cool southern-sourced waters within Glacials. Over the same interval, the CDW signal, that is associated with DWBC flow, is no longer evident in Interglacials. At both Sites, the strongest episode of cool deep-water influence is within MIS2 where deep-dwelling radiolarians exceed 10% of the assemblage (text-fig. 7).

DISCUSSION

Interglacial assemblages

Radiolarian assemblages at ODP Site 1123, and, in particular at Site 1124, are abundant and diverse during Interglacials (text-fig. 2). This is also seen in modern radiolarian assemblages north of the STF (Hollis and Neil 2005) and is consistent with a micronutrient-rich, highly-productive STW inflow (Boyd et al. 2004). At

Site 1124, the strong influence of northern-sourced ECC flow is evident from an abundance of warm-water species. Radiolarian assemblages at Site 1123 are less abundant and diverse during Interglacials than at Site 1124. At Site 1123, we infer advection of micronutrient-poor SAW (Boyd et al. 2004) across or around the eastern edge of Chatham Rise (Chiswell and Sutton 1998; Chiswell 2001). In the area off the eastern rise, the STF-controlling Southland Current (SC) and the ECC are less constrained by the deepening rise (2000m; Chiswell 2001), allowing widening of the front up to 400km. Satellite-derived images of sea surface temperature (SST) in the eastern offshore New Zealand region show both intrusions of SAW north into STW and reverse out-breaks over the STF (Chiswell 2001). SST oscillations, at scales ranging from tens to hundreds of kilometers, however, do not affect the steep thermohaline feature of the STF (Chiswell 2001).

Spumellarian-dominated assemblages at Sites 1123 and 1124 have increased abundance of warm-water families, namely collosphaerids, coccodiscids, tholoniids and nassellarian pterocoryids within Interglacials (text-fig. 3), which are the radiolarian families that typify subtropical and tropical watermasses in the southwest Pacific (Boltovskoy 1987). The high-resolution record at Site 1124 reveals a rapid increase of warm-water taxa at glacial terminations (text-fig. 6). Radiolarian assemblages indicate that warmest conditions and strongest influence of shallow, warm STW occurred at the onset of Interglacials within MIS11 (Site 1123), MIS7 (Sites 1123, 1124) and MIS5 (Sites 1123, 1124) (text-fig. 7). Sea-surface temperature (SST) reconstructions at Site 1123, based on planktic foraminifera, suggest warmest mean annual SSTs of $\sim 19^{\circ}\text{C}$ at the onset of MIS11, 9, 7, and, SSTs of $\sim 18^{\circ}\text{C}$ in initial MIS5 (Crundwell et al. in press). The abrupt increase in tropical and subtropical elements at the onset of Interglacials is consistent with sedimentary evidence for a strengthening of south-flowing subtropical waters of the ECC (e.g. Carter et al. 1999b; Carter 2001; Nelson et al. 2000). Carter et al. (2002) noted that the main driving force of the ECC, namely the Tasman Front/East Australian Current, migrated southward to its present position at $\sim 32^{\circ}\text{S}$ after the Last Glacial Maximum (LGM), which is assumed to allow the current to pass through a major gap in Norfolk Ridge, thus enforcing the downstream ECC. This southward migration of the front presumably occurred in all Interglacials and caused increased abundance of warm-water radiolarians. An increased abundance of deep-dwelling taxa in some Interglacials at Site 1123 (text-fig. 7) is considered to indicate enhanced vertical mixing and is discussed further below.

Glacial assemblages

Reduced abundance and diversity characterize Glacials, especially at Site 1123. This is assumed to be due to the weakened flow of STW. During the LGM, the Tasman Front/East Australian Current was positioned at $\sim 26^{\circ}\text{S}$ (Martinez 1994) and $\sim 600\text{km}$ north of its present position (Carter 2001). Thus, the southward flow of STW was thought to be weakened and partly deflected by Norfolk Ridge (Carter et al. 2002). Concurrent northward incursions of SAW across, and around the deep eastern edge of Chatham Rise (Chiswell and Sutton 1998; Chiswell 2001) would cause particularly low abundance and diversity at Site 1123 (text-fig. 2). Crundwell et al. (in press) also suggest a northward shift of the STF, and migration of SAW over the position of Site 1123 during Glacials. Expansion of ice caps is believed to have intensified temperature gradients, the flow of westerly winds, circumpolar currents and the associated DWBC flow resulting in the northward migration of ocean fronts in the Southern Ocean (Carter 2001; Hall et al. 2001; 2002). Because of the topographic restriction, northward oscillation of the STF

is unlikely over the shallow, central Chatham Rise (Heath 1985; Fenner et al. 1992; Nelson et al. 1993; Carter 2001; Chiswell 2002; Sikes et al. 2002).

Glacial radiolarian assemblages at Sites 1123 and 1124 are dominated by spongodiscids and litheliids and have increased abundance of carpocaniids, cannobotryids, artostrobiids, as well as cool-water actinommids, pyloniids and theoperids (text-fig. 3). Radiolarian paleotemperature and depth indicators also suggest reduced supply of shallow STW to the eastern New Zealand area, and, at the same time, increased influence of cool SAW during Glacials (text-fig. 7). Lowest ST Index values indicate coolest conditions in MIS12 (Site 1123), MIS6 (Sites 1123, 1124), MIS4 (Site 1123) and MIS2 (Sites 1123, 1124; text-fig. 6). Oxygen isotope records at Site 1123 suggest coolest Glacials in MIS 12 and 2 (Hall et al. 2001; 2002); MIS12 is considered to be the coldest Glacial in the past 500,000 years (Howard 1997). Derived from planktic foraminiferal assemblages, Crundwell et al. (in press) propose SSTs of $\sim 10^{\circ}\text{C}$ (MIS6), $\sim 11^{\circ}\text{C}$ (MIS12, 4) and $\sim 12^{\circ}\text{C}$ (MIS2) at Site 1123.

Sedimentological and stable isotope data indicate that the intensity of DWBC flow increases during Glacials and that the flow has shown a progressive increase in successive Glacial stages from $\sim 4\text{ Ma}$ (Hall et al. 2001). This is broadly consistent with the radiolarian record, although the low resolution of the Site 1123 record and the hiatus in the critical interval at Site 1124 make confident interpretation of the deep-water signal difficult. Based on the abundance of deep-water indicators, deep water influence is strongest in the last three Glacial stages (MIS6, 4 and 2) and peaks in MIS2 (text-fig. 7). Prior to MIS7 ($\sim 0.25\text{ Ma}$), there is little indication that deep-water influence is significantly stronger in Glacials than in Interglacial with peaks in deep-water indicators occurring rather randomly through the record. There is little evidence to support the suggestion by Joseph et al. (2004) that DWBC flow became progressively weaker through the Quaternary at Site 1124 due to the current migrating away from the location.

Vertical mixing during Interglacials

Peaks in the abundance of deep-dwelling radiolarian species, such as *C. bicornis* and *S. osculosa*, have been used to identify episodes of high export productivity and enhanced vertical mixing within upwelling areas (Welling et al. 1992; Abelmann and Gowing 1997; Jacot Des Combes et al. 1999; Weinheimer 2001; text-fig. 6). As these are also cool-water species, increases in their abundance during Glacial stages at Sites 1123 and 1124 are an expected feature of cooler-water assemblages. However, significant peaks in Interglacials are possibly caused by deep-water indicators; local changes in oceanographic conditions may have promoted vertical mixing. *C. bicornis* and *S. osculosa* have abundance peaks in Interglacials (MIS 15, 13 and 9) in the lower part of the Site 1123 record and also exhibit small increases in MIS15 and 13 at Site 1124 (text-fig. 4). In the upper part of the two records, peak abundances for these two species are largely restricted to Glacial stages, apart from peaks for *C. bicornis* in MIS5 and MIS3 (text-fig. 4). This suggests that enhanced vertical mixing was primarily a feature of Interglacials prior to $\sim 0.25\text{ Ma}$. However, there is no evidence from the radiolarian faunas to suggest that this resulted in increased export productivity. Indeed, radiolarian abundance and diversity increase at Site 1123 from the base of Interglacial MIS9 and both parameters are stable through this interval at Site 1124 (text-fig. 2). Rather than a paleoproductivity signal, the abundance peak for these two deep-water species in middle Pleistocene Interglacials (MIS15-9) suggests that a compositional difference in the deep water

bathing the two sites, especially Site 1123, occurred at ~2.5 Ma. The cause for this shift is uncertain but it may be related to an overall increase in DWBC flow that begins at ~0.45 Ma (Hall et al. 2001).

SUMMARY AND CONCLUSIONS

Variations in radiolarian abundance, diversity and in the abundance of paleotemperature and paleodepth indicators at Sites 1123 and 1124 during G-I cycles provide useful guides to changes in oceanographic conditions offshore eastern New Zealand during the last 600,000 years.

Radiolarian assemblages north of the STF are abundant and diverse, reflecting nutrient-rich, productive conditions under STW inflow, particularly at Site 1124. A radiolarian paleotemperature proxy, the Subtropical (ST) Index indicates warmest climatic conditions occurred during Interglacial Stages MIS 11, 7 and 5. Diverse Interglacial faunas comprise mostly warm-water and shallow-dwelling taxa that reflect a strong inflow of the subtropical ECC, probably caused by southward shift of the Tasman Front/East Australian Current. Abundance peaks of deep-dwelling taxa within Interglacials between 0.6 and 0.25 Ma (MIS15-9) indicate enhanced vertical mixing but radiolarian assemblages do not indicate that this was associated with high productivity: radiolarian abundance and diversity are highest in the latest Quaternary Interglacials. The ST Index indicates that coolest climatic conditions occurred in MIS 12, 6 and 2. Paleotemperature and paleodepth indicators indicated reduced subtropical inflow during Glacials, particularly at Site 1123. Radiolarian assemblages suggest that the STF may have migrated over Site 1123 during the coolest Glacial episodes, probably due to the strengthening of deep, southern-sourced currents.

ACKNOWLEDGMENTS

VL acknowledges the German Academic Exchange Service (Deutscher Akademischer Austausch Dienst, DAAD); VL and HW thank the German Research Foundation (Deutsche Forschungsgemeinschaft, DFG) and the University of Bremen; VL and CH are grateful for support from the Foundation for Research, Science and Technology through the GNS Global Change Through Time Program. The authors thank the Ocean Drilling Program for providing samples from Sites 1123 and 1124. We are grateful to Ian Hall for providing stable isotope and color reflectance data for Sites 1123 and 1124, and for the revised age model from Site 1123. The authors thank Martin P. Crundwell, George H. Scott and Karin A. F. Zonneveld for helpful discussions and critical review of this work. The thorough analysis and perceptive comments on the manuscript by David B. Lazarus and Jane K. L. Dolven were much appreciated.

REFERENCES

ABELMANN, A., 1988. Freeze-drying simplifies the preparation of microfossils. *Micropaleontology*, 34(4): 361.

ABELMANN, A. and GERSONDE, R., 1988. *Cycladophora davisiana* stratigraphy in Plio-Pleistocene cores from the Antarctic Ocean (Atlantic Sector). *Micropaleontology*, 34(3): 268-276.

ABELMANN, A. and GOWING, M.M., 1997. Spatial distribution pattern of living polycystine radiolarian taxa - baseline study for paleoenvironmental reconstructions in the Southern Ocean (Atlantic Sector). *Marine Micropaleontology*, 30: 3-28.

ABELMANN, A., BRATHAUER, U., GERSONDE, R., SIEGER, R. AND ZIELINSKI, U., 1999. Radiolarian-based transfer function for the estimation of sea surface temperatures in the Southern Ocean (Atlantic Sector). *Paleoceanography*, 14(3): 410-421.

AITA, Y. and SUZUKI, A., 2003. Leg 181: Southwest Pacific Gateways: Sediment drift and deep water fluctuation off Eastern New Zealand. *Monthly Chikyu Special Volume: Deep Sea and a new Earth Biological Science*, Kaiyo-Shuppan, 40: 1-5.

BENSON, R.N., 1966. "Recent Radiolaria from the Gulf of California". Ph.D. thesis, University of Minnesota, Minnesota, 577 pp.

BEVINGTON, P.R. and ROBINSON, D.K., 1991. *Data reduction and Error Analysis for the Physical Sciences*. London, McGraw-Hill Higher Education, Inc.: 328 pp.

BOLTOVSKOY, D., 1987. Sedimentary record of radiolarian biogeography in the equatorial to antarctic western Pacific Ocean. *Micropaleontology*, 33(3): 267-281.

———, 1998. Classification and distribution of South Atlantic recent polycystine Radiolaria. *Paleontologica Electronica*, 1(2): 1-116. [http://www.paleo-electronica.org/1998_2/boltovskoy/issue2.htm]

BOLTOVSKOY, D. and RIEDEL, W.R., 1980. Polycystine Radiolaria from the southwestern Atlantic Ocean plankton. *Revista Espanola de Micropaleontologia*, 12(1): 99-146.

BOLTOVSKOY, D. and JANKILEVICH, S.S., 1985. Radiolarian distribution in East equatorial Pacific plankton. *Oceanologica Acta*, 8(1): 101-123.

BOYD, P.W., MCTAINSH, G., SHERLOCK, V., RICHARDSON, K., NICHOL, S., ELLWOOD, M. and FREW, R., 2004. Episodic enhancement of phytoplankton stocks in New Zealand subantarctic waters: contribution of atmospheric and oceanic iron supply. *Global Biogeochemical Cycles*, 18: 1029, doi:10.1029/2002GB002020.

BRATHAUER, U., ABELMANN, A., GERSONDE, R., NIEBLER, H.-S., and FÜTTERER, D.K., 2001. Calibration of *Cycladophora davisiana* events versus oxygen isotope stratigraphy in the subantarctic Atlantic Ocean - a stratigraphic tool for carbonate-poor Quaternary sediments. *Marine Geology*, 175: 167-181.

CARTER, L., 2001. Currents of change: the ocean flow in a changing world. *Water and Atmosphere*, 9(4): 15-17. NIWA online publications [<http://www.niwascience.co.nz>].

CARTER, R.M., CARTER, L., MCCAVE, N., and THE LEG 181 SHIPBOARD SCIENTIFIC PARTY, 1999a. The DWBC sediment drift record from Leg 181: drilling in the Pacific gateway for the global thermohaline circulation. *JOIDES Journal*, 25(1): 8-13.

CARTER, R.M., MCCAVE, I.N., RICHTER, C., CARTER, L., AND THE LEG 181 SHIPBOARD SCIENTIFIC PARTY, 1999b. *Proceedings of the Ocean Drilling Program, Initial Reports, Southwest Pacific Gateways, Volume 181*. College Station, TX: Ocean Drilling Program, [CD-ROM].

CAULET, J.P., 1986. Radiolarians from the Southwest Pacific. In: Kennett, J.P., Von Der Borch, C.C., et al., Eds. *Initial Reports of the Deep Sea Drilling Project*, Volume 90, Washington DC: US Government Printing Office, 90: 835-861.

CAULET, J.P. and NIGRINI, C., 1988. The genus *Pterocorys* [Radiolaria] from the tropical late Neogene of the Indian and Pacific Oceans. *Micropaleontology*, 34(3): 217-235.

- CASEY, R.E., 1971. Radiolarians as indicators of past and present water-masses. In: Funnel, B.M. and Riedel, W.R., Eds., *The Micropalaeontology of Oceans*. London: Cambridge University Press, 331-341.
- CHISWELL, S.M., 1994. Variability in sea surface temperature around New Zealand from AVHRR images. *New Zealand Journal of Marine and Freshwater Research*, 28: 179-192.
- , 2000. The Wairarapa Coastal Current. *New Zealand Journal of Marine and Freshwater Research*, 34: 303-315.
- , 2001. Eddy energetics in the Subtropical Front over the Chatham Rise, New Zealand. *New Zealand Journal of Marine and Freshwater Research*, 35: 1-15.
- , 2002. Temperature and salinity mean and variability within the Subtropical Front over Chatham Rise, New Zealand. *New Zealand Journal of Marine and Freshwater Research*, 36: 281-298.
- CHISWELL, S.M. and SUTTON, P.J.H., 1998. A deep eddy in the Antarctic Intermediate Water north of the Chatham Rise. *Journal of Physical Oceanography*, 28: 535-540.
- CLARKE, A., CHURCH, J. and GOULD, J., 2001. In: Siedler, G., Church, J. and Gould, J., Eds., *Ocean circulation and climate: observing and modelling the global ocean*, 11-30. San Diego: Academic Press.
- CORTESE, G., 2004. The 300 specimens problem. *Radiolaria: Newsletter of the international association of radiolarian paleontologists*, 22: 13-18.
- CORTESE, G. and ABELMANN, A., 2002. Radiolarian-based paleotemperatures during the last 160 kyr at ODP Site 1089 (Southern Ocean, Atlantic Sector). *Palaeogeography, Palaeoclimatology, Palaeoecology*, 182: 259-286.
- CRUNDWELL, M., SCOTT, G., NAISH, T., and CARTER, L., in press. Glacial-interglacial ocean climate variability during the Mid-Pleistocene transition in the temperate Southwest Pacific, ODP Site 1123. *Palaeogeography, Palaeoclimatology, Palaeoecology*
- DOLVEN, J.K., CORTESE, G. and BJØRKLUND, K.R., 2002. A high-resolution radiolarian derived paleotemperature record for the Late Pleistocene-Holocene in the Norwegian Sea. *Paleoceanography*, 17(4): 1072, 13 pp.
- DOW, R.L., 1978. Radiolarian distribution and the Late Pleistocene history of the Southeastern Indian Ocean. *Marine Micropaleontology*, 3(3): 203-227.
- DWORETZKY, B.A. and MORLEY, J.P., 1987. Vertical distribution of radiolaria in the Eastern equatorial Atlantic: analysis of multiple series of closely-spaced plankton tows. *Marine Micropaleontology*, 12: 1-19.
- FENNER, J., CARTER, L. and STEWART, R., 1992. Late Quaternary paleoclimatic and paleoceanographic change over northern Chatham Rise, New Zealand. *Marine Geology*, 108: 383-404.
- FENNER, J. and DI STEFANO, A., 2004. Late Quaternary oceanic fronts along Chatham Rise indicated by phytoplankton assemblages, and refined calcareous nannofossil stratigraphy for the mid-latitude SW Pacific. *Marine Geology*, 205(1-4): 59-86.
- GODFREY, M.G., ROEBUCK, E.M. and SHERLOCK, A.J., 1988. *Concise Statistics*. London: Edward Arnolds Publishers Ltd., 402 pp.
- HALL, I.R.; MCCAIVE, I.N.; SHACKELTON, N.J.; WEEDON, G.P. and HARRIS, S.E., 2001. Intensified deep Pacific inflow and ventilation in Pleistocene glacial times. *Nature*, 412: 809-812.
- HALL, I.R., CARTER, L. and HARRIS, S.E., 2002. Major depositional events under the deep Pacific inflow. *Geology*, 30(6): 487-490.
- HAMMER, Ø., HARPER, D.A.T. and RYAN, P.D., 2001. PAST: paleontological statistics Software Package for Education and Data Analysis. *Paleontologia Electronica*, 4(1): 9 pp. [hi/palaeo-electronica.org/2001_1/pasVissue1_01.].
- HAYS, J.D., 1965. Radiolaria and Late Tertiary and Quaternary history of Antarctic seas. In: LLANO, G.D., Ed. *Biology of the Antarctic Seas II*. American Geophysical Union, Antarctic Research Series, 5: 125-184.
- HAYS, J.D., IMBRIE, J. and SHACKLETON, N.J., 1976. Variations in the Earth's orbit: Pacemaker of the ice ages. *Science*, 194: 1121-1132.
- HAYS, J.D. and SHACKLETON, N.J., 1976. Globally synchronous extinction of the radiolarian *Stylatractus universus*. *Geology*, 4: 649-652.
- HAYS, J.D. and MORLEY, J.J., 2003. The Sea of Okhotsk: A Window on the Ice Age Ocean. *Deep-Sea Research I*, 50: 1481-1506.
- HAYWARD, B.W.; GRENFELL, H.R.; REID, C.M. and HAYWARD, K.A., 1999. Recent New Zealand shallow-water benthic foraminifera: Taxonomy, ecologic distribution, biogeography, and use in paleoenvironmental assessment. *Institute of Geological and Nuclear Sciences Monograph*, 21: 1-258.
- HEATH, R.A., 1976. Models of the diffusive-advective balance at the Subtropical Convergence. *Deep Sea Research*, 23: 1153-1164.
- , 1985. A review of the physical oceanography of the seas around New Zealand - 1982. *New Zealand Journal of Marine and Freshwater Research*, 19: 79-124.
- HOLLIS, C.J., MILDENHALL, D.C., CROUCH, E.M., and LÜER, V., 2002. Preliminary studies of palynomorphs and radiolarians from Quaternary marine sediment cores, offshore eastern New Zealand. *Institute of Geological and Nuclear Sciences file report 2002*, 2: 1-37.
- HOLLIS, C.J. and NEIL, H.L., 2005. Sedimentary record of radiolarian biogeography, offshore eastern New Zealand. *New Zealand Journal of Marine and Freshwater Research*, 39: 165-193.
- HOLLIS, C.J., NEIL, H.M., LÜER, V., SCOTT, G.H. and MANIGHETTI, B., 2006. Radiolarian-based sea-surface temperature estimates for the last 35,000 years, offshore eastern New Zealand. In: Lüer, V., Hollis, C.J., Campell, H. and Simes, J., Eds. *InterRad 11 and Triassic Stratigraphy Symposium; A joint international conference hosted by the International Association of Radiolarian Paleontologists, IGCP 467 and the Subcommission of Triassic Stratigraphy, 19-24 March 2006, Te Papa, Wellington, GNS Science miscellaneous series II*, Lower Hutt, Institute of Geological and Nuclear Sciences Ltd: 85.
- HOWARD, W.R., 1997. A warm future in the past. *Nature*, 388: 418-419.
- ITAKI, T., 2003. Depth-related radiolarian assemblage in the water-column and surface sediments of the Japan Sea. *Marine Micropaleontology*, 47: 253-270.
- ITAKI, T. and HASEGAWA, S., 2000. Destruction of radiolarian shells during sample drying and its effect on apparent faunal composition. *Micropaleontology*, 46(1): 179-185.
- JACOT DES COMBES, H., CAULET, J.-P., and TRIBOVILLARD, N.P., 1999. Pelagic productivity changes in the equatorial area of the northwest Indian Ocean during the last 400,000 years. *Marine Geology*, 158: 27-55.

- JOHNSON, D.A. and NIGRINI, C., 1980. Radiolarian biogeography in surface sediments of the western Indian Ocean. *Marine Micropaleontology*, 5(2): 111-152.
- , 1982. Radiolarian biogeography in surface sediments of the eastern Indian Ocean. *Marine Micropaleontology*, 7(3): 237-281.
- JOSEPH, L.H., REA, D.K. and VAN DER PLUIJM, B.A., 2004. Neogene history of the Deep Western Boundary Current at Rekohu sediment drift, Southwest Pacific (ODP Site 1124). *Marine Geology*, 205: 185-206.
- KLING, S.A., 1979. Vertical distribution of polycystine radiolarians in the central north Pacific. *Marine Micropaleontology*, 4: 295-318.
- , 1998. Radiolaria. In: HAQ, B.U. AND BOERSMA, A., Eds. *Introduction to marine micropaleontology*, 203-244. New York: Elsevier Science.
- KLING, S.A. and BOLTOVSKOY, D., 1995. Radiolarian vertical distribution patterns across the southern California Current. *Deep Sea Research I*, 42(2): 191-231.
- LAZARUS, D.B., 1990. Middle Miocene to Recent radiolarians from the Weddell Sea, Antarctica, ODP Leg 113. In: barker, P.F., kennett, J.P., et al., Eds., *Proceedings of the Ocean Drilling Program, Scientific Results, Leg 113*. Ocean Drilling Program, College Station, Texas, A&M University, 113: 709-727.
- , 1992. Antarctic Neogene radiolarians from the Kerguelen Plateau, ODP legs 119 and 120. In: Wiese, S.W. and Schlich, R., Eds. *Proceedings of the Ocean Drilling Program, Scientific Results, Leg 20*, Ocean Drilling Program, College Station, Texas, A&M University, 20: 785-810.
- LING, H.-Y., 1974. Polycystine Radiolaria and silicoflagellates from surface sediments of the Sea of Okhotsk. *Bulletin of the Geological Survey of Taiwan*, 24: 1-11.
- LOMBARI, G. AND BODEN, G., 1985. Modern Radiolarian Global distributions. *Cushman Foundation for Foraminiferal Research, Special Publication*, 16A: 125 pp.
- LÜER, V., 2003. *Quaternary radiolarians from offshore eastern New Zealand, Southwest Pacific (ODP Leg 181, Site 1123): importance for correlation and identification of climatic changes*. Diploma Thesis, University of Bremen, Bremen, 105 pp., 11 pls., pdf [http://www-user.uni-Bremen.de/~micropal/lueer_de.htm].
- LÜER, V., HOLLIS, C.J. AND WILLEMS, H., 2006. Late Quaternary radiolarian assemblages as indicators for paleoceanographic changes north of the Subtropical Front, offshore eastern New Zealand, southwest Pacific. In: Lüer, V., Hollis, C.J., Campell, H. and Simes, J., Eds. *InterRad II and Triassic Stratigraphy Symposium; A joint international conference hosted by the International Association of Radiolarian Paleontologists, IGCP 467 and the Subcommission of Triassic Stratigraphy, 19-24 March 2006, Te Papa, Wellington*, 85. GNS Science miscellaneous series II. Lower Hutt: Intitute of Geological and Nuclear Sciences Ltd.
- MARTINEZ, J.I., 1994. Late Pleistocene paleoceanography of the Tasman Sea: implications for the dynamics of the warm pool in the western Pacific. *Palaeogeography, Palaeoclimatology, Palaeoecology*, 112: 19-62.
- MCMILLEN, K.J. and CASEY, R.E., 1978). Distribution of living radiolarians in the Gulf of Mexico and caribbean Sea, and comparison with the sedimentary record. *Marine Micropaleontology*, 3: 121-145.
- MOLINA-CRUZ, A., 1977. Radiolarian assemblages and their relationship to the oceanography of the subtropical southeastern Pacific. *Marine Micropaleontology*, 2:315-352.
- MOORE, T.C., 1973. Method of randomly distributing grains for microscopic examination. *Journal of Sedimentary Petrology*. 43(3): 904-906.
- , 1978. The distribution of radiolarian assemblages in the modern and ice-age Pacific. *Marine Micropaleontology*, 3: 229-266.
- MORLEY, J.J., 1979. A transfer function for estimating paleoceanographic conditions based on deep-sea surface sediment distribution of radiolarian assemblages in the South Atlantic. *Quaternary Research*, 12(3): 381-395.
- MORLEY, J.J. and HAYS, J.D., 1979. Cycladophora davisiana: a stratigraphic tool for Pleistocene north Atlantic and Interhemispheric correlation. *Earth and Planetary Science Letters*, 44: 383-389.
- , 1983. Oceanographic conditions associated with high abundances of the radiolarian Cycladophora davisiana. *Earth and Planetary Science Letters*, 66: 63-72.
- MORLEY, J.J. and SHACKLETON, N.J., 1978. Extension of the radiolarian *Strylactrus universus* as a biostratigraphic datum to the Atlantic Ocean. *Geology*, 6: 309-311.
- MORLEY, J.J. and STEPIEN, J.C., 1985. Antarctic Radiolaria in late winter/early spring Weddell Sea waters. *Micropaleontology*, 31(4): 365-371.
- MORLEY, J.J., TIASE, V.L., ASHBY, M.M. and KASHGARIAN, M., 1995. A high resolution stratigraphy for Pleistocene sediments from North Pacific sites 881, 883, and 887 based on abundance variations of the radiolarian *Cycladophora davisiana*. In: Rea, D.K., Basov, I.A., Scholl, D.W. and Allan, J.F., Eds., *Proceedings of the Ocean Drilling Program, Scientific Results, Volume 145*, 133-140. Ocean Drilling Program, College Station, Texas: A&M University.
- NAKASEKO, K. and NISHIMURA, A., 1982. Radiolaria from the Bottom Sediments of the Bellingshausen Basin in the Antarctic Sea. *Report of the Technology Research Center, J.N.O.C.*, 16: 91-244.
- NELSON, C.S., COOKE, P.J., HENDY, C.H., and CUTHBERTSON, A.M., 1993. Oceanographic and climatic changes over the past 160,000 years at Deep Sea Drilling Site 594 off southeastern New Zealand, southwest Pacific Ocean. *Paleoceanography*, 8: 435-458.
- NELSON, C.S., HENDY, I.L., NEIL, H.L., HENDY, C.H., and WEAVER, P.P.E., 2000. Late Glacial jetting of cold waters through the Subtropical Convergence zone in the Southwest Pacific off eastern New Zealand, and some geological implications. *Palaeogeography, Palaeoclimatology, Palaeoecology*, 156: 103-121.
- NIGRINI, C., 1977. Tropical Cenozoic Artostrobiidae. [Radiolaria]. *Micropaleontology*, 23(3): 241-269.
- NIGRINI, C.A. and MOORE, T.C., 1979. A guide to modern Radiolaria. *Cushman Foundation for Foraminiferal Research, Special Publication*, 16: i-xii, S 1-S 142, N1-N106, 28 pls.
- NIMMERGUT, A. and ABELMANN, A., 2002. Spatial and seasonal changes of radiolarian standing stocks in the Sea of Okhotsk. *Deep-sea Research I*, 49: 463-493.
- PAHNKE, K. and SACHS, J.P., 2006. Sea surface temperatures of southern midlatitudes 0-160 kyr B.P. *Paleoceanography*, doi: 10.1029/2005PA001191.

- PETRUSHEVSKAYA, M.G., 1967. *Radiolarii otryadov Spumellaria I Nassellaria antarkticheskoi oblasti (Antarctic Spumellina and Nassellina radiolarians)*. In: *Issledovaniya Fauny Morei 4(12), Rezultaty Biologicheskikh Issledovaniy Sovetskoi Antarkticheskoi Ekspeditsii 1955 - 1958*, 3. Nauk, Zoologicheskii Institut Akademiya Nauk SSSR: 186 pp.
- , 1971a. Radiolaria in the plankton and recent sediments from the Indian Ocean and Antarctic. In: Funnell, B.M. and Riedel, W.R., Eds., *The Micropalaeontology of Oceans*, 319-329. London: Cambridge University Press.
- , 1971b. Spumellarian and nassellarian radiolaria in the plankton and bottom sediments of the central Pacific. In: Funnell, B.M. and Riedel, W.R., Eds., *The Micropalaeontology of Oceans*, 309-317. London: Cambridge University Press.
- , 1975. Cenozoic radiolarians of the Antarctic, Leg 29, DSDP. In: Kennett, J.P., Hourz, R.E., et al., Eds., *Initial Reports of the Deep Sea Drilling Project, Volume 29*, 541-675. Washington DC, US Government Printing Office.
- PETRUSHEVSKAYA, M.G. and KOSLOVA, G.E., 1972. Radiolaria: Leg 14. Deep Sea Drilling Project. In: Hayes, D.E., Pimm, A.C. et al., Eds. *Initial Reports of the Deep Sea Drilling Project, Volume 14*, 495-648. Washington, DC: US Government Printing Office.
- PISIAS, N.G. and MIX, A.C., 1997. Spatial and temporal oceanographic variability of the eastern equatorial Pacific during the Late Pleistocene: Evidence from Radiolaria microfossils. *Paleoceanography*, 12: 381-393.
- RENZ, G.W., 1976. The distribution and ecology of Radiolaria in the central Pacific: Plankton and surface sediments. *Bulletin of the Scripps Institution of Oceanography of the University of California*, 22: 1-262.
- SANFILIPPO, A., WESTBERG-SMITH, M.J. and RIEDEL, W.R., 1985. Cenozoic Radiolaria. In: Bolli, H.M., Saunders, J.B. and Perch-Nielsen, K., Eds., *Plankton Stratigraphy*, 631-712. London: Cambridge University Press.
- SANFILIPPO, A. and NIGRINI, C., 1998. Code numbers for Cenozoic low latitude radiolarian biostratigraphic zones and GPTS conversion tables. *Marine Micropaleontology*, 33: 109-156.
- SHACKLETON, N.J., and HALL, M.A., 1989. Stable isotope history of the Pleistocene at ODP Site 677. In: BECKER, K., SAKAI, H. et al., Eds. *Proceedings of the Ocean Drilling Program, Scientific Results, Volume 111*, 295-316., College Station, Texas: Ocean Drilling Program.
- SHACKLETON, N.J., BALDAUF, J.G., FLORES, J.-A., IWAI, M., MOORE, T.C., RAFFI, I. and VINCENT, E., 1995. Biostratigraphic summary for Leg 138. In: Pisias, N.G., Mayer, L.A., Janecek, T.R., Palmer-Julson, A. and Van Andel, T.H., Eds. *Proceedings of the Ocean Drilling Program, Scientific Results, Volume 138*, 517-536., College Station, Texas: Ocean Drilling Program.
- SIKES E.L., HOWARD, W.R., NEIL, H.L. AND VOLKMANN, J.K., 2002. Glacial-interglacial sea surface temperature changes across the subtropical front east of New Zealand based on alkenone unsaturation ratios and foraminiferal assemblages. *Paleoceanography*, 17(2): 1012, 10.1029/2001PA000640, 2002.
- SUTTON, P.J.H., 2003. The Southland Current: a subantarctic current. *New Zealand Journal of Marine and Freshwater Research*, 37: 645-652.
- TAKAHASHI, K., 1991. Radiolaria: Flux, Ecology, and Taxonomy in the Pacific and Atlantic. Ocean Biocoenosis Series, 3: 1-303.
- TAKAHASHI, K. AND HONJO, S., 1981. Vertical flux of Radiolaria: A taxon-quantitative sediment trap study from the western tropical Atlantic. *Micropaleontology*, 27(2): 140-190.
- WANG, R. AND ABELMANN, A., 2002. Radiolarian responses to paleoceanographic events of the southern South China Sea during the Pleistocene. *Marine Micropaleontology*, 46: 25-44.
- WARREN, B.A., 1981. Deep circulation of the world ocean. In: Warren, B.A. and Wunsch, C., Eds., *Evolution of Physical Oceanography*, 6-41. Cambridge: Massachusetts Institute of Technology Press.
- WEINHEIMER, A.L., 2001. Radiolarians from Northern Cape Basin, Site 1082. In: WEFER, G., BERGER, W.H. AND RICHTER, C., Eds. *Proceedings of the Ocean Drilling Program, Scientific Results, Volume 175*, 1-16., College Station, Texas: Ocean Drilling Program. [http://www-odp.tamu.edu/publications/175_SR/VOLUME/CHAPTERS/SR175_03.PDF].
- WELLING, L.A., PISIAS, N.G. and ROELOFS, A.K., 1992. Radiolarian microfauna in the northern California Current System: indicators of multiple processes controlling productivity. In: Summerhayes, C.P., Prell, W.L. and Emeis, K.C., Eds., *Upwelling Systems. Evolution since the Early Miocene*, 177-195. London Geological Society: Geological Society Special Publication, 64.
- WELLING, L.A., PISIAS, N.G., JOHNSON, E.S., and WHITE, J.R., 1996. Distribution of polycystine radiolaria and their relation to the physical environment during the 1992 El Nino and following cold event. *Deep-Sea Research II*, 43(4-6): 1413-1434.
- WELLING, L.A. and PISIAS, N.G., 1998. How do radiolarian sediment assemblages represent surface ocean ecology in the central equatorial Pacific?. *Paleoceanography*, 13(2): 131-149.
- YAMASHITA, H., TAKAHASHI, K. and FUJITANI, N., 2002. Zonal and vertical distribution of radiolarians in the western and central Equatorial Pacific in January 1999. *Deep-Sea Research II*, 49: 2823-2862.

Site 1123: Samples were processed using a standard method for preparation of Cenozoic radiolarians (Sanfilippo et al. 1985) incorporating the >63 µm size fraction and using a hand strewn dry method for producing microscope slides, including oven drying of bulk sediments and residues. Sample processing and slide preparation were as followed:

1. Bulk sediment samples are oven-dried (40°C), weighed and transferred into 600 ml glass beakers.
2. 100-150 ml 10% HCl, 20 ml 30% HCl is slowly added.
3. The sediment residue is washed through a 63µm screen, transferred into a 250 ml glass beaker adding a 4:1 solution of 10% H₂O₂ and 5% Na(PO₃)₆, covered with a watchglass while heated and simmered on the hot plate (~1 hour).
4. The clean residue is washed through a 63µm screen, transferred into a 250 ml glass beaker, oven-dried (40°C) and transferred into a waxed paper holder.
5. For radiolarian strewn slide preparation dilute gum tragacanth base is painted on a cover slip-seized central area of a cleaned glass slide and left to dry; slides are labelled and laid out on a waxed paper.
6. Dried residue is sprinkled regularly over the tragacanthed part of the glass slide, the slide is breathed on carefully to making the slide sticky.
7. Two drops of xylene are placed in the centre of the slide using a glass pipette and slowly, 20-25 drops of Entellan-Neu are placed on the residue using a disposable dropper and a cover slip is placed onto the residue.
8. Placed in a flat warm well-ventilated spot the mounting medium hardens in five days.

Site 1124: Samples were freeze-dried and processed (Abelmann 1988). The retrieved >45 µm fraction was transferred to the microscope slides by using a wet settling technique adopted from Moore (1973); Abelmann (1988) and Abelmann et al. (1999). Radiolarian residues were mounted in Norland applying a newly developed quick, cold mounting technique which ensured the production of microscope slides without significant numbers of air bubbles,

especially within radiolarian tests. Formation of bubbles in the matrix and within radiolarian tests has been a longstanding problem with Norland (C. A. Nigrini; K. R. Bjørklund; written communications, 2004). The cold use of xylene was found to be an effective way of avoiding formation of air bubbles. Sample processing and slide preparation methods are specified below.

1. Samples are deep-frozen, freeze-dried, weighed and transferred into a 600 ml glass beaker.
2. The sediment is covered with some demineralized water, 100 ml of a 4:1 solution of 10% H₂O₂ and 5% Na(PO₃)₆ and 100 ml 10% HCl are slowly added while simmering on the hot plate for ~1 hour.
3. The glass beaker is filled up to 600 ml with demineralized water, the residue is washed through a 45µm mesh and transferred into a 50 ml centrifuge plastic tube and kept in solution with demineralized water.
4. A rectangular plastic settling container (95 x 45 x 45 mm) is filled with a 1:2.5 solution of gelatine and water before three clean cover slips (40 x 22 mm) are aligned on the bottom of the container.
5. An automatic pipette is used to evenly distribute a defined amount of suspension which depends on the size of the residue (generally 5-10 ml) into the liquid-filled settling container.
6. After allowing all particles to sink and settle on the cover slips (~2 hours) a siphoning system is used to remove most of the liquid from the container. Soft paper strips are hung into the liquid to slowly remove the remaining water without creating convection.
7. Dry cover slips are removed from the settling container, using a razor blade.
8. For preparation of radiolarian strewn slides the residue-coated cover slip is placed on a cool, flat surface, 2-3 drops of xylene are dropped on the residue using a glass pipette to remove air pockets within and between tests.
9. Once the inter-particle area is dry but the residual grains are still wet, ~10 drops of Norland are slowly placed on each cover slip to be mounted on glass slides; evaporation of xylene occurs at room temperature without the use of heat, e.g. from a hot plate.
10. After ~20 minutes of UV light treatment the mounting medium is hardened and slides are ready for microscopic analysis.

Temporal fluxes of radiolarians along the W-E transect in the central and western equatorial Pacific, 1999-2002

Yusuke Okazaki¹, Koza Takahashi² and Hirofumi Asahi³

¹*Institute of Observational Research for Global Change,*

Japan Agency for Marine-Earth Science and Technology, Natsushima-cho 2-15, Yokosuka 237-0061, Japan

²*Department of Earth and Planetary Sciences, Graduate School of Science,*

Kyushu University, Hakozaki 6-10-1, Fukuoka 812-8581, Japan

³*Ocean Research Institute, University of Tokyo, Minamidai 1-15-1, Nakano-ku, Tokyo 164-8639, Japan*

email: okazaki@jamstec.go.jp

ABSTRACT: Coarse size (>63 μ m) radiolarian fluxes along the Equator in the central and western Pacific between 145°E and 160°W (Stations MT3, MT4, MT5, MT6 and MT7) were examined during January 1999 to January 2003 in order to evaluate how radiolarian assemblages respond to the El Niño Southern Oscillations (ENSO). Radiolarian fluxes were constrained by the water masses: the Western Pacific Warm Pool (WPWP) located in the west and the Equatorial Upwelling Region (EUR) east of the WPWP in the central equatorial Pacific. In general, radiolarian fluxes gradually increased from the western sites to the eastern sites, responding to the increases in nutrient supply and primary production in the euphotic layer. Notable annual cycles of radiolarian fluxes observed at the two Stations with nearly complete time series (MT3 and MT5) were likely corresponding to the rainy seasons of Papua New Guinea (MT3) and the extent of upwelling intensity in the equatorial Pacific (MT3 and MT5). With transition from La Niña to El Niño during 2001 to 2002, high radiolarian fluxes were coincident with cooler surface water. Among the radiolarian taxa, *Lithomelissa* sp. group and *Pseudocubus obeliscus* Haeckel 1887, which were mainly dwelling in the surface water in the EUR, responded distinctively to the WPWP excursion and decreased their fluxes as surface water temperature rose.

INTRODUCTION

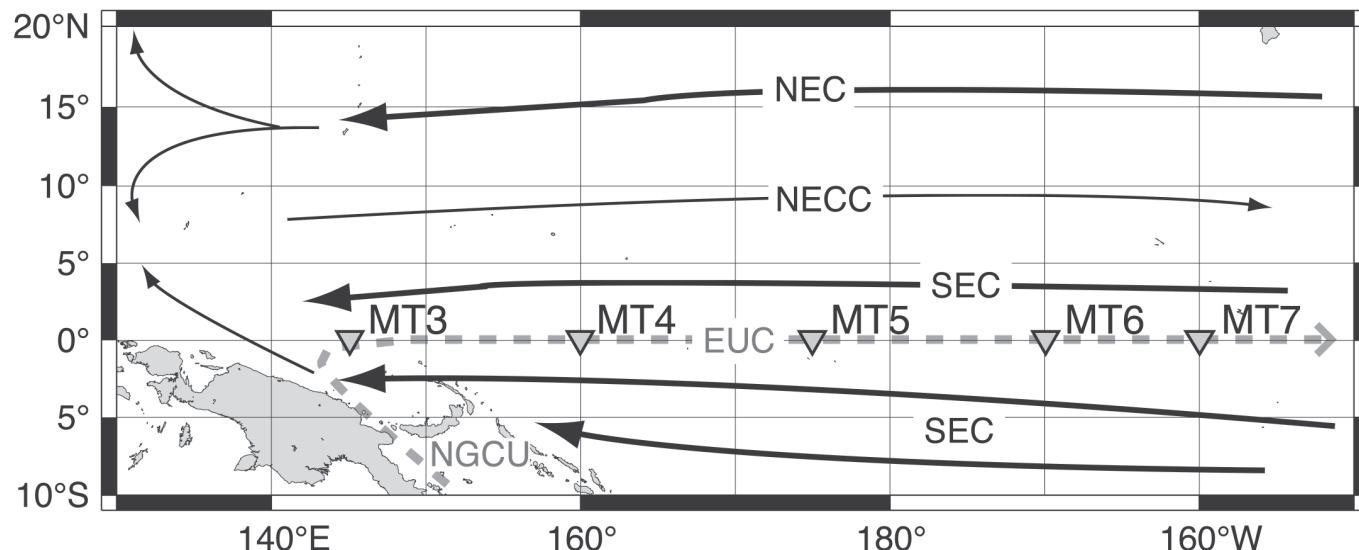
The equatorial Pacific is recognized as one of the most important areas of the oceans to understand global climate change through the El Niño-Southern Oscillation (ENSO). The Western Pacific Warm Pool (WPWP), which is characterized by >28°C sea-surface temperature (Yan et al. 1992), is located in the western equatorial Pacific. Further east in the central equatorial Pacific relatively cool surface waters are found due to the equatorial upwelling (equatorial upwelling region: EUR). The behavior of the WPWP plays a key role in the ENSO, which occurs at intervals of 2-7 years (e.g., Inoue et al. 1996; Picaut et al. 1996). During El Niño years, the warm waters in the WPWP spread eastwards with weakening of the South-East Trades in the western and central equatorial Pacific. The eastward excursion of the WPWP can suppress the equatorial upwelling, which supplies cold, nutrient-rich water to the surface of the equatorial Pacific. Thus, biological production along the equator is greatly influenced by the WPWP (e.g., Mackey et al. 1995; Blanchot and Rodier 1996; Chavez et al. 1996; Le Borgne et al. 1999; Kawahata et al. 2000; Kobayashi and Takahashi 2002; Mackey et al. 2002; Matsumoto et al. 2004).

Radiolarians are siliceous microzooplankton with a high diversity, which dwell in a wide range of depth zones from the surface water down to depths of several thousand meters. Thus, they have the potential to be a proxy of various vertical water masses including not only the surface but also subsurface and intermediate depths. Radiolaria are classified into two taxonomic groups: Polycystina and Phaeodaria. The skeletons of polycystine radiolarians are often preserved in sediments. Hence, they have been used as proxies to reconstruct past climate and environmental changes. On the other hand, phaeodarian radiolarians are readily dissolved in the water column because of their skeletal composition and porous morphology and thus they are rarely preserved in sediments (Takahashi et al. 1983). Previous studies on radiolarian vertical distributions (Petrushevskaya 1971a; Renz 1976;

Welling et al. 1996; Yamashita et al. 2002) and temporal fluxes (Pisias et al. 1986; Welling and Pisias 1998) have been conducted in the equatorial Pacific. Their results indicate that radiolarian assemblages respond strongly to changes in oceanographic conditions with the ENSO. Yamashita et al. (2002) indicated that radiolarian standing stocks increased from west (WPWP) to east (EUR) during La Niña period (January 1999). However, most of these previous studies have focused on the eastern and central equatorial Pacific except for Yamashita et al. (2002). Hence, our knowledge on radiolarian fluxes in the western equatorial Pacific, the centre of the WPWP, is limited. Here, we describe four year-long radiolarian fluxes at five stations along the Equator in the western and central equatorial Pacific and evaluate how radiolarian assemblages respond to the eastward spread of the WPWP with the transition from the La Niña to the El Niño.

MATERIALS AND METHODS

Time-series sediment traps (type SMD26S-6000, Nichiyu-Giken Co. Ltd., Tokyo) with 26 collecting cups were deployed at approximately 2000 and 3000m depths at five stations in the western and central equatorial Pacific (Stations MT3, MT4, MT5, MT6, and MT7) from January 1999 to January 2003 (text-fig. 1; Table 1). Their recovery, maintenance and redeployment have been carried out during the cruises of the R/V Mirai, Japan Agency for Marine-Earth Science and Technology (JAMSTEC). Before the trap deployments, sample bottles were filled with filtered (0.45 μ m) deep seawater containing 3% buffered formalin solution. The samples for radiolarian analyses were sieved through a stainless screen with 1mm mesh to remove larger plankton, and then split into an aliquot size of 1/256 using a high precision rotary sample splitter. The split samples were sieved through a stainless steel screen with 63 μ m mesh. The fraction greater than 63 μ m were filtered through Gelman® membrane filters with a nominal pore size of 0.45 μ m and washed with distilled water to remove salt, dried in an oven at 50°C overnight, and then



TEXT-FIGURE 1

Map showing the locations of the five sediment trap stations on the equator in the western and central Pacific. Representative surface ocean currents and undercurrents are also shown: the North Equatorial Current (NEC), the North Equatorial Counter Current (NECC), the South Equatorial Current (SEC), the Equatorial Undercurrent (EUC), and the New Guinea Coastal Undercurrent (NGCU).

mounted with Canada Balsam on microslides. All coarse-sized radiolarian skeletons (1mm–63µm; expressed as >63µm hereafter) on a microslide were counted with a light microscope and computed to derive radiolarian fluxes (No. radiolarians m⁻² day⁻¹) at each station. We used only >63µm fraction to compare our results with previous studies using >63µm fraction in the equatorial Pacific (Welling et al. 1996, Welling and Piasis 1998, and Yamashita et al. 2002). Species identification of radiolarians was performed according to the taxonomy of the following works: e.g., Benson (1966), Nigrini (1970), Petrushevskaya (1971b), Renz (1976), Nigrini and Moore (1979), Boltovskoy and Riedel (1987), Takahashi (1991), Welling (1996), Boltovskoy (1998) and Björklund et al. (1998).

The southern oscillation index (SOI) data, defined as the sea-level pressure difference between Tahiti and Darwin, were downloaded from the website of Climate Prediction Center (<http://www.ncep.noaa.gov/data/indices/>). The data for the 20°C isothermal depth on the equator between 140°E and 150°W were obtained from the Tropical Atmosphere Ocean (TAO) project website (<http://www.pmel.noaa.gov/tao/>). The sea surface temperature data by the Integrated Global Ocean Services System (IGOSS; Reynolds and Smith 1994) at each trap site were obtained from the following website (<http://ingrid.ldeo.columbia.edu/SOURCES/IGOSS/>). These observations for 1999–2002 are shown in text-figure 2.

We performed a singular spectrum analysis (SSA; Broomhead and King 1986; Vautard and Ghil 1989; Ghil et al. 2002) in order to ascertain the periodicity of the radiolarian fluxes. This analytical method is designed to extract information from time series data-sets and gives general ideas and dynamics underlying them. This method has the advantages of verifying the relative contributions of each frequency or cycle (% variance) found in the time-series data, and in extracting the smoothed curve (reconstructed components: RC) for each cycle. In this study, time-series variation from Stations MT3 and MT5 were longer enough to be subjected to this analysis. Prior to performing the spectrum analysis, the data-sets were standardized (mean=0; standard

deviation=1) and re-sampled at a 20 day interval. The singular spectrum analysis was performed using the “SSA-MTM tool kit” (Ghil et al. 2002) on the total radiolarian fluxes at stations MT3 and MT5.

OCEANOGRAPHIC SETTING

The surface-water circulation in the western equatorial Pacific has three major currents: the North Equatorial Current (NEC: 10°N–25°N), the Equatorial Counter Current (ECC: 4°N–10°N) and the South Equatorial Current (SEC: 4°N–20°S) (text-fig. 1). NEC and SEC flows westward, which pile up water in a warm pool in the western Pacific. Besides these surface currents, the Equatorial Undercurrent (EUC) flows eastward along the equator at a depth of 20–200m. The New Guinea Coastal Undercurrent (NGCU) flows along the north coast of New Guinea, which is entrained in the EUC (Tsuchiya et al. 1989).

The central and eastern equatorial Pacific has nutrient rich surface water and high primary production attributed to equatorial upwelling due to shallow thermoclines (e.g., Mackey et al. 2002; Kobayashi and Takahashi 2002; Matsumoto et al. 2004). On the other hand, the surface water of the WPWP, having a high temperature (>28°C), is oligotrophic due to strong water stratification. Lukas and Lindstrom (1991) suggested that a “barrier layer” between the bottom of the mixed layer and the top of the thermocline isolates the surface water from the nutrient-rich water below the thermocline. Hence, nutrient supply to the surface layer from upwelling is smaller in the western equatorial Pacific than that in the eastern equatorial Pacific. Based on a modeling study, the new production rate is closely related to the mixed-layer concentrations of nitrate and iron, and the 20°C isothermal depth in the upwelling region (Wang et al. 2006). The western edge of the equatorial Pacific upwelling is marked by a sharp salinity front (Rodier et al. 2000). The front shifts longitudinally with El Niño and La Niña events. During the trap-deployment periods, the equatorial Pacific was under the influence of La Niña from 1999 to early 2001 and shifted to El Niño from late 2002 based on SOI variations (text-fig. 2a). During end of 2002, the 20°C isothermal

depth rapidly shallowed (<150m) in the western equatorial Pacific around Stations MT3 and MT4 (text-fig. 2b).

RESULTS

Station MT3 was located at 145°E on the equator in the WPWP region. Weekly SSTs were higher than 28°C throughout the sampling period (text-fig. 2c).

Station MT4 was located at 160°E on the equator. Based on SST variations, the WPWP covered this station throughout the sampled period analogous to Station MT3 (text-fig. 2c-d).

Station MT5 was located at 175°E on the equator, belonging to a weak upwelling region under transitional and La Niña conditions. With the transition from La Niña to El Niño, the warm surface-water covered around Station MT5 after April 2001 (text-fig. 2c-d).

Station MT6 was located at 170°W on the equator in a weak upwelling region. The variation in SST indicated that the WPWP spread around Station MT6 from May 2001 (text-fig. 2c-d). The SST showed apparent seasonal change throughout the sampled period, i.e. lower SST in boreal winter.

Station MT7 was located at 160°W on the equator, belonging to an equatorial upwelling region. The observed SSTs showed greater than 28°C after April 2002, with the eastward spread of the WPWP (text-fig. 2c-d). Analogous to Station MT6, SST exhibited a clear seasonal change at Station MT7.

Total radiolarian fluxes at Stations MT3, MT4, MT5, MT6 and MT7 during 1999-2002 are shown in text-figure 3. And annual fluxes (average flux per day in interval sample during 1999, 2000, 2001 and 2002) of total radiolarians for each trap are also shown in text-figure 4, despite of several sampling hiatuses occurred at each site (see table 1; text-fig. 3). In general, radiolarian fluxes were higher at eastern sites than those at western sites.

A total of 223 radiolarian taxa were identified: 209 Polycystina (90 Spumellaria, 119 Nassellaria); and 14 Phaeodaria (Table 2). Based on previous plankton-tow studies in the equatorial Pacific (Welling et al. 1996; Yamashita et al. 2002), we have selected six abundant taxa to illustrate fluxes for characteristic biogeographical/water depth distributions: (1) WPWP, *Didymocyrtilis tetrathalamus* (Haeckel) 1887; (2) EUR, *Lithomelissa* sp. group, *Pseudocubus obeliscus* Haeckel 1887; (3) Subtropical, *Tetrapyle octacantha* Müller 1858; (4) Equator, *Lophophaena hispida* (Ehrenberg) 1872; (5) Subsurface, *Pseudodictyophimus gracilipes* (Bailey) 1856. Temporal flux and relative abundance changes of the above six radiolarian taxa are shown in text-figures 5 and 6.

Based on a singular spectrum analysis, periodicity of the radiolarian fluxes in MT3 and MT5 clearly reveal the conspicuous annual cycle (frequency: 370 days at MT3; 364 days at MT5). This annual cycle at these two stations was the most significant of all cycles found at both stations (variance: 39.0 % at MT3; 42.3% at MT5) (text-fig. 7).

DISCUSSION

Longitudinal distributions of annual radiolarian fluxes showed a clear difference between the western sites (MT3, MT4) and the eastern sites (MT5, MT6, and MT7) (text-fig. 4): i.e., much higher radiolarian production in the EUR. The results conform with the previous studies in the equatorial Pacific: primary pro-

TABLE 1

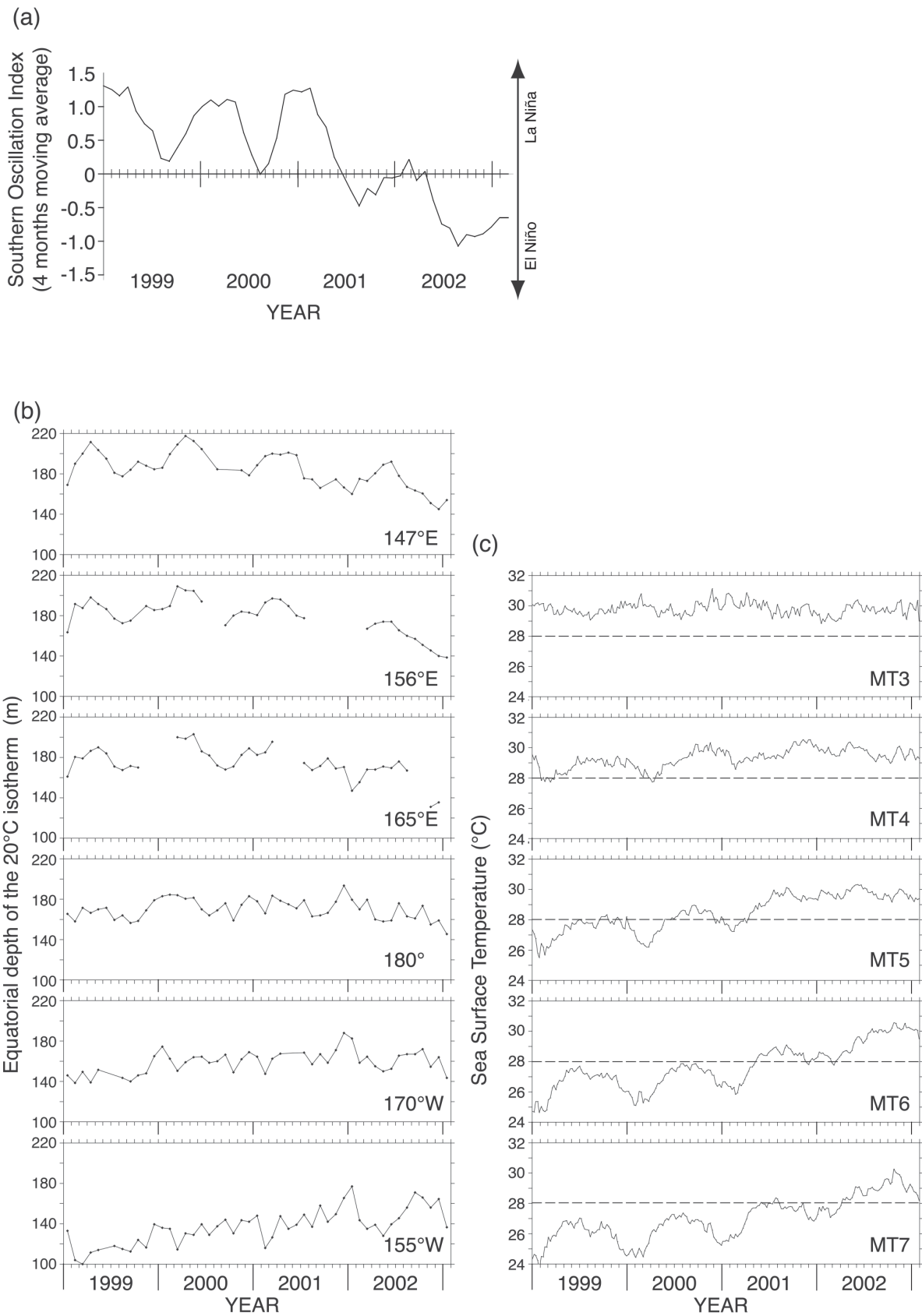
Summary information for the sediment trap samples used in this work.

Trap station	Location	Water depth (m)	Mooring depth (m)	Sampled duration
MT3	0°, 145°E	3680	2060	1999.01.05 - 1999.11.21
"	"	3676	2030	1999.12.01 - 2001.01.01
"	"	3684	1960	2001.02.01 - 2002.02.02
"	"	3684	1962	2002.03.18 - 2002.12.23
MT4	0°, 160°E	2808	1990	1999.12.01 - 2001.01.01
"	"	2811	2070	2001.01.26 - 2002.02.01
MT5	0°, 175°E	4828	3000	1999.01.13 - 1999.12.01
"	"	4820	2970	1999.12.16 - 2001.01.16
"	"	4816	3090	2001.01.22 - 2002.01.27
"	"	4820	3090	2002.02.01 - 2003.01.16
MT6	0°, 170°W	5634	3040	1999.12.16 - 2000.11.01
"	"	5625	2850	2002.02.01 - 2003.01.21
MT7	0°, 160°W	5176	3120	2001.01.16 - 2002.01.16
"	"	5130	3070	2002.01.25 - 2003.01.24

ductivity (e.g., Mackey et al. 1995; Le Borgne 2002), plankton communities such as radiolarians (Yamashita et al. 2002), diatoms (Chavez et al. 1996; Kobayashi and Takahashi 2002), picophytoplankton (e.g., Blanchot and Rodier 1996; Mackey et al. 2002; Matsumoto et al. 2004), and mesozooplankton (Rodier et al. 2000). Settling particles in the equatorial Pacific also showed much higher in the EUR than those in the WPWP (Kawahata and Gupta 2004).

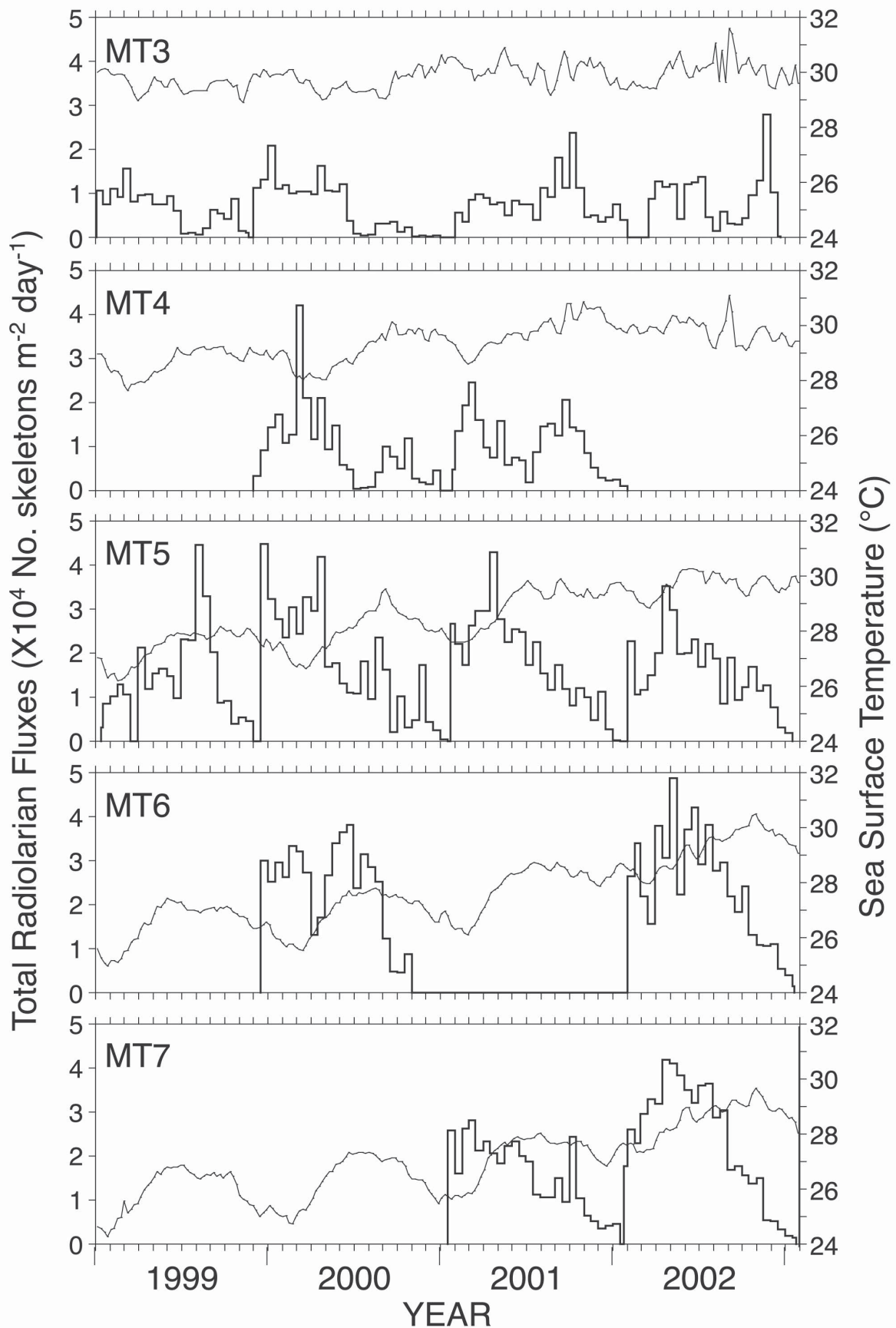
Radiolarian production in the WPWP region seems to be associated with terrestrial/riverine inputs as well as thermocline depth. Mackey et al. (1995) suggested that a barrier layer prevented the supply of upwelled nutrients, yielding low productivity in the WPWP. The barrier layer thins during El Niño period, affecting on the productivity in the WPWP. Terrestrial/riverine inputs also influenced on biological production in the equatorial Pacific particularly off Papua New Guinea around Station MT3 (e.g., Milliman and Meade 1983). Under transitional and La Niña conditions, the rainy season in the Papua New Guinea is from December to March. New Guinea has an annual river discharge of sediments to the ocean of ca. 1.7×10^9 tons due to its relatively weathered rocks, hot weather and heavy rainfall (Milliman et al. 1999). About one half of the sediments discharge to the north side of New Guinea, mainly through the Sepik River. The north side of Papua New Guinea has a narrow shelf and is adjacent to a steep slope. Dissolved and particulate matter of the Sepik River thus empties into the western equatorial Pacific through the New Guinea Coastal Undercurrent (Sholkovitz et al. 1999; Mackey et al. 2002). Monthly changes in radiolarian fluxes at Station MT3 showed different pattern between during 1999-2000 and during 2001-2002 (text-fig. 8). The 1999-2000 period showed high fluxes during January to June, which is largely coincident with the rainy season (December to March) in Papua New Guinea. This suggests that radiolarian production at Station MT3 is closely associated with terrestrial/riverine inputs during La Niña conditions. On the contrary, the following 2001-2002 period exhibited a different pattern of seasonal change and relatively high fluxes were found not only during boreal spring but also during October to November. Under the El Niño condition, the area of high rainfall moves eastward along with the WPWP excursion, resulting a decline of terrestrial/riverine inputs from Papua New Guinea. In such a case, upwelled nutrients may be important for biological production in this region. During 2001-2002, 20°C isothermal depths, which is equivalent to the thermocline, were shallower during boreal autumn to winter than those during boreal spring to summer (text-fig. 2b), which may have contributed to the radiolarian production during October to November.

At Station MT5, temporal radiolarian fluxes in 1999 were different from the other three years, exhibiting a pronounced boreal summer peak (text-fig. 3). Flux peaks of three radiolarian taxa,

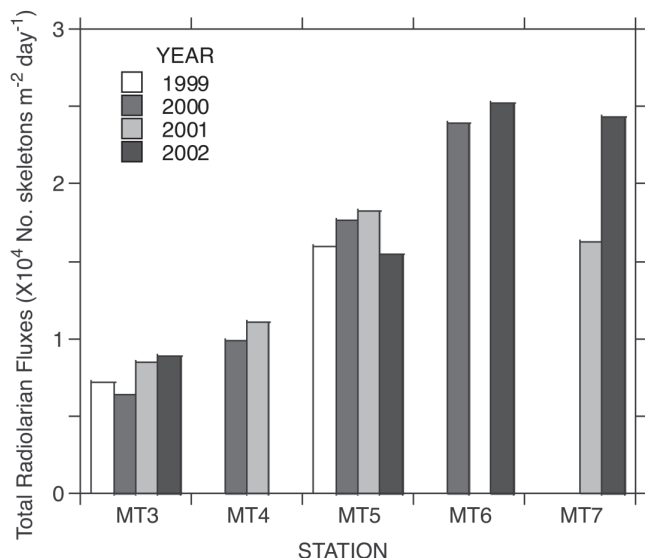


TEXT-FIGURE 2

(a) Temporal changes in the equatorial southern oscillation index (SOI) during January 1999 to February 2003. The SOI data are from the Climate Prediction Center (<http://www.cpc.noaa.gov/data.indices>). (b) Temporal variations of 20°C isothermal depth on the equator at 147°E, 156°E, 165°E, 180°, 170°W, and 155°W. The data are from the Tropical Atmosphere Ocean (TAO) project (<http://www.pmel.noaa.gov/tao/>). (c) The Integrated Global Ocean Services System (IGOSS) sea-surface temperature (Reynolds and Smith 1994) at five stations (Stations MT3, MT4, MT5, MT6 and MT7) during 1999-2002.



TEXT-FIGURE 3
 Total radiolarian fluxes and IGOSS SST anomaly at five stations in the western and central equatorial Pacific during 1999-2002.



TEXT-FIGURE 4
Annual fluxes of total Radiolaria at five trap stations during 1999-2002.

Lithomelissa sp. group, *Lophophaena hispida* and *Pseudocubus obeliscus* occurred within this summer peak interval (text-figs. 5-6). Previous studies suggest that these taxa dwell in the surface layer of the equatorial Pacific and are associated with high productivity and/or upwelled nutrients (Takahashi 1987; Welling et al. 1996; Welling and Pisias 1998; Yamashita et al. 2002). In addition, fluxes of *Pseudodictyophimus gracilipes*, which dwells in the subsurface water with high chlorophyll-a concentrations (Kling 1979; Yamashita et al. 2002), also showed a pronounced peak during boreal summer 1999 (text-fig. 6). These results suggest that the nutrients supplied by the equatorial upwelling could have enhanced the radiolarian production at MT5 during the boreal summer 1999, which is indicated by relating shallow (ca. 170 m) 20°C isothermal depths (text-figs. 2a-b). On the other hand, the radiolarian flux changes during 2000 to 2002 present a saw-tooth annual pattern, i.e., maximum flux peak during January to April and subsequent gradual decrease toward the end of year (text-fig. 3). Such annual patterns occurred at Stations MT6 and MT7 (text-fig. 3), which is related to the strengthened northeast Trade Winds during the boreal winter (Tozuka and Yamagata 2003). *Tetrapyle octacantha*, most abundant radiolarian taxon at Station MT5, is widely distributed in the surface waters of the low to mid latitudes of the North Pacific (central North Pacific: Kling 1979; California Current: Kling and Boltovskoy 1995; equatorial Pacific: Welling and Pisias 1998; Yamashita et al. 2002). In the equatorial Pacific, *T. octacantha* standing stocks increased eastward (Yamashita et al. 2002). This taxon is defined as a subtropical species based on its geographical distributions (e.g., Lombardi and Boden 1985). Welling et al. (1996) and Welling and Pisias (1998) suggested that within the equatorial region *T. octacantha* production is associated with upwelled water although also indicative for subtropical water mass advection from the north. Our results support this suggestion.

Conspicuous annual cycle of the radiolarian fluxes are appeared at stations MT3 and MT5 based on a singular spectrum analysis. The reconstructed components (RC) for this annual cycle at both stations (text-fig. 7) seems to be corresponding to annual climate variation at each station, such as rainy/dry seasons of Papua New Guinea (MT3) and upwelling intensity relating to the seasonal

trade winds in the equatorial Pacific (MT3 and MT5) as mentioned in the previous section.

With transition from La Niña to El Niño during 2001 to 2002, the warm water in the WPWP spread eastward (text-fig. 2) and suppressed upwelling in the EUR. Among the radiolarian taxa, *Lithomelissa* sp. group and *Pseudocubus obeliscus* (abundant standing stocks in the EUR; Yamashita et al. 2002) responded distinctively to the WPWP excursion, decreasing their fluxes as surface water warm - at least at station MT5, the only location with substantial abundances of their fluxes and with a full timeseries to allow comparing SST data (text-fig. 5). As an indicator of the eastward extension of the WPWP, *Didymocyrtis tetrathalamus* was defined as a warm water species based on its geographic distribution, showing high relative abundances in the western tropical Pacific (Lombardi and Boden 1985). In our study, the fluxes and relative abundances of *D. tetrathalamus* were relatively abundant in the WPWP site (Station MT3) but there was no significant relationship between *D. tetrathalamus* and SST. Anderson et al. (1990) suggested that *D. tetrathalamus* has a lower temperature tolerance than indicated by its geographical distribution. During 1992 to 1993, corresponding to El Niño and following cold event, *D. tetrathalamus* fluxes were abundant not on the equator but in the area between 3°N to 9°N and 3°N to 12°N along the transect at 140°W (Welling and Pisias 1998). They suggested that seasonal and interannual oscillations in the meridional current were primary regulator for *D. tetrathalamus* abundances (both flux and relative abundance), while temperature was secondary (Welling and Pisias 1998). Hence, temporal flux changes of *D. tetrathalamus* in our study may reflect not only eastward extension of the WPWP but also advection from the north and/or south driven by the Trade Winds.

CONCLUSIONS

Radiolarian fluxes in the western Pacific warm pool (WPWP: Stations MT3 and MT4) were much lower than those in the equatorial upwelling region (EUR: MT5, MT6 and MT7). Radiolarian production in the WPWP may be associated with terrestrial/riverine inputs as well as nutrient supply by minor upwelling. In the EUR, upwelling intensity is inferred to be the main control on radiolarian production.

Based on the singular spectrum analysis, pronounced annual cycles of total radiolarian fluxes were found at Stations MT3 and MT5, responding to the rainy seasons of Papua New Guinea (MT3) and the extent of upwelling intensity in the equatorial Pacific (MT3 and MT5).

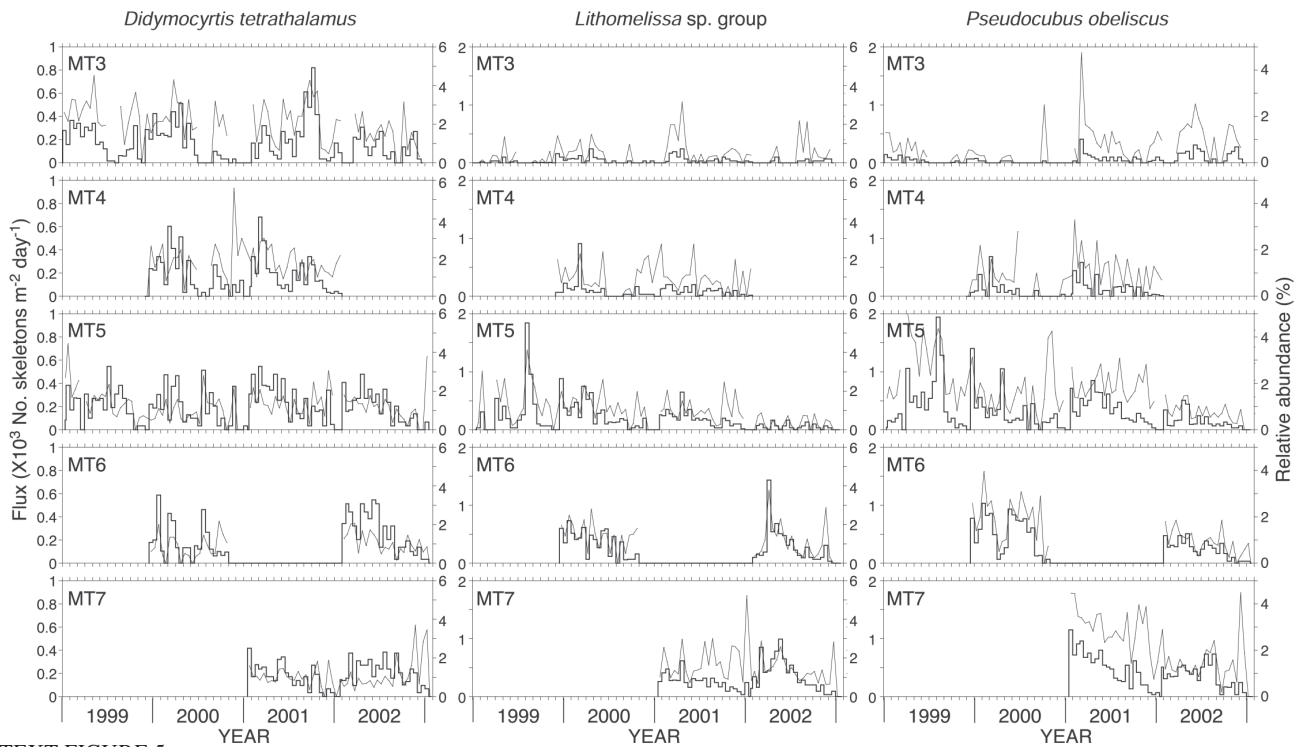
Temporal fluxes in *Lithomelissa* sp. group and *Pseudocubus obeliscus*, which were key species in the EUR, seemed to reflect well the sea-surface temperature changes during the transition from La Niña to El Niño between 2001 and 2002.

TAXONOMIC NOTES

Didymocyrtis tetrathalamus (Haeckel) 1887

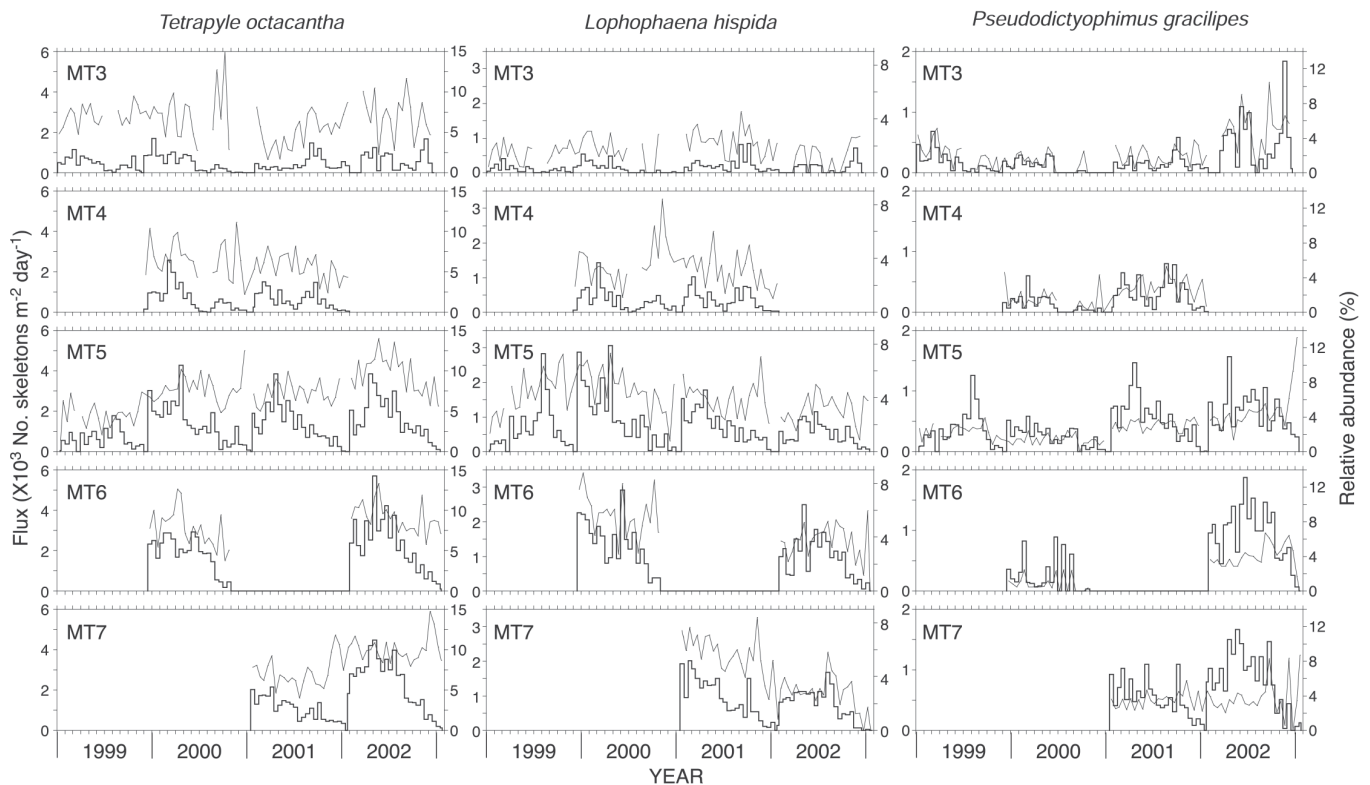
Didymocyrtis tetrathalamus (Haeckel) 1887. - WELLING 1996, p. 210, Pl. 4, Figs. 6-12. - BOLTOVSKOY 1998, p. 49, Figs. 15.77a-c). - TAKAHASHI 1991, p. 79, Pl. 21, Figs. 1-14.

Ommatartus tetrathalamus tetrathalamus (Haeckel) 1887, NIGRINI AND MOORE 1979, p. S49, Pl. 6, Figs. 1a-d.



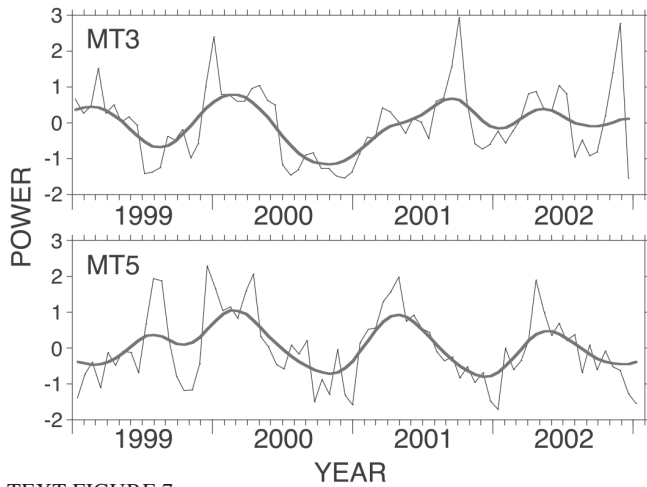
TEXT-FIGURE 5

Temporal fluxes of three radiolarian taxa (*Didymocystis tetrathalamus*, *Lithomelissa* sp. group and *Pseudocubus obeliscus*) at five stations in the western and central equatorial Pacific during 1999-2002.

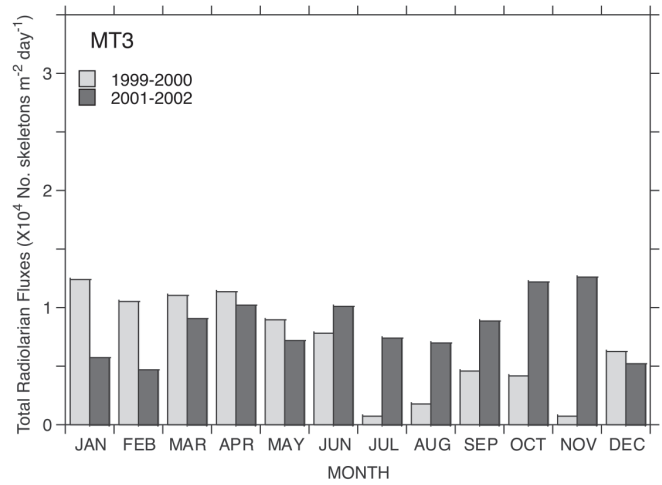


TEXT-FIGURE 6

Temporal fluxes of three radiolarian taxa (*Tetrapyle octacantha*, *Lophophaena hispida* and *Pseudodictyophimus gracilipes*) at five stations in the western and central equatorial Pacific during 1999-2002.



TEXT-FIGURE 7
Standardized total radiolarian fluxes (thin line) and the singular spectrum analysis-reconstructed components (SSA-RC) (1st component: 370 days cycle with 39.0% variance at MT3; 364 days cycle with 42.3% variance at MT5) of total radiolarian fluxes (thick line) at Stations MT3 and MT5.



TEXT-FIGURE 8
Monthly mean fluxes of total radiolarians at Station MT3 during 1999-2000 and 2001-2002.

PLATE 1

- | | |
|--|---|
| <p>1-6. <i>Didymocyrtis tetrathalamus</i> (Haeckel) 1887, scale bar=100µm</p> <p>1-2 <i>Didymocyrtis tetrathalamus</i> (Haeckel) 1887, MR02, MT3 #3</p> <p>3 <i>Didymocyrtis tetrathalamus</i> (Haeckel) 1887, MR02, MT6 #11</p> <p>4, 6 <i>Didymocyrtis tetrathalamus</i> (Haeckel) 1887, MR02, MT3 #9</p> <p>5 <i>Didymocyrtis tetrathalamus</i> (Haeckel) 1887, MR02, MT5 #1</p> <p>7-12 <i>Tetrapyle octacantha</i> Müller 1858, scale bar=100µm</p> <p>7-8 <i>Tetrapyle octacantha</i> Müller 1858, MR02, MT5 #1</p> <p>9, 12 <i>Tetrapyle octacantha</i> Müller 1858, MR02, MT6 #6</p> <p>10, 11 <i>Tetrapyle octacantha</i> Müller 1858, MR02, MT6 #3</p> <p>13-17 <i>Pseudodictyophimus gracilipes</i> (Bailey), scale bar=100µm</p> <p>13 <i>Pseudodictyophimus gracilipes</i> (Bailey), MR02, MT5 #1</p> <p>14 <i>Pseudodictyophimus gracilipes</i> (Bailey), MR02, MT6 #6</p> <p>15 <i>Pseudodictyophimus gracilipes</i> (Bailey), MR02, MT6 #3</p> | <p>16 <i>Pseudodictyophimus gracilipes</i> (Bailey), MR02, MT6 #16</p> <p>17 <i>Pseudodictyophimus gracilipes</i> (Bailey), MR02, MT6 #5</p> <p>18-24 <i>Lithomelissa</i> sp. group, scale bar=50µm</p> <p>18, 24 <i>Lithomelissa</i> sp. group, MR02, MT6 #11</p> <p>19, 22 <i>Lithomelissa</i> sp. group, MR02, MT6 #16</p> <p>20 <i>Lithomelissa</i> sp. group, MR02, MT6 #6</p> <p>21 <i>Lithomelissa</i> sp. group, MR02, MT6 #3</p> <p>23 <i>Lithomelissa</i> sp. group, MR02, MT6 #5</p> <p>25-26 <i>Pseudocubus obeliscus</i> Haeckel 1887, scale bar=50µm</p> <p>25 <i>Pseudocubus obeliscus</i> Haeckel 1887, MT6 #6</p> <p>26 <i>Pseudocubus obeliscus</i> Haeckel 1887, MT6 #5</p> <p>27-29 <i>Lophophaena hispida</i> (Ehrenberg) 1872, scale bar=50µm</p> <p>27 <i>Lophophaena hispida</i> (Ehrenberg) 1872, MR02, MT6 #6</p> <p>28 <i>Lophophaena hispida</i> (Ehrenberg) 1872, MR02, MT6 #3</p> <p>29 <i>Lophophaena hispida</i> (Ehrenberg) 1872, MR02, MT5 #1</p> |
|--|---|

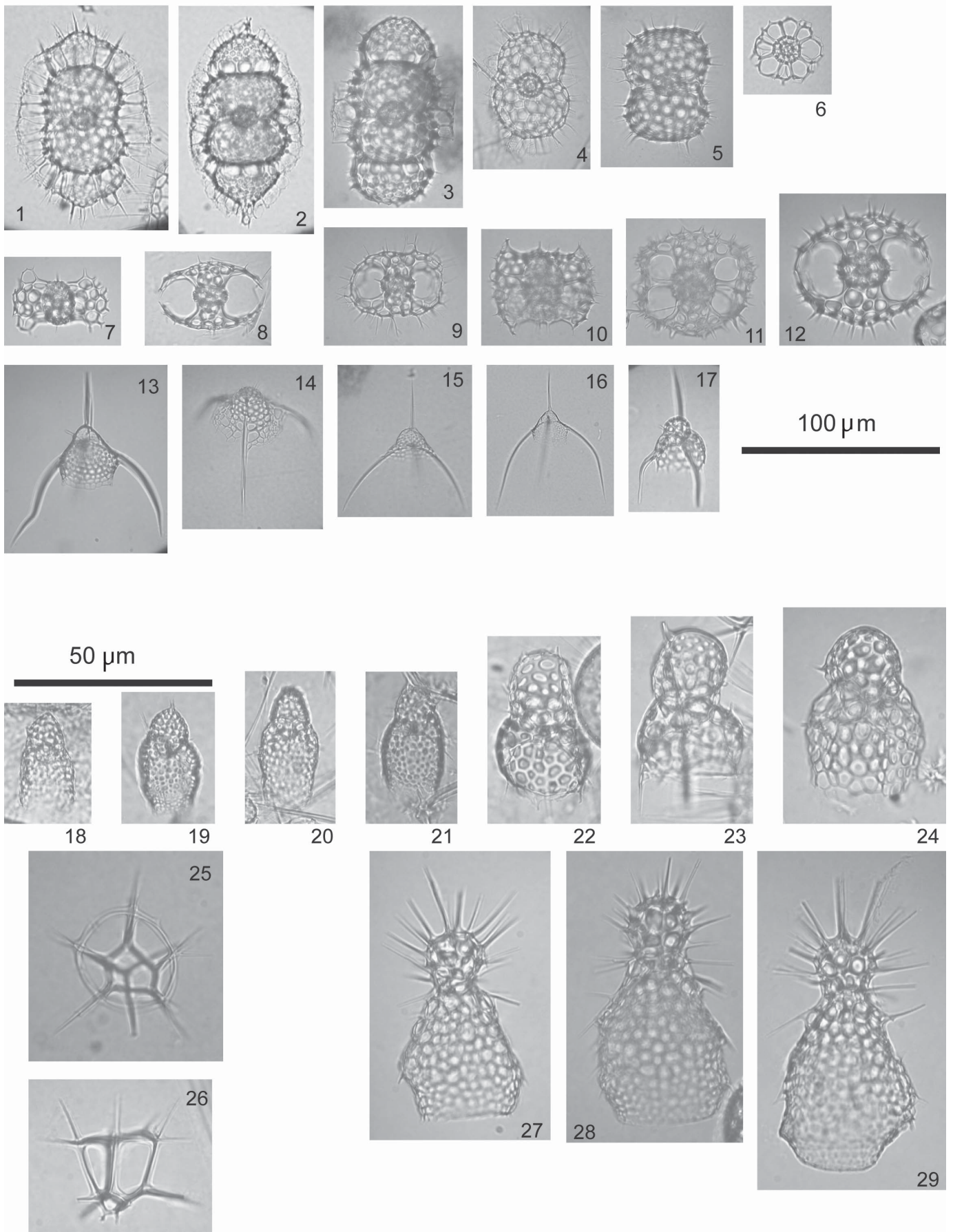


TABLE 2

List of radiolarian taxa identified in the sediment trap samples

Taxa	Current references
<i>Spumellaria</i>	
<i>Acanthosphaera actinota</i> (Haeckel)	Takahashi, 1991, p. 66, Pl. 8, Fig. 1
<i>Acanthosphaera tunis</i> Haeckel	Takahashi, 1991, p. 66, Pl. 8, Figs. 2, 3
<i>Acrosphaera murrayana</i> (Haeckel)	Takahashi, 1991, p. 55, Pl. 1, Figs. 3, 6-11
<i>Acrosphaera spinosa</i> (Haeckel)	Takahashi, 1991, p. 55, Pl. 1, Figs. 1, 2, 4, 5
<i>Actinomma arcadophorum</i> Haeckel	Nigrini and Moore, 1979, p. S29, Pl. 3, Fig. 4
<i>Actinomma boreale</i> Cleve	Cortese and Bjørklund, 1998, p. 151, Pl. 1, Figs. 1-18
<i>Actinomma delicatulum</i> (Dogiel and Reshetnyak)	Welling, 1996, p. 207, Pl. 2, Figs. 5-7
<i>Actinomma leptoderma leptoderma</i> (Jørgensen)	Bjørklund et al, 1998, p. 128, Pl. 1, Fig. 11
<i>Actinomma medianum</i> Nigrini	Nigrini and Moore, 1979, p. S31, Pl. 3, Figs. 5, 6
<i>Actinomma sol</i> Cleve	Boltovskoy, 1998, p. 40, Fig. 15.44
<i>Actinomma</i> spp.	
<i>Actinosphaera acanthophora</i> (Popofsky)	Takahashi, 1991, p. 68, Pl. 9, Figs. 2, 3
<i>Amphirhopalum ypsilon</i> Haeckel	Takahashi, 1991, p. 81, Pl. 17, Figs. 1-3
<i>Arachnosphaera myriacantha</i> Haeckel	Takahashi, 1991, p. 67, Pl. 10, Figs. 11, 12
<i>Astrosphaera hexagonalis</i> Haeckel	Takahashi, 1991, p. 69, Pl. 11, Figs. 1-3
<i>Axoprunum stauraxonium</i> Haeckel	Takahashi, 1991, p. 76, Pl. 14, Figs. 8-10
<i>Cenosphaera</i> spp.	Nigrini and Moore, 1979, p. S43, Pl. 4, Figs. 3a-d
<i>Centroculus octostylus</i> Haeckel	Takahashi, 1991, p. 64, Pl. 7, Fig. 1
<i>Circodiscus</i> spp. group	Takahashi, 1991, p. 82, Pl. 20, Figs. 6-9
<i>Cladococcus abietinus</i> Haeckel	Takahashi, 1991, p. 67, Pl. 10, Fig. 5
<i>Cladococcus cervicornis</i> Haeckel	Takahashi, 1991, p. 67, Pl. 10, Figs. 8-10
<i>Cladococcus scoparius</i> Haeckel	Takahashi, 1991, p. 67, Pl. 10, Figs. 6, 7
<i>Cladococcus viminalis</i> Haeckel	Bjørklund, 1976, p. 1131, Pl. 1, Figs. 10-12
<i>Collosphaera invaginata</i> (Haeckel)	Bjørklund and Goll, 1979, p. 1317, Pl. 3, Figs. 1-9
<i>Collosphaera tubelosa</i> Haeckel	Takahashi, 1991, p. 55, Pl. 2, Figs. 1-3
<i>Collosphaera</i> spp.	
<i>Cubotholus</i> spp.	Boltovskoy, 1998, p. 59, Fig. 2K, 15.84
<i>Dictyocoryne euclidis</i> Haeckel	Welling, 1996, p. 214, Pl. 8, Figs. 1-3
<i>Dictyocoryne profunda</i> Ehrenberg	Nigrini and Moore, 1979, p. S87, Pl. 12, Fig. 1
<i>Dictyocoryne truncatum</i> (Ehrenberg)	Welling, 1996, p. 215, Pl. 9, Figs. 1-6
<i>Didymocyrtes tetrathalamus</i> (Haeckel)	Takahashi, 1991, p. 79, Pl. 21, Figs. 2-14
<i>Dipylissa bensoni</i> Dumitrica	Boltovskoy, 1998, p. 58, Fig. 15.83
<i>Disolenia</i> spp.	
<i>Dorydrupa bensoni</i> Takahashi	Takahashi, 1991, p. 78, Pl. 15, Figs. 11-14
<i>Drupptractus ostracion</i> Haeckel group	Takahashi, 1991, p. 75, Pl. 14, Figs. 3, 4
<i>Dryosphaera dendrophora</i> Haeckel	Takahashi, 1991, p. 70, Pl. 11, Fig. 4
<i>Dryomyomma elegans</i> Jørgensen	Cortese and Bjørklund, 1998, p. 154, Pl. 3, Figs. 17-19
<i>Ellipsoxiphium palliatum</i> Haeckel	Takahashi, 1991, p. 75, Pl. 14, Figs. 11-17
<i>Euchitonia elegans</i> (Ehrenberg)	Takahashi, 1991, p. 80, Pl. 16, Figs. 1-6
<i>Haekeliella macrodoras</i> (Haeckel)	Takahashi, 1991, p. 69, Pl. 10, Figs. 1-4
<i>Heliodiscus asteriscus</i> Haeckel	Nigrini and Moore, 1979, p. S73, Pl. 9, Figs. 1, 2
<i>Heliodiscus echiniscus</i> Haeckel	Takahashi, 1991, p. 89, Pl. 23, Figs. 4-6
<i>Heliodiscus macrococcus</i> Haeckel	Welling, 1996, p. 211, Pl. 6, Figs. 1-11
<i>Hexacromyium elegans</i> Haeckel	Takahashi, 1991, p. 73, Pl. 13, Figs. 4, 5, 7
<i>Hexacontium enthacanthum</i> Jørgensen	Nigrini and Moore, 1979, p. S45, Pl. 5, Figs. 1a, b
<i>Hexacontium hostile</i> Cleve	Takahashi, 1991, p. 72 Pl. 13, Figs. 1, 2
<i>Hexacontium laevigatum</i> Haeckel	Nigrini and Moore, 1979, p. S47, Pl. 5, Figs. 2a, b
<i>Stylosphaera melpomene</i> Haeckel	Takahashi, 1991, p. 75, Pl. 14, Figs. 1, 2
<i>Hexacontium</i> spp.	
<i>Hexalonche amphisiphon</i> Haeckel	Takahashi, 1991, p. 71 Pl. 12, Figs. 13, 14
<i>Hexapyle armata</i> (Haeckel)	Welling, 1996, p. 219, Pl. 12, Figs. 1, 2
<i>Larcopyle buetschlii</i> Dreyer	Nigrini and Moore, 1979, p. S131, Pl. 17, Figs. 1a, b
<i>Larcospira quadrangula</i> Haeckel	Takahashi, 1991, p.92, Pl. 23, Figs. 11, 12
<i>Lithelius minor</i> (Jørgensen)	Nigrini and Moore, 1979, p. S135, Pl. 17, Figs. 3, 4a, b
<i>Lithelius nautiloides</i> Popofsky	Nigrini and Moore, 1979, p. S137, Pl. 17, Fig. 5
<i>Myelastrum</i> spp.	
<i>Phorticium pylonium</i> Haeckel	Welling, 1996, p. 220, Pl. 12, Figs. 10, 11
<i>Plegmosphaera entodictyon</i> Haeckel	Takahashi, 1991, p. 62, Pl. 6, Figs. 8, 10, 11
<i>Plegmosphaera lepticali</i> Renz	Renz, 1976, p. 115, Pl. 1, Fig. 14
<i>Plegmosphaera pachypila</i> Haeckel	Takahashi, 1991, p. 62, Pl. 5, Figs. 7-9
<i>Polysolenia arktios</i> Nigrini	Nigrini and Moore, 1979, p. S11, Pl. 2, Fig. 1
<i>Pylospira octopyle</i> Haeckel	Nigrini and Moore, 1979, p. S139, Pl. 17, Figs. 6a-c

TABLE 2 (continued)
List of radiolarian taxa identified in the sediment trap samples

Table 2. (continued)	
Taxa	Current references
<i>Rhizoplegma boreale</i> (Cleve)	Bjørklund et al., 1998, p. 128, Pl. 1, Fig. 8
<i>Saturnalis circularis</i> Haeckel	Takahashi, 1991, p. 78, Pl. 15, Figs. 15-18
<i>Siphonosphaera</i> spp.	
<i>Sphaeropyle mespilus?</i> Dreyer	Takahashi, 1991, p. 70, Pl. 11, Figs. 7, 8
<i>Spongaster pentas</i> Riedel and Sanfilippo	Takahashi, 1991, p. 86, Pl. 17, Figs. 12-16
<i>Spongaster tetras tetras</i> Ehrenberg	Nigrini and Moore, 1979, p. S93, Pl. 13, Fig. 1
<i>Spongodictyon spongiosum</i> (Müller)	Boltovskoy, 1998, p. 46, Fig. 15.57
Spongodiscidae sp.	
<i>Spongodiscus biconcavus</i> Haeckel	Takahashi, 1991, p. 84, Pl. 19, Figs. 4-6
<i>Spongodiscus resurgens</i> Ehrenberg	Takahashi, 1991, p. 84, Pl. 19, Fig. 1
<i>Spongoliva ellipsoides</i> Popofsky	Renz, 1976, p. 108, Pl. 1, Fig. 5
<i>Spongopyle osculosa</i> Dreyer	Nigrini and Moore, 1979, p. S115, Pl. 15, Fig. 1
<i>Spongosphaera</i> sp. aff. <i>Helioides</i> Haeckel	Takahashi, 1991, p. 64, Pl. 7, Figs. 4, 7, 8
<i>Spongosphaera polycantha</i> Müller	Takahashi, 1991, p. 64, Pl. 7, Figs. 2, 3, 5
<i>Spongotrochus glacialis</i> Popofsky	Nigrini and Moore, 1979, p. S115, Pl. 15, Fig. 2a-d
<i>Spongurus cylindricus</i> (Haeckel)	Takahashi, 1991, p.85, Pl. 17, Figs. 6-9
<i>Spongurus pylomaticus</i> Riedel	Nigrini and Moore, 1979, p. S65, Pl. 15, Figs. 3a, b
<i>Spongurus spindalis</i> Welling	Welling, 1996, p. 212, Pl. 5, Figs.4, 5
<i>Stylochlamyidium venustum</i> (Bailey)	Ling et al, 1971, p. 711, Pl. 1, Figs. 7, 8
<i>Stylodictya aculeata</i> Jørgensen	Nigrini and Moore, 1979, p. S101, Pl. 13, Figs. 3, 4
<i>Stylodictya validispina</i> Jørgensen	Nigrini and Moore, 1979, p. S103, Pl. 13, Figs. 5a, b
<i>Styptosphaera spongiacea</i> Haeckel	Renz, 1976, p. 116, Pl. 1, Fig. 13
<i>Tetrapyle octacantha</i> Müller	Takahashi, 1991, p. 90, Pl. 23, Figs. 9, 10
<i>Thecosphaera inermis</i> (Haeckel)	Boltovskoy, 1998, p. 48, Fig. 15.38
<i>Tholospira cervicornis</i> Haeckel group	Takahashi, 1991, p. 91, Pl. 22, Figs. 7-9, 12
<i>Xiphatractus pluto</i> (Haeckel)	Takahashi, 1991, p. 77, Pl. 15, Figs. 1-3
<i>Xiphosphaera gaea</i> Haeckel	Takahashi, 1991, p. 70, Pl. 12, Figs. 1, 2
<i>Xiphosphaera tesseractis</i> Dreyer	Takahashi, 1991, p. 70, Pl. 12, Figs. 3-5
Nassellaria	
<i>Acanthodesmia vinculata</i> Müller	Takahashi, 1991, p. 102, Pl. 28, Figs. 6-8
<i>Acrobotrys</i> spp.	Boltovskoy, 1998, p. 87, Fig. 15.171
<i>Amphiplecta acrostoma</i> Haeckel	Welling, 1996, p. 231, Pl. 16, Fig.11
<i>Androspyris</i> spp.	
<i>Anthocrytidium ophirensis</i> (Ehrenberg)	Nigrini and Moore, 1979, p. N679, Pl. 25, Fig. 1
<i>Anthocrytidium zanguibaricum</i> (Ehrenberg)	Nigrini and Moore, 1979, p. N69, Pl. 25, Fig. 2
<i>Arachnocalpis</i> spp.	
<i>Arachnocorys pentacantha</i> Popofsky	Welling, 1996, p. 227, Pl. 14, Figs.21-23
<i>Arachnocorys umbellifera</i> Haeckel	Welling, 1996, p. 227, Pl. 14, Figs.24-27
<i>Artobotrys boreale</i> (Cleve)	Bjørklund et al, 1998, p. 130, Pl. 2, Figs. 4, 5
<i>Artostrobos annulatus</i> (Bailey)	Takahashi, 1991, p. 128, Pl. 38, Figs. 9, 10
<i>Artostrobos joergensenii</i> Petrushevskaya	Bjørklund et al, 1998, p. 130, Pl. 2, Figs. 17-19
<i>Botryocephalina armata</i> Petrushevskaya	Boltovskoy, 1998, p. 87, Fig. 15.173
<i>Botryocyrtilis elongatum</i> Takahashi	Takahashi, 1991, p. 135, Pl. 46, Figs. 8, 9
<i>Botryocyrtilis scutum</i> (Harting)	Takahashi, 1991, p. 135, Pl. 46, Figs. 6, 7
<i>Botryopyle dictyocephalus</i> Haeckel	Boltovskoy, 1998, p. 88, Fig. 15.174
<i>Botryostrobos aquilonaris</i> (Bailey)	Nigrini and Moore, 1979, p. N99, Pl. 27, Fig. 1
<i>Botryostrobos auritus/australis</i> group (Ehrenberg)	Nigrini and Moore, 1979, p. N101, Pl. 27, Fig. 2a-d
<i>Callimitra annae</i> Haeckel	Takahashi, 1991, p. 99, Pl. 26, Fig. 14
<i>Callimitra emmae</i> Haeckel	Takahashi, 1991, p. 100, Pl. 26, Fig. 15
<i>Callimitra solocicribrata</i> Takahashi	Takahashi, 1991, p. 100, Pl. 27, Figs. 10, 11
<i>Cantharospyris platybrata</i> Haeckel	Takahashi, 1991, p. 106, Pl. 31, Fig. 5
<i>Carpocanarium papillosum</i> (Ehrenberg)	Nigrini and Moore, 1979, p. N27, Pl. 21, Fig. 3
<i>Carpocanistrum</i> spp.	Nigrini and Moore, 1979, p. N23, Pl. 21, Figs. 1a-c
<i>Centrobotrys thermophila</i> Petrushevskaya	Takahashi, 1991, p. 135, Pl. 46, Figs. 1, 2
<i>Cephalospyris cancellata</i> Haeckel	Takahashi, 1991, p. 105, Pl. 31, Figs. 3, 4
<i>Cladoscenium ancoratum</i> Haeckel	Takahashi, 1991, p. 94, Pl. 24, Figs. 9-14
<i>Clathrocanium coarctatum</i> Ehrenberg	Boltovskoy, 1998, p. 64, Fig. 15.114
<i>Clathrocorys giltschii</i> Haeckel	Takahashi, 1991, p. 101, Pl. 27, Figs. 1-3, 9
<i>Clathrocorys murrayi</i> Haeckel	Takahashi, 1991, p. 101, Pl. 27, Figs. 4-8
<i>Clathrocyclas monumentum</i> (Haeckel)	Takahashi, 1991, p. 112, Pl. 34, Figs. 9-11
<i>Conarachnium facetum</i> (Haeckel)	Takahashi, 1991, p. 118, Pl. 39, Fig. 7
<i>Conarachnium parabolicum</i> (Popofsky)	Takahashi, 1991, p. 118, Pl. 39, Figs. 5, 6

TABLE 2 (continued)

List of radiolarian taxa identified in the sediment trap samples

Table 2. (continued)	
Taxa	Current references
<i>Conarachnium aff. polyacanthum</i> (Popofsky)	Takahashi, 1991, p. 118, Pl. 39, Figs. 1-4
<i>Cornutella profunda</i> Ehrenberg	Takahashi, 1991, p. 113, Pl. 35, Figs. 3-9
<i>Corocalyptra columba</i> (Haeckel)	Boltovskoy, 1998, p. 71, Fig. 15.132
<i>Cycladophora bicornis</i> (Popofsky)	Takahashi, 1991, p. 122, Pl. 41, Figs. 4-6, 8-11
<i>Cycladophora cornutoides</i> Kling	Motoyama, 1997, p. 57, Pl. 1, Figs. 1-3
<i>Cycladophora davisiana</i> Ehrenberg	Motoyama, 1997, p. 57, Pl. 1, Figs. 4-10
<i>Cyrtopera languncula</i> Haeckel	Takahashi, 1991, p. 119, Pl. 40, Figs. 3-6
<i>Dictyocodon elegans</i> (Haeckel)	Takahashi, 1991, p. 117, Pl. 37, Figs. 6, 7, 9
<i>Dictyocodon palladius</i> Haeckel	Takahashi, 1991, p. 117, Pl. 37, Figs. 8, 10, 11
<i>Dictyophimus crisiæ</i> Ehrenberg/hirundo (Haeckel) group	Welling, 1996, p. 234, Pl. 19, Figs. 1-5
<i>Dictyophimus aff. infabricatus</i> Nigrini	Takahashi, 1991, p. 116, Pl. 37, Figs. 3-5
<i>Dictyophimus macropterus</i> (Ehrenberg)	Takahashi, 1991, p. 116, Pl. 39, Figs. 8-11
<i>Dictyophimus</i> spp.	
<i>Dimelissa thoracites</i> (Haeckel) group	Welling, 1996, p. 225, Pl. 14, Figs. 1-8
<i>Eucecryphalus danaes</i> (Haeckel)	Welling, 1996, p. 238, Pl. 22, Figs. 7-9
<i>Eucecryphalus gegenbauri</i> Haeckel/cervus (Ehrenberg) group	Welling, 1996, p. 238, Pl. 22, Figs. 1-6
<i>Eucecryphalus tricostatus</i> (Haeckel)	Takahashi, 1991, p. 110, Pl. 33, Figs. 4, 6
<i>Eucyrtidium anomalum</i> (Haeckel)	Boltovskoy, 1998, p. 75, Fig. 15.138
<i>Eucyrtidium acuminatum</i> (Ehrenberg)	Takahashi, 1991, p. 124, Pl. 42, Figs. 9, 10, 16, 17, 20
<i>Eucyrtidium hexagonatum</i> Haeckel	Nigrini and Moore, 1979, p. N63, Pl. 24, Figs. 4a, b
<i>Eucyrtidium hexastichum</i> (Haeckel)	Welling, 1996, p. 234, Pl. 18, Figs. 13-14
<i>Eucyrtidium</i> spp.	
<i>Gonosphaera primordialis</i> Jørgensen	Bjørklund, 1976, p. 1143, Pl. 9, Figs. 7-10
<i>Helotholus histicosa</i> Jørgensen	Boltovskoy, 1998, p. 65, Fig. 15.113
<i>Lamprocyclus maritialis</i> group? Haeckel	Boltovskoy, 1998, p. 81, Fig. 15.158
<i>Lamprocyrtis nigriniae</i> (Caulet)	Welling, 1996, p. 243, Pl. 24, Figs. 13, 14
<i>Lampromitra</i> spp.	Welling, 1996, p. 230, Pl. 16, Figs. 1-6
<i>Lipmanella</i> spp.	
<i>Lipmanella virchowii</i> (Haeckel)	Takahashi, 1991, p. 122, Pl. 40, Figs. 19-21
<i>Liriospyris reticulata</i> (Ehrenberg)	Takahashi, 1991, p. 107, Pl. 31, Figs. 14-16
<i>Liriospyris thorax</i> (Haeckel)	Takahashi, 1991, p. 106-107, Pl. 31, Figs. 10-13
<i>Litharachnium tentorium</i> Haeckel	Takahashi, 1991, p. 114, Pl. 35, Figs. 14-18
<i>Lithomelissa</i> sp. group	
<i>Lithopera bacca</i> Ehrenberg	Takahashi, 1991, p. 119, Pl. 40, Figs. 1, 2
<i>Lithostrobus hexagonalis</i> Haeckel	Takahashi, 1991, p. 122, Pl. 41, Figs. 1-3
<i>Lophophaena butschlii</i> (Haeckel)	Boltovskoy, 1998, p. 66, Fig. 15.108
<i>Lophophaena hispida</i> (Ehrenberg)	Boltovskoy, 1998, p. 66, Fig. 15.109
<i>Lophophaena cylindrica</i> (Cleve)	Takahashi, 1991, p. 96, Pl. 25, Figs. 3-5
<i>Lophophaena nadezdae</i> Petrushevskaya	Welling, 1996, p. 229, Pl. 15, Figs. 8-10
<i>Lophophaena variabilis</i> (Popofsky)	Welling, 1996, p. 228, Pl. 15, Fig. 7
<i>Lophospyris</i> juvenile form group	Takahashi, 1991, p. 102, Pl. 28, Figs. 1-4
<i>Lophospyris pentagona hyperborea</i> (Jørgensen) emend. Goll	Takahashi, 1991, p. 103, Pl. 29, Figs. 1-3, 5-10
<i>Lophospyris pentagona pentagona</i> (Ehrenberg) emend. Goll	Takahashi, 1991, p. 102, Pl. 28, Figs. 9-14
<i>Lophospyris pentagona quadriforis</i> (Haeckel) emend. Goll	Takahashi, 1991, p. 102, Pl. 28, Fig. 5
<i>Neosemantis distephanus</i> Popofsky	Takahashi, 1991, p. 95, Pl. 27, Fig. 12
<i>Nephrospyris renilla renilla</i> Haeckel	Takahashi, 1991, p. 104, Pl. 30, Fig. 7-9
<i>Paradictyum paradoxum</i> Haeckel	Petrushevskaya, 1971b, Fig. 138
<i>Peridium longispinum</i> Jørgensen	Bjørklund, 1998, p. 130, Pl. 2, Figs. 26, 27
<i>Peridium</i> spp.	Welling, 1996, p. 222, Pl. 13, Figs. 10-13
<i>Peripyramis circumtexta</i> Haeckel	Takahashi, 1991, p. 113, Pl. 35, Figs. 10-13
<i>Peromelissa phalacra</i> Haeckel	Takahashi, 1991, p. 97, Pl. 25, Figs. 11-15
<i>Phormospyris stabilis capoi</i> Goll	Welling, 1996, p. 250, Pl. 28, Figs. 3-5
<i>Phormospyris stabilis scaphipes</i> (Haeckel)	Takahashi, 1991, p. 103, Pl. 29, Figs. 11, 12, 14
<i>Phormospyris stabilis stabilis</i> (Goll)	Takahashi, 1991, p. 104, Pl. 30, Figs. 2-5
<i>Phormostichoartus corbula</i> (Harting)	Takahashi, 1991, p. 129, Pl. 44, Figs. 14-16
<i>Phormacantha hystrix</i> (Jørgensen)	Takahashi, 1991, p. 95, Pl. 26, Fig. 3
<i>Plectacantha</i> spp.	Welling, 1996, p. 221, Pl. 13, Figs. 1-9
<i>Plectagonidium deflandrei</i> Cachon and Cachon	Cachon and Cachon, 1969, p. 236, Pl. 39, Fig. 1
<i>Pseudocubus obeliscus</i> Haeckel	Takahashi, 1991, p. 95, Pl. 26, Fig. 1
<i>Pseudodictyophimus bicornis</i> (Ehrenberg)	Welling, 1996, p. 223, Pl. 13, Figs. 13, 14
<i>Pseudodictyophimus gracilipes</i> (Bailey)	Bjørklund, 1998, p. 130, Pl. 2, Fig. 8
<i>Pseudodictyophimus</i> spp.	
<i>Pterocanium korotnevi</i> (Dogiel and Reshetnyak)	Nigrini and Moore, 1979, p. N39, Pl. 23, Figs. 1a, b

TABLE 2 (continued)
List of radiolarian taxa identified in the sediment trap samples

Table 2. (continued)	
Taxa	Current references
<i>Pteroscenium pinnatum</i>	Boltovskoy, 1998, p. 83, Fig. 15.162
<i>Pterocanium polypylum</i>	Welling, 1996, p. 235, Pl. 19, Figs. 11, 12
<i>Pterocanium praetextum</i>	Nigrini and Moore, 1979, p. N41, Pl. 23, Fig. 2
<i>Pterocanium trilobum</i> (Haeckel)	Boltovskoy, 1998, p. 78, Fig. 15.145
<i>Pterocorys hertwigii</i> (Haeckel)	Boltovskoy, 1998, p. 82, Fig. 15.155
<i>Pterocorys sabae</i> (Ehrenberg)	Welling, 1996, p. 245, Pl. 25, Figs. 8-10
<i>Pterocorys zancleus</i> (Müller)	Nigrini and Moore, 1979, p. N89, Pl. 25, Figs. 11a, b
<i>Siphocampe arachnea</i> (Ehrenberg)	Abelmann, 1992, p. 382, Pl. 5, Fig. 15
<i>Spirocorytis subscalaris</i> Nigrini	Takahashi, 1991, p. 127, Pl. 44, Figs. 3-6
<i>Corocalyptra kruegeri</i> Popofsky	Boltovskoy, 1998, p. 72, Fig. 15.136
<i>Stichopilium bicorne</i> Haeckel	Nigrini and Moore, 1979, p. N91, Pl. 26, Figs. 1a, b
<i>Tetracorethra tetracorethra</i> (Haeckel)	Takahashi, 1991, p. 123, Pl. 41, Figs. 17, 18
<i>Tetraphormis dodecaster</i> (Haeckel)	Takahashi, 1991, p. 108, Pl. 32, Fig. 7
<i>Tetraphormis rotula</i> (Haeckel)	Takahashi, 1991, p. 108, Pl. 32, Figs. 1-3
<i>Tetraplecta pinigera</i> Haeckel	Takahashi, 1991, p. 93, Pl. 24, Figs. 1-5
<i>Theocorys veneris</i> Haeckel	Takahashi, 1991, p. 120, Pl. 40, Figs. 11-14
<i>Theocorythium trachelium</i> (Ehrenberg)	Takahashi, 1991, p. 121, Pl. 40, Figs. 15, 16
<i>Theophormis callipilium</i> Haeckel	Takahashi, 1991, p. 108, Pl. 32, Figs. 9-12
<i>Tholospyris baconiana</i> (Haeckel)	Takahashi, 1991, p. 106, Pl. 31, Figs. 6-8
<i>Tholospyris</i> sp. group	Takahashi, 1991, p. 106, Pl. 27, Figs. 15-17
<i>Lophocorys undulata</i> (Popofsky)	Takahashi, 1991, p. 120, Pl. 40, Figs. 9, 10
<i>Trisulcus triacanthus</i> Popofsky	Boltovskoy, 1998, p. 69, Fig. 15.106
<i>Zygocircus productus</i> (Hertwig) group	Takahashi, 1991, p. 101, Pl. 27, Figs. 13, 14
Phaeodaria	
<i>Borgertella caudata</i> (Wallich)	Takahashi, 1991, p. 148, Pl. 54, Figs. 13-17
<i>Castanella</i> spp.	
<i>Challengeron tizardi</i> (Murray)	Takahashi, 1991, p. 139, Pl. 48, Figs. 13-16
<i>Challengeron willemoesii</i> Haeckel	Takahashi, 1991, p. 138, Pl. 47, Figs. 1-14
<i>Challengerosium avicularia</i> Haecker	Takahashi, 1991, p. 140, Pl. 49, Figs. 1-13
<i>Conchelimium capsula</i> Borgert	Takahashi, 1991, p. 157, Pl. 61, Figs. 1-5, 7, 8, 10
<i>Conchidium argiope</i> Haeckel	Takahashi, 1991, p. 157, Pl. 62, Figs. 1, 2
<i>Euphysetta elegans</i> Borgert	Takahashi, 1991, p. 146, Pl. 53, Figs. 1-10
<i>Euphysetta staurocodon</i> Haeckel	Takahashi, 1991, p. 146, Pl. 53, Figs. 11-14
<i>Lirella bullata</i> (Stadium and Ling)	Takahashi, 1991, p. 149, Pl. 55, Figs. 8-11
<i>Lirella melo</i> (Cleve)	Takahashi, 1991, p. 149, Pl. 55, Figs. 12-18
<i>Medustta ansata</i> Borgert	Takahashi, 1991, p. 147, Pl. 54, Figs. 1-7
<i>Porospathis holostoma</i> (Cleve)	Takahashi, 1991, p. 150, Pl. 57, Figs. 1-8
<i>Protocystis auriculata</i> Takahashi	Takahashi, 1991, p. 142, Pl. 50, Figs. 4-7

***Tetrapyle octacantha* Müller 1858**

Tetrapyle octacantha Müller 1858. - NIGRINI and MOORE 1979, p.125, Pl. 16, Figs. 3a, b. - TAKAHASHI 1991, p. 90. Pl. 23, Figs. 9-10. - WELLING 1996, p. 219, Pl. 12, Figs. 3-9.

Octopyle stenoza Haeckel 1887. - NIGRINI and MOORE 1979, p. S123, Pl. 16, Figs. 2a, b. - TAKAHASHI 1991, p. 90. Pl. 23, Fig. 8.

Octopyle stenoza group? Haeckel 1887. - BOLTOVSKOY 1998, p. 58, Figs. 15.80b-c (not 15.80a).

Remarks: In the present study, *Octopyle stenoza* Haeckel 1887 is included in *Tetrapyle octacantha* Muller 1858 following the definition of Welling (1996).

***Pseudodictyophimus gracilipes* (Bailey) 1856**

Pseudodictyophimus gracilipes (Bailey) 1856. - PETRUSHEVSKAYA 1971b, Fig. 48 (1-6). - TAKAHASHI 1991, p.116, Pl. 37, Figs. 12-14.

- WELLING 1996, p. 223, Pl. 13, Figs. 16-20. - BJØRKLUND 1998, p. 130, Pl. 2, Fig. 8.

Dictyophimus gracilipes Bailey 1856. - BOLTOVSKOY 1998, p. 73, Figs. 15.142a, b.

Pseudodictyophimus gracilipes tetracanthus (Popofsky) 1913. - PETRUSHEVSKAYA 1971b, Fig. 49 (1-6).

Pseudodictyophimus tetracanthus (Popofsky) 1913. - WELLING 1996, p. 224, Pl. 13, Figs. 21-22.

Pseudodictyophimus platycephalus (Haeckel) 1887. - WELLING 1996, p. 224, Pl. 13, Fig. 23.

Remarks: *Pseudodictyophimus tetracanthus* (Popofsky) 1913 and *Pseudodictyophimus platycephalus* (Haeckel) 1887 are considered as member of *P. gracilipes* because Petrushevskaya (1971b) describes *tetracanthus* as a subspecies of *P. gracilipes*. Welling (1996) mentioned that *platycephalus* is probably a variant of *P. tetracanthus*.

Lithomelissa sp. group

Lithomelissa setosa Jørgensen 1900, TAKAHASHI 1991, Pl. 25, Figs. 16-22.

Remarks: As it can be seen in the illustrations of Takahashi (1991), the definition of *L. setosa* at the time was broader than referring as a single species. Therefore, we categorized this taxonomic group as *Lithomelissa* sp. group.

Pseudocubus obeliscus Haeckel 1887

Pseudocubus obeliscus Haeckel 1887, PETRUSHEVSKAYA 1971b, Fig. 76 (1-6) . – TAKAHASHI 1991, p. 95, Pl. 26, Fig. 1. – BOLTOVSKOY 1998, p. 68, Figs. 15.122a, b.

Lophophaena hispida (Ehrenberg) 1872

Lophophaena hispida (Ehrenberg) 1872. – PETRUSHEVSKAYA 1971b, Fig. 61 (1-3); WELLING 1996; p. 228, Pl. 15, Figs. 2-6; BOLTOVSKOY 1998, p. 66, Figs. 15.109a-d.

ACKNOWLEDGMENTS

We gratefully thank Prof. Hodaka Kawahata of the Ocean Research Institute, University of Tokyo for providing valuable sediment trap samples. We acknowledge captain, crew, technicians, and scientists on board the R/V Mirai Cruises, JAMSTEC, for their efforts in collecting sediment trap samples. We are grateful to Prof. Kjell Bjørklund, Dr. Helene Jacot des Combes, Dr. Isao Motoyama, Dr. Shin-ichi Kamikuri and Dr. David Lazarus for their critical and constructive comments to improve our manuscript. This study was financially supported by the following program to YO: the Sasakawa Scientific Research Grant from The Japan Science Society, The Moritani Scholarship Foundation, and the JSPS Project No. 18710022. The deployment of sediment traps were supported by the GCMAPS program (Global carbon cycle and related mapping based on satellite imagery) promoted by the MEXT.

REFERENCES

ABELMANN, A., 1992. Radiolarian taxa from Southern Ocean sediment traps (Atlantic sector). *Polar Biology*, 12: 373-385.

ANDERSON, O. R., BRYAN, M. and BENNETT, P., 1990. Experimental and observational studies of radiolarian physiological ecology: 4. Factors determining the distribution and survival of Didymocystis tetrathalamus tetrathalamus with implications for paleoecological interpretations. *Marine Micropaleontology*, 16: 155-167.

BENSON, R. N., 1966. "Recent Radiolaria from the Gulf of California." Ph.D. thesis, University of Minnesota, 577pp.

BJØRKLUND, K. R., 1976. Radiolaria from the Norwegian Sea, Leg 38 of the Deep Sea Drilling Project. *Initial Reports of the Deep Sea Drilling Project*, 38: 1101-1168.

BJØRKLUND, K. R. and GOLL, R. M., 1979. Internal skeletal structures of Collosphaera and Trisolenia: a case study of repetitive evolution in the Collosphaeridae (Radiolaria). *Journal of Paleontology*, 53: 1293-1326.

BJØRKLUND, K. R., CORTESE, G., SWANBERG, N. and SCHRADER, H. J., 1998. Radiolarian faunal provinces in surface sediments of the Greenland, Iceland and Norwegian (GIN) Seas. *Marine Micropaleontology*, 35: 105-140.

BLANCHOT, J. and RODIER, M., 1996. Picophytoplankton abundance and biomass in the western tropical Pacific Ocean during the 1992 El Niño year: results from flow cytometry. *Deep-Sea Research I*, 43: 877-895.

BOLTOVSKOY, D., 1998. Classification and distribution of South Atlantic Recent Polycystine Radiolaria. *Paleontologica Electronica*, 1: 1-116 pp.

BOLTOVSKOY, D. and RIEDEL, W. R., 1987. Polycystine Radiolaria of the California Current region: seasonal and geographic patterns. *Marine Micropaleontology*, 12: 65-104.

BROOMHEAD, D. S. and KING, G., 1986. Extracting qualitative dynamics from experimental data. *Physica D*, 20: 217-236.

CACHON, J. and CACHON, M., 1969. Revision systematique des Nassellaires Plectoidea a propos de la description d'un nouveau representant, *Plectagonidium deftlandrei* nov. gen. nov. sp. *Archiv für Protistenkunde*, 111: S. 236-251.

CHAVEZ, F. P., BUCK, K. R., SERVICE, S. K., NEWTON, J. and BARBER, R. T., 1996. Phytoplankton variability in the central and eastern tropical Pacific. *Deep-Sea Research II*, 43: 835-870.

CORTESE, G. and BJØRKLUND, K. R., 1998. The taxonomy of boreal Atlantic Ocean Actinomma (Radiolaria). *Micropaleontology*, 44: 149-160.

GHIL, M., ALLEN, R. M., DETTINGER, M. D., IDE, K., KONDRASHOV, D., MANN, M. E., ROBERTSON, A. SAUNDERS, A., TIAN, Y., VARADI, F. and YIOU, P., 2002. Advanced spectral methods for climatic time series, *Review of Geophysics*, 40: 3.1-3.41, 10.1029/2000RG000092.

INOUE, H. Y., ISHII, M., MATSUEDA, H. and AOYAMA, M., 1996. Changes in longitudinal distribution of the partial pressure of CO₂ (pCO₂) in the central and western equatorial Pacific, west of 160°W. *Geophysical Research Letters*, 23: 1781-1784.

KAWAHATA, H. and GUPTA, L. P., 2004. Settling particles flux in response to El Niño/Southern Oscillation (ENSO) in the equatorial Pacific. In: Shiomi, M. and Kawahata, H., Eds., *Global environmental change in the ocean and on land*, 95-108. Tokyo: Terra.

KAWAHATA H., SUZUKI, A. and OHTA, H., 2000. Export Fluxes in the Western Pacific Warm Pool. *Deep-Sea Research I*, 47: 2061-2091.

KLING, S. A., 1979. Vertical distribution of Polycystine radiolarians in the central North Pacific. *Marine Micropaleontology*, 4: 295-318.

KLING, S.A. and BOLTOVSKOY, D., 1995. Radiolarian vertical distribution patterns across the southern California Current. *Deep-Sea Research I*, 42, 191-231.

KOBAYASHI, F. and TAKAHASHI, K., 2002. Distribution of diatom along the Equatorial transect in the western central Pacific during the 1999 La Niña condition, *Deep-Sea Research II*, 49: 2801-2821.

LE BORGNE, R., RODIER, M., LE BOUTEILLER, A. and MURRAY, J. W., 1999. Zonal variability of plankton and particle export flux in the equatorial Pacific upwelling between 165°E and 150°W. *Oceanologica Acta*, 22: 57-66

LE BORGNE, R., BARBER, R. T., DELCROIX, T., INOUE, H. Y., MACKAY, D. J. and RODIER, M., 2002. Pacific warm pool and divergence: temporal and zonal variations on the equator and their effects on the biological pump, *Deep-Sea Research II*, 49: 2471-2512.

LOMBARI, G. and BODEN, G., 1985. *Modern radiolarian global distributions*. Washington, Cushman Foundation for Foraminiferal Research, Special Publication No. 16A, 125 pp.

- LUKAS, R. and LINDSTROM, E., 1991. The mixed layer of the western equatorial Pacific. *Journal of Geophysical Research*, 96: 3343-3357.
- MACKEY, D. J., PARSLow, J., HIGGINS, H. W., GRIFFITHS, F. B., and O'SULLIVAN, J. E., 1995. Plankton productivity and biomass in the western Pacific: biological and physical controls. *Deep-Sea Research II*, 42: 499-535.
- MACKEY, D. J., O' SULLIVAN, J. E. and WATSON, R. J., 2002. Iron in the western Pacific: a riverine or hydrothermal source for iron in the Equatorial Undercurrent? *Deep-Sea Research I*, 49: 877-893.
- MATSUMOTO, K., FURUYA, K. and KAWANO, T., 2004. Association of picophytoplankton distribution with ENSO events in the equatorial Pacific between 145°E and 160°W. *Deep-Sea Research I*, 51: 1851-1871.
- MILLIMAN, J. and MEADE, R. H., 1983. World-wide delivery of river sediment to the oceans. *Journal of Geology*, 91: 1-21.
- MILLIMAN, J., FARNSWORTH, K. L. and ALBERTIN, C. S., 1999. Flux and fate of fluvial sediments leaving large islands in the East Indies. *Journal of Sea Research*, 41: 97-107.
- MOTOYAMA, I., 1997. Origin and evolution of *Cycladophora davisiana* Ehrenberg (Radiolaria) in DSDP Site 192, Northwest Pacific. *Marine Micropaleontology*, 30: 45-63.
- NIGRINI, C., 1970. Radiolarian assemblages in the North Pacific and their application to a study of Quaternary sediments in core V20-130. In: HAYS, J. D., Ed. *Geological Investigations of the North Pacific* 139-183. The Geological Society of America, Memoir 126.
- NIGRINI, C. and MOORE, T. C. Jr., 1979. *A guide to modern Radiolaria*. Washington, Cushman Foundation for Foraminiferal Research, Special Publication No. 16, 342 pp.
- PETRUSHEVSKAYA, M. G., 1971a. Spumellarian and nassellarian Radiolaria in the plankton and bottom sediments of the central Pacific. In: Fumnel, B. M., Riedel, W. R., Eds, *The Micropaleontology of Oceans*, pp. 309-317.
- , 1971b. *Radiolyarii Nassellaria v planktone Mirovogo Okeana*. Issledovaniya Fauny Morei 9. Leningrad: NAUKA, 294 pp.
- PICAUT, J., IOUALALEN, M., MENKES, C., DELCROIX, T. and MCPHADEN, M. J., 1996. Mechanism of the zonal displacements of the Pacific Warm Pool: Implications for ENSO. *Science*, 274: 1486-1489.
- PISIAS, N. G., MURRAY, D. W., and ROELOFS, A. K., 1986. Radiolarian and silicoflagellate response to oceanographic changes associated with the 1983 El Niño. *Nature*, 320: 259-262.
- RENZ, G. W., 1976. The distribution and ecology of radiolaria in the central Pacific: plankton and surface sediments. *Bulletin of the Scripps Institution of Oceanography*, 22:1-267 pp.
- REYNOLDS, R. W. and SMITH, T. M., 1994. Improved global sea surface temperature analysis. *Journal of Climate*, 7: 929-948. <http://ingrid.ldeo.columbia.edu/SOURCES/IGOSS>
- RODIER, M., ELDIN, G. and BORGNE, R., 2000. The western boundary of the Equatorial Pacific upwelling: some consequences of climatic variability on hydrological and planktonic properties. *Journal of Oceanography*, 56: 463-471.
- SHOLKOVITZ, E. R., ELDERFIELD, H., SZYMCZAK, R. and CASEY, K., 1999. Island weathering : river sources of rare earth elements to the Western Pacific Ocean. *Marine Chemistry*, 68: 39-57.
- TAKAHASHI, K., 1987. Radiolarian flux and seasonality: climatic and El Niño response in the subarctic Pacific, 1982-1984. *Global Biogeochemical Cycles*, 1: 213-231.
- TAKAHASHI, K., 1991. Radiolaria: flux, ecology, and taxonomy in the Pacific and Atlantic. In: Honjo, S., Ed, *Ocean Biocoenosis*, Series 3, Woods Hole Oceanography Institute Press, Woods Hole, 303 pp.
- TAKAHASHI, K., HURD, D. C. and HONJO, S., 1983. Phaeodarian Skeletons: their role in silica transport to the deep sea. *Science*, 222: 616-618.
- TOZUKA, T. and YAMAGATA, T., 2003. Annual ENSO. *Journal of Physical Oceanography*, 33: 1564-1578.
- TSUCHIYA, M., LUKAS, R., FINE, R. A., FIRING, E. and LINDSTROM, E., 1989. Source waters of the Pacific Equatorial Undercurrent. *Progress in Oceanography*, 23: 101-147.
- VAUTARD, R. and GHIL, M., 1989. Singular spectrum analysis in nonlinear dynamics, with applications to paleoclimatic time series. *Physica D*, 35: 395-424.
- WANG, X. J, CHRISTIAN, J. R, MURTUGUDDE, R. and BUSALACCHI, A. J., 2006. Spatial and temporal variability in new production in the equatorial Pacific during 1980-2003: Physical and biogeochemical controls. *Deep-Sea Research II*, 53: 677-697.
- WELLING, L. A., 1996. "Environmental control of radiolarian abundance in the central equatorial Pacific and implications for paleoceanographic reconstructions." Ph.D. thesis, Oregon State University, Corvallis, 314 pp.
- WELLING, L. A. and PISIAS, N. G., 1998. Radiolarian fluxes, stocks, and population residence times in surface waters of the central equatorial Pacific. *Deep-Sea Research I*, 45: 639-671.
- WELLING L. A., PISIAS, N. G., JOHNSON, E. S. and WHITE, J. R., 1996. Distribution of polycystine radiolaria and their relation to the physical environment during the 1992 El Niño and following cold event. *Deep-Sea Research II*, 43: 1413-1434.
- YAMASHITA, H., TAKAHASHI, K. and FUJITANI, N., 2002. Zonal and vertical distribution of radiolarians in the western and central Equatorial Pacific in January 1999. *Deep-Sea Research II*, 49: 2823-2862.
- YAN, X. H., HO, C. R., ZHENG, Q. and KLEMAS, V., 1992. Temperature and size variabilities of the Western Pacific Warm Pool. *Science*, 258: 1643-1645.

